UNIVERSITAT DE BARCELONA

Teleconnexions atmosfèriques i resposta oceanogràfica a les mars Mediterrània Nordoccidental i Cantàbrica

Aitor Rumín Caparrós

TELECONNEXIONS ATMOSFÈRIQUES I RESPOSTA OCEANOGRÀFICA A LES MARS MEDITERRÀNIA NORD-OCCIDENTAL I CANTÀBRICA

Aitor Rumín Caparrós

Memòria de Tesis Doctoral

Dirigida per la **Dra. Anna Sànchez Vidal** i el **Dr. Miquel Canals Artigas**

Programa de Doctorat de Ciències del Mar, Universitat de Barcelona

Departament de Dinàmica de la Terra i de l'Oceà

Facultat de Ciències de la Terra, Universitat de Barcelona

UNIVERSITAT DE BARCELONA

Universitat de Barcelona GRC Geociències Marines

Aquesta Tesi s'emmarca dins el Programa de Doctorat de Ciències del Mar de la Universitat de Barcelona i ha estat realitzada al Departament de Dinàmica de la Terra i de l'Oceà de la mateixa Universitat, dins el Grup de Recerca en Geociències Marines, reconegut per la Generalitat de Catalunya com a Grup de Recerca Consolidat (refs. 2009 SGR 1305 i 2014 SGR 1068). Durant el període d'elaboració de la Tesi, el doctorand ha gaudit d'una beca FPI (*Formación de Personal Investigador*) del *Ministerio de Economía y Competitividad* (ref. BES-2010-036214). Dues estades breus, a *l'Istituto di Scienze Marine* (ISMAR) del *Consiglio Nazionale delle Ricerche* (CNR) italià i al *Centro Oceanográfico de Gijón* de l'*Instituto Español de Oceanografía*, han estat finançades pel programa d'*Ayudas a la movilidad predoctoral para la realización de estancias breves en centros de I+D del Subprograma Estatal de Movilidad del Ministerio de Economía y Competitividad*. Altres ajuts que el doctorand ha rebut per assistir a congressos i cursos han estat concedits per la Facultat de Geologia (ara Facultat de Ciències de la Terra) de la Universitat de Barcelona a través del programa d'Ajuts a la Mobilitat de la Comissió de Recerca de la Facultat i pel Seté Programa Marc de la Comissió Europea *(FP7/2007-2013)*. El treball i els resultats de recerca que es mostren en aquesta Tesi són vinculats principalment al projecte DOS MARES (*Cañones y taludes profunDOS en los MARES Mediterráneo y Cantábrico: desde la sincronía entre forzamientos externos a los recursos vivos*, 2010-13, ref. CTM2010-21810-C03-01) del *Plan Nacional de I+D+i*. A més, hem rebut el suport dels projectes europeus HERMIONE (*Hotspot Ecosystem Research and Man's Impact on European Seas*, 2009-12, ref. FP7-ENV-2008-1-226354) i PERSEUS (*Policy-oriented marine Environmental Research in the Southern EUropean Seas, 2012-15*, ref. GA 287600), i del projecte GRACCIE (*Multidisciplinary Research Consortium on GRadual and Abrupt Climate Changes, and their Impacts on the Environment*, 2007-13, ref. CSD2007-00067) del programa CONSOLIDER-INGENIO 2010.

A voltes, les coses, senzillament, passen.

Peter Theodore Landsberg (1922-2010)

Portada: Adaptació d'un fragment de l'obra de Piet Mondrian "Broadway Boogie-Woogie"

Als meus pares, a la meva iaia i a l'Elena

AGRAÏMENTS

Sempre havia imaginat que escriuria els agraïments en algun indret ben especial. Vaig intentar escriure'ls als Pirineus, mes no ho vaig aconseguir. Vaig intentar escriure'ls a la costa del Garraf, mes tampoc ho vaig aconseguir. Finalment, he trobat el lloc ideal, front d'una estufa de llenya d'un *lodge* situat a Padepani (Nepal), a 2700 metres d'alçada, envoltat de gent de diferents nacionalitats i cultures ben dispars.

El seu estat d'ànim alegre però alhora tens, possiblement per la incertesa que genera el no saber ben bé com seran les etapes que encara els hi queden per davant, em recorda com em vaig sentir el primer dia en que vaig aparèixer pel departament a fer una entrevista amb un tal doctor Canals, de qui havia sentit parlar a la facultat pels seus treballs sobre "cascading" al golf de Lleó. Tot i el meu neguit inicial, l'entrevista va anar prou bé i en Miquel em va oferir l'oportunitat de començar una Tesi en el grup que ell mateix dirigeix. No em va costar massa decidir-me i el resultat és la Tesi doctoral que es presenta a continuació. És a ell a qui vull donar les gràcies en primer lloc, no solament per haver-me donat aquesta oportunitat i per haver confiat en mi tot aquest temps, sinó que també per engrescar-me a participar en campanyes oceanogràfiques, congressos, reunions i sobretot per haver-me donat l'oportunitat d'adquirir una sèrie de coneixements i aptituds que m'han ajudat a madurar i ser molt més exigent amb la feina ben feta.

A la segona persona a qui voldria agrair la confiança que ha dipositat en mi és a l'Anna Sànchez. Sense la seva ajuda no hagués pogut acabar aquesta Tesi. Mercès pels teus consells i també per guiar-me durant tot aquest llarg camí. Gràcies per les teves correccions en tots i cadascun dels treballs que he publicat.

A tota la penya que ha estat o forma part actualment de la 336, una sala que deixa nafra: Rayo, Rubén, Patri POVEA, Eli Costa, Mayte, Mapache (Valero), X. Tubau, Andreu, Yaniel, Nicolaaaaaa i Barriuso. Gràcies per tots aquests anys. Mai oblidaré les filosofades del savi Valero i les rèpliques d'en Rubén, ni les discussions per l'aire condicionat o la calefacció, ni tantes coses viscudes tots plegats en aquesta, la nostra sala. A tots vosaltres, mil gràcies companys!

A la gent que sou o heu format part del GRCGM (i espero no deixar-me a ningú): Marc Cerdà, David Amblàs, Albert, Oli, Maria, Mercè, JudOt, Jalme, Oriol Veres, Pilar, Aaron, Esther, Liam, José Noel, Anna Ayyyyma, Galderic, J.L. Casamor, Leo, Rut Pedrosa, Ruth Duran i al gran savi Toni Calafat.

A la Montse Guart, per haver-me ajudat tot aquest temps amb les feines del laboratori, per ser sempre tan alegre, per tenir tan bon humor i estar sempre predisposada a ajudar amb el que calgui, dins i fora del laboratori, moltes gràcies!

Muchas gracias Silvia por tu gran labor, echaré de menos nuestras muy breves (pero siempre productivas) conversaciones matutinas.

Voldria agrair en especial a la Rut Pedrosa, la meva compi de fatigues del GRCGM, amb qui tant he compartit i amb qui tant, espero, compartiré. Rut, gràcies per tots aquest anys, per aguantar els meus alts i baixos, per ajudar-me sempre que m'ha calgut i en definitiva, per ser com ets. Tramperus Power 4ever!

A l'Oli, perquè tenies raó, she was like the winter... she was coming. Grazas pola túa compañía durante todos estos anos. Grazas polos teus consellos e por axudarme sempre que o precisei.

A la Patri (a qui en aquest document vull fer justícia a l'honor dels POVEA escrivint bé el seu cognom: POVEA, i no PoveDa) per totes les pink panthers que hem compartit... Amb qui les compartiré ara? Gràcies per deixar-me ser el teu little finger ;-)

No puc oblidar d'agrair molt especialment als RASPBERRYS: Rayo, Amblàs i Costris:

- Rayo, Rayini, ets i seràs sempre algú molt especial per mi.
- Costris (SergiO Costa), vagis on vagis sempre seràs algú ben important per mi. Sobretot si de tant en quan em portes a fer un bon esmorzar de funcionari allà on tu ja saps ;-)
- Al gran Amblàs, a qui admiro. Saps que l'olla de Núria sempre serà nostra. T'espero per repetir-la any darrera any.

A la família i amics, i en especial al Xavi Tambu (Oculouo), per tants anys d'amistat... Ich liebe dich!

Tubau, reservo en especial per tu algunes línies també. Gràcies per haver compartit tot aquest temps amb mi, en especial els últims anys de Tesi. Tu mateix em vas escriure un dia que durant una Tesi no només es forja el coneixement, sinó també les amistats. Doncs ho comparteixo totalment. Gràcies per la teva amistat.

Marc, no m'oblido pas de tu, gràcies per fer-me molt més planera la última etapa de la Tesi, gràcies pels teus consells i per la teva amistat. Noves rutes moteres ens esperen!

A la gente de Gijón y en especial a los "Asturianos al Caloreta" (Tamara, Nestor y Sdena) y a Lucie. Gracias por haberme acogido tan y tan bien en Gijón.

A Renate, Mikel y especialmente a César y Raquel, gracias por haberme tratado tan bien durante mi estancia en el IEO de Gijón. Gracias por vuestra ayuda, dedicación y amistad.

A Katrin e Jacopo, grazie per avermi insegnato tanto di MATLAB, grazie mille per il vostro aiuto, la vostra pazienza e dedizione.

I a l'Elena. Algú em va dir en una ocasió que arribaries com l'hivern i així vas fer. Gràcies per entendre'm com ho fas, i per voler compartir la teva història amb la meva. Sense tu mai hagués pogut portar aquesta Tesi a bon port.

I finalment, a mons pares per l'educació i per l'afecte que m'heu donat. Gràcies per estar sempre al meu costat, per estimar-me com ho heu fet, pel vostre esforç i per ajudar-me a fer realitat els meus somnis.

I com un bon amic em va dir un bon dia, mai diguis d'aquesta aigua no en beuré, doncs és un error i cal provar-la; sempre acaba agradant més del que inicialment ens pensem.

Gràcies a tots!

ÍNDEX

RESUM

Hom considera que els oceans són sistemes altament complexos, la dinàmica dels quals depèn de la interrelació de processos físics, químics i biològics. En aquests context, l'estudi dels intercanvis verticals de matèria i energia des de la superfície cap a l'oceà profund esdevé essencial per a entendre i predir l'impacte dels canvis en el sistema climàtic de la Terra sobre la dinàmica oceànica i els l'ecosistema marins.

Aquesta Tesi està centrada en el reconeixement del paper dels forçaments externs (règim de vents, pèrdues de calor, aportacions fluvials, acció de l'onatge, i altres), inclosa llur variabilitat intra- i interanual, damunt la hidrografia i les transferències de matèria i energia des de la plataforma cap al talús i els ambients més profunds a través dels canyons submarins. En aquest context, ens hem centrat en l'estudi un canyó mediterrani altament actiu, el canyó del cap de Creus, i en un gran canyó de la mar Cantàbrica, el canyó d'Avilés. El fet que tots dos canyons es trobin gairebé a la mateixa latitud, sotmesos recurrentment als mateixos règims atmosfèrics regionals, ens ha permès investigar les teleconnexions atmosfèriques entre ambdues àrees i llurs conseqüències oceanogràfiques i ecosistèmiques.

L'anàlisi combinada de la variabilitat temporal dels fluxos de partícules i dels paràmetres meteorològics, hidrològics i oceanogràfics en tots dos canyons ha permès determinar les seves respostes als forçaments físics. Els principals processos que governen la transferència de matèria particulada més enllà de la plataforma continental a través del canyó del cap de Creus són: (1) les cascades d'aigua densa de plataforma (DSWC, de l'anglès *Dense Shelf Water Cascading*), desencadenades pel refredament sobtat, l'evaporació i la salinització de les aigües superficials de la plataforma continental durant episodis perllongats de vents del nord, freds i secs, i (2) els episodis d'enfonsament d'aigua (*downwelling*) que tenen lloc durant les llevantades, les quals provoquen l'augment de l'alçada de les ones, el reforçament de la circulació ciclònica i l'apilament massiu d'aigua carregada de sediment contra la costa que acaba provocant el seu enfonsament cap al talús. En canvi, la transferència de matèria particulada més enllà de la plataforma a través del canyó d'Avilés, ocorre majoritàriament durant els episodis de resuspensió de matèria particulada que tenen lloc amb motiu del desenvolupament de temporals i degut a l'augment de l'alçada de les ones i els corrents prop del fons. La direcció del vent i dels corrents que impulsa

determinen si la matèria resuspesa arriba al canyó majoritàriament per la superfície o pel fons.

El present estudi confirma que els canyons submarins del cap de Creus i d'Avilés són conductes preferents per al transport de matèria particulada esmentat adés i palesa el seu potencial com a vectors preferents per a la transferència del senyal dels forçaments externs des de la plataforma cap als respectius marges i conques profundes. La prevalença de la fracció terrígena en els fluxos de matèria particulada enregistrats en ambdós canyons, revela que la resuspensió de dipòsits terrígens a la plataforma continental representa la principal font de partícules vers els canyons del cap de Creus i d'Avilés. La segona font de matèria particulada a tots dos canyons és la producció marina primària, els fluxos procedents de la qual (matèria orgànica, carbonat de calci i òpal) mostren una gran variabilitat que depèn sobretot del règim hidrodinàmic i de les explosions (*blooms*) estacionals de fitoplàncton.

D'altra banda, a més dels episodis de *downwelling* associats a tempestes marines i de les DSWC (al canyó del cap de Creus), i dels episodis de resuspensió i transport de matèria particulada que tenen lloc associats al desenvolupament de temporals (al canyó d'Avilés), els processos oceanogràfics més energètics a les dues àrees estudiades són la convecció profunda (al golf de Lleó) i la convecció intermèdia (a la mar Cantàbrica). Quan els forçaments d'origen atmosfèric que impliquen l'arribada de masses d'aire fred i sec són prou intensos i afecten alhora totes dues àrees, es produeix una resposta oceanogràfica simultània que palesa l'existència de teleconnexions atmosfèriques.

Creiem que aquesta Tesi presenta un alt interès per la comunitat científica i també per la gestió dels recursos marins, doncs és fruit d'un nou enfocament en l'estudi de les relacions entre l'atmosfera i la dinàmica oceànica, la biogeoquímica marina i el funcionament dels ecosistemes marins entesos en sentit ampli. I té el valor afegit de demostrar que aitals relacions poden establir-se entre àrees separades per masses continentals, com és el cas del golf de Lleó i de la mar Cantàbrica, situats a banda i banda de la península Ibèrica.

La integració de dades provinents de l'observació meteorològica i oceanogràfica, i del modelat numèric, que s'ha dut a terme en aquesta Tesi podria fer-se extensible, en el futur, a les dades de pesca de les mars del nord la península

Ibèrica. Aquest esforç permetria segurament assolir una millor comprensió dels vincles entre els processos físics i biogeoquímics i la variabilitat dels recursos vius fins al punt, en una situació ideal, de poder plantejar models de gestió paral·lels entre les dues àrees, els quals incorporessin plenament els coneixements assolits.

RESUMEN

Los océanos son sistemas altamente complejos, cuya dinámica viene determinada por la interrelación de diversos procesos físicos, químicos y biológicos. Por ello, el estudio de los intercambios verticales de materia y energía desde la superficie hacia el océano profundo resulta esencial para entender y predecir el impacto de los cambios en el sistema climático de la Tierra sobre la dinámica oceánica y los ecosistemas marinos.

Esta Tesis está centrada en el reconocimiento del papel que ejercen los forzamientos externos (régimen de viento, pérdidas de calor, aportes fluviales, acción del oleaje, y otros), incluida su variabilidad intra- e interanual, sobre la hidrografía y las transferencias de materia y energía desde la plataforma hacia el talud y los ambientes más profundos a través de los cañones submarinos. En este contexto, nos hemos centrado en el estudio de un cañón mediterráneo altamente activo, el cañón del cabo de Creus, y en un gran cañón del mar Cantábrico, el cañón de Avilés. El hecho de que los dos cañones se encuentren prácticamente a la misma latitud, sometidos recurrentemente a los mismos regímenes atmosféricos regionales, nos ha permitido investigar las teleconexiones atmosféricas entre ambas áreas y sus consecuencias oceanográficas y ecosistémicas.

A partir del análisis combinado de la variabilidad temporal de los flujos de partículas y de los parámetros meteorológicos, hidrológicos y oceanográficos en los dos cañones hemos podido determinar sus respuestas a los forzamientos físicos. Los principales procesos que gobiernan la transferencia de materia particulada más allá de la plataforma continental a través del cañón del cabo de Creus son: (1) las cascadas de agua densa de plataforma (DSWC, del inglés *Dense Shelf Water Cascading*), desencadenadas por el enfriamiento súbito, la evaporación y la salinización de las aguas superficiales de la plataforma continental durante episodios prolongados de vientos del norte, fríos y secos, y (2) los episodios de hundimiento de agua (*downwelling*) que tienen lugar durante las tormentas de levante, las cuales provocan el aumento de la altura del oleaje, el reforzamiento de la circulación ciclónica y el apilamiento masivo de agua cargada de sedimentos contra la costa que acaba provocando su hundimiento hacia el talud. Por el contrario, la transferencia de materia particulada más allá de la plataforma a través del cañón de Avilés, ocurre principalmente durante los episodios de

resuspensión de materia particulada que tienen lugar con motivo del desarrollo de temporales y debido al aumento de la altura del oleaje y de las corrientes cerca del fondo. La dirección del viento y de las corrientes que impulsa tras estos periodos, determinan si la materia resuspendida llega al cañón mayoritariamente por la superficie o por el fondo.

El presente estudio confirma además que los cañones submarinos del cabo de Creus y de Avilés son conductos preferentes para el transporte de materia particulada, demostrando su potencial como vectores preferentes para la transferencia de la señal de los forzamientos externos desde la plataforma hacia los respectivos márgenes y cuencas profundas. La prevalencia de la fracción terrígena en los flujos de materia particulada registrados en ambos cañones revela que la resuspension de depósitos terrígenos en la plataforma continental representa la principal fuente de partículas de los cañones del cabo de Creus y de Avilés. La segunda fuente de materia particulada en ambos cañones es la producción marina primaria, los flujos procedentes de la cual (materia orgánica, carbonato de calcio y ópalo) muestran una gran variabilidad que depende sobretodo del régimen hidrodinámico y de las explosiones (*blooms*) estacionales de fitoplancton.

Por otro lado, además de los episodios de *downwelling* asociados a tormentas marinas y las DSWC (en el cañón del cabo de Creus), y de los episodios de resuspensión y transporte de materia particulada que tienen lugar con motivo del desarrollo de temporales (en el cañón de Avilés), los procesos oceanográficos más energéticos en las dos áreas estudiadas son la convección profunda (en el golfo de León) y la convección intermedia (en el mar Cantábrico). Cuando los forzamientos de origen atmosférico que implican la llegada de masas de aire frío y seco son suficientemente intensos y afectan de manera sincrónica a las dos áreas, se produce una respuesta oceanográfica simultánea que evidencia la existencia de teleconexiones atmosféricas.

Creemos que esta Tesis presenta un elevado interés para la comunidad científica y también para la gestión de los recursos marinos, pues es fruto de un nuevo enfoque en el estudio de las relaciones entre la atmósfera y la dinámica oceánica, la biogeoquímica marina y el funcionamiento de los ecosistemas marinos entendidos en sentido amplio. I tiene el valor añadido de demostrar que tales relaciones pueden establecerse entre áreas separadas por masas continentales,

como es el caso del golfo de León y del mar Cantábrico, situados a un lado y otro de la península Ibérica.

Así, la integración de datos provenientes de la observación meteorológica y oceanográfica, y del modelado numérico llevado a cabo en esta Tesis podría hacerse extensible, en el futuro, a los datos de pesca de los mares del norte de la península Ibérica. Este esfuerzo facilitaría una mejor comprensión de los vínculos entre los procesos físicos y biogeoquímicos, y de la variabilidad de los recursos vivos. En una situación ideal, se podrían incluso plantear modelos de gestión paralelos entre las dos áreas, incorporando para ello todos los conocimientos logrados.

ABSTRACT

The oceans are considered to be highly complex systems, whose dynamics depend on the interrelation of physical, chemical and biological processes. In this context, the study of the vertical exchanges of matter and energy from the surface to the deep ocean is essential for understanding and predicting the impact of changes in the Earth's climate system on ocean dynamics and marine ecosystems.

This Thesis aims at understanding the role of external forcings (wind regime, heat losses, riverine inputs, wave action, and others), including their intra- and interanual variability, on the hydrography and the transfer of matter and energy from the continental shelf to the slope and the deeper environments through submarine canyons. In this context, we have focused on a highly active Mediterranean canyon, the Cap de Creus Canyon, and in a large canyon of the Cantabrian Sea, the Aviles Canyon. The fact that the two canyons are practically at the same latitude, thus recurrently subjected to the same regional atmospheric regimes, has allowed us to investigate the atmospheric teleconnections between both areas and their oceanographic and ecosystemic consequences.

The integrated analysis of the temporal variability of particle fluxes together with meteorological, hydrological and oceanographic parameters in both submarine canyons, has allowed to determine their response to physical forcings. The principal processes that govern the transfer of particulate matter beyond the continental shelf through the Cap de Creus Canyon are: (1) Dense Shelf Water Cascading (DSWC), triggered by cooling, evaporation or salinization in the surface layer of shallow areas of the continental shelf during events of cold, dry, and persistent northerly winds, and (2) downwelling events related to the occurrence of eastern storms that cause increased wave height, the strengthening of the cyclonic circulation and the massive stacking of sediment-laden water against the coast, which ultimately ends up sinking downslope. In contrast, the off-shelf transfer of particulate matter through the Aviles canyon principally occurs during resuspension events caused by large waves and near bottom currents developing at the occasion of severe northern storms. Wind direction and subsequent wind-driven currents determine if resuspended matter reach the canyon mainly by surface or bottom transport.

This study confirms that the Cap de Creus and the Aviles submarine canyons act as preferential pathways for transporting particulate matter, and proves their potential as preferential vectors for transferring the signal of the external forcings from the shelf to their respective margins and deep basins. The dominance of the terrigenous fraction in the particulate matter fluxes recorded in both canyons reveals that the resuspension of terrigenous deposits on the continental shelf represent the main source of particles. Marine primary production is the second main source of particulate matter in both canyons. Its fluxes of major components (organic matter, opal and calcium carbonate) show high variability, which depend mainly on the hydrodynamic regime and the seasonal development of phytoplanktonic blooms.

On the other hand, besides the downwellig episodes linked to the occurrence of marine storms and the DSWC (in the Cap de Creus submarine canyon), and the resuspension and transport episodes occurring during the occasion of severe storms (in the Avilés submarine canyon), the most energetic oceanographic processes in both studied areas are deep convection (in the Gulf of Lion) and intermediate depth convection (in the Cantabrian Sea). When atmospheric forcing involving the arrival of cold and dry air masses is severe enough and spreads over the two areas, a simultaneous oceanographic response occurs, which in turn evidences the existence of atmospheric teleconnections.

We believe that this Thesis is of great interest for the scientific community and also for the management of marine resources, as it is the result of a new approach in the study of the relations between the atmosphere and the ocean dynamics, marine biogeochemistry and the marine ecosystems functioning understood in a broad sense. It also has the added value of demonstrating that such relations can be established between areas separated by continental masses, as is the case of the Gulf of Lion and the Cantabrian Sea, located at each side of the Iberian Peninsula.

The integration of meteorological and oceanographic observations, and numerical modeling that has been carried out in this Thesis could be extended, in the future, to the fisheries data of the seas to the north of the Iberian Peninsula. This effort would lead to an improved understanding of the links between physical and biogeochemical processes, and resource variability to the point that, ideally, management plans could fully integrate such knowledge.

PRESENTACIÓ I OBJECTIUS

La vida al nostre planeta se sustenta bàsicament gràcies als intercanvis de matèria i energia entre la litosfera, l'oceà i l'atmosfera. Les interaccions entre l'oceà i l'atmosfera, que es troben en permanent contacte, regulen normalment el temps meteorològic i el clima.

L'oceà superficial es considerat com una capa d'amortiment entre l'atmosfera i l'oceà profund. Els forçaments atmosfèrics, com ara els canvis en el règim de vents, en la temperatura de l'aire o en el balanç d'evaporació, en modifiquen les seves propietats i estructura. En determinades circumstàncies, les aigües modificades per la interacció amb l'atmosfera poden ésser transportades, per diferents mecanismes, fins nivells intermedis i profunds, mesclant-se amb les aigües que allí hi hagi. A la Mediterrània nord-occidental, per exemple, el refredament brusc, l'evaporació i la salinització de les aigües de damunt la plataforma continental per causa de vents persistents del nord, freds i secs, dóna lloc a la formació d'aigües denses de plataforma i al seu posterior enfonsament en forma de cascada talús avall fins la conca situada a més de 2.500 metres de fondària. És el procés denominat "cascades d'aigües denses de plataforma" (DSWC, de l'anglès *Dense Shelf Water Cascading*) (*cf.* aptat 1.4.3). El mateix forçament atmosfèric desencadena, a mar oberta, el refredament de l'aigua superficial i, subseqüentment, la mescla vertical i l'homogeneïtzació de la columna d'aigua. Es tracta del procés anomenat "convecció oceànica". Aquests dos processos contribueixen activament a la modificació i la formació de les masses d'aigua pregones de la mar Mediterrània, i a l'intercanvi de nutrients entre la superfície i la conca profunda. Situada just a l'altra banda dels pirineus, i pràcticament a la mateixa latitud, la mar Cantàbrica presenta també episodis de convecció oceànica hivernal en resposta a l'acció persistents de vents freds i secs del nord, el quals modifiquen les propietats i l'estructura de les masses d'aigua superficials així com el flux de nutrients des de profunditats intermèdies fins la capa fòtica.

Aquesta Tesi és una contribució a l'estudi de les interaccions oceà-atmosfera que va més enllà de l'escala eminentment localista de la majoria de treballs previs en aquest camp realitzats a les mars que envolten la península Ibèrica. Volem

esbrinar si hi ha cap patró de teleconnexió[1] entre el golf de Lleó, a la Mediterrània nord-occidental, i la mar Cantàbrica, a l'Atlàntic nord-oriental, i en cas de ser-hi escatir les conseqüències oceanogràfiques i ecosistèmiques que se'n deriven.

En el cas de la teleconnexió mediterrània-cantàbrica, els mateixos forçaments atmosfèrics (*e.g.* arribada de masses d'aire continentals fredes i seques) afectarien de forma sincrònica ambdues àrees, influint directament sobre l'intercanvi d'energia i massa entre els ambients soms i els profunds. Tanmateix, la màxima expressió dels forçaments externs associats a les teleconnexions atmosfèriques adopta formes diferents a una i altra àrea d'acord amb les estructures hidrogràfiques de cadascuna: (I) DSWC i convecció oceànica profunda a la Mediterrània i (II) mescla vertical reforçada i aprofundiment de la capa de mescla hivernal a la mar Cantàbrica (Fig. P.1).

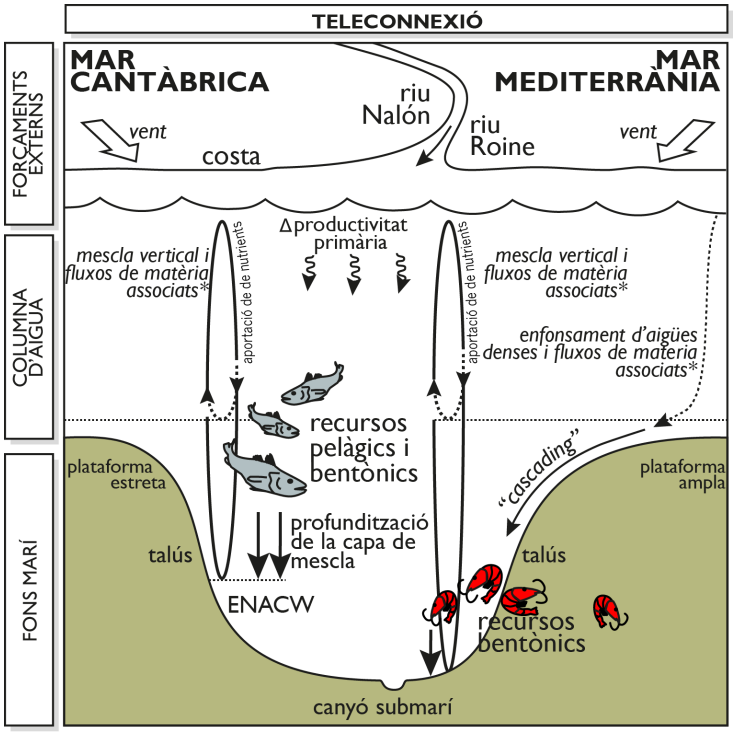

* Materia orgànica, sílice biogènica, carbonats i litogènics

[1] El terme "teleconnexió" es refereix a un patró recurrent i persistent d'anomalies de circulació atmosfèrica i, per tant, de pressió, que afecta una àrea geogràfica extensa. Els patrons de teleconnexió o, més senzillament, les "teleconnexions", també són coneguts com a modes preferents de variabilitat de baixa freqüència (és a dir, d'escala temporal llarga). Tot i que generalment les teleconnexions solen durar entre setmanes i mesos, de vegades poden ser més persistents, representant així una part significativa de la variabilitat estacional i interanual de la circulació atmosfèrica. Moltes teleconnexions tenen abast regional i fins i tot planetari i, en conseqüència, poden afectar continents i conques oceàniques senceres, i també mars regionals amb masses continentals interposades, com és el cas de la Mediterrània nord-occidental i la mar Cantàbrica. Les teleconnexions influeixen directament en la temperatura atmosfèrica, la precipitació, els vents, la formació i el recorregut de les tempestes, i tantes altres variables i processos, i indirectament sobre els ecosistemes terrestres i marins. Per tot això, hom les considera sovint responsables de situacions meteorològiques anòmales que afecten simultàniament àrees geogràfiques molt extenses (http://www.cpc.ncep.noaa.gov/data/teledoc/teleintro.shtml).

D'acord amb el que acabem d'exposar, l'objectiu general d'aquesta Tesi és saber si hi ha teleconnexions atmosfèriques efectives entre les mars Mediterrània nord-occidental i Cantàbrica que afectin la dinàmica oceànica d'ambdues àrees.

Els objectius específics d'aquesta Tesi són:

1) Esbrinar el paper dels forçaments externs (règim de vents, pèrdues de calor, aportacions fluvials, onatge i altres) i l'impacte de la seva variabilitat interanual en el transport de matèria particulada al llarg del canyó submarí del cap de Creus (golf de Lleó, mar Mediterrània nord-occidental).

2) Establir l'origen de la matèria particulada i identificar els forçaments externs que condicionen la variabilitat espaciotemporal dels fluxos de partícules al canyó submarí d'Avilés (mar Cantàbrica).

3) Un cop establerta l'existència de teleconnexions atmosfèriques efectives entre la Mediterrània nord-occidental i la mar Cantàbrica, escatir si les respostes que es produeixen són sincròniques, caracteritzar aitals respostes i llurs possibles semblances i diferències des dels punts de vista oceanogràfic i biogeoquímic (fluxos de matèria), i valorar les conseqüències ecosistèmiques que en cada cas se'n derivin.

Aquesta Tesi s'emmarca de manera preeminent dins el projecte d'investigació DOS MARES, l'objectiu general del qual era entendre el funcionament de sistemes de canyons submarins i talussos profunds adjacents en dos marges continentals amb característiques contrastades, concretament els marges de la Mediterrània nord-occidental i de la mar Cantàbrica, mitjançant un estudi coordinat, multidisciplinari, integrat i sincrònic dels ambients pelàgics i bentònics de les dues àrees.

Figura P.1 (veure figura a la pàgina anterior). Esquema conceptual on es relacionen els forçaments externs, els principals processos oceanogràfics (com les DSWCs i la convecció de mar oberta) i els trets morfològics generals de les dues àrees estudiades en aquesta Tesi. Es mostren els efectes de la teleconnexió atmosfèrica entre les mars Mediterrània nord-occidental i Cantàbrica, així com els seus impactes sobre els ecosistemes pelàgic i bentònic profunds de mar oberta. ENACW: Aigua Central de l'Atlàntic Nord-Est (de l'anglès *East North Atlantic Central Water*). Esquema adaptat de la memòria científica-tècnica del projecte DOS MARES (ref. CTM2010-21810-C03-01).

ESTRUCTURA DE LA TESI

Aquesta Tesi es presenta com a compendi de publicacions i inclou tres articles, dos dels quals ja publicats en revistes indexades al *Science Citation Index* de l'*ISI Web of Knowledge*. El tercer ha estat sotmès recentment a una revista igualment indexada.

La memòria de Tesi s'estructura en quatre capítols. Al primer hom introdueix al lector en l'àmbit científic en que s'emmarca aquest treball, i també es presenta l'àrea d'estudi, la metodologia i les eines emprades.

El segon capítol es dedicat als resultats principals assolits en aquesta Tesi, recollits en les tres publicacions esmentades més amunt. Es mostra una còpia completa i fidedigna dels articles publicats o sotmesos, en que el doctorand és el primer autor. Per a cada article hom aporta la referència bibliogràfica completa o, en el cas del tercer article, les dades de la revista on ha estat tramès el manuscrit. Al primer article, publicat a la revista *Biogeosciences* i titulat *External forcings, oceanographic processes and particle flux dynamics in Cap de Creus submarine canyon, NW Mediterranean Sea*, s'hi integren dades meteorològiques i oceanogràfiques i resultats d'anàlisis biogeoquímiques que han permès caracteritzar la matèria particulada transportada al canyó submarí del cap de Creus durant dos hiverns consecutius marcadament diferents en termes meteorològics.

El segon article, publicat a la revista Progress in Oceanography i titulat *Particle fluxes and their drivers in the Avilés submarine canyon and adjacent slope, central Cantabrian margin, Bay of Biscay,* es basa en els resultats del monitoratge continu del canyó submarí d'Avilés i el talús adjacent al llarg d'un any. La combinació de dades metoceàniques, d'imatgeria satel·litària i biogeoquímiques ha permès aclarir quines són les fonts de matèria particulada en aquest marge així com els forçaments atmosfèrics que desencadenen el seu transport.

El tercer article, tramés a la revista Progress in Oceanography i titulat *Ocean system response to atmospheric forcing and synchronous extreme events over mid-latitudes: the Cantabrian Sea and the Gulf of Lion case study*, demostra l'existència d'un acoblament atmosfèric efectiu entre la Mediterrània nord-occidental i la mar

Cantàbrica, i estableix les conseqüències oceanogràfiques que en resulten. Aquest article representa la culminació de l'objectiu principal de la Tesi.

Els capítols tercer i quart són dedicats a la discussió dels resultats i a les conclusions obtingudes a partir dels articles presentats al segon capítol. La discussió i les conclusions representen un esforç per establir les relacions i sintetitzar els tres articles que formen el cos de la Tesi, tot i donant resposta als objectius inicialment plantejats. Finalment, el capítol cinquè inclou tota la bibliografia citada en aquesta Tesi.

Capítol 1
Introducció

1.1 L'ATMOSFERA I L'OCEÀ

L'atmosfera és una capa formada per gasos, inclòs el vapor d'aigua, i partícules en suspensió que embolcalla el nostre planeta. És en contacte permanent amb la superfície de l'oceà, amb el qual intercanvia de forma constant energia en forma de calor, aigua, gasos i sals. Els gasos que s'incorporen a l'atmosfera provinents de l'oceà tenen efectes altament rellevants sobre el clima. Per exemple, el vapor d'aigua absorbeix la radiació infraroja reflectida a la superfície de la Terra, impedint així que s'escapi cap a l'espai, fet determinant per a que la temperatura mitjana superficial del nostre planeta sigui apta per la vida (*e.g.* Kiehl i Trenberth, 1997; Held i Soden, 2000). D'altra banda, els gasos que penetren a l'oceà des de l'atmosfera poden influir, entre d'altres, en les característiques fisicoquímiques de l'aigua de mar, l'estabilitat química dels sediments i la distribució de la vida marina (*e.g.* Kump, 1989; Doney *et al.,* 2007; Cooley i Doney, 2009; Gattuso i Hansson, 2011; Zeebe, 2012).

A la Terra, la dinàmica atmosfèrica és governada per les diferències de pressió que es produeixen a conseqüència de les variacions en la insolació segons la latitud. És ben conegut que la radiació solar incident per unitat de superfície disminueix progressivament de l'equador cap als pols. Això fa que les masses d'aire tendeixin a desplaçar-se des de les latituds equatorials, més càlides i amb pressions baixes, cap a les latituds altes, més fredes i amb pressions elevades. No hi ha, però, una sola cel·la atmosfèrica de circulació convectiva des de l'equador fins als pols a cada hemisferi. Degut a l'efecte de Coriolis, durant el transport des de l'equador cap a les regions polars al nord i al sud, les masses d'aire són desviades gradualment cap a l'est a l'hemisferi nord, i cap a l'oest a l'hemisferi sud. Al llarg d'aquest transport, l'aire sec per efecte de la descompressió, el refredament i la pèrdua d'humitat per precipitació mentre ascendeix a les regions equatorials va irradiant calor cap a l'espai exterior i esdevé progressivament més dens. Quan ha recorregut, aproximadament, un terç del seu camí cap a les latituds altes, l'aire s'ha tornat prou dens com per descendir de nou cap a la superfície terrestre. Gran part d'aquest aire retorna cap a l'equador, desviant-se novament per l'efecte de Coriolis, cap a la dreta (*i.e.* d'est a oest) a l'hemisferi nord i cap a l'esquerra a l'hemisferi sud. En el seu retorn cap a l'equador l'aire va absorbint calor i humitat, cosa que fa minvar la seva densitat fins que, de nou, acabar ascendint a les regions equatorials completant així el circuit convectiu conegut com a cel·la de

Hadley (Fig. 1.1). La interacció a la zona equatorial de les cel·les de Hadley dels hemisferis nord i sud dona lloc als vents alisis.

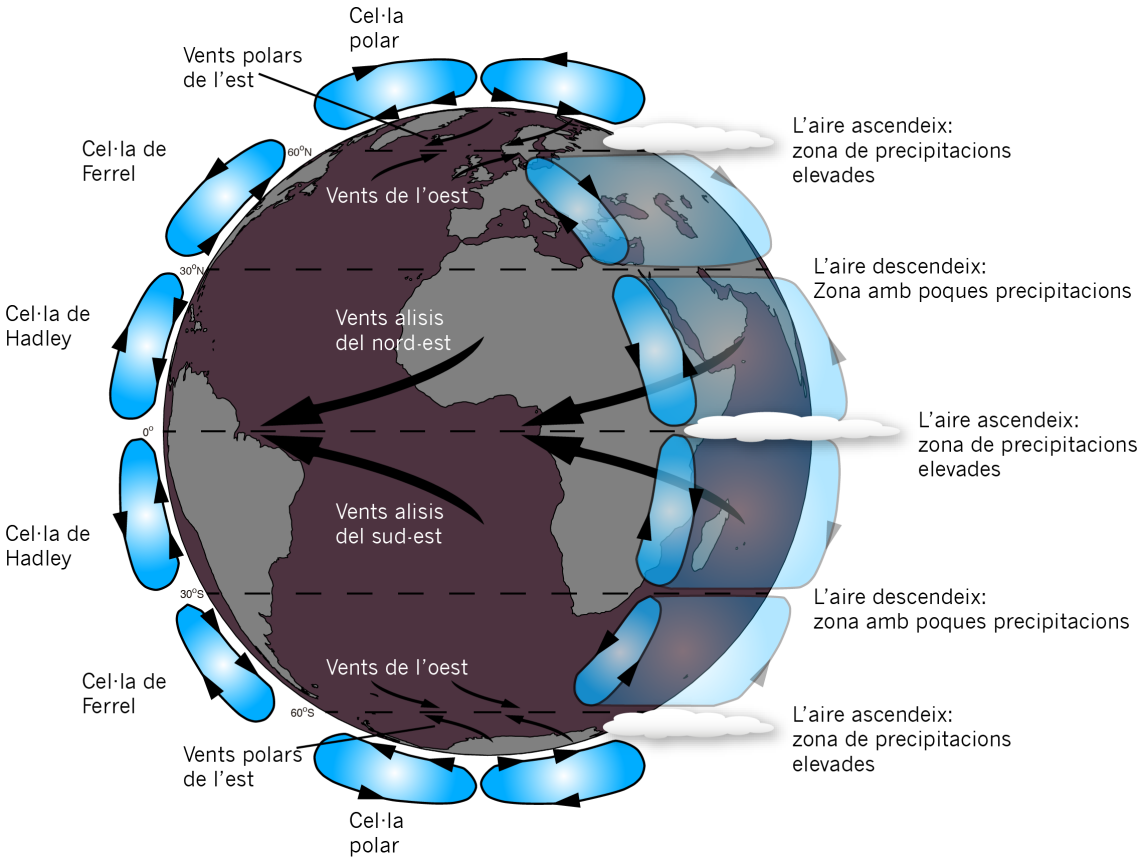

Figura 1.1. Model de circulació atmosfèrica, amb tres cel·les latitudinals, què respon a la distribució de la quantitat d'energia solar que arriba a la Terra segons la latitud. L'efecte de Coriolis desvia els vents cap a la dreta a l'hemisferi nord i cap a l'esquerra a l'hemisferi sud (modificada de Garrison, 1993).

A les latituds mitges d'ambdós hemisferis, entre 30 i 50-60º de latitud, s'hi desenvolupa una altra gran cel·la de circulació atmosfèrica, anomenada cel·la de Ferrel (Fig. 1.1). Aquestes cel·les es formen per la interacció, a les capes altes de l'atmosfera, de part de l'aire descendent de la cel·la de Hadley amb aire que prové dels pols. També en aquest cas, l'efecte de Coriolis desvia el vent en superfície cap a la dreta (*i.e.* cap al l'esquerra a l'hemisferi sud), donant lloc així a vents de l'oest (Fig. 1.1). Aquests vents transporten l'aire en superfície cap a les latituds altes de cada hemisferi. Pel camí, l'aire va absorbint humitat i calor fins que torna a ascendir a 50-60º de latitud, tot i tancant el circuit d'aquesta cel·la.

Les regions polars tenen les seves pròpies cel·les de circulació atmosfèrica convectiva, anomenades justament "cel·les polars". L'aire refredat als pols es desplaça per superfície en direcció a l'equador mentre és desviat cap a l'oest. Aquest situació és a l'origen dels vents polars de l'est (Fig. 1.1). Quan arriba a 50-60º de latitud, laques massa d'aire polar ja ha absorbit prou humitat i calor per ascendir i retornar seguidament per les capes altes de l'atmosfera cap als pols, tancant la cel·la polar.

Els forçaments atmosfèrics associats a les grans cel·les convectives de la circulació atmosfèrica global exerceixen un efecte determinant sobre els corrents superficials i la circulació oceànica en general (Fig. 1.2).

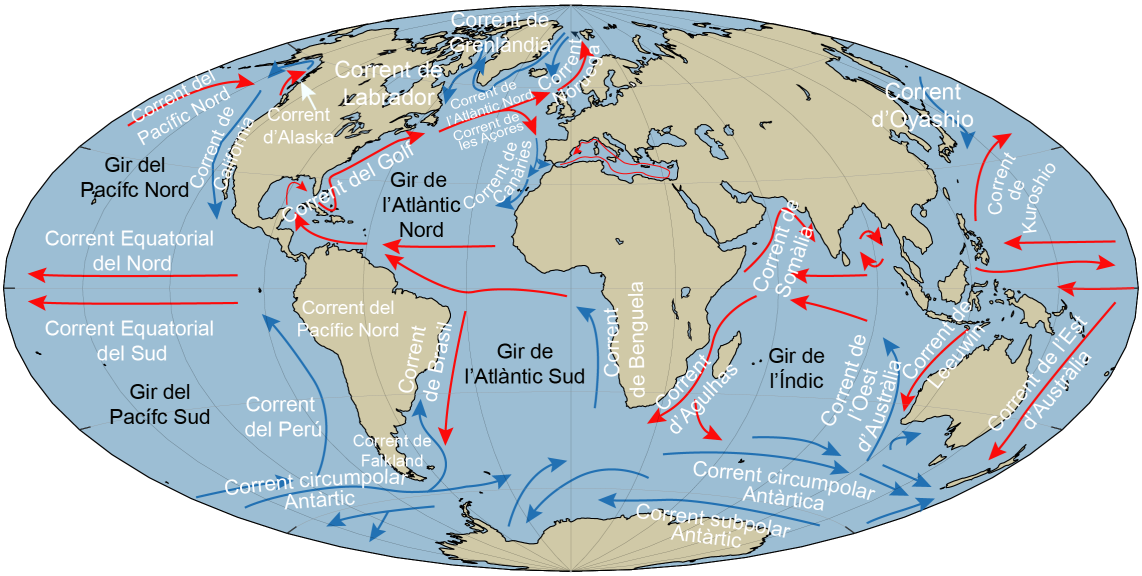

Figura 1.2. Circulació oceànica superficial global. Els corrents càlids són indicats en vermell, mentre que els freds són en blau. També s'indiquen els principals girs oceànics (modificada de Garrison, 1993).

Cal dir que en els corrents superficials hi participa tan sols el 10% del volum total d'aigua dels oceans, essent sobretot l'estrès friccional del vent i en menor mesura l'expansió tèrmica de l'aigua les principal forces impulsores de la circulació superficial (*e.g.* Gill, 1982; Vallis, 2006; Olbers *et al.,* 2012). L'escalfament solar fa que l'aigua s'expandeixi lleugerament. Conseqüentment, el nivell del mar prop de l'equador, on la insolació superficial és màxima, és aproximadament 8 cm més alt que a les regions temperades. Contràriament, prop dels pols, on la insolació superficial és mínima, el refredament intens fa que l'aigua es contragui en una proporció similar a l'expansió

que experimenta a l'equador (*e.g.* Mellor, 1996; Stewart, 2008). Aquesta petita diferència global del nivell del mar genera un pendent molt lleuger que fa que les aigües equatorials càlides flueixin cap als pols en resposta a les forces gravitacionals. Mentre es desplacen, aquestes aigües són desviades per l'efecte de Coriolis, circumstància que contribueix al desenvolupament d'un flux lent i circular d'aigua a cadascuna de les grans conques oceàniques que hi ha a banda i banda de l'equador. Aquest flux lent és anticiclònic a l'hemisferi nord i ciclònic a l'hemisferi sud i, en el cas de l'oceà Atlàntic, dona lloc al gir de l'Atlàntic nord a l'hemisferi nord i al gir de l'Atlàntic sud a l'hemisferi sud (Fig. 1.2).

Nogensmenys, els corrents superficials a l'oceà són impulsats en primera instància pels vents. La major part de l'energia dels vents de superfície és concentra, però, en els vents alisis d'ambdós hemisferis (Fig. 1.1). D'aquest fet en resulta el desenvolupament d'un patró circular de circulació, paral·lel en gran mesura als marges de les grans conques oceàniques, el qual és anticiclònic a l'hemisferi nord i ciclònic a l'hemisferi sud (Fig. 1.2). Alguns d'aquests corrents són com una mena de rius enmig de la mar, molt ràpids i amb límits ben definits. El corrent del Golf, que neix al golf de Mèxic, n'és un bon exemple (*e.g.* Stommel, 1958). Les seves prolongacions, el corrent de l'Atlàntic nord i el corrent de Noruega, transporten aigua càlida des del golf fins el mateix oceà Àrtic (Fig. 1.2) (*e.g.* Orvik i Niiler, 2002). Altres corrents superficials, però, són més lents i difusos, com el corrent de Canàries (Fig. 1.2) (*e.g.* Navarro-Pérez i Barton, 2001; Pelegrí et al., 2005).

A més d'impulsar els corrents superficials, els vents també provoquen moviments verticals a les masses d'aigua. L'espiral d'Ekman ajuda a entendre aquests moviments. Així, a l'hemisferi nord, per causa de l'efecte de Coriolis degut a la rotació de la Terra, la capa superficial es desvia 90º cap a la dreta respecte la direcció del vent. En absència de Coriolis, com succeeix a l'equador, la capa d'aigua superficial es desplaçaria en la mateixa direcció del vent. Quan el vent bufa prop de la costa i paral·lelament a la mateixa, l'estrès friccional generat a la superfície de l'oceà que fa que, depenent del sentit del vent respecte a la línia de costa, les aigües superficials es desplacin cap a la costa o en sentit oposat, mar endins. Per tant, a l'hemisferi nord, quan la costa queda a l'esquerra respecte al sentit del vent, el transport de la capa superficial és cap a mar oberta. El desplaçament de les aigües costaneres cap a mar endins afavoreix l'ascens de les aigües subsuperficials a escassa distància de la costa.

Aquest procés es coneix amb el nom d'aflorament o *upwelling*. En canvi, quan la costa queda a la dreta respecte al sentit del vent, el transport de la capa superficial és cap a la costa, on es produeix un apilament d'aigües superficials que pot provocar el seu enfonsament o *downwelling*.

Els afloraments i enfonsaments d'aigües afecten la temperatura i la productivitat biològica superficials de l'oceà. Les aigües que arriben a la superfície durant els episodis d'aflorament provenen de nivells inferiors i són, per tant, més fredes que les que s'han desplaçat mar endins. A més, les aigües d'aflorament transporten nutrients cap a la zona fòtica, la qual cosa provoca explosions, o *blooms*, fitoplanctòniques. Atès que el fitoplàncton representa la base de la cadena tròfica marina, moltes de les principals pesqueries mundials se sustenten gràcies a aquest procés (*e.g.* la pesqueria de l'anxoveta *Engraulis ringens* a l'aflorament costaner del Perú, o les pesqueries de l'anomenat banc saharià i d'Àfrica del sud-oest) (*e.g.* Balguerías *et al.,* 2000; Tarazona i Arntz, 2001; Arístegui *et al.,* 2009; Ohman *et al.,* 2013). En canvi, les aigües superficials descendents durant els episodis d'enfonsament són relativament calentes i pobres en nutrients. Conseqüentment, els enfonsaments fan minvar la productivitat biològica i transporten calor, oxigen i altres substàncies dissoltes cap a les grans fondalades marines.

Els episodis d'aflorament i enfonsament costaners també influencien el clima a escala regional i fins i tot planetària. Per exemple, al Pacífic la superfície de l'oceà s'escalfa i refreda cíclicament en resposta a la intensitat dels alisis. Al seu torn, aquests canvis en la temperatura superficial de l'oceà desencadenen canvis en els patrons de pluja globals. Els episodis del *Niño* i la *Niña* són expressions extremes d'aquesta variabilitat que comporten greus sequeres en unes regions i pluges intenses en altres.

A les mars que envolten la península Ibèrica també s'hi produeixen afloraments i enfonsaments costaners. Per exemple, davant la costa gallega, quan el vent bufa intensament i persistent des del nord tot i arrossegant la capa d'aigua superficial cap al sud. El transport d'Ekman generat desplaça cap a mar obert (és a dir, cap a la dreta) les aigües superficials costaneres, circumstància de propicia l'ascens d'aigües fredes profundes (Fraga, 1981; Prego *et al.,* 2001; Gomez-Gesteira *et al.,* 2006) (Fig. 1.3).

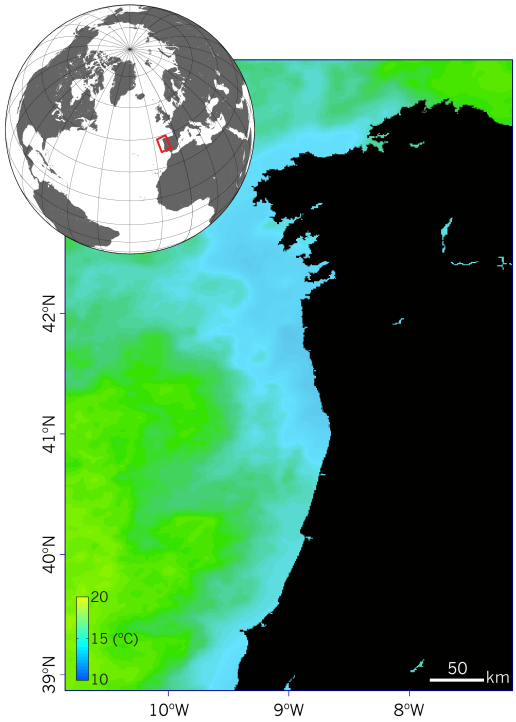

Figura 1.3. Imatge de temperatura de les aigües marines superficials al llarg de la costa occidental del nord de la península Ibèrica corresponent al dia 17 de juliol de 2010. La imatge il·lustra un episodi d'aflorament costaner (colors blaus). La imatge està feta a partir de dades satel·litàries de temperatura superficial de l'aigua de la *National Oceanic and Atmospheric Administration* (NOAA) (http://www.esrl.noaa.gov).

1.2 FONTS I FLUXOS DE PARTÍCULES A L'OCEÀ

Entenem com a matèria particulada la població de partícules en suspensió que quedaria retinguda en un filtre de 45 μm de pas de malla. Les aigües marines contenen matèria particulada molt diversa, des de frústuls de diatomees, coccòlits, closques de foraminífers i restes esquelètiques i no esquelètiques de molts altres organismes marins fins petits fragments de roques introduïts pels rius, les glaceres i el vent, i també per altres vies. Atenent a les seves fonts principals és habitual classificar la matèria particulada marina com a biogènica o terrígena.

Fluxos de matèria particulada biogènica. La vida als oceans se sustenta gràcies a la producció primària a càrrec dels organismes autòtrofs (fitoplàncton). Aquests organismes, rics en molècules orgàniques assimilables pels organismes que ocupen els

següents nivells de la cadena tròfica, són consumits per organismes heteròtrofs (zooplàncton), degradats per microorganismes, o dissolts a la columna d'aigua un cop morts. Segons Honjo *et al*. (1982), els principals components de les partícules biogèniques que sedimenten a través de la columna d'aigua a l'oceà són esquelets de carbonat de calci (de coccòlits, pteròpodes i foraminífers), closques de silici biogènic (òpal produït per diatomees, silicoflagel·lats i radiolaris) i matèria orgànica particulada (MOP). Aquesta darrera és formada per una mescla d'organismes vius, restes d'organismes morts i pellets fecals. De tots els components principals de les partícules biogèniques que sedimenten a través de la columna d'aigua, el component menys resistent a la degradació és la MOP. Bona part de la MOP cau, a la curta o a la llarga, en el si de la columna d'aigua cap al fons. Durant la caiguda es va degradant, de manera que a 1000 m de profunditat la degradació de la MOP ja és gairebé completa (Martin *et al*., 1987). L'òpal, els carbonats i les partícules terrígenes presents a la columna d'aigua poden associar-se amb la MOP i alterar els fluxos provinents de la capa fòtica. Aquests components minerals actuen de llast, fet que fa augmentar la quantitat de MOP que s'exporta cap als fons marins (Armstrong *et al*., 2002; Klaas i Archer, 2002; François *et al*., 2002). Els minerals llast protegeixen la MOP de la degradació per l'increment de la velocitat de sedimentació i mitjançant processos d'adsorció. Les partícules minerals adsorbeixen components orgànics en els seus porus, protegint-los així físicament de ser hidrolitzats per l'acció dels microorganismes. Així doncs, hom pot subdividir el flux total de MOP que s'exporta cap al fons marí en una fracció "protegida" pels minerals llast i una de "no protegida", que es remineralitzada (és a dir, es degrada) al llarg del seu recorregut per la columna d'aigua (Fig. 1.4).

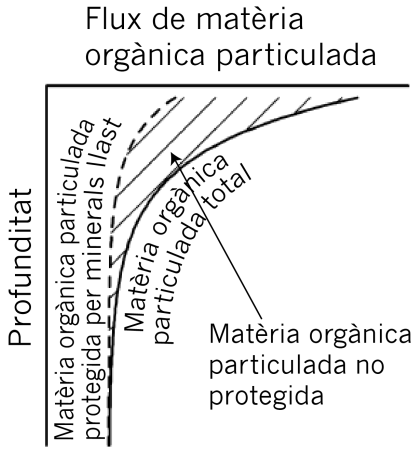

Figura 1.4. Esquema del flux de matèria orgànica particulada total (línia sòlida) i del flux matèria orgànica particulada protegida per minerals llast (línia discontínua) dins la columna d'aigua. L'àrea ratllada correspon a la matèria orgànica particulada no protegida (modificat d'Armstrong *et al*., 2002).

Els fluxos de partícules a l'oceà, definits com la mesura de la taxa de transferència de matèria des d'un reservori qualsevol a un altre (Honjo, 1996), determinen la distribució dels elements clau per la vida i asseguren el sosteniment de l'ecosistema marí profund. Cal tenir present també que, d'acord amb Margalef (1978), és molt més probable que un àtom arribi al fons formant part d'una partícula que d'una dissolució. Aquesta circumstància posa de manifest que entendre els processos que controlen la formació, la degradació i el transport de matèria particulada a l'oceà és del màxim interès per conèixer els cicles biogeoquímics marins i el seu paper en la biologia dels oceans.

Fluxos de matèria particulada terrígena. Els sediments terrígens són formats majoritàriament per fragments de roques descompostes per processos de meteorització química i física. Com a resultat de la meteorització química, els components solubles de les roques es dissolen i són transportats cap a l'oceà pels anomenats "agents de transport". La meteorització física, per la seva part, fragmenta les roques en partícules de mida menor mitjançant processos mecànics com la gelifracció o la dilatació i la contracció provocades per oscil·lacions tèrmiques pronunciades. Les partícules resultants d'aital fragmentació són transportades cap al mar pels rius, les glaceres i el vent, que són els principals agents de transport.

El quars és un dels minerals més comuns en els sediments terrígens marins. Es tracta d'un mineral molt resistent a l'alteració química que arriba a l'oceà sense patir pràcticament cap canvi en la seva composició. En canvi, altres grups minerals, com els feldspats, són força difícils de trobar en els sediments marins terrígens doncs, a més d'alterar-se en contacte amb l'aigua de mar, en el transcurs del seu transport cap a l'oceà solen meteoritzar-se amb facilitat tot i donant lloc a minerals del grup de les argiles. Els minerals argilosos, formats per silicats d'alumini hidratats, són dominants en els sediments marins de gra fi. Donada la seva capacitat d'absorbir ions en la seva estructura cristal·lina, les argiles són una font de nutrients i d'elements químics essencials (com el ferro, el coure i altres) per a la vida als oceans (*e.g.* Bader *et al.,* 1960; Ding i Henrichs, 2002; Kennedy *et al.,* 2002; Satterberg *et al.,* 2003).

La fracció terrígena dels sediments marins inclou també altres components, com productes derivats del vulcanisme emergit i submergit, partícules cosmogènics i compostos hidrogènics, formats per precipitació de minerals dissolts a l'aigua de mar. Aquesta precipitació sovint es produeix en microambients especials, com ara dins les

closques de foraminífers, on és relativament comú la precipitació de pirita i glauconita. Per altra banda, els compostos hidrogènics poden formar o dominar determinats dipòsits, cas de les acumulacions de fosforites en zones amb alta productivitat primària o dels camps de nòduls polimetàl·lics. Hom parla aleshores de dipòsits o sediments "químics". Les acumulacions de sals per evaporació i precipitació són un altre exemple de dipòsits químics (*e.g.* Seibold i Berger, 1993).

1.3 FLUXOS DE MATÈRIA PARTICULADA ALS MARGES CONTINENTALS

Cada any els rius transporten prop de tretze mil milions de tones de sediment cap a l'oceà (Syvitski et al., 2005). Gran part de la càrrega sòlida transportada pels rius queda retinguda, però, de forma natural, en deltes i estuaris, i només una petita fracció s'escapa dels marges continentals i assoleix les grans fondalades marines. I això sense comptar que en l'Era de l'Home, l'Antropocè, en que vivim, una part significativa queda també retinguda en la munió d'embassaments construïts en moltíssimes conques fluvials (Syvitski et al., 2005).

Els marges continentals són la part submergida dels continents i, per tant, són una franja d'amplada variable que se situa entre les terres emergides i les grans fondalades marines. (Divins, 2003). Com és prou conegut, hom diferencia tres tipus de marges: (i) actius, situats al llarg de límits de placa en que es produeix subducció d'escorça oceànica sota escorça continental; (ii) passius, situats en posició d'intraplaca i originats pels processos de *rifting* o distensió intracontinental que donen lloc a la formació de conques oceàniques; i (iii) de cisalla, menys comuns, situats al llarg de grans falles transformants (Kearey et al., 2009). En el context d'aquesta Tesi els que ens interessen són els marges passius, que inclouen les províncies fisiogràfiques de plataforma, talús i glacis continentals i contenen les acumulacions de sediment més grans del planeta (Fig. 1.5).

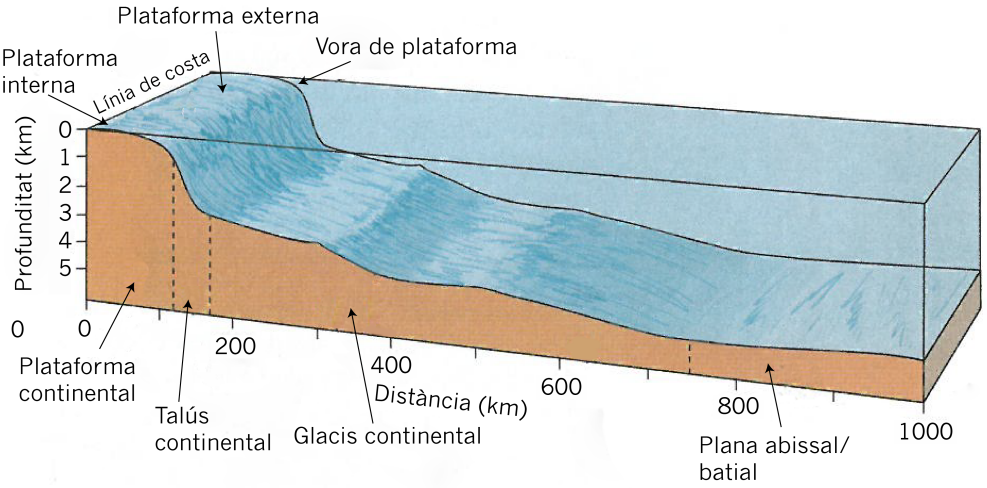

Figura 1.5. Províncies fisiogràfiques d'un marge continental passiu. L'esquema inclou també la plana abissal o plana batial, aquesta última pels casos en que, com a la Mediterrània occidental, no s'assoleixen fondàries de plana abissal. L'escala vertical està exagerada 20 vegades respecte l'horitzontal (modificada de Gross i Gross, 1996).

Els talussos continentals són sovint excavats per canyons submarins, els quals poden estendre's fins la plataforma i el glacis continental. Generalment, el seu traçat és perpendicular a les isòbates. Els canyons són discontinuïtats morfològiques situades a cotes més baixes que els relleus circumdants, la qual cosa facilita l'atrapada i la canalització de matèria particulada (Monaco *et al*., 1990; Heussner *et al*., 1999). Els canyons molt endentats a la plataforma continental tenen un alt potencial per a capturar sediments litorals (Canals et al., 2013). Les partícules sedimentàries són subseqüentment transportades canyó avall cap al marge i la conca pregona. En contrast, als talussos o segments del talús sense presència de canyons submarins el transport de matèria particulada és més difús (compareu a i b a la Fig. 1.6).

A més de ser conductes preferents pels moviments de les masses d'aigua canyó amunt i avall i pel transport de sediments cap al marge distal i la conca pregona (Gardner, 1989; Puig i Palanques, 1998, Hung *et al*., 2003; Canals *et al*., 2006), alguns canyons també es comporten com a depocentres sedimentaris i de material particulat en concret (Hickey *et al*., 1986; Palanques *et al*., 2005). Les condicions hidrodinàmiques imperants als canyons submarins faciliten la resuspensió i la

formació de capes nefeloides[2] que generalment s'escampen mar endins sustentades per les picnoclines (Gardner, 1989). Certs processos, com els corrents de terbolesa, afavoreixen la resuspensió i carreguen de matèria particulada les aigües, les quals esdevenen lleugerament més denses que les aigües circumdants. Aquest diferencial de densitat i el pendent, per petit que sigui, activen les forces gravitacionals i són suficients per provocar el desplaçament canyó o talús avall, i en règim turbulent, de les aigües involucrades. Les seves grans eficiència i capacitat de transport fan que els corrents de terbolesa transportin grans quantitats de sediment, inclosa matèria particulada, des de la plataforma continental fins els ambients profunds, temàtica que ha estat estudiada bastament des dels treballs pioners de Morgenstern (1967) i Middleton i Hampton (1973) fins els més recents de Shanmugam (2002) i Talling et al. (2012).

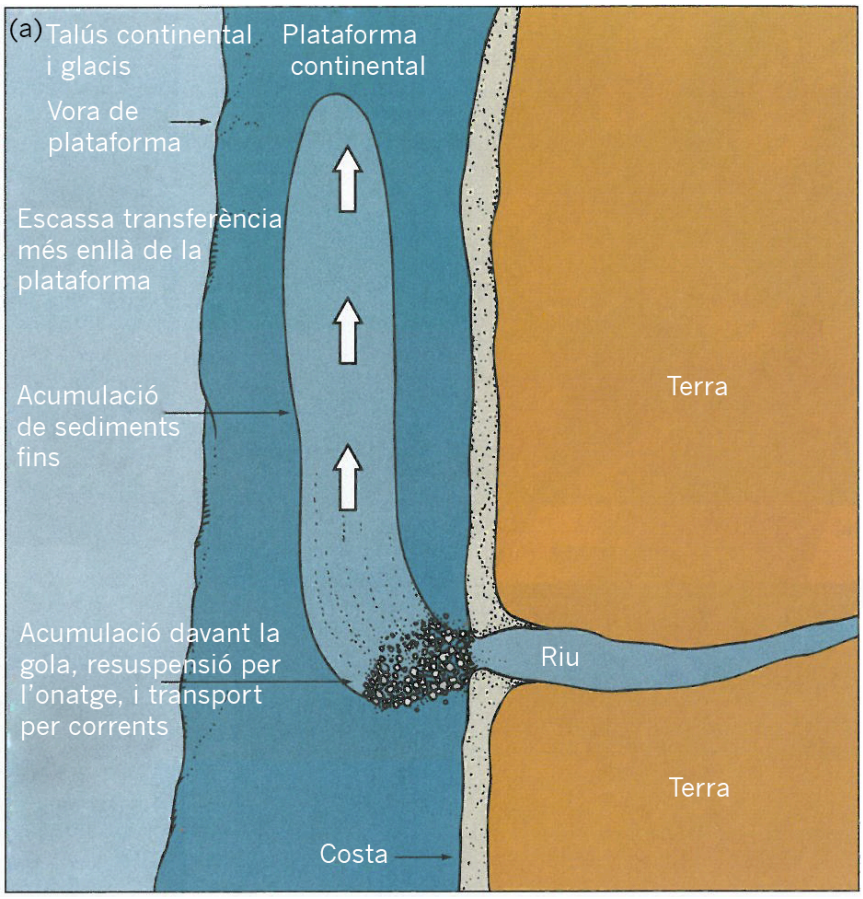

[2] Capes amb concentracions de partícules en suspensió pel damunt de la concentració ambient, formades per MOP fina i sediments argilosos.

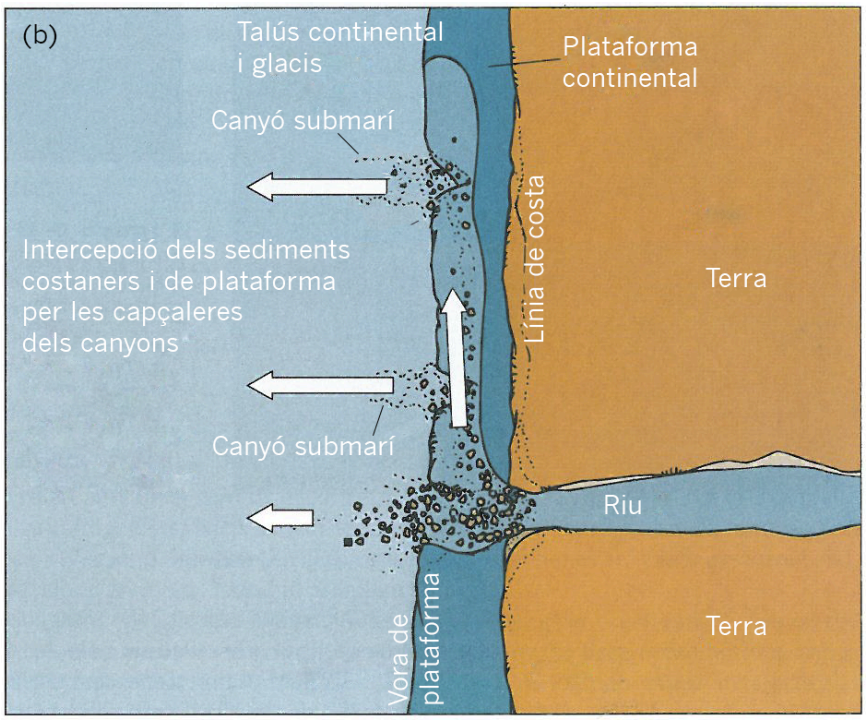

Figura 1.6. Transport de sediment de providència fluvial al llarg i a través (a) d'una plataforma continental ampla i no entallada per canyons submarins (veure figura a la pàgina anterior), i (b) d'una plataforma estreta i entallada per canyons submarins. A (a) els sediments s'acumulen en estuaris i deltes i a la plataforma, i molt pocs s'escapen més enllà de la vora de plataforma. A (b) els sediments poden arribar més fàcilment al marge i a la conca pregons mercès a la seva canalització pels canyons submarins entallats a la plataforma (modificada de Gross i Gross, 1996).

1.4 ÀREES D'ESTUDI: EL GOLF DE LLEÓ I LA MAR CANTÀBRICA

1.4.1 SITUACIÓ GEOGRÀFICA

Les mars Mediterrània nord-occidental i Cantàbrica són dues mars marginals de la mar Mediterrània i de l'oceà Atlàntic, respectivament (Fig. 1.7a). Els seus marges continentals són solcats per nombrosos canyons submarins que connecten les plataformes continentals respectives amb el talús, el glacis i la conca pregona. El golf de Lleó, que s'estén des del cap de la Croisette al nord-est fins al cap de Creus al sud-oest, forma el límit septentrional de la Mediterrània nord-occidental. Presenta una plataforma continental força ampla (~70 km), en forma de mitja lluna (Fig. 1.7a).

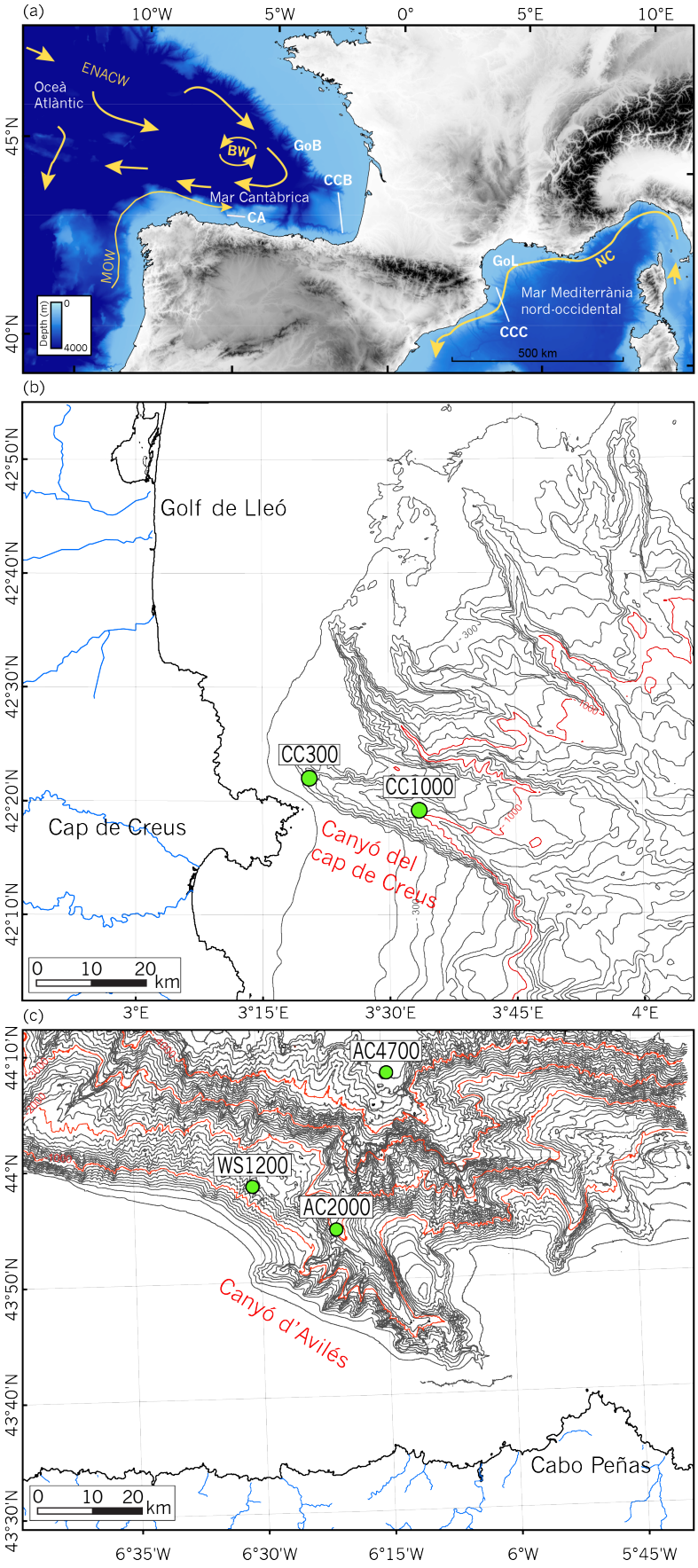
(a)
10°W
5°W
0°
5°E
10°E
45°N
40°N
Oceà Atlàntic
ENACW
BW
GoB
CCB
Mar Cantàbrica
CA
MOW
Depth (m)
0
4000
GoL
NC
Mar Mediterrània nord-occidental
CCC
500 km
(b)
42°50'N
42°40'N
42°30'N
42°20'N
42°10'N
Golf de Lleó
CC300
CC1000
Cap de Creus
Canyó del cap de Creus
0 10 20 km
3°E
3°15'E
3°30'E
3°45'E
4°E
(c)
44°10'N
44°N
43°50'N
43°40'N
43°30'N
AC4700
WS1200
AC2000
Canyó d'Avilés
Cabo Peñas
0 10 20 km
6°35'W
6°30'W
6°15'W
6°W
5°45'W

Els canyons del seu talús continental formen una xarxa dendrítica i la majoria penetren la plataforma continental externa, tot i que alguns, com el de Lacaze-Duthiers i el del cap de Creus, s'estenen fins la plataforma mitja i interna. Els principals canyons del golf de Lleó desemboquen al glacis i a la plana batial algero-balear (Canals, 1985; Berné et al., 2004).

Per la seva banda, la mar Cantàbrica limita pel sud el golf de Biscaia, que té una fisiografia marcadament asimètrica. Mentre al marge cantàbric, que s'estén cap a l'oest fins el cap Ortegal, la plataforma continental es molt estreta (~12 km d'ample en alguns indrets) i obre pas a un talús continental força abrupte, al marge gascó, que acaba pel nord al cap de Pointe de Pern, la plataforma continental té una amplada molt notable, de més de 140 km en algun indret (Fig. 1.7a). El gran canyó submarí de Capbretó, de 270 km de llargada, i que discorre d'est a oest, separa els marges cantàbric i gascó del golf de Biscaia (Bourillet et al., 2007).

Els marges del golf de Lleó i de la mar Cantàbrica són situats en el mateix rang latitudinal, entre 42º i 44º N, i entre 43º i 45º N, respectivament.

Figura 1.7 (vegeu il·lustració a la pàgina anterior). (a) Mapa topo-batimètric general de la regió que compren les mars Mediterrània nord-occidental i Cantàbrica. Hom indica també la situació dels golfs de Lleó (GoL), i de Biscaia (GoB), així com dels canyons del cap de Creus (CCC), d'Avilés (CA) i del Capbretó (CCB). Dades batimètriques de la *General Bathymetric Chart of the Oceans* (GEBCO). En groc s'indiquen els patrons de circulació regionals i les masses d'aigua. A la mar Cantàbrica, BW (de l'anglès *Bottom Water*): Aigua de Fons; ENACW (de l'anglès *East North Atlantic Central Water*): Aigua Central de l' Atlàntic Nord-Est; MOW (de l'anglès *Mediterranean Outflow Water*): Aigua de Sortida Mediterrània. A la mar Mediterrània nord-occidental participen en el NC, de més superficial a més profunda, la MAW (de l'anglès *Modified Atlantic Water*): Aigua Atlàntica Modificada; la WIW (de l'anglès *Western Intermediate Water*): Aigua Intermèdia d'Hivern de la conca occidental; i la LIW (de l'anglès *Levantine Intermediate Water*): Aigua Intermèdia Llevantina. Per sota s'hi troba la WMDW (de l'anglès *Western Mediterranean Deep Water*) i les seves variants en funció de la intensitat i influència dels processos de cascades d'aigües denses de plataforma i de convecció de mar oberta del golf de Lleó i sectors propers (vegeu text principal). (b) Mapa batimètric del marge continental del canyó del cap de Creus on s'indica la posició dels ancoratges CC300 i CC1000 (cf. caps. 2.1 i 2.3). Isòbates cada 100 m. En vermell s'indica la isòbata de 1000 m. (c) Mapa batimètric del marge continental del canyó d'Avilés on s'indica la posició dels ancoratges WS1200, AC2000 i AC4700 (*cf*. caps. 2.2 i 2.3). Isòbates cada 100 m. En vermell s'indiquen les isòbates de 1000, 2000, 3000 i 4000 m.

1.4.2 FORÇAMENT METEOROLÒGIC

Els patrons de variabilitat atmosfèrica de llarg abast a les latituds mitjanes de l'Atlàntic nord i del sud-oest d'Europa estan determinats principalment per la interacció entre dues cel·les atmosfèriques: la cel·la d'altes pressions subtropicals i la cel·la de baixes pressions subpolars (Figs. 1.1 i 1.8). Aquestes cel·les, conegudes com a alta de les Açores i baixa d'Islàndia, presenten una forta estacionalitat.

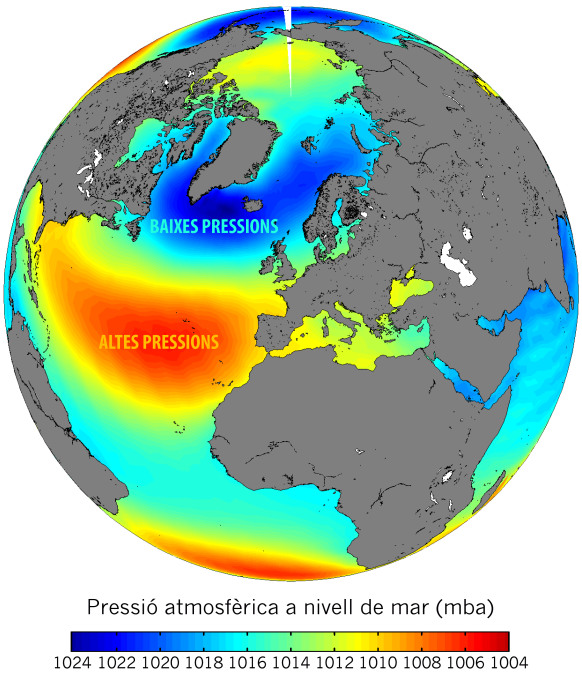

Figura 1.8. Mitjana històrica de la pressió atmosfèrica a nivell de mar pel període 1968-1996. Computat a partir de dades del *NOAA National Climatic Data Center, Derived NCEP Reanalysis Products Surface Level* (http://www.esrl.noaa.gov).

A l'hivern, l'anticicló es debilita i la depressió s'intensifica i es desplaça cap al sud-est, cap als voltants de les illes Canàries. Contràriament, a l'estiu, l'anticicló de les Açores es reforça i la depressió d'Islàndia es debilita. Fruit d'aquesta variabilitat, en resulta l'existència de dues estacions ben diferenciades, amb diferents patrons de vents i pluges a l'Atlàntic nord i al sud-oest europeu. Aquestes dues cel·les experimenten, a més, una forta variabilitat interanual correlacionada estadísticament amb uns índex numèrics coneguts com Oscil·lació de l'Atlàntic Nord (NAO, de l'anglès *North Atlantic Oscilation*, identificada per Wallace i Gutzier, 1981) i l Patró de l'Atlàntic Oriental (EAP,

de l'anglès *East Atlantic Pattern*, definit també per Wallace i Gutzier, 1981). L'índex NAO representa la diferència de pressió entre l'anticicló de les Açores i la baixa d'Islàndia. De forma general, una NAO positiva implica que la diferència de pressió entre l'anticicló de las Açores i la baixa d'Islàndia és més gran que la seva mitjana climatològica, és a dir que hi ha un gradient latitudinal de pressió fort. Aquesta situació afavoreix el domini de l'anticicló al sud-oest d'Europa i a l'Atlàntic nord, i facilita que les borrasques i els fronts actius es desviïn cap el nord-oest del continent europeu, on provoquen més precipitacions i vents més intensos i persistents del que és habitual (Fig. 1.9a).

Contràriament, una NAO negativa està relacionada amb un afebliment tant de l'anticicló de les Açores com de la baixa d'Islàndia i, per tant, comporta un gradient latitudinal de pressió modest. És una situació que afavoreix el redireccionament dels fronts actius cap el sud-oest d'Europa, on s'instal·len règims de vents dèbils que propicien hiverns més humits i temperats a la regió mediterrània i al sud-oest d'Europa, i hiverns freds al nord del continent (Fig. 1.9a). Thompson i Wallace (1998) s'adonaren que la NAO era la manifestació local d'un patró més global, conegut com Oscil·lació de l'Àrtic (AO, de l'anglès *Arctic Oscillation*). L'AO explica gran part de la variància de les anomalies hivernals de la temperatura de l'aire en superfície a l'hemisferi nord. En la seva fase negativa, el sistema de baixes pressions polars (també conegut com el vòrtex polar) sobre l'Àrtic és més dèbil, cosa que provoca un corrent en raig, o *jet stream*, més feble. Sota aquestes condicions, l'aire fred de l'Àrtic pot assolir les latituds meridionals d'Europa (Fig. 1.9b).

L'EAP és el segon mode de variabilitat atmosfèrica regional. Conceptualment parlant és força similar a la NAO. Consisteix també en un dipol nord-sud de centres d'anomalies de pressió altes i baixes tot i que desplaçats cap al sud-est respecte a la posició dels centres considerats per la NAO. Això fa que sovint l'EAP sigui interpretat simplement com un patró NAO desplaçat cap al sud. En la seva fase positiva, l'EAP presenta un potent centre d'acció ciclònic sobre l'Atlàntic nord que dirigeix els fronts actius cap el sud-est i sud d'Europa (Fig. 1.9c). Sota aquesta configuració, el sud d'Europa experimenta hiverns amb temperatures i precipitacions per sobre de la mitjana. Contràriament, la fase negativa de l'EAP està relacionada amb l'establiment un potent centre d'acció anticiclònic a l'oest d'Irlanda que afavoreix el desenvolupament de vents del nord persistents, freds i secs sobre el sud-oest d'Europa (Fig. 1.9c).

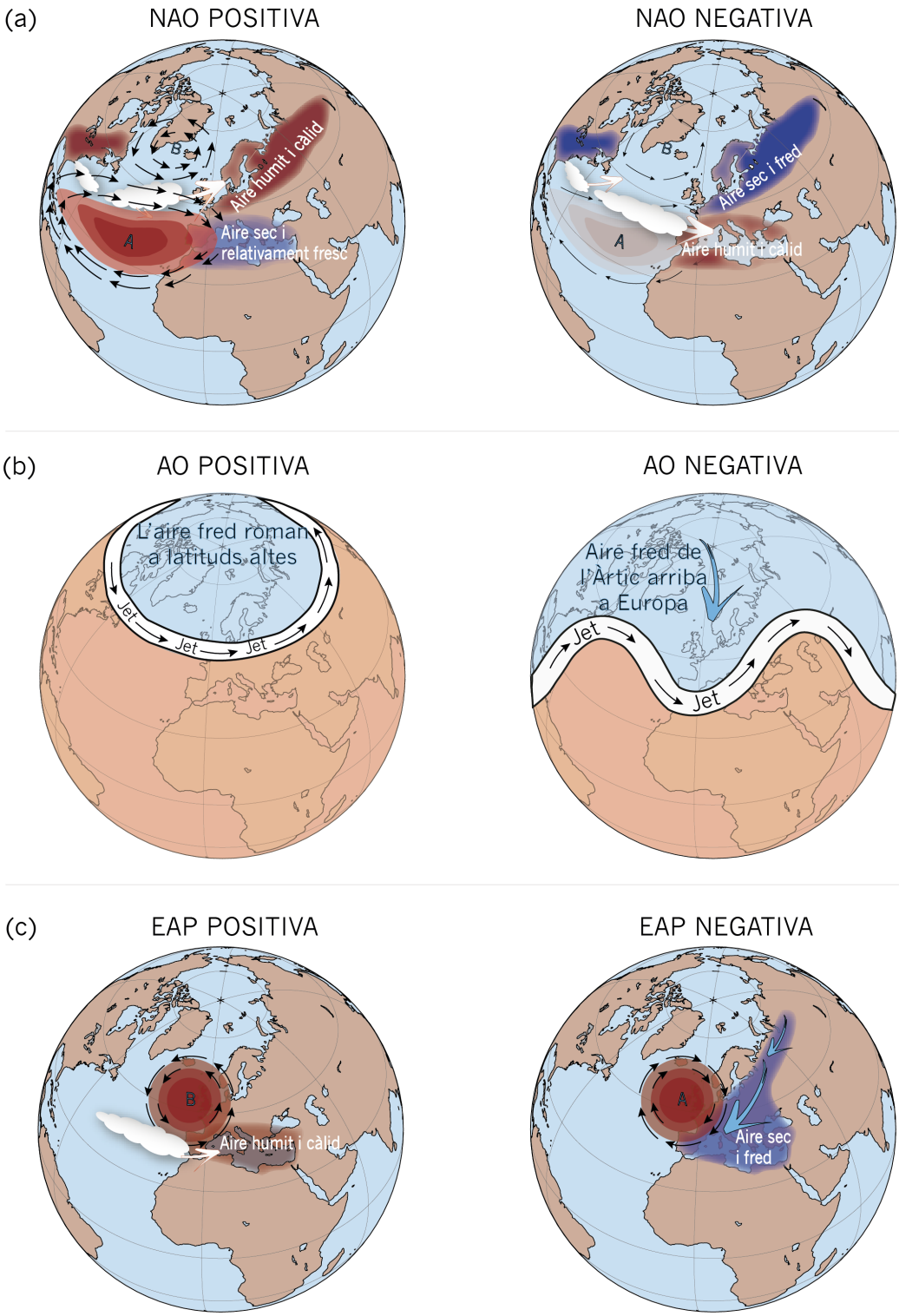

Figura 1.9. Representació de les anomalies atmosfèriques associades a les fases positives i negatives de (a) l'Oscil·lació de l'Atlàntic Nord (NAO), (b) l'oscil·lació de l'Àrtic (AO), i (c) el Patró de l'Atlàntic Oriental (EAP) (modificada de https://www.wunderground.com).

1.4.3 CIRCULACIÓ GENERAL I HIDROGRAFIA

La resposta de l'oceà envers les variacions en l'estructura atmosfèrica determinada per l'anticicló de les Açores i la borrasca d'Islàndia és l'establiment de patrons de circulació oceànica superficial també permanents.

Mar Mediterrània nord-occidental. La circulació superficial a la Mediterrània nord-occidental està estretament vinculada al Corrent del Nord (NC, de l'anglès *Northern Current*), també coneguda a la literatura com a Corrent liguroprovençal i Corrent nord-català. A l'àrea d'estudi, el NC es manifesta com un corrent baroclínic[3] i geostròfic[4] que discorre en sentit ciclònic paral·lel al talús continental superior (Fig. 1.7a), amb un flux màxim de 1,5-2 Sv a ~700 m de fondària, segons Albérola *et al*. (1995), Conan i Millot (1995) i Sammari *et al*. (1995). Addicionalment, el NC està afectat per factors topogràfics i batimètrics. A l'hivern, la canalització dels vents de l'oest o *westerlies* (Fig. 1.1), per la vall del Roine i per la depressió que hi ha entre els Pirineus i el massís Central es tradueix en vents intensos, persistents, freds i secs del nord (tramuntana) i del nord-oest (mestral). L'estudi dels principals patrons de circulació a la mar Mediterrània mostrà que la interacció entre la circulació atmosfèrica i l'orografia regional té un impacte directe sobre la circulació termohalina a escala de conca (Millot i Taupier-Letage, 2005). D'acord amb Millot (1999), Quan la tramuntana i el mestral són poc intensos, la part superior del NC penetra sobre la plataforma del golf de Lleó i tot i fluint en sentit antihorari ocupa pràcticament tota la columna aigua. Sota aquesta configuració, el NC i l'efecte de Coriolis desvien cap a la dreta, és a dir cap a la costa, la descàrrega fluvial del Roine, que és el riu amb més cabal de tota la Mediterrània occidental. Es facilita així el transport de les aigües i sediments d'aquest riu paral·lelament a la línia de costa en direcció de la península del cap de Creus, incorporades a la deriva litoral. Contràriament, la intensificació de la tramuntana i el mestral empenyen el NC cap a indrets més profunds i allunyats de la costa, situació que facilita la barreja i l' homogeneïtzació de les aigües de plataforma amb les del Roine mentre es desplacen cap a mar oberta.

La hidrografia del golf de Lleó i de la conca pregona adjacent està caracteritzada per una distribució en quatre capes o masses d'aigua (Fig. 1.10).

[3] Flux la densitat del qual varia amb la profunditat i en la horitzontal.
[4] Un Flux geostròfic és aquell en el que les forces dels gradient de pressió i de Coriolis són en equilibri.

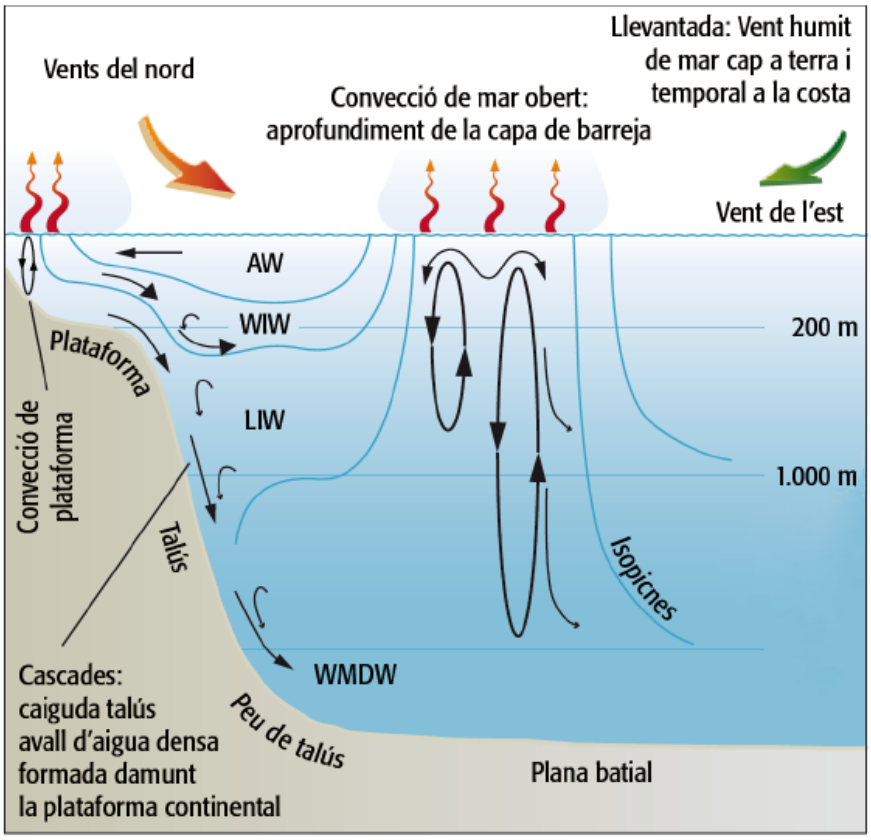

Figura 1.10. Estructura hidrogràfica del golf de Lleó i de la conca pregona adjacent. Hom indica els forçaments atmosfèrics, així com els seus efectes i els processos que desencadenen (cortesia de M. Canals, a partir de Pusceddu *et al.*, 2010).

La capa més superficial està ocupada per Aigua Atlàntica (AW, de l'anglès *Atlantic Water*) procedent de l'estret de Gibraltar, la qual es va modificant progressivament (*e.g.* incrementa la seva salinitat) a mesura que recircula per la Mediterrània (Millot, 1999). A l'hivern, sota condicions severes de vents el nord, l'AW es pot refredar sense mesclar-se amb les capes d'aigua immediatament inferiors. Aquesta situació dóna lloc a la formació d'una massa d'aigua que apareix de forma intermitent al golf de Lleó entorn els 200 m de fondària anomenada Aigua Intermèdia Occidental (WIW, de l'anglès *Western Intermediate Water*) (Salat i Font, 1987). Just davall d'aquesta massa d'aigua i ocupant les capes intermèdies entre ~200 i 500 metres, hi ha l'Aigua Intermèdia Llevantina (LIW, de l'anglès *Levantine Intermediate Water*) (Lacombe i Tchernia, 1972; Guibout, 1987), formada per convecció intermèdia (>300 m de profunditat) a la Mediterrània oriental. La LIW es propaga lentament des de la conca oriental cap a l'occidental travessant del canal de Sicília. La massa d'aigua més profunda és l'Aigua

Fonda de la Mediterrània Occidental (WMDW, de l'anglès *Western Mediterranean Deep Water*) (Lacombe *et al*., 1985). Aquest massa d'aigua està escassament estratificada i es genera a partir del refredament intens de les aigües superficials i l'activació subseqüent de DSWC i de convecció profunda de mar oberta (vegeu més avall) al golf de Lleó (López-Jurado et al., 2005; Canals et al., 2006; Schroeder et al., 2010; Durrieu de Madron et al., 2013). Les aigües denses arrosseguen en el seu descens cap al fons de la conca volums més o menys grans de la WIW i la LIW. La WMDW omple tota la conca profunda de la Mediterrània occidental (Schroeder et al., 2010).

Les aigües de la Mediterrània nord-occidental són sensibles a un seguit de processos altament energètics, amb potencial per modificar llurs propietats. A l'hivern, el reforçament i la persistència de la tramuntana i el mestral provoca refredament i evaporació intensos a les aigües superficials del golf de Lleó, tant a la plataforma com a mar oberta. Conseqüentment, les aigües de superfície esdevenen més fredes i més salines i, per tant, més denses. A la plataforma, a les etapes inicials, s'inicia un procés de convecció soma i d'escapament de les aigües denses que s'estenen cap al talús superior on assoleixen els nivells de la WIW (Dufau-Julliand *et al*., 2004). Però si l'increment de densitat de les aigües de plataforma és prou gran aleshores poden caure fins el talús inferior, el peu de talús i fins i tot la conca, tot i mesclant-se amb la LIW i la WMDW durant el seu recorregut (Fig. 1.10). Es tracta del procés conegut com a "cascades d'aigües denses de plataforma" (DSWC) esmentat més amunt (Canals et al., 2006).

Convé assenyalar que el talús continental del golf de Lleó està solcat per un elevat nombre de canyons submarins (Fig. 1.7b) que actuen com a conductes preferents per al transport de les aigües denses i carregades de sediment que es desplacen des de la plataforma cap a la conca profunda durant els episodis de DSWC (Canals *et al*., 2006; Palanques *et al*., 2006). Les DSWCs són un tipus de corrents submarins impulsats únicament pels contrastos de densitat de l'aigua, en que és el moviment de l'aigua el que incorpora partícules sedimentàries en suspensió turbulenta. En canvi, en els corrents de terbolesa és el moviment del núvol de partícules en suspensió el que incorpora les aigües circumdants. En el cas de les DSWCs hom ha mesurat *in situ*, i a 30 m sobre el fons, velocitats de més d'1 m s^{-1} (Canals et al., 2006; Durrieu de Madron et al., 2013). Les aigües denses de plataforma formades al golf de Lleó també poden escampar-se cap al sud pel damunt de la plataforma i el talús continentals, on són

capturades per altres canyons submarins com el de La Fonera o fins i tot el de Blanes, més al sud (Ulses et al., 2008; Ribó et al., 2011). Les DSWCs transporten enormes volums d'aigua, sediments, MOP i contaminants, i són capaces de modificar el relleu submarí a gran escala, amb afectacions majors sobre els ecosistemes pelàgics i bentònics profunds (Canals et al., 2006; Lastras et al., 2007; Company et al., 2008; Puig et al., 2008 i 2013; Salvadó et al., 2012a, 2012b, 2013).

A mar oberta, enfora de la plataforma continental, el refredament i l'evaporació de les aigües superficials dona lloc a episodis de convecció oceànica, la qual pot ésser profunda (MEDOC Group, 1970). De fet, es tracta d'un procés d'aprofundiment ràpid de la capa de mescla amb destrucció de la termoclina preexistent i homogeneïtzació de la columna d'aigua (Schroeder *et al*., 2010; Durrieu de Madron et al., 2013). Depenent de la intensitat del forçament atmosfèric, aquesta homogeneïtzació pot afectar tota la columna d'aigua fins al fons (Bethoux *et al*., 2002; L'Hévéder *et al*., 2012). Les aigües fondes neoformades en una fase de propagació pel fons de la conca que pot durar mesos. La convecció profunda de mar oberta a la Mediterrània nord-occidental, juntament amb les DSWC, és el principal mecanisme de renovació de la WMDW (López-Jurado et al., 2005; Canals et al., 2006; Schroeder et al., 2010; Puig et al., 2013). Quan les condicions atmosfèriques es suavitzen, el sistema torna al cap d'un temps a la "normalitat", és a dir a la situació d'estratificació prèvia, fet que comporta l'aïllament de les capes més profundes ventilades per la convecció respecte als nivells més superficials.

Mar Cantàbrica. La configuració atmosfèrica permanent definida per l'anticicló de les Açores i la borrasca d'Islàndia determina els patrons també permanents de la circulació oceànica superficial al golf de Biscaia i a la mar Cantàbrica en particular. La circulació de les masses d'aigua situades sota la capa de mescla superficial al golf de Biscaia ha estat descrita en nombrosos treballs, entre els que destaquen els de van Aken (2000a, b i 2001), molt complerts.

Les masses d'aigua semiprofundes i profundes del golf de Biscaia o bé s'han format al nord de l'oceà Atlàntic, o bé són el resultat de la barreja d'aigües d'orígens diversos (Pollard *et al*., 1996; Iorga i Lozier, 1999a). Com és natural, l'estructura de la columna d'aigua al golf de Biscaia, i dins seu a la mar Cantàbrica, ve imposada per la distribució de les masses d'aigua a l'Atlàntic nord-est (Lavín *et al*., 2006).

Just per sota de la capa de mescla la primera massa d'aigua és l'Aigua Central de l'Atlàntic Nord-Est (ENACW, de l'anglès *East North Atlantic Central Water*) (Fig. 1.11). L'ENACW es forma per mescla hivernal a l'interior del gir anticiclònic delimitat pel corrent de l'Atlàntic nord i pel corrent de les Açores, dintre el nord-est de les Açores i el marge atlàntic europeu (Fig. 1.2) (Pollard i Pu, 1985; Pollard *et al*., 1996). D'acord amb Colas (2003), Al golf de Biscaia, l'ENACW forma un flux cap a l'est centrat a 46ºN aproximadament, el qual impulsa un gir anticiclònic que afecta a tot el sector meridional del golf (Fig. 1.7a).

Sota l'ENACW hi circula l'Aigua de Sortida Mediterrània (MOW, de l'anglès *Mediterranean Outflow* Water) (Fig. 1.11), a profunditats compreses entre 500 i 1500 m (Iorga i Lozier, 1999a). Quan la MOW ix de l'estret de Gibraltar arriba al cap de Sant Vicenç des d'on es dirigeix cap al nord tot i resseguint el marge portuguès fins assolir l'anomenada conca del Tajo, on es bifurca en dues branques guiada per l'efecte de Coriolis i per la topografia del talús, una que es desvia cap a l'oest i forma un gir anticiclònic, i una altra que continua propagant-se cap al nord (Iorga i Lozier, 1999b). Aquestes dues branques es retroben més al nord i a l'alçada de la costa gallega la intensa mescla diapicna[5] les uniformitza en una única branca, més homogènia, que flueix al llarg de la costa nord de la península, tot i entrant al golf de Biscaia on ressegueix el talús cantàbric d'oest a est (Fig. 1.7a). Aquest corrent, conegut com a Corrent cap al Pol Ibèric (IPC, de l'anglès *Iberian Poleward Current*), transporta aigües càlides i salines, incloses les de la MOW, des de latituds meridionals i domina la circulació a la plataforma i el talús del golf de Biscaia, especialment a l'hivern (Frouin *et al*., 1990; Haynes i Barton, 1990).

L'Aigua de Fons (BW, de l'anglès *Bottom Water*) s'estén des de davall de la MOW fins al fons (Fig. 1.11). És formada per la mescla de diferents masses d'aigua: Aigua Profunda de l'Atlàntic Nord (NADW, de l'anglès *North Atlantic Deep Water*), Aigua Profunda Abaixada (LDW, de l'anglès *Lowered Deep Water*) i Aigua de Fons Antàrtica (ABW, de l'anglès *Antarctic Bottom Water*) (Botas *et al*., 1989; Pingree i Le Cann, 1992; van Aken, 2000a). Certs estudis mostren que la BW presenta un patró de circulació ciclònic a la plana abissal del golf de Biscaia (Fig. 1.7a), a prop del peu del marge continental (Dickson *et al*., 1985; Paillet i Mercier, 1997).

[5] Mescla a través de nivells amb diferents densitats, de *dia*, "a través de", i *pyknós*, "espès, dens".

Les aigües superficials i intermèdies de la mar Cantàbrica també són sensibles a processos energètics amb potencial suficient com per modificar-ne les seves propietats (Fig. 1.11).

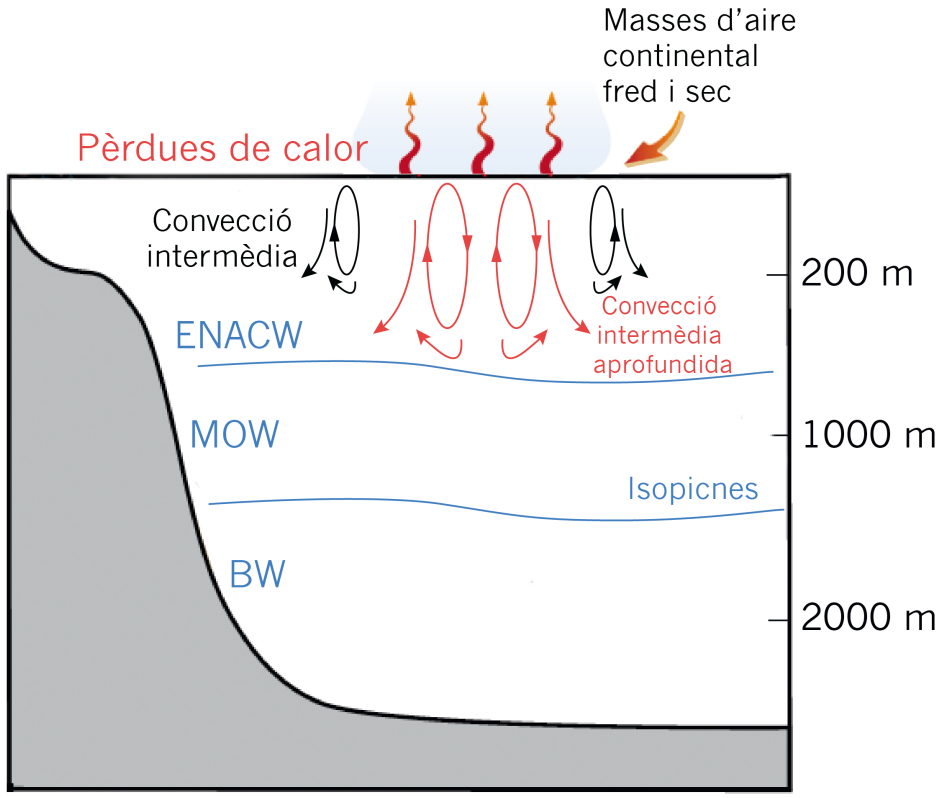

Figura 1.11. Estructura de la columna d'aigua al golf de Biscaia acompanyada d'una representació esquemàtica dels processos de convecció intermèdia i convecció intermèdia aprofundida (en vermell), amb les masses d'aigua involucrades. La convecció intermèdia aprofundida comporta un aprofundiment anòmal de la capa de mescla, que assoleix el nucli de l'Aigua Central de l'Atlàntic Nord-Est (ENACW, de l'anglès *East North Atlantic Central Water*).

Generalment, a l'àrea cantàbrica i, per extensió, al golf de Biscaia, la capa de mescla hivernal amb prou feines excedeix els 250 m de profunditat (González-Pola *et al.*, 2007). Però en hiverns extremadament freds i secs (*e.g.* l'hivern del 2005) l'estructura hidrogràfica sol experimentar una transformació major, de manera que la capa de mescla pot assolir els 400 m de fondària o gairebé (Somavilla *et al.*, 2009, 2011). Aquest aprofundiment anòmal de la capa de mescla provoca la ventilació[6] d'aigües que habitualment estan totalment aïllades i desconnectades de l'atmosfera, i a canvis

[6] Procés pel qual es transporta aigua (i gasos dissolts, com l'oxigen) des de la superfície de la capa de mescla cap a nivells més profunds.

hidrogràfics que poden ser detectats fins i tot dos anys més tard de l'ocurrència d'hiverns particularment severs (Somavilla *et al*., 2011).

1.5 METODOLOGIA

1.5.1 DISSENY DE L'EXPERIMENT

L'estudi dels fluxos de partícules a les mars Mediterrània nord-occidental i Cantàbrica, inclosa la seva variabilitat espaciotemporal, s'ha dut a terme mitjançant l'ús d'ancoratges instrumentats equipats amb trampes de sediment seqüencials, correntòmetres i turbidímetres (Fig.1.12a, b).

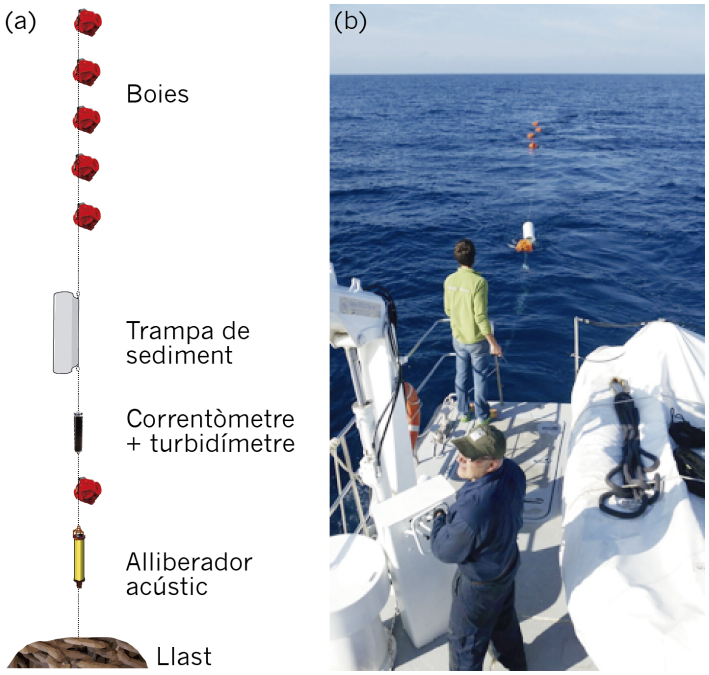

Figura 1.12. (a) esquema d'un dels ancoratges instrumentats emprats en aquesta Tesi. (b) maniobra de desplegament d'un ancoratge instrumentat des de la popa d'una embarcació.

Trampes de sediment seqüencials. L'ús de les trampes de sediment de mostreig seqüencial (Honjo, 1996) va suposar tota una revolució en l'enfocament de l'estudi dels fluxos de partícules a l'oceà. En aquesta Tesi hem emprat les trampes PPS3 de Technicap, que tenen forma cilíndrica-cònica, una ràtio alçada/diàmetre de 2,5 i un embut receptor amb una àrea de captació de 0,125 m^2 (Heussner *et al*., 1990). Aquest

embut desemboca en un "carrusel" rotatori equipat amb 12 ampolles recol·lectores (Fig. 1.13).

Figura 1.13. "Carrusel" rotatori d'una trampa de sediment PPS3 amb les ampolles recol·lectores plenes de matèria particulada.

Les trampes de sediment són raonablement eficaces alhora de recollir matèria particulada descendent dins la columna d'aigua. Tot i això, llur eficiència es pot veure compromesa quan algun factor extern, com un corrent intens i persistent, fa que la trampa s'inclini (Gardner, 1985). La millor manera de minimitzar aquests efectes és mitjançant un bon dimensionament de la flotabilitat que "estira" l'ancoratge cap amunt, afavorint així que la trampa es mantingui en posició vertical. Bonnin *et al.* (2008) van concloure que per sota de 82 cm s^{-1} de velocitat del corrent les trampes no s'inclinaven més de 15º, i que tal inclinació no afectava significativament llur eficiència en la captura de partícules.

Abans de ser fondejades, hom netejà minuciosament les trampes de sediment emprades en aquest estudi, i totes les parts susceptibles d'estar en contacte amb la matèria interceptat fou submergit 12 hores en una solució 0,5 M d'HCl. Les ampolles recol·lectores eren plenes d'una solució formolada al 5% (v/v), preparada amb formaldehid al 37-38% i aigua de mar filtrada a 0,45 µm i neutralitzada amb borat de sodi a un pH de 7,5-8. Hom emprà aquesta solució per prevenir tant la degradació de la matèria particulada com per evitar la fragmentació i la degradació dels organismes nedadors que de forma ocasional acaben dins les ampolles recol·lectores.

Correntòmetres. Aquests instruments permeten establir les relacions entre les estructures hidrogràfiques i la circulació marina, i el transport de matèria particulada. Des dels primers models, els correntòmetres han evolucionat enormement al llarg del temps. Així, un model clàssic com l'*ANDERAA RCM 7*, que encara s'utilitza, mesura la velocitat del corrent mitjançant un rotor mecànic i la direcció amb una aleta que s'orienta segons el mateix corrent. Avui, però, hom utilitza majoritàriament correntòmetres basats en el principi Doppler de retrodispersió de les ones acústiques. A més, els correntòmetres solen mesurar altres paràmetres, com la temperatura, la pressió i la conductivitat de l'aigua per mitjà de sensors addicionals afegits a la unitat principal. En aquest treball, hom ha utilitzat dos models de correntòmetres doppler, l'*AANDERA RCM9* (Fig. 1.14a) i el *Nortek Aquadopp* (Fig. 1.14b). Tots dos models mesuren la velocitat i la direcció del corrent, la temperatura i la pressió.

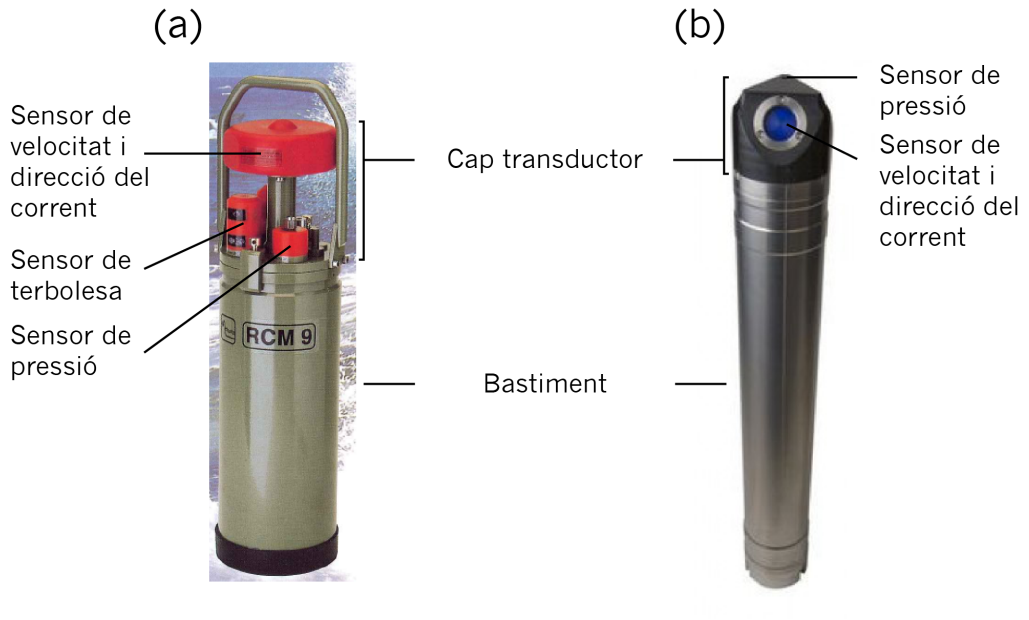

Figura 1.14. Els dos models de correntòmetres doppler utilitzats en aquesta Tesi: (a) AANDERA RCM9 i (b) Nortek Aquadopp (http://www.aanderaa.com, http://www.nortek-es.com/).

Turbidímetres. Són aparells que permeten mesurar la terbolesa de l'aigua per mitjà de mètodes òptics (transmitància i retrodispersió). En aquesta Tesi, la terbolesa s'ha mesurat amb un *Seapoint Turbidity Meter*, que detecta la llum dispersada per les partícules en suspensió tot i generant un voltatge que és directament proporcional a la seva concentració (Baker i Lavelle, 1984; Bishop, 1986). La terbolesa es mesura en

Unitats de Terbolesa de Formazina (FTU, de l'anglès *Formazin Turbidity Units*), les quals hem transformat en concentracions de partícules en suspensió (mg L^{-1}) mitjançant les corbes de calibratge de Guillén *et al*. (2000). Els fluxos laterals de sediment hom els ha obtingut multiplicant la concentració de partícules en suspensió per la velocitat del corrent. Convé remarcar que les mesures de fluxos verticals de matèria particulada obtinguts amb trampes de sediment i les de fluxos horitzontals obtinguts amb turbidímetres solen discrepar força. És una qüestió que ha estat àmpliament debatuda a la literatura (*e.g.* Gardner, 1989; Gardner i Walsh, 1990; Walsh i Gardner, 1992; Bonnin *et al*., 2008). Les explicacions sobre aquestes discrepàncies són diverses, Entre elles, la ineficiència de les trampes per capturar partícules advectades, i la presència de partícules gruixudes que sedimentarien ràpidament en el mateix material advectat, les quals donarien lloc a lectures de terbolesa baixes.

Ancoratges. A la Mediterrània nord-occidental hom fondejà dos ancoratges instrumentats al curs superior, a una profunditat nominal de 300 m, i al curs mig, a una fondària nominal de 1000 m, del canyó submarí del cap de Creus, a les estacions anomenades CC300 i CC1000, respectivament (Fig. 1.7b). Cada ancoratge fou equipat amb una trampa de sediment ubicada a 25 m sobre el fons, i un correntòmetre i un turbidímetre a 23 m sobre el fons (Taula 1.1). Les trampes de sediment recolliren mostres durant els hiverns de 2009-10, 2010-11 i 2012-13, amb una freqüència de 15-16 dies. És a dir, que cada 15-16 dies es canviava automàticament d'ampolla recol·lectora situada a l'eixida inferior de la trampa. Els correntòmetres i els turbidímetres enregistraren dades a intervals de 30 minuts durant 90 segons en els mateixos períodes de mostratge.

A la mar Cantàbrica hom fondejà tres ancoratges instrumentats, situats al curs mig del canyó d'Avilés, a 2000 m de profunditat nominal (estació AC2000), a la boca del canyó a 4700 m (estació AC4700) i al talús continental obert a l'oest del canyó, a 1200 m de fondària nominal (estació WS1200) (Fig. 1.7c). L'estació AC2000 inclogué dos nivells de trampes i correntòmetres, un a 1200 m (AC2000T), amb la trampa a 822 m sobre el fons i el correntòmetre a 820 m sobre el fons, i l'altre a 2000 m (AC2000B) de profunditat, amb una trampa a 46 m sobre el fons i un correntòmetre a 44 m sobre el fons. Aquest darrer duia acoblat un turbidímetre a la mateixa profunditat (Taula 1.1). L'estació AC4700 inclogué una sola trampa a 46 m sobre el fons. L'estació WS1200 fou equipada amb dos nivells de correntòmetres, un a 160 m del fons i l'altre a 46 m

del fons, aquest darrer amb un turbidímetre acoblat, i una trampa de sediment a 46 m del fons (Taula 1.1). Les trampes de sediment recolliren mostres durant un any, de març de 2012 a març de 2013, amb una freqüència de mostreig de 15-16 dies excepte les tres últimes ampolles de febrer de 2013, que romangueren obertes set dies per tal d'ajustar l'interval de mostreig total a les dates de recuperació dels ancoratges. Els correntòmetres i turbidímetres enregistraren dades a intervals de 15 minuts als nivells superiors i de 30 minuts als nivells inferiors de les línies instrumentades, sempre durant 90 segons.

Taula 1.1 (vegeu taula a la pàgina següent). Metadades de tots els ancoratges i instruments desplegats a les dues àrees d'estudi (*cf.* Cap. 1.4). Hom indica també els períodes de mostreig a cada estació, dividits en període 1 (P1), període 2 (P2) i període 3 (P3).

Localització geogràfica	Codi estació	Profunditat estació (m)	Instrumentació	Metres sobre el fons (m)	Metres reals de profunditat de l'instrument (m)	Període de mostreig
Canyó del Cap de Creus	CC300	P1:342 P2: 338	Trampa de sediment	30	P1: 312 P2: 308	P1: Novembre 2009-maig 2010 P2: Desembre 2010-maig 2011
			Correntòmetre	7	P1: 335 P2: 331	
			Turbidímetre	7	P1: 335 P2: 331	
Canyó del Cap de Creus	CC1000	P1: 980 P2: 920 P3: 959	Trampa de sediment	25	P1: 955 P2: 895 P3:934	P1: Novembre 2009-maig 2010 P2: desembre 2010-juny 2011 **P3:** Desembre 2012-juny 2013
			Correntòmetre	23	P1: 957 P2: 897 P3: 936	
			Turbidímetre	23	P1: 957 P2: 897 P3: 936	
Talús obert a l'oest del canyó d'Avilés	WS1200	P1: P2:	Trampa de sediment	46	P1: 1170 P2: 1241	P1: Març 2012-setembre 2012 P2: Setembre 2012-abril 2013
			Correntòmetre	44	P1: 1172 P2: 1243	
			Turbidímetre	44	P1: 1172 P2: 1243	
Canyó d'Avilés	AC2000T	P1: 2122 P2: 2103	Trampa de sediment	822	P1: 1234 P2: 1219	
			Correntòmetre	820	P1: 1236 P2: 1221	
Canyó d'Avilés	AC2000B	P1: 2122 P2: 2103	Trampa de sediment	46	P1: 2076 P2:2057	
			Correntòmetre	44	P1: 2078 P2: 2059	
			Turbidímetre	44	P1: 2078 P2: 2059	
Canyó d'Avilés	AC4700	P1: 4726 P2: 4775	Trampa de sediment	46	P1: 4680 P2: 4729	

1.5.2 MÈTODES ANALÍTICS

Després de recuperar els ancoratges instrumentats, hom emmagatzemà a 2-4ºC i en condicions de foscor, i fins la seva anàlisi, les ampolles amb les mostres de matèria particulada. Les mostres foren processades seguint el procediment descrit per Heussner *et al*. (1990), amb lleugeres modificacions. En primer lloc, hom procedí a l'extracció dels organismes nedadors (*i.e.* els que entraren dins les trampes per moció activa i no pas per l'acció de la gravetat) per tal d'evitar errors en la quantificació dels fluxos. Els de major mida foren retirats per filtració a través d'una malla d'1 mm, mentre que els organismes més petits d'1 mm foren retirats manualment amb unes pinces de laboratori sota un microscopi de dissecció. Tot seguit, hom dividí la mostra en volums iguals per mitjà d'una bomba peristàltica d'alta precisió, la qual distribuí la mostra en parts alíquotes seguint un patró cíclic. A continuació, les parts alíquotes foren centrifugades repetidament i netejades amb aigua Milli-Q per extreure'n el formaldehid i la sal. Finalment, hom les liofilitzà. Cada submostra alíquota fou pesada per tal d'obtenir el pes total de la mostra, i utilitzada per a la determinació de la composició elemental de la matèria particulada.

Composició elemental. L'anàlisi elemental l'hem aplicat a la quantificació dels continguts de carboni i nitrogen a les mostres de les trampes de sediment. Primer hom procedí a la combustió de les mostres a 1020ºC a partir de la injecció d'oxigen. Els gasos generats foren arrossegats amb heli a través d'uns reactius que reduïren el nombre d'espècies gasoses resultants de la combustió a N_2, CO_2, i H_2O. Seguidament, hom passà les mostres per un cromatògraf de gasos amb detector de conductivitat tèrmica, obtenint un seguit de mesures a partir de les quals hom avaluà els continguts de carboni i nitrogen.

L'anàlisi elemental de les mostres es dugué a terme als Centres Científics i Tecnològics de la Universitat de Barcelona emprant un analitzador elemental Thermo EA Flash 1112. Per a la determinació del carboni orgànic, hom pesà una petita part de la mostra (20 mg, aproximadament) que fou introduïda seguidament en una petita càpsula de plata. A continuació les mostres foren atacades amb addicions successives de parts alíquotes de 100 μL d'HCl al 25%. Entre una addició i la següent, hom assecà les mostres durant 8 hores a 60 ºC seguint Nieuwenhuize *et al*. (1994). Aquest procediment fou repetit fins que l'efervescència de la mostra desaparegué, assegurant

així la completa dissolució dels carbonats. Finalment, les mostres foren barrejades amb pentaòxid de vanadi, un catalitzador que accelera l'oxidació, i analitzades a l'analitzador elemental. La determinació del carboni total fou realitzada seguint el mateix procediment, però sense l'atac amb HCl per eliminar els carbonats.

Hom obtingué així els percentatges de carboni orgànic i carboni total, i també el percentatge de carboni inorgànic, d'acord amb l'expressió *carboni inorgànic = carboni total carboni orgànic*. Els valors de carboni orgànic i inorgànic permeteren calcular els continguts de MOP (carboni orgànic x 2) i de carbonat de calci (multiplicant el carboni inorgànic per la ràtio de la massa molecular del carbonat de calci [100/12], tot i assumint que tot el carboni inorgànic és contingut dins del carbonat de calci).

Sílice biogènica. Els continguts de sílice biogènica (diòxid de silici hidratat), o òpal, també foren analitzats als Centres Científics i Tecnològics de la Universitat de Barcelona mitjançant un espectròmetre d'emissió atòmica de plasma acoblat inductivament (ICP-AES, de l'anglès *Inductive Coupled Plasma Atomic Emission Spectrometer*). L'ICP-AES es basa en la ionització i l'excitació dels elements químics (Si i Al, en el nostre cas) a l'interior d'un plasma d'argó a 7000°C i s'utilitza per a la seva determinació quantitativa. Durant el procés de desexcitació, els elements presents a la mostra en forma d'àtoms i ions produeixen una radiació electromagnètica característica a la zona del UV-Visible, la qual pot ser separada d'acord amb la seva longitud d'ona. Seguidament, hom precedeix a la detecció i la quantificació dels diferents espectres d'emissió.

La quantitat d'òpal de les mostres fou determinada seguint el protocol descrit per Mortlock i Froelich (1989) i la readaptació de Fabrés *et al*. (2002). Primerament hom extragué la sílice amorfa de les mostres per mitjà de dues digestions de 2,5 hores a 85ºC en una solució de carbonat de sodi (Na_2CO_3) 0,5M. El material resultat d'ambdues digestions fou centrifugat, d'on hom obtingué un lixiviat que hom analitzà mitjançant ICP-AES. Durant la primera digestió de la mostra, hom aconseguí la dissolució total de la sílice biogènica i de part de la sílice no biogènica provinent d'aluminosilicats com les argiles. A partir de la segona digestió, en que el silici de la mostra provenia únicament dels aluminosilicats, hom calculà una relació silici/alumini utilitzable com a factor de correcció per al contingut de silici de la primera digestió:

$$Si_{biogènic} = Si_1 - Al_1 \times (\frac{Si_2}{Al_2})$$

on, Si_1 i Al_1 són les concentracions d'aquest element en el primer lixiviat i Si_2 i Al_2 són les concentracions obtingudes a la segona digestió. Finalment, hom obtingué el contingut d'òpal multiplicant el valor obtingut per al silici biogènic per 2,4 tot i assumint que la composició de l'òpal és $SiO_2 \cdot 0{,}4H_2O$, d'acord amb Mortlock i Froelich (1989).

Fracció terrígena. Hom calculà l'abundància de la fracció terrígena a partir de les dades anteriors, sostraient a la massa total la part corresponent a la suma dels components biogènics, és a dir carbonat de calci, MOP i òpal), segons l'expressió:

$$\%\ material\ litogènic = 100 - (\%\ carbonat\ de\ calci + \%\ MO\ + \%\ òpal)$$

Mida de gra. La distribució granulomètrica de les mostres fou efectuada mitjançant un difractòmetre làser *Beckman Coulter LS230 Laser Diffraction Particle Size Analyzer* o, simplement, *Coulter*. Aquest instrument està format per dos mòduls, un d'òptic i un de fluid a través dels quals passa la mostra en solució. Un cop introduïdes a l'aparell, les mostres són il·luminades amb un làser monocromàtic. Cada partícula dispersa la llum segons la seva mida, i unes lents concentren els feixos de llum en un detector que mesura la distribució angular de la llum difractada a diferents intervals de temps, obtenint així la distribució granulomètrica de la mostra introduïda.

Les mostres analitzades al *Coulter*, foren atacades prèviament amb peròxid d'hidrogen (H_2O_2) al 10% per tal d'eliminar la MOP. A cada mostra, hom repetí l'atac fins que va deixar de fer efervescència, indicant així la completa eliminació de la MOP. Seguidament, i per tal de prevenir la formació d'agregats, les mostres foren agitades amb una solució disgregant de polifosfat de sodi a l'1‰ durant 4 hores en una coctelera de laboratori.

1.5.3 DADES SUPORT ADDICIONALS DE FONTS DIVERSES

L'estudi dels forçaments externs directament responsables de nombrosos processos oceanogràfics i indirectament dels fluxos de partícules requereix l'ús de múltiples variables, tant meteorològiques (*e.g.* velocitat i direcció del vent, i temperatura de l'aire) com oceanogràfiques (*e.g.* temperatura de l'aigua a prop del fons, velocitat i direcció dels corrents, concentració de sediments en suspensió, i altres), disponibles en bases de dades gestionades per diverses institucions.

Les dades de temperatura de l'aire i precipitació corresponen a les estacions meteorològiques de Perpinyà i Sant Sebastià, representatives de la mar Mediterrània nord-occidental i de la mar Cantàbrica, respectivament, i les vàrem extreure del *NOAA National Climatic Data Center*.

Pel canyó del cap de Creus, les dades d'onatge s'extragueren d'una boia costanera localitzada davant de Leucata (Fig. 2.1), al Llenguadoc-Rosselló, gestionada pel *Centre d'Études Techniques Maritimes et Fluviales* del *Ministère de l'Ecologie, de l'Energie, du Développement durable et de la Mer,* França. Pel canyó d'Avilés, les dades d'onatge es van obtenir de la boia meteoceànica del Cabo Peñas (Fig. 2.7), gestionada per *Puertos del Estado* (Álvarez-Fanjul *et al*., 2003). Donat que l'alçada de l'onatge varia d'una onada a l'altra, hom sol utilitzar l'alçada significativa (Hs) de l'onatge, equivalent a l'alçada mitja del terç de les onades més altes. En conseqüència, en aquesta Tesi hem emprat l'Hs.

En l'estudi del canyó del cap de Creus, els valors de direcció i intensitat del vent s'extragueren de l'estació meteorològica de Portbou (Fig. 2.1), administrada pel Servei Meteorològic de Catalunya. Les dades de la direcció i intensitat del vent per a l'estudi del canyó d'Avilés es van obtenir a partir de la boia metoceànica del Cabo Peñas.

Les dades de descarrega fluvial dels principals rius que desemboquen al golf de Lleó, incloent el Roine, l'Erau, l'Orb, l'Aglí, el Tec i la Tet, les va proporcionar el *Laboratoire Hydraulique et de Mesures de la Compagnie Nationale du Rhône*. Les dades de descàrrega dels rius Nalón i Narcea, que són els principals rius que desemboquen prop de la capçalera del canyó d'Avilés, les va proporcionar el grup d'empreses d'energia EDP.

Les dades de concentracions de clorofil·la-a i de producció primària neta, i les imatges de satèl·lit en color veritable provenen del sensor *Moderate Resolution Imaging Spectoradiometer* (MODIS) instal·lat al satèl·lit *Aqua*, i foren proporcionades pel *Goddard Earth Sciences* (GES) *Data and Information Services Center* (DISC).

Les dades dels fluxos de calor entre l'atmosfera i l'oceà (*e.g.* pèrdues de calor sensible, latent i turbulent) emprades en aquesta Tesi provenen de l'anàlisi retrospectiva (o reanàlisi) d'una àmplia varietat de sistemes d'observació, juntament amb models numèrics elaborats per la NASA en el marc del projecte *Modern-Era Retrospective analysis for Research and Applications* (MERRA), el GES-DISC, i la *National Oceanic and Atmospheric Administration* (NOAA) en el marc del *National Centers of Environmental Prediction* (NCEP) *and National Center for Atmospheric Research* (NCAR) *atmospheric model reanalysis* (Kalnay *et al*., 1996) que administra i distribueix el NOAA *Earth System Research Laboratory*. Les dades necessàries per calcular les pèrdues de calor netes (pèrdues de calor sensible, latent, d'ona llarga i ona curta) i els fluxos de densitat de les aigües superficials (temperatura superficial de l'aigua, salinitat de les aigües superficials, precipitació i evaporació) van ser extretes del NOAA NCEP/NCAR *atmospheric model reanalysis*.

Altres dades oceanogràfiques complementàries (*e.g.* temperatura de l'aigua a prop del fons, velocitat i direcció dels corrents, i altres) utilitzades en l'estudi de les teleconnexions atmosfèriques entre les mars Mediterrània nord-occidental i Cantàbrica hom les obtingué a partir d'una sèrie d'instruments instal·lats en diverses estacions de mesura (Fig. 2.18). A la Mediterrània, a més de l'estació CC1000, hom va utilitzar les dades provinents de dos ancoratges equipats amb sensors de temperatura, un al canyó de Lacaze-Duthiers (LCD) a 1000 m de profunditat i un altre anomenat LION a l'àrea MEDOC (MEDOC group, 1970) a 2400 m, tots dos gestionats pel CEFREM, del *CNRS* i la Universitat de Perpinyà. Hom emprà també dades de la boia meteorològica Lion (LMB, de l'anglès *Lion Meteorological Buoy*) de *Météo-France*, equipada amb sensors de temperatura de l'aigua des de la superfície fins a 200 m de profunditat, també a prop de l'àrea MEDOC, igualment fondejada a ~2400 m de profunditat. A més, donat que els registres a la mar Mediterrània no són tan homogenis ni continus com a la mar Cantàbrica, hom usà dades dels treballs de Mertens i Schott (1998), Bethoux *et al*. (2002) i Somot *et al*. (2016). A la mar Cantàbrica, els registres oceanogràfics (*e.g.* temperatura de l'aigua diferents profunditats, velocitat i direcció

dels corrents, i altres) procediren de la boia oceànica número 7 del projecte Radiales (Valdés *et al*., 2002; Bode *et al*., 2012) de l'*Instituto Español de Oceanografía*, que arriba fins a 2580 m de profunditat.

L'entorn de computació utilitzat en aquesta Tesi ha estat MATLAB, programari d'anàlisi numèrica i visualització de dades dissenyat específicament per al treball científic.

Capítol 2
Resultats

2.1 EXTERNAL FORCINGS, OCEANOGRAPHIC PROCESSES AND PARTICLE FLUX DYNAMICS IN CAP DE CREUS SUBMARINE CANYON, NW MEDITERRANEAN SEA

A. Rumín-Caparrós[1], A. Sanchez-Vidal[1], A. Calafat[1], M. Canals[1], J. Martín[2], P. Puig[2], and R. Pedrosa-Pàmies[1]

[1]GRC Geociències Marines, Dept. d'Estratigrafia, Paleontologia i Geociències Marines, Universitat de Barcelona, 08028 Barcelona, Spain
[2]Institut de Ciències del Mar (CSIC), Passeig Marítim de la Barceloneta 37-49, 08003, Barcelona, Spain

Biogeosciences, 10, 3493-3505, 2013
www.biogeosciences.net/10/3493/2013/
doi:10.5194/bg-10-3493-2013

2.1.1 ABSTRACT

Particle fluxes (including major components and grain size), and oceanographic parameters (near-bottom water temperature, current speed and suspended sediment concentration) were measured along the Cap de Creus submarine canyon in the Gulf of Lions (GoL; NW Mediterranean Sea) during two consecutive winter-spring periods (2009-2010 and 2010-2011). The comparison of data obtained with the measurements of meteorological and hydrological parameters (wind speed, turbulent heat flux, river discharge) have shown the important role of atmospheric forcings in transporting particulate matter through the submarine canyon and towards the deep sea.

Indeed, atmospheric forcing during 2009-2010 and 2010-2011 winter months showed differences in both intensity and persistence that led to distinct oceanographic responses. Persistent dry northern winds caused strong heat losses (14.2×10^3 W m^{-2}) in winter 2009-2010 that triggered a pronounced sea surface cooling compared to Winter 2010-2011 (1.6×10^3 W m^{-2} lower). As a consequence, a large volume of dense

shelf water formed in winter 2009-2010, which cascaded at high speed (up to ~ 1 m s^{-1}) down Cap de Creus Canyon as measured by a currentmeter in the head of the canyon. The lower heat losses recorded in winter 2010-2011, together with an increased river discharge, resulted in lowered density waters over the shelf, thus preventing the formation and downslope transport of dense shelf water.

High total mass fluxes (up to 84.9 g m^{-2} d^{-1}) recorded in winter-spring 2009-2010 indicate that dense shelf water cascading resuspended and transported sediments at least down to the middle canyon. Sediment fluxes were lower (28.9 g m^{-2} d^{-1}) under the quieter conditions of Winter 2010-2011. The dominance of the lithogenic fraction in mass fluxes during the two winter-spring periods points to a resuspension origin for most of the particles transported down canyon. The variability in organic matter and opal contents relates to seasonally controlled inputs associated with the plankton spring bloom during March and April of both years.

2.1.2 INTRODUCTION

Atmospheric-ocean interactions play a key role in the modification of oceanographic processes. Shifts in wind regime and air temperature are among the most important forcing variables in the atmosphere, triggering modifications in thermohaline properties of water, and therefore, in the hydrographic configuration of the upper part of the water column. There are several mechanisms that can transport and mix these atmospheric-modified shallow waters with intermediate or even deep waters. For example, cooling, evaporation or freezing in the surface layer of shallow areas of the continental shelf trigger the formation of dense water that eventually spills over the shelf edge onto the continental slope (see Ivanov et al., 2004, for a review). This causes the transmission of the atmospheric signal from shallow to deep waters within a short time range

In the Gulf of Lions (GoL) there are three major mechanisms by which superficial waters are modified and transported from the surface to deep sea regions. The first is storm-induced downwelling. This is related to the occurrence of E-SE winds that cause increased wave height and shelf sediment resuspension. The excess of water and suspended sediment piled in the inner shelf of the GoL, together with the reinforcement of the coastal current, forces shelf waters to flow towards the southwest and sink mainly through the Cap de Creus Canyon (Palanques et al., 2008).

Furthermore, E-SE winds transfer humid marine air towards the coastal relief, where the air is obstructed and results in orographic rainfall and an increase in river discharge. The delivery of riverine particles and the increased shelf sediment resuspension during E-SE storms augments the export of suspended sediments towards the deep sea (Palanques et al., 2006, 2008; Guillén et al., 2006; Sanchez-Vidal et al., 2012).

The second mechanism is dense shelf water cascading (DSWC). This is linked to cold, dry, and persistent N-NW winds that induce sea-atmosphere heat losses and mixing of shelf waters (Millot, 1990). As a result, shelf waters become dense and sink, overflowing the shelf edge, and cascade downslope (preferentially through submarine canyons) until they reach their equilibrium depth (Durrieu de Madron et al., 2005).

Both mechanisms (i.e., E-SE storms and DSWC) can occur separately or in parallel, and are responsible for the remobilization and transport of sediments to the deep sea (Canals et al., 2006; Heussner et al., 2006; Palanques et al., 2006, 2008; Puig et al., 2008) and the variability in the biogeochemical composition of settling particles (Sanchez-Vidal et al., 2009; Pasqual et al., 2010). The occurrence of these events represents an important source of food to the deep ecosystems and influences the ecology of its deep-sea populations, as described, for instance, by Company et al. (2008) and Pusceddu et al. (2010). Furthermore, these events contribute to the transport and dispersion of persistent organic pollutants in the marine continental GoL shelf and open sea-waters (Salvadó et al., 2012).

The third mechanism is deep-intermediate convection (MEDOC Group, 1970), which is caused again by the occurrence of cold, dry, and persistent N-NW winds that induce a heat and buoyancy loss of offshore waters in the Gulf of Lions, the Ligurian Sea and the Catalan Sea (Schroeder et al., 2010). This leads to mixing at great depths and homogenization of the water column in open sea regions. Recent studies have also documented the potential of such atmospheric-driven phenomena to remobilize sediments at depths below 2000 m in the northwestern Mediterranean basin (Martín et al., 2010).

With the aim of investigating the relationship between atmospheric forcings and the oceanographic processes and near-bottom particle fluxes, two mooring lines were

deployed during two consecutive winter-spring periods (2009-2010 and 2010-2011) in the Cap de Creus Canyon at 300 m and 1000 m water depths. After three decades of year-round continuous monitoring of hydrosedimentary processes in the western GoL, and after considering several studies from both in situ observations (e.g. Canals et al., 2006; Heussner et al., 2006; Palanques et al., 2008; Puig et al., 2008) and numerical modeling (e.g. Ulses et al., 2008a, b), it appears that the most dynamic period in terms of water, sediment and organic matter export are the winter and early spring months. This is the time when dense shelf water forms and cascades downslope, occasional eastern storms occur, and the most prominent yearly planktonic bloom takes place (Fabres et al., 2008; Pasqual et al., 2010). For these reasons, the experiment described here focuses on these months and combines atmospheric data (wind speed and direction, air temperature and heat fluxes) with measured physical parameters (near-bottom temperature and current speed) and particle fluxes (total mass and main components) to assess the atmospheric variables that govern sediment transport to the deep sea floor during these two winter-spring periods. The manuscript is structured as follows: in Sect. 2.1.3 the hydrological and oceanographic settings of study area are presented. Material and methods are presented in Sect. 2.1.4. Section 2.1.5 describes data on the external forcings during the studied period (atmospheric conditions, river discharge, wave height and chlorophyll a concentration), and particle flux and oceanographic data obtained with the sediment traps and the current meters. Section 2.1.6 compares all data obtained and discusses the role of atmospheric forcing in the transport of particulate matter through the Cap de Creus submarine canyon. Finally, Sect. 2.1.7 contains the main conclusions of the study.

2.1.3 STUDY AREA

The GoL is a river-dominated micro-tidal continental margin that extends from the Cap Croisette, in the northeastern corner of the GoL, to the Cap de Creus at its southwestern limit (Fig. 2.1). The main morphological characteristic of its sea floor is its crescent-shaped shelf and the numerous submarine canyons incising the slope and shelf-break. The sea surface circulation in the GoL is linked to the Northern Current (NC), which in the study area manifests itself as a geostrophic jet flowing cyclonically along the slope over the 1000-2000 isobaths (Millot, 1999). The NC is associated with a permanent shelf-slope density front which separates shelf fresh coastal waters, directly influenced by the discharge of the Rhône River, from open-sea waters.

Seasonal variations of the structure and intensity of the NC have been observed, with the current being narrower, deeper and more intense during winter (Millot, 1999).

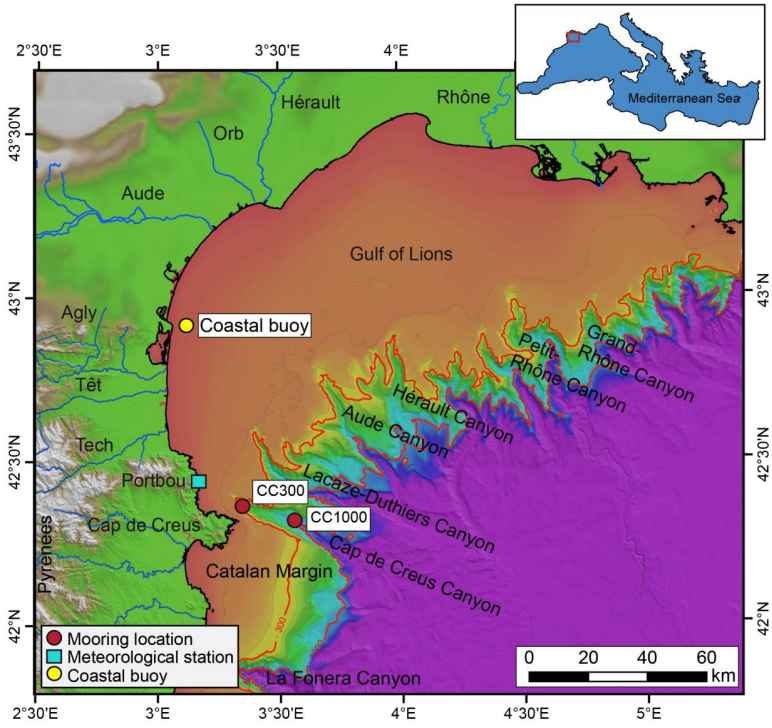

Fig. 2.1. Topo-bathymetric map of the Cap de Creus Canyon and neighboring areas: the northern Catalan margin at the South and the Gulf of Lions (northwestern Mediterranean) at the North. Locations of moorings (red dots), the meteorological station in Portbou (light blue square) and the Leucate coastal buoy (yellow dot) are shown. Top-right red square indicates where the heat fluxes and Chl a concentration maps have been obtained. Bathymetric data published by Canals et al. (2004).

Fresh water inputs into the GoL are mainly from three different hydrographic basins: the Alps in the northern part of the GoL (Rhône River), the Massif Central mountains (Hérault and Orb) and the Pyrenees mountains (Agly, Aude, Tech and Têt rivers). The Rhône River drains much of the water coming from the snowmelt of the Alps and its inputs represent more than the 90 % of the total annual freshwater inputs of the GoL (Bourrin et al., 2006). On the other hand, the Hérault and Orb rivers, and the Agly, Aude, Tech and Têt rivers, drain the Massif Central and the Pyrenees mountains

respectively and, unlike the Rhône River, they are mainly controlled by a Mediterranean climatic regime, with short and intense flash flood events (Serrat et al., 2001).

The absence of significant tidal motions makes the combination of the atmospheric forcings (as the prevailing wind fields), the internal dynamics of the currents (and their interaction with the bathymetry) and the main river discharges the major source of variability in the oceanographic parameters of the GoL.

2.1.4 MATERIAL AND METHODS

2.1.4.1 SAMPLE COLLECTION AND PREPARATION

Two mooring lines were deployed from November 2009 to May 2010 and from December 2010 to June 2011 along the axis of the Cap de Creus submarine canyon (Fig. 2.1). Moorings were deployed at the canyon head and upper canyon course (as described by Lastras et al., 2007) at 300 m and 1000 m depth, respectively, and were defined as CC300 and CC1000 according to the deployment depth. Each moored line was equipped with a PPS3 Technicap sequential sampling sediment trap with a 0.125 m^2 collecting surface and a 2.5 height/diameter ratio in its cylindrical part (Heussner et al., 1990). Each trap was equipped with 12 receiving cups and was deployed at 25 m above the bottom with sampling intervals of 15 days. The collecting cups were filled with a buffered 5 % (v/v) formaldehyde solution in 0.45 µ filtered seawater. Each moored line included an Aanderaa RCM9 current meter deployed at 5 m above the bottom (CC300) and 23 m above the bottom (CC1000) equipped with a turbidimeter with a sampling interval of 30 min. Turbidity units, recorded in Formazin Turbidity Units (FTU), were transformed into suspended sediment concentrations (SSC) (mg L^{-1}) using the general calibration of Guillén et al. (2000). A technical failure of the current meter deployed at 1000 m in both years resulted in the complete absence of data at this water depth.

2.1.4.2 ANALYTICAL METHODS

After recovery, samples were processed according to a modified version of Heussner et al. (1990). Large swimming organisms were removed by wet sieving through a 1 mm nylon mesh, and organisms of less than 1 mm were handpicked under a microscope

with fine tweezers. Samples were split into aliquots using a high-precision peristaltic pump robot and freeze-dried prior to chemical analysis.

Total carbon, organic carbon, and nitrogen contents were analyzed at "Centres Científics i Tecnològics" of the "Universitat de Barcelona" using an elemental organic analyzer Thermo EA Flash 1112 (Thermo Scientific, Milan, Italy) working in standard conditions recommended by the supplier of the instrument. For the organic carbon analysis, samples were first decarbonated with repeated additions of 100 µL of 25 % HCl until no effervescence was observed. Between each acidification step a 60 ºC drying lapse of 8 h was carried out. Organic matter (OM) content was calculated as twice the organic carbon content. The inorganic carbon content was calculated as total carbon minus organic carbon and the carbonate content was calculated assuming that all the inorganic carbon is contained within calcium carbonate ($CaCO_3$), using the molecular mass ratio of 100/12.

Biogenic silica was analyzed using a two-step 2.5 h extraction with 0.5 M Na_2CO_3 separated by filtration of the leachates. Si and Al contents of both leachates were analyzed with an Inductive Coupled Plasma Atomic Emission Spectroscopy (ICP-AES), correcting the Si content of the first leachate by the Si/Al ratio of the second one. Once corrected, Si concentrations were transformed to opal by multiplying by a factor of 2.4 (Mortlock and Froelich, 1989).

The siliciclastic fraction was obtained by subtracting from the total mass the part corresponding to the major biogenic components, assuming that the amount of siliciclastics (%) was = 100 - (% OM + % $CaCO_3$ + % Opal).

Grain size analyses were performed on a Coulter LS 230 Laser Particle Size Analyzer after organic matter oxidation with 10 % H_2O_2.

2.1.4.3 METEOROLOGICAL, HYDROLOGICAL AND OCEANOGRAPHIC DATA

The exchange of energy between the atmosphere and the sea surface takes place through turbulent and radiative energy fluxes. Mathematically, the net air-sea heat exchange (*Qnet*) is the sum of four components:

$$Q_{net} = Q_{sh} + Q_{lh} + Q_{sw} + Q_{lw}, \quad (2.1)$$

where Q_{sh} is the sensible heat flux (SHF), Q_{lh} is the latent heat flux (LHF), Q_{sw} is the short-wave flux, and Q_{lw} is the long-wave flux. The sum of the sensible and latent heat fluxes ($Q_{sh} + Q_{lh}$, named turbulent heat flux) is linearly proportional to the wind speed and the air-sea temperature or humidity difference, while the sum of the short-wave and long-wave fluxes ($Q_{sw} + Q_{lw}$, named radiative flux) is function of air temperature, humidity, and cloudiness (Deser et al., 2010).

According to Josey (2003) and Schroeder et al. (2010), LHF, and to a lesser extent SHF, control anomalies in the winter net heat exchanges in the GoL. Both parameters are calculated as follows:

$$Q_{sh} = \rho\, c_p\, C_h\, u\, [\, T_s - (\, T_a + \Upsilon z\,)], \quad (2.2)$$

$$Q_{lh} = \rho\, L C_e\, u\, (\, q_s - q_a\,), \quad (2.3)$$

where ρ is the air density at observation level, c_p the specific heat capacity of the air at constant pressure, L is the latent heat of evaporation of water, C_h is the transfer coefficient for the SHF, u is the wind speed, T_s and T_a are the sea surface temperature and the surface air temperature corrected for the adiabatic lapse rate respectively, z is the height at which the air temperature is measured, C_e is the transfer coefficient for the LHF, and q_s and q_a are the specific humidity at the sea surface and the atmospheric specific humidity at the reference level, respectively (Josey et al., 1999). LHF and SHF in the study area have been acquired as part of the activities of NASA's Science Mission Directorate, archived and distributed by the Goddard Earth Sciences (GES) Data and Information Services Center (DISC). The source used has been the Modern Era Retrospective-analysis for Research and Applications (MERRA), which uses the GEOS-5 Data Assimilation System with the adoption of a joint analysis with the National Centers for Environmental Prediction (NCEP) and of a set of physics packages for the atmospheric general circulation model. The study of the sea-atmosphere interactions has been gridded from 42.1° N to 43.4° N; and from 3.1° E to 5° E (Fig. 2.1).

Significant wave height (Hs) data have been obtained from the Leucate coastal buoy (Fig. 2.1), provided by the "Centre d'Études Techniques Maritimes Et Fluviales" ("Ministère de l'Ecologie, de l'Energie, du Développement durable et de la Mer", CANDHIS, France).

Wind speed and direction have been acquired from the automatic meteorological station in Portbou (see location in Fig. 2.1), maintained by "Servei Meteorològic de Catalunya" ("Generalitat de Catalunya").

Riverine discharges have been obtained from the "Laboratoire Hydraulique et Mesures" from the Compagnie Nationale du Rhône. The rivers considered are the Rhône River, because it is the main contributor of freshwater inputs of the GoL, and the Hérault, Orb, Agly, Aude, Tech and Têt rivers, in order to consider the freshwater inputs from most of the small rivers discharging into the GoL.

Data on concentration of the photosynthetic pigment Chlorophyll a (Chl *a*) have been obtained from the Goddard Earth Sciences (GES) Data and Information Services Center (DISC), using as a source the Moderate Resolution Imaging Spectoradiometer (MODIS) onboard the Aqua satellite. Chl *a* concentration is calculated using remotely sensed observations of the ocean surface with visible wavelength data. For our study, Chl *a* concentration has been gridded, including the mooring location and most of the GoL area (Fig. 2.1).

2.1.5 RESULTS

2.1.5.1 EXTERNAL FORCINGS

Winter 2009-2010 in the Cap de Creus area (northern Catalonia) was characterized by very low temperatures. Air temperatures were approximately 2 ºC lower than the average climatic values registered in the climatic atlas of Catalonia (Martín-Vide and Raso Nadal, 2008). Several wind episodes with severe N-NW winds were recorded during late December 2009 (with speeds reaching up to 40 m s^{-1}), mid-January 2010 (up to 47 m s^{-1}), and mid-February 2010 (up to 44 m s^{-1}) (Fig. 2.2a). At the same time the cumulative turbulent heat losses (LHF and SHF) reached values of 14.2×10^3 W m^{-2} through the entire winter, from November 2009 until the end of March 2010.

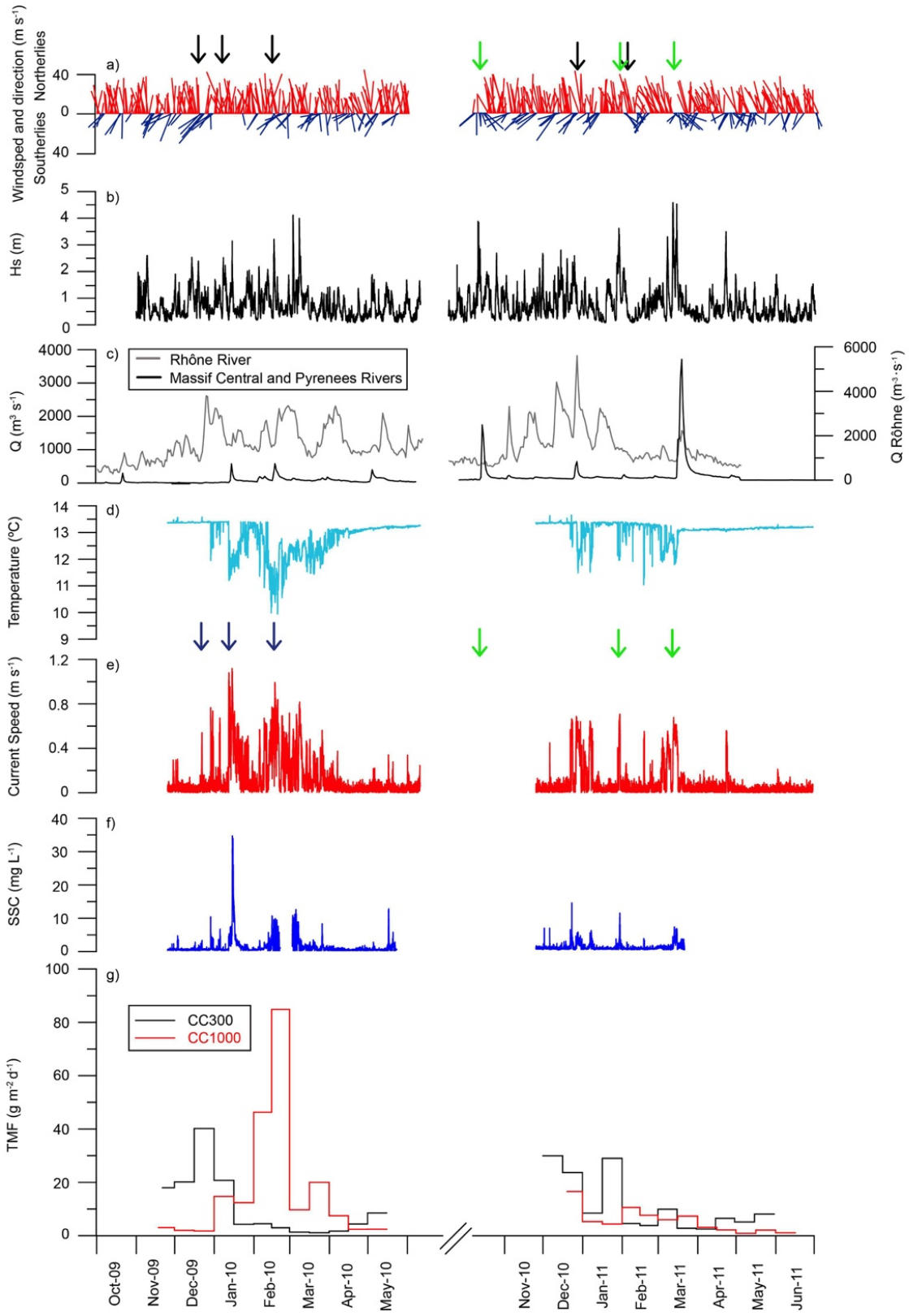
a)
Windsped and direction (m s-1)
Southerlies Northerlies
40
0
40
b)
Hs (m)
5
4
3
2
1
0
c)
Rhône River
Massif Central and Pyrenees Rivers
Q (m3 s-1)
4000
3000
2000
1000
0
6000
4000
2000
0
Q Rône (m3 s-1)
d)
Temperature (ºC)
14
13
12
11
10
9
e)
Current Speed (m s-1)
1.2
0.8
0.4
0
f)
SSC (mg L-1)
40
30
20
10
0
g)
CC300
CC1000
TMF (g m-2 d-1)
100
80
60
40
20
0
Oct-09
Nov-09
Dec-09
Jan-10
Feb-10
Mar-10
Apr-10
May-10
Nov-10
Dec-10
Jan-11
Feb-11
Mar-11
Apr-11
May-11
Jun-11

The second winter studied was on average 1 ºC warmer than the previous one. N-NW velocities reached speeds of up to 45 m s^{-1} during late December 2010, and up to 42 m s^{-1} in early February 2011 (Fig. 2.2a). Strong wind events were concentrated in the first half of the winter, so the cumulative turbulent heat loss for the whole winter (from November until the end of March), was 1.6×10^3 W m^{-2} lower than the previous winter.

Two very important increases in the discharge of rivers draining the Pyrenees and the Massif Central are well distinguished in October 2010 and in March 2011 (Fig. 2.2c, 2.3d). During both events the Hérault River reached 40 and 850 m^3 s^{-1}, the Orb River reached 91 and 899 m^3 s^{-1}, the Agly River reached 741 and 635 m^3 s^{-1}, the Aude River reached 399 and 561 m^3 s^{-1}, the Tech River 239 and 512 m^3 s^{-1}, and the Têt 245 and 366 m^3 s^{-1}, respectively. Considering that the Rhône river basin is not affected by the Mediterranean climate characterized by its limited rainfall regime (Ludwig et al., 2003), its basal discharge was always very high compared to the rest of the rivers, presenting a much more regular flow rate during the whole period of around 2,000 m^3 s^{-1} (Figs. 2.2c, 2.3e). The higher water discharge in the whole time series was registered at the very end of December 2010, with 5,600 m^3 s^{-1}.

Maximum significant wave height (Hs) was recorded in March in both winters in the context of a reinforcement of easterly winds (Fig. 2.2a, b), in agreement with larger swell due to the longer fetch distance of E winds. During winter 2009-2010, the maximum Hs recorded was of 4 m, while during the next winter the maximum Hs was 4.6 m.

Fig. 2.2 (see figure in previous page) (a) Temporal variability of northerly winds (red) and southerly winds (blue). Black arrows highlight severe N-NW wind episodes and green arrows the occurrence of eastern storms (b) Significant wave height (Hs); (c) Daily fluvial discharges of the Rh oneˆ River in grey and the sum of the main small rivers flowing to the Gulf of Lions (Hérault, Orb, Agly, Aude, Tech and Têt) in black; (d) near-bottom temperature recorded at CC300; (e) near-bottom current speed recorded at CC300, (f) suspended sediment concentration (SSC) as recorded by the currentmeter at 300 m of water depth; (g) total mass flux at 300 (black) and 1000 m (red) of water depth. Blue arrows show period of intense heat losses and DSWC event (as in Figs. 2.3 and 2.5), and green arrows the occurrence of eastern storms (as in Fig. 2.5).

Chl *a* concentration images showed increased pigment concentrations during March, reflecting the well-known seasonal phytoplankton bloom in the region (e.g. Estrada et al., 2011) (Fig. 2.4).

2.1.5.2 NEAR-BOTTOM CURRENT REGIME AND DOWNWARD PARTICLE FLUXES

Time series of near-bottom water temperature, current speed, near-bottom suspended sediment concentration (SSC) at CC300, and downward total mass flux (TMF) at both CC300 and CC1000, are shown in Fig. 2.2d-g.

2.1.5.2.1 WINTER 2009-2010

November 2009 was characterized by relatively stable oceanographic conditions at the CC300 station, with no major changes in near-bottom water temperature and current speeds below 0.29 m s^{-1}. At the very end of December 2009, a drop in near-bottom water temperature (to 11.98 ºC) was recorded concomitantly with increased current speeds (0.77 m s^{-1}) and SSC (10.41 mg L^{-1}). This event lasted a couple of days. At the same time TMF reached 40.2 g m^{-2} d^{-1} at CC300 while no significant increase was recorded at CC1000.

In mid-January 2010 near-bottom water temperature at CC300 decreased abruptly more than 2 ºC (from 13.40 to 11.21 ºC), and current speed and SSC increased up to 1.12 m s^{-1} and 34.68 mg L^{-1}, respectively. The lower temperatures and high current speeds were maintained for approximately 16 days. Total mass flux (TMF) at CC300 reached only 20.1 g m^{-2} d^{-1} and at CC1000 increased slightly up to 14.7 g m^{-2} d^{-1} (Fig. 2.2g).

In February 2010 the longer event started, which lasted for one and a half months and was characterized by persistent low bottom water temperature (as low as 9.95 ºC) and high velocities (up to 0.99 m s^{-1}). SSC also increased considerably but did not reach the levels of the previous month, being almost 4 times lower. While no variation in TMF was recorded at the CC300 station, TMF at CC1000 registered a sharp increase up to values of 84.9 g m^{-2} d^{-1}.

2.1.5.2.2 WINTER 2010-2011

The second monitored winter presented smaller magnitude anomalies in near-bottom water temperature, current speed and SSC at the CC300 station. At the end of December 2010 water temperature dropped more than 1.5 ºC (to 11.49 ºC) and current speed increased up to 0.68 m s^{-1} and SSC up to 14.57 mg L^{-1}. These anomalies lasted for 17 days. TMF values at the CC300 and CC1000 stations increased up to 23.7 g m^{-2} d^{-1} and 16.6 g m^{-2} d^{-1}, respectively (Fig. 2.2g).

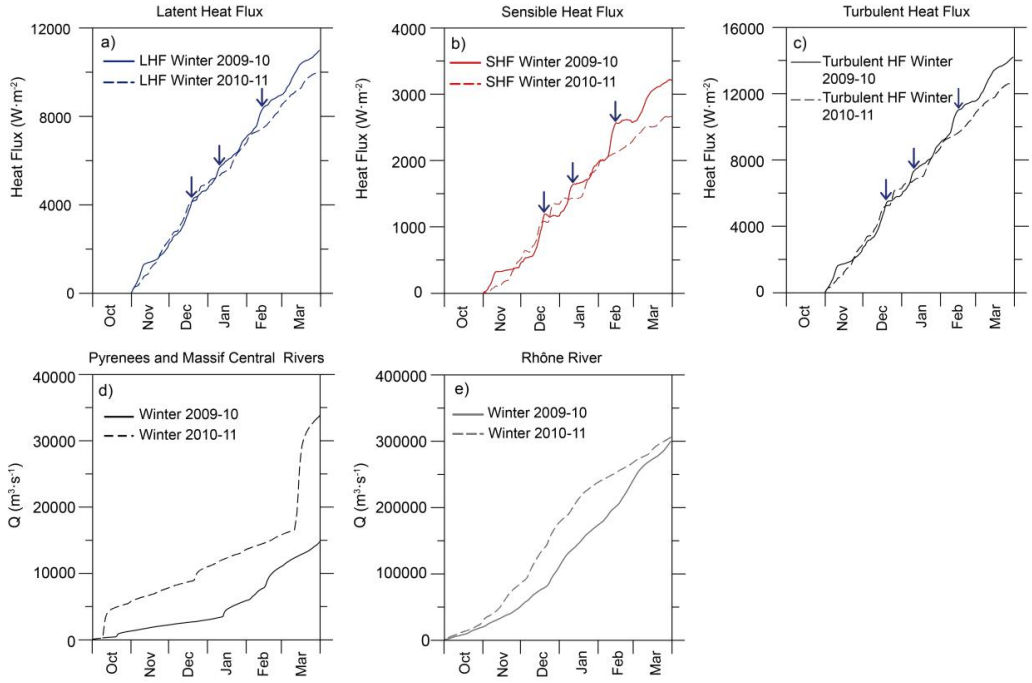

Fig. 2.3. (a) Cumulated Latent Heat Flux for winter-spring 2009-2010 (continuous line) and 2010-2011 (dashed line); (b) Cumulated Sensible Heat Flux for winter-spring 2009-2010 (continuous line) and 2010-2011 (dashed line); (c) Cumulated Turbulent Heat Flux for winter-spring 2009-2010 (continuous line) and 2010-2011 (dashed line); (d) Cumulated river discharge from the Hérault, Orb, Agly, Aude, Tech and Têt rivers for winters 2009-2010 (continuous line) and 2010-2011 (dashed line); (e) Cumulated river discharge from the Rhône river for winters 2009-2010 (continuous line) and 2010-2011 (dashed line). Blue arrows show period of intense heat losses (as in Figs. 2.2 and 2.5).

January and February 2011 were characterized by relatively stable conditions, except for a discrete (lasting less than 2 days) water temperature drop recorded

concomitantly with increased current speeds (up to 0.71m s^{-1}) recorded at the end of January 2011. At the same time, SSC peaked at 11.53 mg L^{-1} and TMF at CC300 reached values up to 28.9 g m^{-2} d^{-1}. No increased TMF was recorded at the CC1000 station.

In March 2011 slight temperature drops (to 11.07 ºC), increased current speeds (0.68 m s^{-1}) and increased SSC (7.37 mg L^{-1}) were again recorded (Fig. 2.2g). TMF increased slightly at CC300 (up to 9.9 g m^{-2} d^{-1}) and after 15 days at CC1000 (up to 7.3 g m^{-2} d^{-1}) (Fig. 2.2g).

2.1.5.3 MAIN COMPONENTS OF SETTLING PARTICLES

The temporal variability of the main components (OM, $CaCO_3$, opal and siliciclastics) at the two stations during the winter-spring periods studied is shown in Fig. 2.5. As repeatedly observed in this region, the siliciclastic component is the main contributor to TMF at all stations and at all depths (Heussner et al., 2006; Pasqual et al., 2010), representing almost 70 % of the total flux. Furthermore, during the second monitored winter-spring 2010-2011, the siliciclastic relative abundance decreased with depth from CC300 to CC1000.

In general the OM relative abundance of TMF during both periods showed a clear temporal variability, displaying almost always higher concentrations at the CC300 station. During the first period maximum concentration values were recorded during the end of March 2010 at CC300 (up to 4.68 %) and during late April 2010 at CC1000 (up to 3.42 %). During the second monitored period, maximum peaks were reached in late February 2011 at CC300 (4.38 %) and late
April 2011 in CC1000 (3.61 %).

$CaCO_3$ relative abundance during the first monitored winter-spring period peaked in late January and February 2010 in CC300 and late January 2010 in CC1000, and accounted for up to 30.49% of the total flux. During the second period values were significantly lower at the CC300 station, increasing in March-April 2011 up to 28.23 and 30.54% of the CC300 and CC1000 flux.

Opal represented always less than 4% of the mass flux. During the first monitored winter-spring opal relative abundance increased in December 2009 (up to 1.99 %) and March-April 2010 (up to 2.01 %) at both stations. During the second period, the seasonal increase of opal was more evident, increasing in very late April 2011 up to values of 1.93% at CC300, and 3.43% at CC1000.

2.1.5.4 GRAIN SIZE

During the two monitored periods, approximately 90 % of the particles were mainly silt-sized (between 4 and 63 µm) whereas 10 % of the particles where clay-sized (< 4 µm). A few samples included sand-sized particles (> 63 µm).

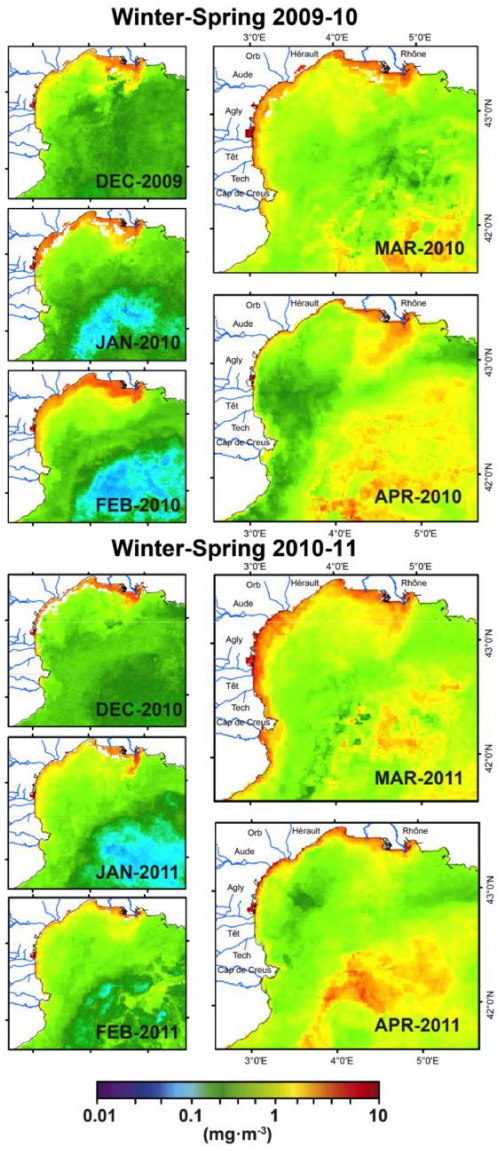

Fig. 2.4. Sequence of monthly mean Chlorophyll a concentration in the study area during both winter-spring periods.

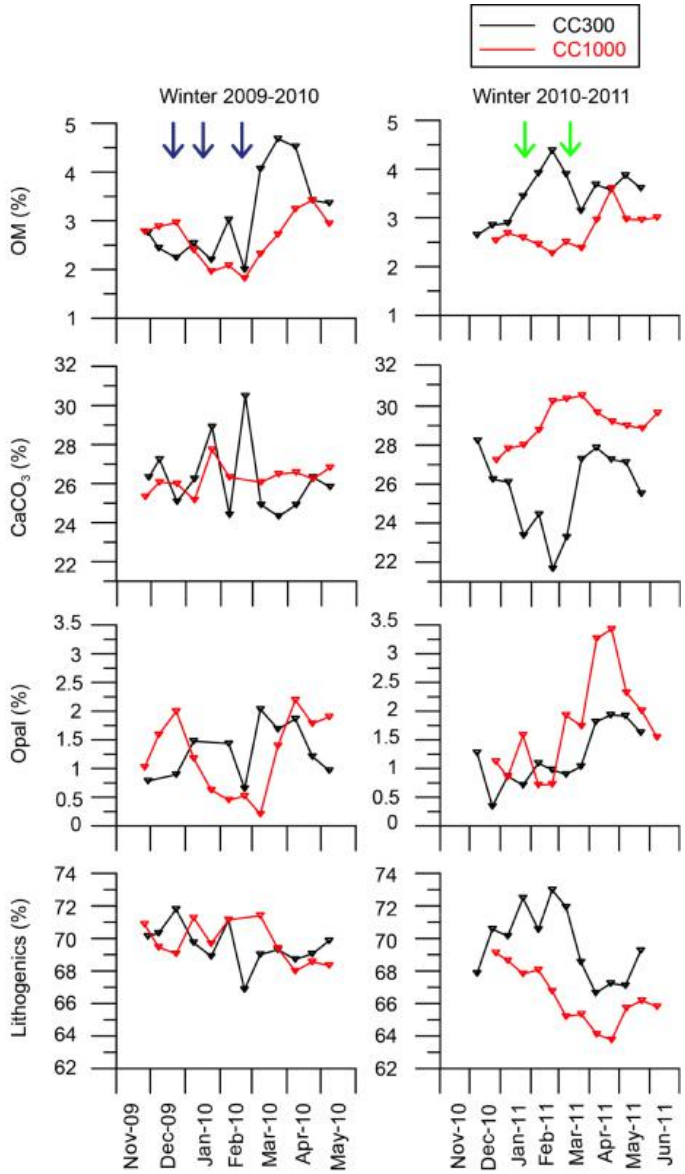

Fig. 2.5. Temporal variability of the main components of the settling particles ($CaCO_3$, Organic Mater (OM), opal and siliciclastics) of the two stations during the two winter-spring periods studied. Black line represents the CC300 station whereas the red line represents the CC1000. (a) Winter-spring 2009-2010. (b) Winter-spring 2010-2011. Blue arrows show periods of intense heat losses and DSWC event (as in Figs. 2.2 and 3), and green arrows show eastern storms events (as in Fig. 2.2).

The grain size distributions display many fluctuations (Fig. 2.6). During the first winter-spring, the low amount of mass obtained from the sediment cups at CC300 from mid-January to mid-April 2010 prevented grain size determination. However, the available

data show coarsening of the sediments collected during the second half of December 2009 with respect to the samples collected at the beginning and at the end of the evaluated time series (very late November 2009 and early May 2010, respectively). Samples collected during February 2010 in CC1000 also displayed a clear coarsening with respect to the initial and final conditions (Fig. 2.6a).

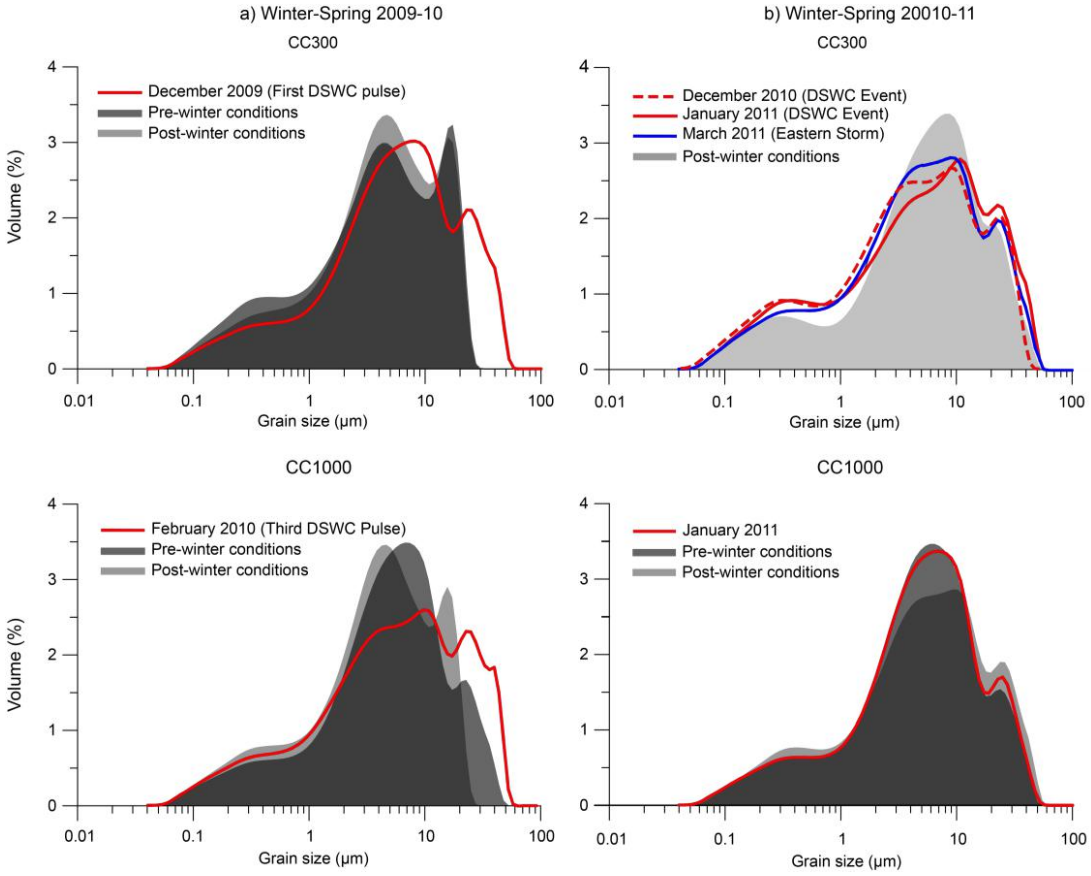

Fig. 2.6. Grain size distribution of sediment trap samples. Black represents the grain size distribution at the beginning of the winter (initial conditions) and gray the grain size distribution at the end of the winter (final conditions). Red and blue lines represent the grain size distribution during main transport events. (a) Grain size distribution at CC300 and CC1000 during winter 2009-2010. (b) Grain size distribution at CC300 (dashed line for December 2010 DSWC event and continuous line for January 2011 DSWC event) and CC1000 during winter 2010-2011.

During the second winter-spring, smaller changes in the grain size distribution of the sediments collected by the sediment traps were recorded. Nevertheless, the samples

collected at CC300 during mid-late January 2011 and during the first half of March 2011 displayed a clear coarsening with respect to the initial and final conditions (end of December 2010 and first half of June 2011, respectively) (Fig. 2.6b). No remarkable changes were recorded in CC1000 during the second winter-spring evaluated.

2.1.6 DISCUSSION

2.1.6.1 ATMOSPHERIC FORCING OF PARTICLE FLUXES IN WINTER 2009-2010

Winter 2009-2010 was characterized by the occurrence of several wind storms that triggered important changes in the water column structure and the sediment transport downcanyon. The northern windstorms occurring in December 2009 resulted in strong sea-atmosphere heat losses in the studied area (Fig. 2.3a-c). Cumulated SHF increased 640 W m^{-2} in less than two weeks (Fig. 2.3b), which represents an average of sensible heat losses of 58 W m^{-2} per day. These values are higher than those reported by Schroeder et al. (2010) for "normal" winters in the nearby convection zone, where most extreme heat losses are believed to occur (42-43° N, 4-5 °E). Consequently, at the end of December 2009 shelf waters lost temperature, became denser and sank, overflowing the shelf edge and cascading downslope through the Cap de Creus submarine canyon, as shown by the decrease in near-bottom water temperature at the upper canyon. This process, known as DSWC, has been recently studied in detail in several papers (e.g. Canals et al., 2006; Heussner et al., 2006; Palanques et al., 2006). The DSWC event started in December 2009, lasted for about 2 months and was formed by 3 main pulses of water.

The first DSWC pulse was recorded at the end of December 2009. This event increased down-canyon suspended sediment fluxes mainly by increasing the current speed up to 0.77m s^{-1} and caused an increase in the TMF up to 40.2 g m^{-2} d^{-1} at CC300 (Fig. 2.2e, g). In addition, grain size distributions of the particles collected by the sediment trap display a clear coarsening during this pulse (Fig. 2.6a). This means that the cascading currents were strong enough to resuspend and transport coarse particles in suspension from the shelf downwards to the basin. Nevertheless, currents were not strong enough to transport sediment deeper in the canyon, as suggested by the low TMF measured at

CC1000. Overall, data suggest that the sediment eroded and transported by the dense water plume settled in somewhere between CC300 and CC1000.

From the end of December 2009 to mid-January 2010, several cold and dry northern windstorms with high wind speeds led to a continued period of heat losses. This sustained heat loss triggered a continued cooling of the surface waters and thus a loss of buoyancy. In consequence, DSWC was reactivated in mid-January, as confirmed by the decrease in the near-bottom water temperature and the sharp increase in the current speed and in the SSC at CC300. The strong intensification in current speed (up to 1.12m s^{-1}) and in SSC (up to 34.68 mg L^{-1}) denoted a major escape of resuspendible fine sediments from the shelf and down the canyon. Furthermore, the TMF at both CC300 and CC1000 increased slightly, evidencing that, this time, cascading waters reached probably the middle canyon course. In addition, the coarsening of the samples collected during this event at CC1000 indicates that, effectively, the cascading waters flowed downcanyon, reaching depths of at least 1000 m.

The third DSWC pulse started February 2010. At this stage, the superficial waters of the GoL were probably completely unstratified as a result of the continued wind cooling and mixing processes that took place during the winter. Winter cumulated SHF in the beginning of February was higher than 520 W m^{-2} (note the high slope of SHF in February 2010 Fig. 2.3b) and the cumulated turbulent heat losses were around 11×10^3 W m^{-2}. This might have caused surface water temperature to decrease, resulting in pronounced buoyancy losses of the coastal waters of the GoL. This situation led shelf waters to cascade downslope continuously for a prolonged time period (from the beginning of February 2010 until the beginning of March 2010), as can be seen by the long and marked drop in near-bottom water temperature (of more than 3 ºC) and the notable increase in the current speed at the upper canyon (Fig. 2.2d, e). However, this event resulted in a small increase in down-canyon suspended sediment fluxes at CC300. Guillén et al. (2006) suggested that the "memory" of the past events on the shelf plays a crucial role in sediment dynamics as the recurrence of the preceding storms reduces the availability of fresh shelf sediments that can be resuspended. This also suggests that those events in December 2009 and January 2010 cleaned erodible sediments in the upper canyon and thus cascading waters in February flowed without a significant suspended sediment transport to CC300 (Fig. 2.2g). However, cascading

waters may have eroded part of the sediments trapped between the two moorings in the upper-middle canyon, thus triggering an increased arrival of particles, with the maximum fluxes recorded at the CC1000 station (Fig. 2.2g). This is also confirmed by the grain size distributions of particles settling during that event, which repeatedly show coarsening when compared to the pre- and post-winter conditions (Fig. 2.6a). Overall, the results demonstrate the multi-step sediment transport by cascading pulses, first from the shelf to the upper canyon, and then from the upper canyon to the middle canyon, as observed in winter 2006 by Pasqual et al. (2006) and Palanques et al. (2012). In addition, the arrival of resuspended particles through the southern flank of the canyon may have caused TMF to increase only at middle canyon depths and not at the canyon head (Canals et al., 2006; Martín et al., 2013). Even though with decreasing current speeds (and thus with decreasing capacity of eroding sediments), the DSWC pulse triggered another increase in TMF at the CC1000 station in the end of March 2010, at the very end of the cascading event.

2.1.6.2 ATMOSPHERIC FORCING OF PARTICLE FLUXES IN WINTER 2010-2011

An eastern windstorm with high E winds and Hs up to 3.9 m affected the Cap de Creus area in fall 2010. This episode was followed by increased river discharge in the rivers adjacent to the study area, which altogether reached 1,661 $m^3\ s^{-1}$ (Fig. 2.2c). As the mooring lines were not yet deployed, we cannot investigate the impact of this eastern storm on the sediment transport downcanyon.

The following months were characterized by the occurrence of cold and dry northern windstorms. Cumulative turbulent heat fluxes from the beginning of November 2010 to late December 2010 were about 400 $W\ m^{-2}$ higher than during the same months in the previous winter. Heat loss triggered a loss of buoyancy and the occurrence of DSWC along the submarine canyon. In fact, it seems that there is a certain heat loss threshold above which DSWC occurs, as can be seen when comparing the two winters evaluated (Fig 2.3a-b). During the first winter it was not until turbulent heat fluxes (Fig. 2.3c) reached values of about 6×10^3 $W\ m^{-2}$ that the first DSWC event occurred. The same happened during winter 2010-2011 - the first dense shelf water pulse was recorded, as a near-bottom water temperature drop, when winter cumulative turbulent heat fluxes reached values of around 6×10^3 $W\ m^{-2}$ (Fig. 2.3c).

The DSWC event of December 2010 lasted for 17 days and triggered increased current speeds. The consequences of this event were a rapid but discrete increase in the current speed, SSC and TMF in the canyon head (Fig. 2.2e-g). Furthermore, the newly formed water plume became dense enough to cascade along the canyon, reaching depths of at least 1000 m as the TMF of the CC1000 recorded values of approximately 16.6 g m^{-2} d^{-1} (Fig. 2.2g).

Turbulent heat losses from the beginning of January until March 2011 were lower than the previous 2009-2010 winter. Furthermore, the increased river discharge recorded in the Rhone River throughout winter, together with the punctual discharge from the smaller rivers opening to the Gulf of Lions, suggest the presence of a large amount of light freshwater in the shelf. This might have inhibited dense water formation through increased buoyancy of surface waters.

In late January 2011 a slight temperature drop indicates the arrival of dense shelf waters. The occurrence of a concomitant eastern storm with Hs of up to 3.6 m suggests that the eastern storm reactivated punctually DSWC, despite the freshwater inhibition. Indeed it is well known that eastern storms cause intense shelf sediment resuspension, which can decrease buoyancy and form a downcanyon flow (Palanques et al., 2006; Sanchez-Vidal et al., 2012). This is demonstrated by the increased current speed (0.71 m s^{-1}), SSC (11.02 mg L^{-1}) and TMF (up to 29.0 g m^{-2} d^{-1}) at the canyon head. The turbid flow might have stopped before reaching the CC1000 station as no significant TMF increase was recorded. The grain size of the samples collected during this event presented a clear coarsening at CC300 but not at CC1000 (Fig. 2.6b).

In mid-March 2011, another eastern storm occurred, with Hs of more than 4.5 m, which was accompanied by a significant increase in the Massif Central and Pyrenees rivers discharge (Figs. 2.2c, 2.3d). Increased current speeds (up to 0.68 m s^{-1}) and SSC (up to 7.37 mg L^{-1}) were recorded. The fact that flooding occurred several days after the main pulse of downcanyon sediment transport suggest again, that erosion from the adjacent shelf was the main source of particles introduced in the canyon during mid-March 2011 (Martín et al., 2013). The turbid flow did not penetrate into the canyon deeper than about 350 m. The coarsening of the grain size of the particles collected at CC300 suggest that near-bottom currents during this event where strong enough to

resuspend and transport coarse particles in suspension from the shelf to the canyon head (Fig. 2.6b).

2.1.6.3 VARIABILITY IN COMPOSITION OF THE SETTLING PARTICLES AND CHL A

2.1.6.3.1 PRINCIPAL VARIATIONS IN THE COMPOSITION OF THE SETTLING PARTICLES OF WINTER-SPRING 2009-2010

Winter 2009-2010 dense shelf water pulses caused TMF to increase and to be dominated by the siliciclastic fraction (more than 67 %) (Fig. 2.5). During December 2009, and January and February 2010, the composition of the settling particles was relatively constant, showing that DSWC pulses transported homogenized materials from the same origin (i.e. the shelf and upper slope) towards the basin (as reported before by Pasqual et al. (2010)). Furthermore, during these events, the non-siliciclastic fraction was close to the values reported by Heussner et al. (2006), with ~ 20-30 % $CaCO_3$, 2-3 % OM, and opal was virtually absent. These values were also close to those reported by Roussiez et al. (2006) for the superficial sediments from the shelf and upper slope (31 % $CaCO_3$, 1-4 % OM and opal nearly absent or under detection limit).

In the end of the winter and beginning of spring, the changes in the composition of the settling particles responded to a seasonal control. The higher variability in the biological signal (i.e. OM and opal content) occurred in response to the biological spring bloom recorded during March and April 2010 (Fig. 2.4). The less severe hydrodynamic conditions (end of the major cascading pulse) also favored the reduction of the input of resuspended lithogenic particles.

The $CaCO_3$ relative abundance displayed an apparently random pattern with higher values in January and February 2010, which are not related to OM and opal peaks (Fig. 2.5). The resuspension and transport of carbonated shell remains from the shelf is the most plausible explanation, as suggested by Martín et al. (2006) in the nearby La Fonera submarine canyon (Fig. 2.1).

2.1.6.3.2 COMPOSITION VARIABILITY OF SETTLING PARTICLES DURING WINTER-SPRING 2010-2011

In the context of a milder and wetter 2010-2011 winter-spring period, the high lithogenic fraction in settling particles suggests also a dominant resuspended origin, especially in the shallower station, which was the more affected by the main sediment transport events. However, primary production products (i.e. OM and opal) dilution due to increased lithogenic sediments resuspension was lower, most likely because of the weakened main transport events. This was also evident in the relative abundance of $CaCO_3$ and especially at the CC1000 station, which was impacted by less events than the preceding winter and spring. Nevertheless, at CC300 the $CaCO_3$ relative abundance decreased progressively until the end of February 2011. At the same time, an increase of OM and lithogenic contributions were recorded, which in absence of any primary production event suggests the arrival of OM-rich resuspended material. The occurrence of a weakened dense shelf water cascading may have triggered a selective winnowing of fine (and OC-rich, following Tesi et al., 2010 and Sanchez-Vidal et al., 2008) particles (Ferré et al., 2005; Bourrin et al., 2008) that sedimented in the head of the canyon. The development of the phytoplanktonic bloom in spring 2011 (Fig. 2.4) may have increased the contribution of $CaCO_3$, together with OM and opal to maximum levels (Fig. 2.5).

2.1.7 CONCLUSIONS

This study compares hydro-sedimentary processes and associated particle fluxes in the westernmost submarine canyon of the Gulf of Lions, at the outlet of the shelf and slope cyclonic circulation system of the area, during the winters and part of the springs of 2009-2010 and 2010-2011. During these periods, contrasting atmospheric forcings developed and led to unequal modifications of the thermohaline properties of the upper ocean layer.

A more pronounced ocean-to-atmosphere heat transfer (up to 14.2 × 103 W m^{-2}) occurred in winter 2009-2010, which triggered a stronger cooling of the water over the continental shelf, compared to winter 2010-2011. This situation resulted in an increase in the density of surface water, which sank and cascaded at higher velocities (up to 0.99 m s^{-1}) down the Cap de Creus canyon. The higher current speeds recorded during

winter 2009-2010 caused higher erosion, resuspension and ultimately transport of sediment to the mid-canyon reach. In contrast, reduced heat losses were recorded (12.6 × 103 W m^{-2}) during winter 2010-2011, which, together with a high volume of cumulated freshwater over the shelf, inhibited the penetration of dense shelf water down to the middle canyon. A noticeable eastern storm that occurred during this winter-spring, resulted in peak near-bottom currents of 0.68 m s^{-1} at 300 m and the export of particles only down to the upper canyon reach.

The lithogenic fraction was dominant in the particle fluxes of the two winter-spring seasons, which point to a resuspension origin, despite the comparatively milder character of the 2010-2011 winter. The variability in OM and opal contents followed a seasonal pattern in response to the plankton spring bloom during March and April 2010 and 2011.

The $CaCO_3$ relative abundance also showed a noticeable variability both within each winter-spring and between the two winter-spring periods. Variability sources are, however, different. The apparently random pattern of $CaCO_3$ in 2009-2010 is attributed to the resuspension of relict carbonate shells during the multi-pulse, deep-penetrating DSWC of that winter. In contrast, the weakened transport events during winter-spring 2010-2011 triggered the resuspension of only fine (and OM-rich) particles. Furthermore, the lower advection of resuspended sediments favored an increase in the relative content of the biogenic components (OM, opal and $CaCO_3$) during the spring bloom.

These results confirm that DSWC plays a key role in governing the timing, composition and volumes of particle fluxes that are exported down Cap de Creus canyon, while eastern storms similar to the one recorded in winter-spring 2010-2011 can also contribute to enhance erosion, resuspension and the off-shelf transport of particles independently of the occurrence of DSWC.

Acknowledgements. This research has been supported by the EC-funded HERMIONE (FP7-ENV-2008-1-226354) and PERSEUS RTD projects (FP7 287600), and by the Spanish projects GRACCIE (CSD2007-00067) and DOS MARES (CTM2010-21810-C03-01). J. Martín was funded through a JAE-DOC contract within the Program “Junta Para la Ampliación de Estudios”, granted by Consejo Superior de Investigaciones Científicas

and co-financed by the European Social Fund. Generalitat de Catalunya is acknowledged for support to GRC Marine Geosciences through its Grups de Recerca Consolidats grant 2009 SGR 1305. We thank D. Amblas and the crew of the vessels Lluerna and Felipe for their dedication during mooring operations. We also thank M. Guart for helping with the laboratory work, X. Rayo for his technical assistance when using Geographic Information Systems, A. Micallef for improving the English, and two anonymous referees for their valuable comments.

2.1.8 REFERENCES

Bourrin, F., Durrieu de Madron, X., 2006. Contribution of the study of coastal rivers and associated prodeltas to sediment supply in north-western Mediterranean Sea (Gulf of Lions), Life and Environment 56, 307-314.

Bourrin, F., Durrieu de Madron, X., Heussner, S., Estournel, C., 2008. Impact of winter dense water formation on shelf sediment erosion (evidence from the Gulf of Lions, NW Mediterranean), Continental Shelf Research 28, 1984-1999.

Canals, M., Casamor, J.L., Urgeles, R., Farrán, M., Calafat, A.M., Amblas, D., Willmott, V., Estrada, F., Sánchez, A., Arnau, P., Frigola, J., Colás, S., 2004. Mapa del relleu submarí de Catalunya, 1:250 000; Institut Cartogràfic de Catalunya, Barcelona, Spain, 1 map.

Canals, M., Puig, P., Durrieu de Madron, X., Heussner, S., Palanques, A., Fabres, J., 2006. Flushing submarine canyons, Nature 444, 354-357.

Company, J.B., Puig, P., Sardà, F., Palanques, A., Latasa, M., Scharek, R., 2008. Climate influence on deep sea populations, PloS one 3, e1431.

Deser, C., Alexander, M.A., Xie, S.-P., Phillips, A.S., 2010. Sea Surface Temperature Variability: Patterns and Mechanisms, Annual Review of Marine Science 2, 115-143.

Durrieu de Madron, X., Zervakis, V., Theocharis, A., Georgopoulos, D., 2005. Comments to “Cascades of dense water around the world ocean”, Progress in Oceanography 64, 83-90.

Estrada, M., 1996. Primary production in the Northwestern Mediterranean, Scientia Marina 60, 55-64.

Fabres, J., Tesi, T., Velez, J., Batista, F., Lee, C., Calafat, A., Heussner, S., Palanques, A., Miserocchi, S., 2008. Seasonal and event controlled export of organic matter from the shelf towards the Gulf of Lions continental slope, Continental Shelf Research 28, 1971-1983.

Ferré, B., Guizien, K., Durrieu de Madron, X., Palanques, A., Guillén, J., Grémare, A., 2005. Fine-grained sediment dynamics during a strong storm event in the inner-shelf of the Gulf of Lion (NW Mediterranean), Continental Shelf Research 25, 2410-2427.

Guillén, J., Palanques, A., Puig, P., Durrieu de Madron, X., Nyffeler, F., 2000. Field calibration of optical sensors for measuring suspended sediment concentration in the Western Mediterranean, Scientia Marina 64, 427-435.

Guillén, J., Bourrin, F., Palanques, A., Durrieu de Madron, X., Puig, P., Buscail, R., 2006. Sediment dynamics during wet and dry storm events on the Têt inner shelf (SW Gulf of Lions), Marine Geology 234, 129-142.

Heussner, S., Ratti, C., Carbonne, J., 1990. The PPS 3 time-series sediment trap and the trap sample processing techniques used during the ECOMARGE experiment, Continental Shelf Research 10, 943-958.

Heussner, S., Durrieu de Madron, X., Calafat, A., Canals, M., Carbonne, J., Delsaut, N., Saragoni, G., 2006. Spatial and temporal variability of downward particle fluxes on a continental slope: Lessons from an 8-yr experiment in the Gulf of Lions (NW Mediterranean), Marine Geology 234, 63-92.

Ivanov, V.V., Shapiro, G.I., Huthnance, J.M., Aleynik, D.L., Golovin, P.N., 2004. Cascades of dense water around the World Ocean. Progress in Oceanography 60, 47-98.

Josey, S.A., 2003. Changes in the heat and freshwater forcing of the eastern Mediterranean and their influence on Deep Water Formation, Journal of Geophysical Research 108, C02032.

Josey, S.A., Kent, E.C., Taylor, P.K., 1999. New insights into the ocean heat budget closure problem from analysis of the SOC air sea flux climatology, Journal of Climate 12, 2856-2880.

Lastras, G., Canals, M., Urgeles, R., Amblas, D., Ivanov, M., Droz, L., Dennielou, B., Fabrés, J., Schoolmeester, T., Akhmetzhanov, A., Orange, A., García-García, A., 2007. A walk down the Cap de Creus canyon, Northwestern Mediterranean Sea: Recent processes inferred from morphology and sediment bedforms, Marine Geology 246, 176-192.

Ludwig, W., Meybeck, M., Abousamra, F., 2003. Riverine transport of water, sediments, and pollutants to the Mediterranean Sea, UNEP MAP Technical report Series 141, UNEP/MAP Athens, 111 pp.

Martín, J., Palanques, A., Puig, P., 2006. Composition and variability of downward particulate matter fluxes in the Palamós submarine canyon (NW Mediterranean), Journal of Marine Systems 60, 75-97.

Martín, J., Miquel, J.C., Khripounoff, A., 2010. Impact of open sea deep convection on sediment remobilization in the western Mediterranean, Geophysical Research Letters 37, L13604.

Martín, J., Durrieu de Madron, X., Puig, P., Bourrin, F., Palanques, A., Houpert, L., Higueras, M., Sanchez-Vidal, A., Calafat, A.M., Canals, M., Heussner, S., Delsaut, N., Sotin, C., 2013. Sediment transport along the Cap de Creus Canyon flank during a mild, wet winter, Biogeosciences 10, 3221-3239.

Martín-Vide, J., Raso Nadal, J.M., 2008. Atlas climàtic de Catalunya, Període 1961-1990, Institut Cartogràfic de Catalunya, Barcelona.

MEDOC Group: Observation of formation of deep water in the Mediterranean Sea, 1969, 1970. Nature 227, 1037-1040.

Millot, C.A., 1999. The Gulf of Lions' hydrodynamic. Cont. Shelf Res., 10, 885-894, 1990.Millot, C., Circulation in the Western Mediterranean Sea, Journal of Marine Systems 20, 423-442.

Mortlock, R.A., Froelich, P.N., 1989. A simple method for the rapid determination of biogenic opal in pelagic marine sediments, Deep-Sea Research Part A: Oceanographic Research Papers 36, 1415-1426.

Palanques, A., Durrieu de Madron, X., Puig, P., Fabres, J., Guillén, J., Calafat, A., Canals, M., Heussner, S., Bonnin, J., 2006. Suspended sediment fluxes and transport processes in the Gulf of Lions submarine canyons, The role of storms and dense water cascading, Marine Geology 234, 43-61.

Palanques, A., Guillén, J., Puig, P., Durrieu de Madron, X., 2008. Storm-driven shelf-to-canyon suspended sediment transport at the southwestern Gulf of Lions, Continental. Shelf Research 28, 1947-1956.

Palanques, A., Puig, P., Durrieu de Madron, X., Sanchez-Vidal, A., Pasqual, C., Martín, J., Calafat, A., Heussner, S., Canals, M., 2012. Sediment transport to the deep canyons and open-slope of the western Gulf of Lions during the 2006 intense cascading and open-sea convection period, Progress in Oceanography 106, 1-15.

Pasqual, C., Sanchez-Vidal, A., Zúñiga, D., Calafat, A., Canals, M., Durrieu de Madron, X., Puig, P., Heussner, S., Palanques, A., Delsaut, N., 2010. Flux and composition of settling particles across the continental margin of the Gulf of Lion: the role of dense shelf water cascading, Biogeosciences 7, 217-231.

Puig, P., Palanques, A., Orange, D.L., Lastras, G., Canals, M., 2008. Dense shelf water cascading and furrows formation in the Cap de Creus Canyon, northwestern Mediterranean Sea, Continental Shelf Research 28, 2017-2030.

Pusceddu, A., Bianchelli, S., Canals, M., Sanchez-Vidal, A., Durrieu De Madron, X., Heussner, S., Lykousis, V., de Stigter, H., Trincardi, F., Danovaro, R., 2010. Organic matter in sediments of canyons and open slopes of the Portuguese, Catalan, Southern Adriatic and Cretan Sea margins, Deep Sea Research Part I: Oceanographic Research Papers 57, 441-457.

Roussiez, V., Ludwig, W., Monaco, A., Probst, J.L., Bouloubassi, I., Buscail, R., Saragoni, G., 2006. Sources and sinks of sedimentbound contaminants in the Gulf of Lions (NW

Mediterranean Sea): A multi-tracer approach, Continental Shelf Research 26, 1843-1857.

Salvadó, J.A., Grimalt, J.O., López, J.F., Durrieu de Madron, X., Heussner, S., Canals, M., 2012. Transformation of PBDE mixtures during sediment transport and resuspension in marine environments (Gulf of Lion, NW Mediterranean Sea), Environmental Pollution 168, 87-95.

Sanchez-Vidal, A., Pascual, C., Kerhervé, P.A., Calafat, A., Heussner, S., Palanques, A., Durrieu de Madron, X., Canals, M., Puig. P., 2008. Impact of dense shelf water cascading on the transfer of organic matter to the deep Western Mediterranean Basin, Geophysical Research Letters 35, L05605.

Sanchez-Vidal, A., Pasqual, C., Kerhervé, P., Heussner, S., Calafat, A., Palanques, A., Durrieu de Madron, X., Canals, M., Puig, P., 2009. Across margin export of organic matter by cascading events traced by stable isotopes northwestern Mediterranean Sea, Limnology and Oceanography 54, 1488-1500.

Sanchez-Vidal, A., Canals, M., Calafat, A., Lastras, G., Pedrosa-Pàmies, R., Menéndez, M., Medina, R., Company, J.B., Hereu, B., Romero. J., Alcoverro, T., 2012. Impacts on the Deep-Sea Ecosystem by a Severe Coastal Storm, PLoS one 7, e30395.

Schroeder, K., Josey, S.A., Herrmann, M., Grignon, L., Gasparini, G.P., Bryden, H.L., 2010. Abrupt warming and salting of the Western Mediterranean Deep Water: Atmospheric forcings and lateral advection, Journal of Geophysical Research 115, C08029.

Serrat, P., Ludwig, W., Navarro, B., Blazi, J.L., 2001. Variabilité spatio-temporelle des flux de matières en suspension d'un fleuve côtier méditerranéen: la Têt (France), Spatial and temporal variability of sediment fluxes from a coastal Mediterranean river: the Têt (France), Comptes Rendus de l'Académie des Sciences – seriesIIA 333, 389-397.

Tesi, T., Puig, P., Palanques, A., Goñi, M.A., 2010. Lateral advection of organic matter in cascading-dominated submarine canyons, Progress in Oceanography 84, 185-203.

Ulses, C., Estournel, C, Bonnin, J., Durrieu de Madron, X., Marsaleix, P., 2008a. Impact of storms and dense water cascading on shelf-slope exchange in the Gulf of Lions (NW Mediterranean), Journal of Geophysical Research 113, CO2010.

Ulses, C., Estournel, C., Durrieu de Madron, X., Palanques, A., 2008b. Suspended sediment transport in the Gulf of Lion (NW Mediterranean): impact of extreme storms and floods, Continental Shelf Research 28, 2048-2070.

2.2 PARTICLE FLUXES AND THEIR DRIVERS IN THE AVILÉS SUBMARINE CANYON AND ADJACENT SLOPE, CENTRAL CANTABRIAN MARGIN, BAY OF BISCAY

A. Rumín-Caparrós[a], A. Sanchez-Vidal[a], C. González-Pola[b], G. Lastras[a], A. Calafat[a], M. Canals[a]

[a]GRC Geociències Marines, Departament de Dinàmica de la Terra i de l'Oceà, Universitat de Barcelona, E-08028 Barcelona, Spain
[b]Instituto Español de Oceanografía, C.O. Gijón, Avda. Príncipe de Asturias 70 bis, E-33212 Gijón, Spain

Progress in Oceanography 144, 39-61, 2016.
http://dx.doi.org/10.1016/j.pocean.2016.03.004 0079-6611/

2.2.1 ABSTRACT

The Avilés Canyon in the central Cantabrian margin is one of the largest submarine canyons in Europe, extending from the shelf edge at 130 m depth to 4765 m depth in the Biscay abyssal plain. In this paper we present the results of a year-round (March 2012 to April 2013) study of particle fluxes in this canyon and the adjacent continental slope. Three mooring lines equipped with automated sequential sediment traps, high-accuracy conductivity-temperature recorders and current meters allowed measuring total mass fluxes and their major components (lithogenics, calcium carbonate, opal and organic matter) in the settling material jointly with a set of environmental parameters. The integrated analysis of the data obtained from the moorings together with remote sensing images and meteorological and hydrographical data has shed light on the sources of particles and the across- and along margin mechanisms involved in their transfer to the deep.

Our results allow interpreting the dynamics of the sedimentary particles in the study area. Two factors play a critical role: (i) direct delivery of river-sourced material to the narrow continental shelf, and (ii) major resuspension events caused by large waves and

near bottom currents developing at the occasion of the rather frequent severe storms that are typical of the Cantabrian Sea. Wind direction and subsequent wind-driven currents largely determine the way sedimentary particles reach the canyon. While westerly winds favour the injection of sediments into the Avilés Canyon mainly by building an offshore transport in the bottom Ekman layer, easterly winds ease the offshore advection of particulate matter towards the Avilés Canyon and its adjacent western slope principally through the surface Ekman layer. Furthermore, repeated cycles of semidiurnal tides add an extra amount of energy to the prevailing bottom currents and actively contribute to keep a permanent background of suspended particles in near-bottom waters.

High contents of lithogenics in settling particles at the three mooring stations confirm that riverine inputs are the principal source of particles to the Avilés Canyon, including the lowermost canyon, and the adjacent open slope. Primary production also has a strong influence on the amount and the composition of particulate matter, with more than 30% of the total mass flux being of biogenic origin (organic matter, opal and calcium carbonate).

2.2.2 INTRODUCTION

Submarine canyons are large seafloor geomorphological features connecting the shallower with the deeper sections of continental margins (Shepard, 1981; Nittrouer and Wright, 1994; Xu et al., 2002; Canals et al., 2006; Mulder et al., 2012). Multiple studies have demonstrated that submarine canyons act as pathways for water movements, lithogenic and biogenic materials (Gardner, 1989; Puig and Palanques, 1998; Hung et al., 2003; Palanques et al., 2006a), hot spots of biodiversity and biological productivity (Vetter, 1994; Vetter and Dayton, 1998; Gili et al., 1999; Vetter et al., 2010).

One of the main aims of the Spanish DOS MARES project (Deep-water submarine canyons and slopes in the Mediterranean and Cantabrian seas: from synchrony of external forcings to living resources) was to understand how the signal of different forcings is transferred and how it affects the deep ecosystem in submarine canyons and continental slopes around the Iberian Peninsula, with an emphasis on the Avilés Canyon in the Cantabrian margin of the Bay of Biscay. Processes controlling particulate

matter transport (e.g. atmosphere and gravitational-driven) have been studied in submarine canyons all over the world (Drake and Gorsline, 1973; Hickey et al., 1986; Durrieu de Madron, 1994; van Weering et al., 2002; Puig et al., 2004a; Paull et al., 2005; Xu et al., 2010; Pierau et al., 2011). In the Iberian Peninsula there is a strong contrast between Atlantic margin settings and Mediterranean ones, including physiography and water depth, water mass structure and ocean dynamics.

In the Western Mediterranean Sea, east of the Iberian Peninsula, the best-studied canyons are those located in the Gulf of Lion and the Catalan margin. Some of those canyons, especially Cap de Creus Canyon, experience high energy events in the form of seasonal dense shelf water cascading, a type of flow that erodes the shelf and slope floor and funnels large volumes of water and sediments into the deep margin and basin (Canals et al., 2006; Heussner et al., 2006). Cascading is triggered by strong, persistent, cold and dry northern winds, causing heat loss and an increase in the density of shelf waters that eventually overflow the shelf and cascade down the slope. Coastal downwelling caused by eastern storms also enhances downcanyon sediment transport (Martín et al., 2006; Palanques et al., 2006a; Bonnin et al., 2008; Sanchez-Vidal et al., 2012). In addition to heavy precipitation and river floods carrying significant amounts of sediments and forming surface plumes along the coast, Eastern winds push surface waters against the coastline, where high waves and associated currents lead to major resuspension events of inner shelf sediments. Part of the sediment load resulting both from river floods and shelf resuspension is ultimately captured by canyons having their heads at short distance from the coastline and then is exported down-canyon (Canals et al., 2013). River floods have also been identified as the main drivers for down-canyon sediment transport in submarine canyons off southern Spain, in the Alborán Sea (Palanques et al., 2005). Bottom trawling practiced on the shelf around canyon heads and along canyon flanks also results in sediment gravity flows that move into the canyon axis, as recently shown in La Fonera Canyon, in the north Catalan margin (Puig et al., 2012).

The Atlantic continental margin west of Iberia hosts some particularly large submarine canyons according to global standards, such as Nazaré, Lisbon-Setúbal and Cascais canyons (Arzola et al., 2008; Tyler et al., 2009; Martín et al., 2011; de Stigter et al., 2011). In contrast with microtidal environments such as the Western Mediterranean Sea, Atlantic tidal currents are strong enough to trigger resuspension and remobilise

particulate matter (Oliveira et al., 2007), especially in upper canyon sections (de Stigter et al., 2007, 2011). The role of shelf storms, eventually combined with river floods, over particulate matter transport from the upper to the middle course of Nazaré Canyon is discussed in Martín et al. (2011). Also in the Atlantic is the northern Iberian, or Cantabrian margin forming the southern bound of the Bay of Biscay. The Cantabrian margin is cut by several, deeply incised submarine canyons and is bounded to the east by the large, more than 2000 km long Cap Breton Canyon, where tidally-induced hydrodynamic events are able to remobilise and sustain a permanent up-and down-canyon transport of particulate matter (Mulder et al., 2012). Shelf storms also play a key role in modulating sediment transport down Cap Breton Canyon. However, in the Cap Ferret submarine canyon, in the eastern margin of the Bay of Biscay, Schmidt et al. (2014) found only a limited downslope particle transfer from the shelf to the basin along the canyon attributed to the disconnection of this canyon from major sediment sources. Further north, in the north-eastern margin of the Bay of Biscay, in the Audierne and Blackmud canyons, particulate matter is resuspended and remobilised by strong tidal hydrodynamics (Mulder et al., 2012).

These studies support the relevance of external forcings on sediment dynamics and particle fluxes within submarine canyons and in the adjacent continental slopes. The external forcings referred to in the previous paragraphs are either atmospherically driven (wind storms, river floods, winter cooling and mixing), gravity driven (tides) or anthropogenic driven (trawling induced resuspension) and all of them are capable of triggering significant sediment transport events in the submarine canyons off the Iberian Peninsula. In addition, the overall margin configuration, including the distance of canyon heads to the nearest shoreline, largely determines the capability of submarine canyons to trap coastal sediment and funnel it down course (Canals et al., 2013).

The above-mentioned background information underlines the existence of a knowledge gap on the behaviour of submarine canyons incised in the Cantabrian margin that our study contributes to fill in, as it is the first of its nature in the central Cantabrian margin. The present study focuses on sediment transfer and particle fluxes from shallow to deep, thus aiming to improve the understanding of the functioning of submarine canyons at large and of Avilés Canyon in particular. Avilés Canyon can be considered as a representative of submarine canyons in the Northeast Atlantic, so that

the high productivity and biodiversity associated with these features (Vetter, 1994; De Leo et al., 2010; Vetter et al., 2010) can be better understood, assessed and managed.

2.2.3 REGIONAL SETTING

The Avilés Canyon is the main, 80 km long trunk of a canyon system that consists of three main branches with contrasting morphologies: the El Corbiro and La Gaviera canyons to the east and the Avilés Canyon itself to the west (Fig. 2.7). El Corbiro and La Gaviera merge before opening into the lowermost course of the Avilés Canyon, which opens to the Biscay abyssal plain at 4765 m depth (Lastras et al., 2012; Gómez-Ballesteros et al., 2013).

Several rivers discharge along the Cantabrian coastline. Their flows are modulated by a typical oceanic climate, with a rainy season starting in November and ending in May and a drier season taking place from June to October (Prego et al., 2008). The main contributor of freshwater and terrigenous sediment to the coastline close to Avilés Canyon head is the 138 km long Nalón River opening into the 15 km long Pravia estuary. The Nalón River is fed by a 4893 km^2 catchment area and has an annual average flow of 109 $m^3\ s^{-1}$ according to Prego et al. (2008), with annual peaks up to 1250 $m^3\ s^{-1}$. These values make the Nalón River watershed and flow the largest in the Cantabrian river system (Prego et al., 2008). Its main tributary is the 111 km long Narcea River with a catchment area of 1135 km^2 and a mean annual discharge of 16 $m^3\ s^{-1}$ (‘‘Confederación Hidrográfica del Cantábrico” online resources in http://chcantabrico.es/index.php/es/atencionciudadano/documentos/documentos-de-la-web/search/lang,es-es/). The Nalón River discharge presents a strong seasonal character following the above-referred rainy and dry seasons. Eight main dams in the Nalón watershed, of which the tallest are Tanes in Nalón River upper course and La Barca in Narcea River, with 95 and 74 m of dam height, respectively (www.seprem.es), and a number of smaller ones, do not have an influence strong enough to wipe off the natural seasonal regime. However, the amounts of sediment trapped behind those dams has not been quantified yet. Of the twenty-eight Cantabrian rivers investigated by Prego et al. (2008), the Nalón River is the one with the highest load (836 $m^3\ s^{-1}$) of total suspended solids (TSS) and is identified as the most important Cantabrian river in terms of TSS contribution to the Bay of Biscay with 379.900 t y^{-1} representing 33% of the total.

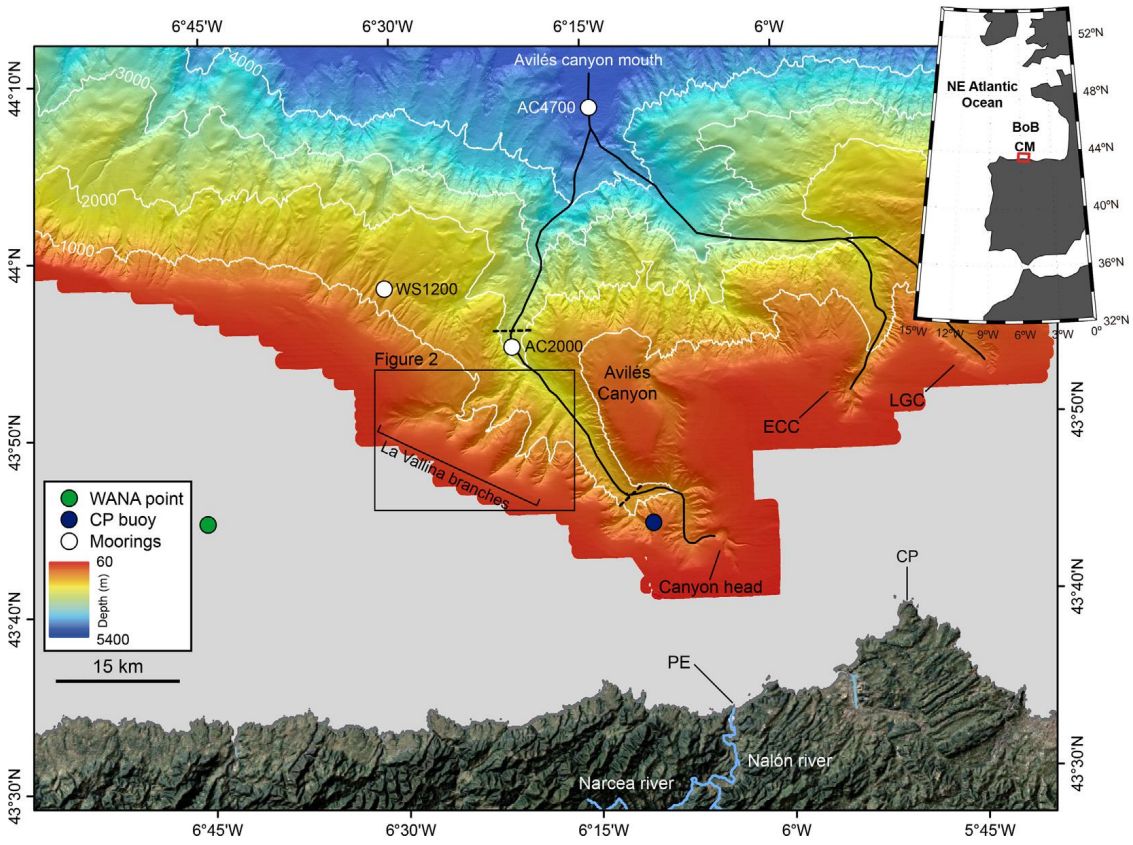

Fig. 2.7. Shaded relief bathymetric map of the Avilés submarine canyon and surrounding shelf, slope and deep basin. The location of the El Corbiro Canyon (ECC) and the La Gaviera Canyon (LGC) are indicated. Location of moorings (white dots), Cabo Peñas coastal buoy (blue dot) and WANA point 1053075 (green dot) are also presented. Dashed black lines mark the boundaries of the upper and middle canyon course. The black box includes La Vallina branches illustrated in Fig. 2.8. Land topography from the NASA's Lance rapid response MODIS satellite true colour images. Depth is in meters. The top right map represents the NE Atlantic Ocean with the Cantabrian margin (CM) forming the southern bound of the Bay of Biscay (BoB). (For interpretation of the references to colour in this figure legend, the reader is referred to the web version of this article.)

Consistently with its geographical location, the water column structure in the Bay of Biscay, and the Cantabrian Sea in particular, corresponds to the Northeast Atlantic one (Lavín et al., 2006). Namely: (1) surface waters extending down to the winter maximum depth (250 m) of the mixed layer (González-Pola et al., 2007), which are characterized by a pronounced inter-annual variability linked to seasonal cycles; (2) the East North

Atlantic Central Water (ENACW) from the base of the mixed layer down to 400-600 m; (3) the Mediterranean Outflow Water (MOW) that is located below the ENACW and extends down to depths of 500-1500 m (Iorga and Lozier, 1999a); and (4) the Bottom Water (BW) extending down to the seafloor as a deep water mass formed after the mixing of several water masses including the North Atlantic Deep Water (NADW), the Lowered Deep Water (LDW) and Antarctic Bottom Water (ABW) (Botas et al., 1989; Pingree and Le Cann, 1992; van Aken, 2000a).

The ENACW results from winter mixing over the area surrounded by the North Atlantic Current (NAC) and the Azores Current (AC) (Pollard and Pu, 1985; Pollard et al., 1996). Two varieties of ENACW are defined according to their origin, temperature and salinity (Ríos et al., 1992). The denser variety, or subpolar mode of the ENACW, forms in the southern border of the NAC. In the Bay of Biscay it flows weakly and experiences an anticyclonic recirculation (Pingree, 1993). The lighter variety, or subtropical mode of the ENACW, forms at the northern boundary of the AC and is conveyed along the northwestern and north Iberian upper continental slope by the Iberian Poleward Current (IPC) (Haynes and Barton, 1990). The IPC circulates poleward along the western and northern Iberian continental shelf and slope, eventually reaching the French Armorican shelf (Pingree and Le Cann, 1990). The MOW results from the outflow of Mediterranean dense deep water into the Atlantic Ocean through the Gibraltar Strait. The northern branch of the MOW flows along the Western Iberian margin as a slope current (Iorga and Lozier, 1999a, 1999b; van Aken, 2000b) and reaches the Bay of Biscay with speeds between 2 and 3 cm s^{-1} (Pingree and Le Cann, 1990; Díaz del Río et al., 1998). The BW draws a cyclonic recirculation cell over the Biscay abyssal plain with a poleward current velocity of 1.2 cm s^{-1} nearby the foot of the continental margin (Dickson et al., 1985; Paillet and Mercier, 1997).

Seasonal wind patterns have a significant impact on the sea surface circulation over the shelf and slope of the study area (Charria et al., 2013). NNE to easterly winds, typically more common from April to September, induce a westward shelf and slope surface circulation and promote coastal upwelling. The presence of the Avilés Canyon system seems to enhance upwelling during such situations, which results in an up-canyon flow (Ruiz-Villarreal et al., 2004). In contrast, NW winds, which can be very strong and usually are dominant from October to March, lead to an eastward shelf and slope surface circulation and coastal downwelling. Under these conditions, the

submarine canyon does not seem to have any effect on the incident slope current (Ruiz-Villarreal et al., 2004). The influence of the IPC surface flow over the western Iberian and Cantabrian slopes in winter extends to the first 200-300 m depth so impacting the upper slope (Frouin et al., 1990; Haynes and Barton, 1990; Pingree and Le Cann, 1990, 1992; Serpette et al., 2006; Friocourt et al., 2007; Le Cann and Serpette, 2009).

Semi-diurnal tidal oscillations on the Avilés shelf are highly energetic and can dominate current dynamics (Fanjul et al., 1997). Barotropic tides above steep topographies such as submarine canyons give rise to internal tides, especially where the slope gradient becomes critical (i.e. wherever the topographic slope matches the propagation angle of the internal tide beams) (Baines, 1982; Cacchione et al., 2002). According to data from ‘‘Puertos del Estado”, the mean meso-tidal range at the coast close to Avilés Canyon for the period 1996-2013 ranged between 1.95 m and 4.68 m at neap and spring tides, respectively, and exceeded 5 m during equinoctial tides. In the Bay of Biscay, the dominance of the semi-diurnal barotropic forcing over the shelf-break and slope makes the internal tide to be markedly semi-diurnal (Pingree and New, 1989). The capability of such tides to influence sedimentary processes by triggering bottom currents fast enough to resuspend sediment has been described in the nearby Aquitanian margin of the Bay of Biscay (Durrieu de Madron et al., 1999).

2.2.4 MATERIALS AND METHODS

2.2.4.1 FORCING CONDITIONS

Wind speed and direction at 3 m above the sea surface and wave height and direction were obtained from Cabo Peñas Sea-watch buoy measuring waves as well as atmospheric and oceanographic parameters at an hourly frequency (Álvarez Fanjul et al., 2003). The buoy, which belongs to the Deep Water Network from ‘‘Puertos del Estado”, is moored at 615 m of water depth on a sort of plateau in the western flank of the Avilés Canyon upper course (Fig. 2.7). Near surface currents are not corrected for platform motion and all the data gathered by the network buoys is subject to a quality control procedure to find inconsistencies and other anomalies in the datasets.

The buoy data have been crosschecked by linear correlation (not shown) with the coded WANA point 1053075 (see location in Fig. 2.7) in order to further validate the wind and wave data used in our work. The WANA network delivers hourly averaged time series of wind (at 10 m above the sea surface) and wave parameters obtained from a reanalysis product performed by ‘‘Puertos del Estado” in collaboration with ‘‘Agencia Estatal de Meteorología”.

The wind-drag-induced Ekman transport perpendicular to the coastline (Q_y) is normally taken as an Upwelling Index (UI). This index is an estimate of across-slope transport depending on local wind. In our study, the dominant orientation of the coastline is in the east-west direction and the UI magnitude expresses volume of water transported in the north-south direction by lineal km of shore (in $m^3\ s^{-1}\ km^{-1}$). UI has been calculated from Cabo Peñas buoy wind data according to Bakun (1973) using equation

$$UI = Q_y = -\frac{\tau_x}{f \cdot \rho_w}, \tag{2.4}$$

where τ_x is the wind stress for the *x* component, f is the Coriolis parameter calculated as $f = 2\Omega \sin \Phi$ at 43° of latitude, and ρ_w is seawater density (1025 kg m^{-3}). Upwelling is characterized by positive values of Q_y whereas negative values are indicate of water masses piling up towards the coast (i.e. downwelling). The wind stress for the *x* component is calculated with equation

$$\tau_x = \rho_a \cdot C_d \cdot \sqrt{U^2 + V^2} \cdot U, \tag{2.5}$$

where ρ_a is the density of air, U and V are the eastward and north-ward wind components, respectively, and C_d is the neutral drag air coefficient computed following Smith (1988).

Discharges by Nalón River and its main tributary, the Narcea River, measured from gauging stations located at 23 and 22 km from the river mouth, respectively, have been obtained from EDP group of companies.

Estimates of Chl-a concentrations are from the Giovanni online data system, developed and maintained by the NASA Goddard Earth Sciences (GES) Data and Information

Services Center (DISC), using the Moderate Resolution Imaging Spectroradiometer (MODIS) as our data source. Data have been gridded from 43.4ºN to 45ºN, and from 7.5ºW to 4ºW in order to include the mooring locations and the areas adjacent to Avilés Canyon. Net primary production data were downloaded from the Ocean Productivity website (http://www.science.oregonstate.edu/ocean.productivity/) and calculated using the Vertically Generalized Production Model (VGPM) (Behrenfeld and Falkowski, 1997). For VGPM, net primary production is a function of chlorophyll, available light, and the photosynthetic efficiency.

Forcing conditions have also been considered indirectly by means of a two-way statistical ANOVA analysis intended to examine the factors responsible for the variability of Total Mass Fluxes (TMFs) in the Avilés Canyon and in its western slope. For this analysis, two fixed factors were considered: month of collection and trap depth (Table 2.2; see Section 2.2.5.3).

A cross-correlation analysis has been performed in order to check the extent of the correlation between the external forcings and the TFMs temporal variability (Table 2.3; see Section 2.2.5.3). Given that raw time series with different time steps ranging from hourly to daily periods present occasional gaps, data were resampled at regular and continuous time series prior to the statistical analysis. All data were re-sampled to a time step equivalent to the sampling period of the sediment traps and such time lapse has been used as a ‘‘lag” to evaluate time-lagged correlations between time series. Gaps in TMFs in AC2000T trap were linearly interpolated considering the low variability of TMFs in the other sediment traps during the data gap (Fig. 2.10).

2.2.4.2 MULTIBEAM DATA ACQUISITION

Prior to the deployment of the mooring lines, and in order to accurately identify the more convenient locations to install them, a seabed high-resolution bathymetric survey including the acoustic characterization of the seabed of the Avilés Canyon and the adjacent continental slope was performed. Multibeam data covering 5682 km^2 of the Cantabrian margin around the Avilés Canyon was acquired in October-November 2011 during the COCAN cruise onboard R/V ‘‘Miguel Oliver”. Data were obtained with a Simrad EM302D multibeam echosounder operated in equidistant mode with swath widths between 600 m on the shelf and 6000 m on the abyssal plain. The complete

dataset was processed onboard using Caris HIPS and SIPS software, resulting in a general 20 m-grid-size digital terrain model.

2.2.4.3 EXPERIMENTAL DESIGN

The high-resolution multibeam bathymetry maps evidenced the complex morphology of the Avilés Canyon system and the adjacent continental slope. Jointly with backscatter imagery (not shown), multibeam bathymetry served as background information to decide where to deploy the mooring lines to investigate the across margin transport of particulate matter and characterise the associated ambience conditions, both within and outside the Avilés Canyon. Two moorings (AC2000 and AC4700) where placed in the middle course and lowermost course of the canyon at 2000 m and 4700 m depth, respectively (Fig. 2.7 and Table 2.1). AC2000 was deployed in order to capture sediment fluxes eventually arriving from both the shelf-incising set of tributaries known as La Vallina branches and from the Avilés Canyon head and upper course (see Section 2.2.5.1). AC4700 was deployed in a very flat area where the Avilés Canyon widens significantly and opens into the Biscay abyssal plain down course of La Gaviera Canyon mouth which main tributary is El Corbiro Canyon (Fig. 2.7). Therefore, AC4700 was well suited to capture sediment fluxes arriving from the entire Avilés Canyon system. A third mooring (WS1200) was deployed as a control station at 1200 m depth in the open slope west of Avilés Canyon (Fig. 2.7).

All mooring lines were equipped with automated sequential sediment traps, high-accuracy conductivity-temperature recorders and current meters. They were deployed during one complete annual cycle in two consecutive periods, from March 2012 to September 2012 and from September 2012 to March 2013.

Station	Water Depth (m)	Meters above the bottom (m)	Meters below surface (m)	TWF (g m^{-2} d^{-1})	Lithogenic		$CaCO_3$		OM		Opal	
					%	Flux (g m^{-2} d^{-1})	%	Flux (g m^{-2} d^{-1})	%	Flux (g m^{-2} d^{-1})	%	Flux (g m^{-2} d^{-1})
WS1200	1200	46	1154	0.99	61.42	0.54	26.78	0.30	8.62	0.078	3.09	0.09
AC2000T (mid-water)	2000	822	1178	0.43	61.32	0.30	24.93	0.14	10.25	0.05	3.00	0.0021
AC2000B (near-bottom)	2000	46	1954	1.98	66.98	1.37	24.42	0.47	6.52	0.14	2.20	0.07
AC4700	4700	46	4654	0.33	53.05	0.17	35.19	0.12	7.42	0.025	4.36	0.017

Table 2.1. Average annual fluxes (g m^{-2} d^{-1}) and relative contribution of each of the major constituents to particle fluxes in the Avilés Canyon and adjacent open slope to the west.

The AC2000 mooring line was equipped with two Aquadopp current meters at 44 and 820 m above the bottom (mab), and two PPS3 sediment traps coupled with SBE37 recorders at 46 m and 822 mab. Hereafter, AC2000T and AC2000B will be used to refer to the mid-water (at 820 mab or 1200 m of water depth) and near-bottom levels in this mooring, respectively. The AC4700 mooring line was equipped with a single RCM8 current meter at 44 mab and a PPS3 sediment trap at 46 mab. The WS1200 mooring line was equipped with a pair of current meters, which were an Aquadopp acoustic Doppler current meter at 160 mab and an Aanderaa RCM8 rotor current meter at 44 mab, and a Technicap PPS3 sediment trap coupled with a SBE37 high-accuracy conductivity-temperature recorder at 46 mab.

The PPS3 Technicap sequential sediment traps have a 0.125 m^2 collecting surface and a 2.5 height/diameter ratio in its cylindrical part. They are equipped with 12 receiving cups (Heussner et al., 1990), which were filled with a buffered 5% (v/v) formaldehyde solution in 0.45 μm filtered seawater. This solution is used to prevent the degradation of the collected particles in the retrieving cups and also to avoid fragmentation and degradation of swimmers occasionally entering the sampling cups. All traps collected settling particles synchronously and uninterruptedly with a sampling interval of 15-16 days during the first and second deployment periods except the last three collecting bottles of February 2013, which remained opened 7 days in order to adjust the total sampling interval to the scheduled recovery dates. Traps worked properly from 16th March 2012 to 23rd September 2012, and from 1st October 2012 to 8th March 2013, except AC2000T, which stopped collecting samples before the end of the first deployment period, on the first of August 2012.

Aandera and Aquadopp current meters were set to collect data at 15 minutes intervals at upper levels and 30 minutes near the bottom. A technical failure of the current meter deployed at AC4700 resulted in the complete data loss at this water depth.

2.2.4.4 TRAP COLLECTION EFFICIENCY

Trap collection efficiency has been checked by examining the pitch and roll sensors of the current meters. Efficiency can be compromised by trap tilting (Gardner, 1985) and also due to the potential of perturbation of trap mouths on

lateral flows causing biases in the collection of sinking particles (e.g. Baker et al., 1988; Gardner et al., 1997; Buesseler et al., 2007 and references therein).

Data from the current meter pressure sensors show that sediment trap tilting never exceeded 11°, even during current speeds as high as 40 cm s^{-1}. According to Gardner (1985) TMFs would not have been affected (see explanation on how TMFs have been calculated in Section 2.2.4.6). Our results compare well with those obtained by Bonnin et al. (2008) in their collecting efficiency experiment using the same PPS3 Technicap sediment traps. These authors concluded that their mooring lines were maintained taut, close to vertical, never tilting more than 15°, during strong current episodes (up to 82 cm s^{-1}).

Since we do not have enough information to detect any effect of perturbation by trap mouths on lateral flows, and in order to be consistent with the extensive published data using the same sediment traps in other locations around the Iberian Peninsula and beyond (e.g. Heussner et al., 1999; Fabrés et al., 2002; Miquel et al., 2011; Stabholz et al., 2013), we assume that hydrodynamics over the trap mouth did not bias mass fluxes.

2.2.4.5 SEDIMENT TRAP SAMPLE PROCESSING AND ANALYTICAL METHODS

After recovery, samples were stored in the dark at 4 °C until they were processed following a modified version of the methodology of Heussner et al. (1990). Swimming organisms were removed in two steps according to its size: large swimmers were removed by wet sieving through a 1 mm nylon mesh and organisms of less than 1 mm were handpicked using fine tweezers under a microscope. A high-precision peristaltic pump robot was used to split samples into aliquots through repeated division of the sample. Samples were then rinsed repeatedly with Milli-Q water, centrifuged to remove formaldehyde and salt, and freeze-dried before chemical analyses. The dried fraction was weighted to obtain the total mass. TMFs were calculated as follows:

$$TMF\ (g\ m^{-2}\ d^{-1}) = \frac{Sample\ dry\ weight\ (g)}{Collecting\ area\ (m^2) \cdot sampling\ interval\ (days)}, \qquad (2.6)$$

Total carbon, organic carbon (OC) and nitrogen (N) contents were analysed at ‘‘Centres Científics i Tecnològics” of ‘‘Universitat de Barcelona” using an elemental analyser Thermo EA Flash 1112. In order to determine the OC content, samples were first decarbonated with 25% HCl through repeated addition of 100 µL aliquots until no effervescence was observed. Between each acidification, samples were dried during 8 h at 60 ºC. Organic matter (OM) content was calculated as twice the organic carbon content. Inorganic carbon content was calculated as total carbon minus organic carbon. Carbonate content was calculated assuming that all inorganic carbon is contained within calcium carbonate ($CaCO_3$), using the molecular mass ratio of 100/12.

Biogenic silica was analysed by extracting the amorphous silica by means of a two-step 2.5 h extraction with 0.5 M Na_2CO_3 separated by centrifugation of the leachates according to Fabrés et al. (2002). Si and Al contents of leachates were analysed with Inductive Coupled Plasma Atomic Emission Spectrometer (ICP-AES). The Si content of the first leachate was corrected by the Si/Al ratio of the second one, and corrected biogenic Si concentrations were transformed to opal by multiplying by a factor of 2.4 (Mortlock and Froelich, 1989).

Abundance of the lithogenic fraction was obtained by subtracting from the total mass the part corresponding to major biogenic components, assuming that the amount of lithogenics (%) was = 100 (%OM + %$CaCO_3$ + %opal).

2.2.4.6 CALCULATION OF LATERAL FLUXES OF SUSPENDED SEDIMENT

Advection of suspended matter in Avilés Canyon and in the slope west to the canyon has been calculated from data acquired by the current and turbidity meters deployed near the bottom. Recorded Nephelometric Turbidity Units (NTU) have been converted to suspended sediment concentration (SSC) using Eq. (4) by Guillén et al. (2000):

$$SSC\ (g\ m^{-3}) = 1.74 \cdot Turbidity\ (NTU) - 1.32 \qquad (2.7)$$

SSC has been multiplied by current speed to obtain the magnitude (in g m^{-2} s^{-1}) of lateral fluxes (LF).

2.2.5 RESULTS

2.2.5.1 MORPHOLOGY OF THE AVILÉS CANYON

The Avilés Canyon is incised about 25 km in the central Cantabrian continental shelf, which is 45 km wide west of the canyon but only 13 km wide ahead of the canyon tip located 18 km WNW of the large coastal promontory of Cabo Peñas (Fig. 2.7). The tip of the canyon is at 130 m water depth and opens to a canyon head and upper course that display three sharp bends probably related to the underlying tectonic lineations (Lastras et al., 2012).

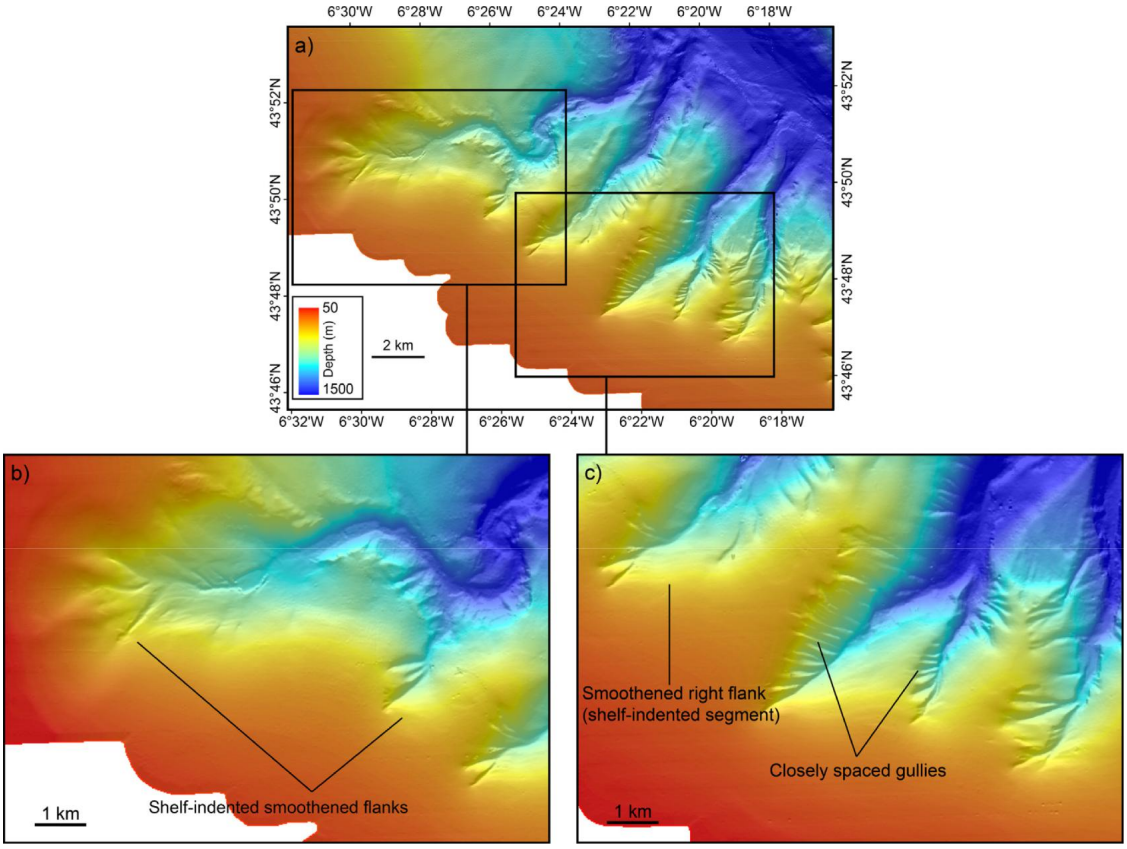

Fig. 2.8. Shaded relief images of tributaries entering the Avilés Canyon from its western flank. (a) General view of tributaries incised in the western flank of the Avilés Canyon middle course and lower upper course. (b) Zoom in of La Vallina westernmost branch showing a dominantly smoothened relief. (c) Zoom in of a set of La Vallina branches showing a smoothened relieve mainly of the right flanks of shelf-incised segments. Note the presence of some flank gullies locally forming closely spaced sets. See Fig. 2.7 for location. (For interpretation to colour in this figure, the reader is referred to the web version of this article.)

Several tributaries join the Avilés Canyon upper and middle course, mostly through its western flank at axial depths ranging between 1300 and 2100 m (Fig. 2.7). The group named La Vallina branches includes four main tributaries, which are SW-NE oriented and also markedly incised on the shelf (Fig. 2.8a-c). With the only exception of the western most branch, La Vallina branches are straight or nearly straight. The two eastern branches show smoothened right flanks along the length incised in the continental shelf, which oppose to gullied left flanks (Fig. 2.8b and c). In the two western branches, the two flanks look moderately smoothened with some gullies occurring locally. The lower Avilés Canyon is SSW-NNE oriented and its increasingly wide floor is interrupted by a series of overdeepenings (Lastras et al., 2012). The Avilés Canyon mouth opens to the Biscay abyssal plain in an area occupied by a faint sedimentary wave field (Gómez-Ballesteros et al., 2013).

2.2.5.2 EXTERNAL FORCINGS

Nalón River discharge time series show increased values in early February 2012 (up to 1071 m^3 s^{-1}), mid April 2012 (602 m^3 s^{-1}), late January 2013 (853 m^3 s^{-1}), and late March 2013 (669 m^3 s^{-1}). Other less marked increased discharge episodes occurred in November and December 2012 (up to 300 m^3 s^{-1}) and February-March 2013 (up to 484 m^3 s^{-1}) (Fig. 2.9a).

High Chl-a concentrations during March 2012 and April 2013 (Fig. 2.9b) correspond to the well-known seasonal phytoplankton spring bloom in the region (e.g. Fernández and Bode, 1991).

The wind regime during the entire monitoring period from March 2012 to March 2013 is characterized by a recurrent alternation between easterly and westerly winds as a response to the coastal polarization of winds (Fig. 2.9c). Higher wind speeds were recorded during westerly wind bursts (Fig. 2.9c and d). However, there were also several periods of strong winds with an important meridional component (such as December 2012, Fig. 2.9c and d). Wave direction (i.e. the direction from which waves arrive to the study area in degrees counted clockwise from the geographical North) shows a marked northwest component during the studied period (Fig. 2.9e). Maximum significant wave heights (Hs) were recorded in mid April 2012 and during late January-early February 2013 (Fig. 2.9f) under predominant westerly winds.

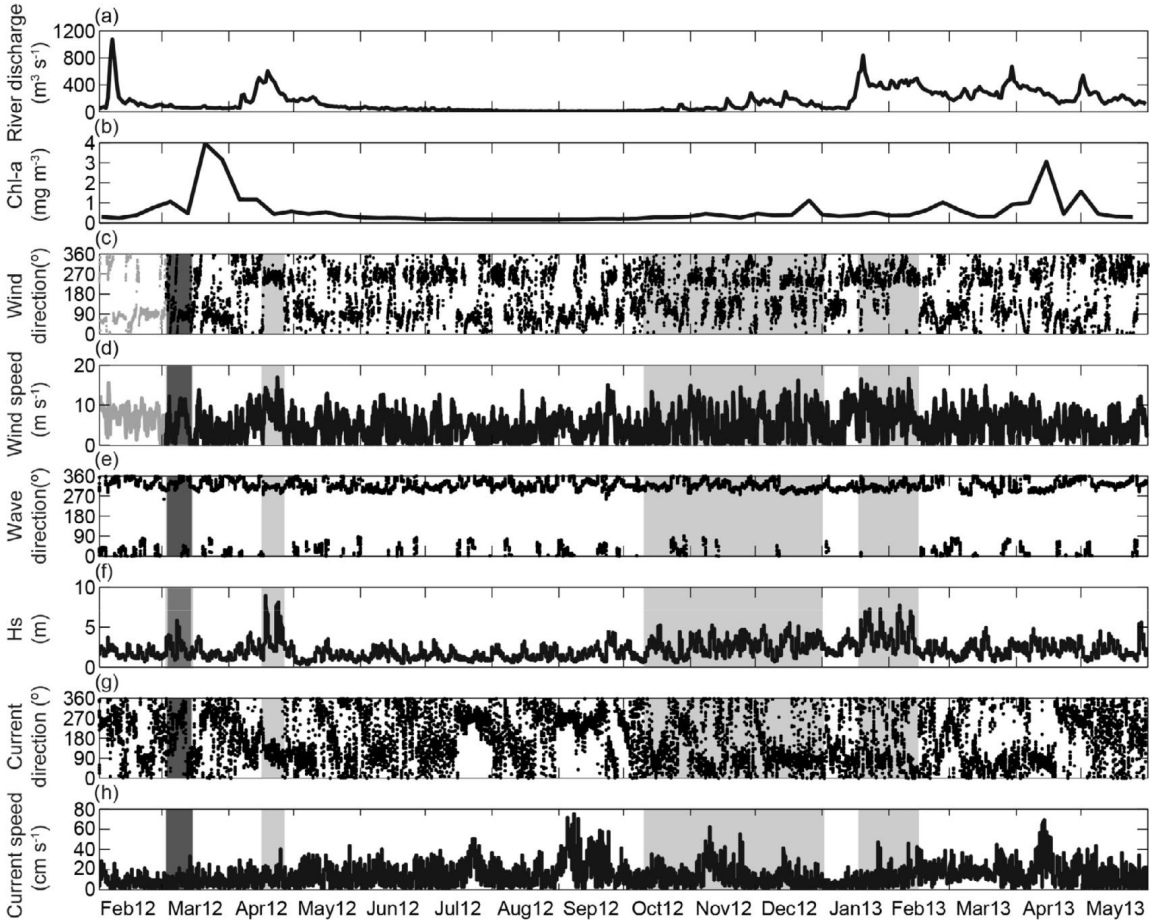

Fig. 2.9. (a) Water discharge of Nalón River encompassing the studied annual cycle (March 2012-April 2013). (b) Temporal evolution of monthly mean Chlorophyll-a concentration centred over the Avilés Canyon. (c) Wind direction at Cabo Peñas coastal buoy with dots representing the direction from which the wind is blowing. (d) Wind speed. (e) Wave direction at Cabo Peñas coastal buoy with dots representing the direction from which the waves are arriving. (f) Significant wave height (Hs) at Cabo Peñas Seawatch coastal buoy. (g) Current direction measured by the currentmeter installed in the Cabo Peñas buoy at 3 m depth. (h) Current speed at 3 m depth measured by the currentmeter of the Cabo Peñas buoy. Note that wind direction and speed records start about one month later (in grey data from the WANA point 1053075, see location in Fig. 2.7) than wave and current data due to a technical failure of the buoy's meteorological sensors. Shaded areas highlight specific events discussed in the text.

2.2.5.3 SPATIAL DISTRIBUTION AND VARIABILITY OF MASS FLUXES

The time series of vertical TMFs recorded in the sediment traps deployed in the Avilés Canyon and on the nearby open slope are shown in Fig. 2.10. TMFs fluctuate at least one order of magnitude within all stations.

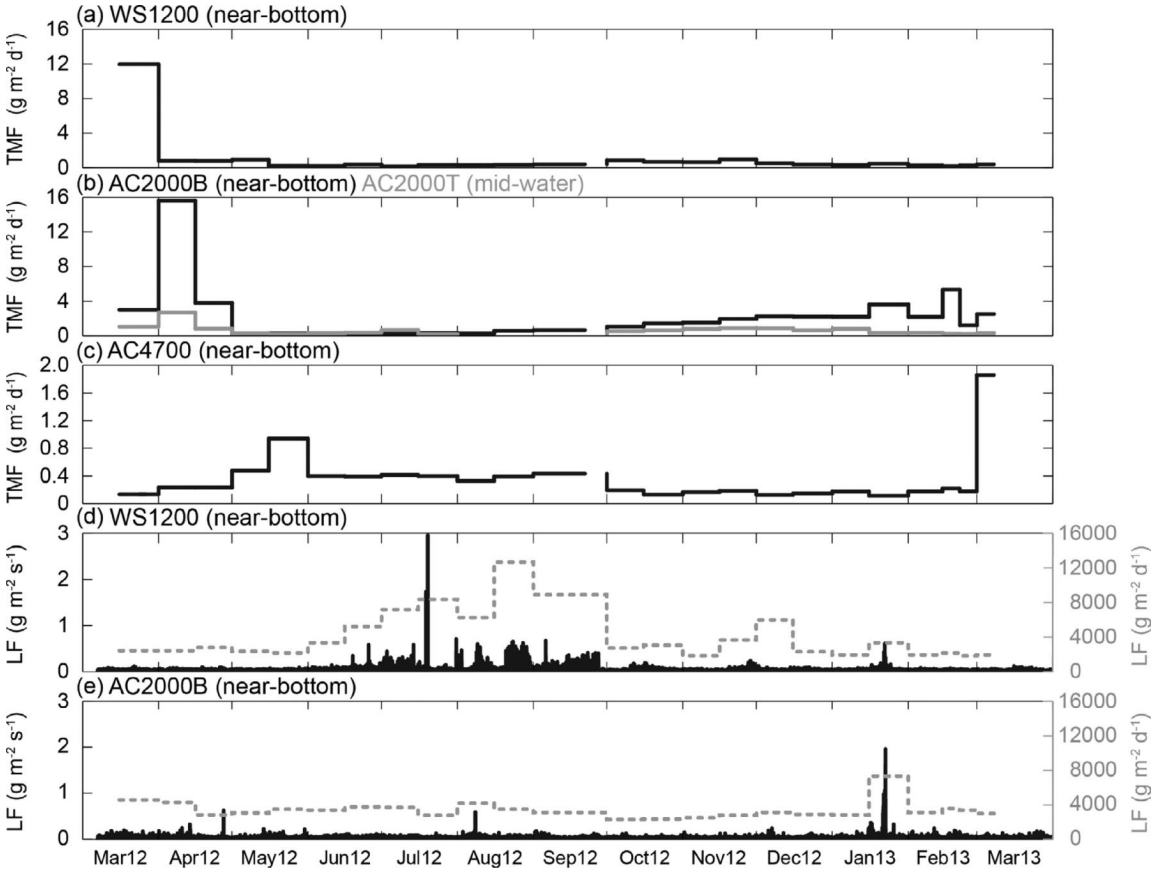

Fig. 2.10. Total mass fluxes (TMF) and lateral fluxes (LF) in the mooring stations deployed within the Avilés Canyon and on the open upper slope to the west. (a) TMFs at the open upper slope station WS1200 (near-bottom) west of the canyon. (b) TMFs in the middle course station for levels AC2000B (black stepped line, near-bottom) and AC2000T (grey stepped line, mid-water). (c) TMFs in the lowermost canyon course station AC4700 (near-bottom). (d and e) LFs at WS1200 (near-bottom) and AC2000B (near-bottom) in black. The grey dashed line represents re-sampled lateral fluxes adjusted to time steps equal to the sampling interval of the sediment traps.

At the WS1200 (near-bottom) open slope station west of Avilés Canyon, TMFs reached a maximum of 11.94 g m^{-2} d^{-1} in March 2012, whereas during the rest of

the experiment, values remained below 1 g m^{-2} d^{-1}, with a minor increase in autumn 2012 (Fig. 2.10a).

In the Avilés Canyon middle course AC2000 station, TMFs increase with increasing trap depth. At the near-bottom level (AC2000B), higher fluxes occurred during the mid-end of winter and in spring (15.65 g m^{-2} d^{-1} in April 2012, which represents the top value of TMFs recorded in all stations, and up to 5.24 g m^{-2} d^{-1} in February 2013). Relatively low fluxes were recorded during the rest of the year (between 0.19 and 2.12 g m^{-2} d^{-1}) (Fig. 2.10b), although a continuously increasing trend in TMF took place from October 2012 until almost the end of the experiment. In contrast, in the upper level (AC2000T), TMFs varied from a maximum of 2.57 g m^{-2} d^{-1} in April 2012 to a relative minimum of 0.047 g m^{-2} d^{-1} in July 2012. In October 2012 TMFs increased again until reaching a second relative maximum of 0.74 g m^{-2} d^{-1} in November and December 2012. From December 2012 to the end of the experiment, TMFs decreased progressively to 0.046 g m^{-2} d^{-1} recorded in February 2013 (Fig. 2.10b). In comparison with the deeper AC2000B trap, variability in TMFs at the shallower AC2000T is much smaller.

When compared with previous stations the TMFs at the near-bottom AC4700 canyon lowermost course station are much lower, usually around or below 0.35 g m^{-2} d^{-1}, except for two peaks of up to 0.94 and 1.86 g m^{-2} d^{-1} recorded in May 2012 and March 2013, respectively (Fig. 2.10c).

The ANOVA analysis shows that the interaction between the month of collection and the trap depth are the main source of variance in the studied area (31%). The month of collection by itself is also significant, representing 21% of the overall variability, which by extension suggests that the variability in TMFs mostly relates to the seasonality of the external forcings. Therefore, these two variables account for 52% of TMFs variability. However, 40% of the variability remains unexplained (residual) (Table 2.2).

As shown in Table 2.3, the highest correlation coefficient (>0.7) between time series of external forcings and TMFs corresponds to wave height and wind speed at time lag 1 (15 days) for the mid-water (1200 m of water depth) trap AC2000T. Good correlation coefficients (0.6) are also found for these two variables again at time lag 1 for the near-bottom (1954 m of water depth) trap AC2000B. There is a

good correlation (0.7) for the same middle canyon station AC2000 at both levels, mid-water and near-bottom, with total river discharge at time lag 3 (45 days).

Factors	SS	DF	% Total variability	*F*	*p*
Trap depth	5.22E+08	2	8	134.23	<0.001
Month of collection	1.35E+09	11	21	134.23	<0.001
Trap depth / month of collection	1.99E+09	22	31	46.60	<0.001
Residual (unexplained)	2.53E+09	1303	40		
Total	7.67E+09	1338	100		

Table 2.2. Results of the three-way ANOVA performed on total mass fluxes (TMFs). The sum of the squares (SS), the degree of freedom (DF), the relative contribution to the overall variability of TMFs of each of the factors considered, and the F value and its probability ‘‘p” are presented.

At the near-bottom, western open slope trap WS1200 the correlation of TMFs and the three variables considered in Table 2.3 is weaker (0.4-0.5) and occurs at time lag 2 (30 days) for wave height and wind speed and at time lag 4 (60 days) for total river discharge. Except for wind speed, high cross-correlation coefficients between AC4700 and the external forcings in Table 2.3 have been found at negative time lags, which are non-representative and therefore will not be considered in the discussion.

Station		Wind speed	Wave height	Total river discharge
WS1200	Correlation coefficient	0.458 (lag 2)	0.459 (lag 2)	0.507 (lag 4)
AC2000T (mid-water)	Correlation coefficient	0.716 (lag 1)	0.722 (lag 1)	0.681 (lag 3)
AC2000B (near-bottom)	Correlation coefficient	0.626 (lag 1)	0.639 (lag 1)	0.667 (lag 3)
AC4700 (near-bottom)	Correlation coefficient	0.73 (lag 0)	0.68 (lag 3)	0.69 (lag 3)

Table 2.3. Overall cross-correlation coefficients between time series of external forcings and total mass fluxes during the studied period. Each time lag unit corresponds to 15 days.

LFs are markedly different in the near-bottom stations WS1200 and AC2000B (Fig. 2.10d and e). In the open slope station WS1200, LFs show a background

level close or slightly above 0.05 g m^{-2} s^{-1} and below 0.1 g m^{-2} s^{-1} during most of the time, with some spikes from June to September 2012 and in January 2013. The most prominent of them occurred in July 2012 reaching 3 g m^{-2} s^{-1} (Fig. 2.10d). It was also in January 2013 when peak LFs (up to 2 g m^{-2} s^{-1}) were recorded in station AC2000B, where a few minor spikes are also visible (e.g. at the end of April 2012 and in the first half of August 2012, both with 0.6 g m^{-2} s^{-1}) above a similar background level than in WS1200 (Fig. 2.10e).

2.2.5.4 MEAN COMPOSITION OF PARTICLE FLUXES AND CHANGES THROUGH TIME

Lithogenics clearly dominate settling particles at all stations, with averaged annual values between 53.05% and 66.98%, and fluxes around 0.17 and 1.37 g m^2 d^{-1} (Table 1). The temporal variability of the lithogenic content is quite similar between all stations but AC2000B (Fig. 2.11a), with higher values during autumn and winter (i.e. from September 2012 to February 2013) and lower values during spring and summer (i.e. from March 2012 to August 2012). AC2000B shows the highest averaged annual value and also the lowest range of interannual variation (i.e. from 62.42% to 74.11%) (Fig. 2.11a and Table 2.1). The lithogenic contribution to TMFs is never less than 37% (Fig. 2.11a). On average it is almost six percentage points lower in AC2000T (mid-water) than in AC2000B (near-bottom), and fourteen percentage points lower in AC4700 (near-bottom) than in AC2000B. This results evidence a decrease in the percentage of lithogenics with, first, increasing distance to the seafloor and, second, increasing canyon depth.

Annualy averaged $CaCO_3$ fluxes are lower than lithogenics, ranging between 0.12 and 0.47 g m^2 d^{-1} (Table 2.1). $CaCO_3$ relative contents display a trend opposite to the lithogenics one, with lower percentage values during autumn and winter (i.e. from September 2012 to February 2013) and slightly higher values during spring and summer (i.e. from March to August 2012) (Fig. 2.11b). Higher variations were recorded during spring especially at the lowermost canyon and open western slope, where the $CaCO_3$ annualy averaged percentage is the highest among all traps. Similarly to the lithogenics, AC2000B shows the lowest range of interannual variation (i.e. from 17.16% to 30.7%), in parallel with the lowest annually averaged value, close to the one of AC2000T, with 24.42% and 24.93%, respectively (Fig. 2.11b and Table 2.1). For the two near-bottom traps deployed inside the canyon, the $CaCO_3$ annual mean content increases with water depth, being about ten

percentage points higher at the lowermost canyon (AC4700) than in the middle canyon (AC2000B) (Table 2.1). It is noteworthy that during the second half of the studied period, $CaCO_3$ records in all traps present a rather similar evolution.

OM fluxes are relatively low, with averaged annual values ranging from 0.025 to 0.14 g m^2 d^{-1} and averaged percentages around 8-10% (Table 2.1). The atomic N to OC ratio (N:OC), which is widely used to examine OM sources and source changes in settling particles, is on average 0.11 for all traps (Fig. 2.11c). Our time series show enhanced N:OC ratios (0.12-0.16) and OM relative abundance (16-18%) at station WS1200 in May 2012 and March 2013, thus indicating a marked spring seasonal signal on settling particles at this station. Similar variations were recorded at the upper trap AC2000T of station AC2000 (Fig. 2.11c), which also displays the highest annual OM contents (Table 2.1). Both traps, WS1200 and AC2000T, are in the 1150-1200 m depth range below the sea surface (Table 2.1). In contrast, settling particles at the near-bottom traps AC2000B and AC4700 within the canyon show rather stable N:OC ratios and OM relative abundances (around 0.8-0.13% and 6.5-8.6%, respectively), with only minor fluctuations except for a peak recorded at AC4700 in June 2012 (reaching 12%). By the end of the time series OM contents at all traps and stations reached minimum values to start increasing again till the end of the sampling period in March 2013. This increase was particularly important at WS1200 and AC2000T (Fig. 2.11c). The parallelism of the OM records for these two traps is noticeable and, except for the above-mentioned final part of the time series, they do not seem to be correlated with the near-bottom traps AC2000B and AC4700 (Fig. 2.11c).

Averaged annual opal fluxes range between 0.017 and 0.09 g m^{-2} d^{-1} (Table 2.1) and opal relative abundance shows different patterns depending on mooring location and water depth (Fig. 2.11d).

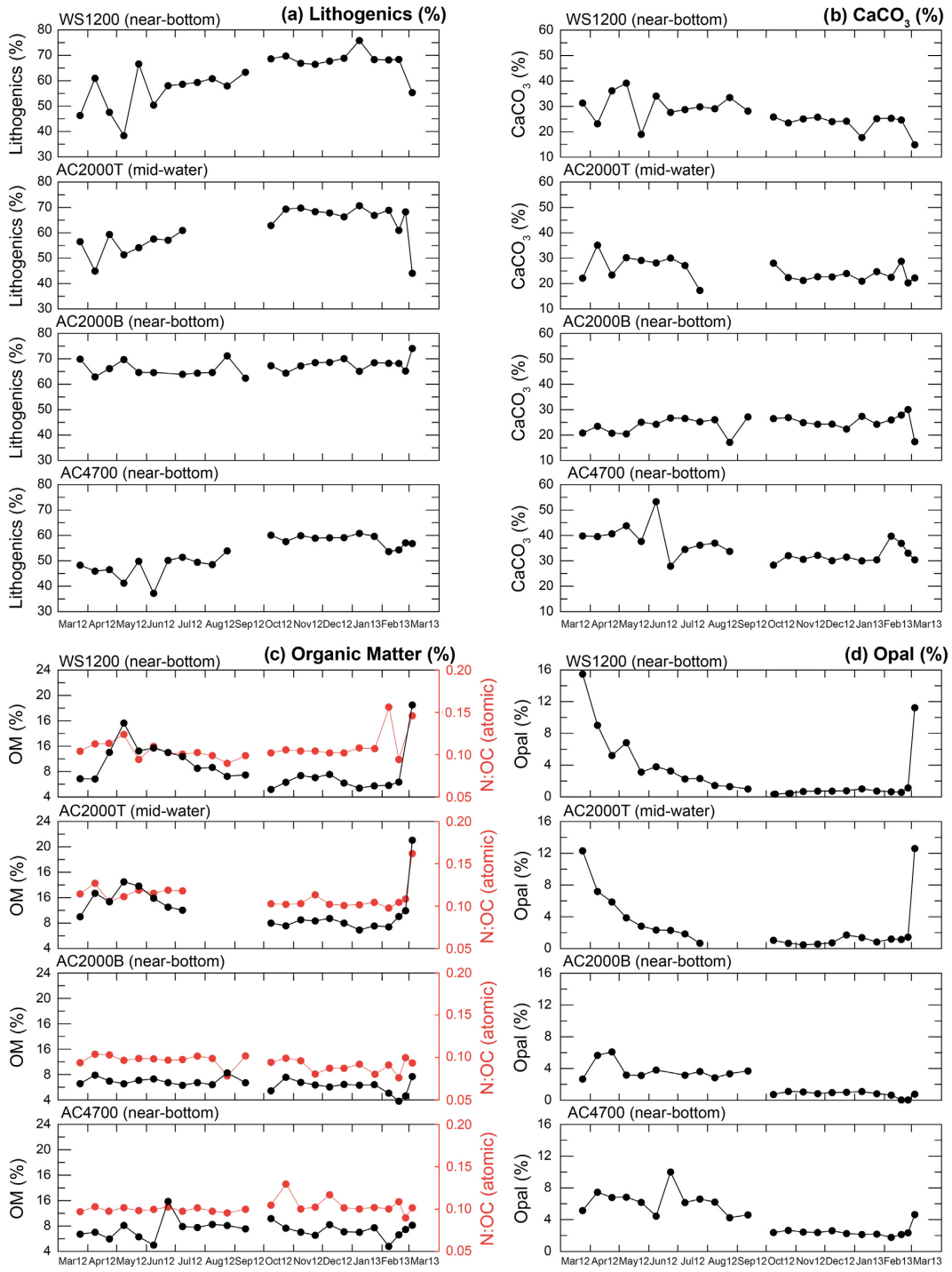

Fig. 2.11. Temporal variability of the main components of the settling particle fluxes collected by the sediment traps in the mooring stations deployed within and on the open slope west of Avilés Canyon during the studied annual cycle (March 2012-April 2013). (a) Lithogenics. (b) $CaCO_3$. (c) Organic matter (black dots), molar nitrogen:organic carbon ratios (N:C, red dots). (d) Opal. Codes of mooring stations and levels correspond to those in Figs. 2.7 and 2.11, and in Table 2.1. (For interpretation of the references to colour in this figure legend, the reader is referred to the web version of this article.)

At the two traps in the same depth range below the sea surface, the western open slope WS1200 (near-bottom) and the AC2000T (mid-water) over the middle canyon, opal content shows an obvious temporal variability peaking up at 12% in March 2012 and March 2013. In the other two, in-canyon, near-bottom traps AC2000B and AC4700, opal contents do not show a clear seasonal signal and the fluctuation rate is much lower, especially for AC2000B (Fig. 2.11c). Similarly to OM, enhanced opal relative abundances were recorded by the end of the observational period at all stations, weakly at AC2000B and strongly at WS1200 and AC2000T. Contribution of opal relative abundance to the total mass does not represent more than 15% at any trap, and opal mean annual content remains in the range from 2.20% to 4.36%, with the lowest and highest values corresponding to the near-bottom canyon traps AC2000B and AC4700, respectively. WS1200 and AC2000T display very similar values (3% and 3.09%).

2.2.6 DISCUSSION

2.2.6.1 PARTICLE SOURCES AND DISPERSAL PATTERNS

Our results show the dominance of river-sourced lithogenics in sinking particles in the study area. Quartz, feldspars, heavy minerals and aluminosilicates mainly constitute these particles. The dispersion of riverine water and lithogenic particles in the vicinity of the Avilés submarine canyon appears to be affected by seasonal reversals of sea surface circulation. During autumn and winter, the prevailing westerly winds induce an eastward shelf-slope circulation associated with downwelling conditions, which pushes sediment-loaded river plumes away from Avilés Canyon to the east, towards Cabo Peñas and beyond, as shown in the MODIS image of 21 January 2013 (Fig. 2.12a). Eastward surface currents associated with an onshore surface Ekman transport may also lead to the coastal confinement of river plumes, as also shown in Fig. 2.12a. Below the surface layer where Ekman transport occurs, there must be a compensatory circulation, directed in opposite sense. Downwelling conditions due to westerly wind forcing will then lead to an eastward shelf current that (if interacting with the bottom, which is generally the case under winter high energy conditions) corresponds to offshore transport in the bottom Ekman layer. This is because in a bottom Ekman layer the Ekman transport is directed to the right of the bottom stress, in the same way that in a surface Ekman layer the Ekman transport is directed 90º to the right of the wind stress in the Northern Hemisphere. However, given that the stress at

the seafloor is in the opposite direction of the prevailing current, the bottom Ekman transport is 90º to the left of the surface current, with the Ekman spiral turning counterclockwise with increasing depth in the Northern Hemisphere (Taylor and Sarkar, 2008).

Westerly wind pulses also reinforce the entrance of the eastward-flowing poleward slope currents over the Cantabrian margin (e.g. González-Pola et al., 2005), which extend from the surface to about 250-400 m depth (Pingree and Le Cann, 1990; Gil and Gomis, 2008). On the contrarily, during spring and summer, with prevailing easterly winds, the shelf circulation is mainly westward (Charria et al., 2013). This surface currents are associated with an upwelling component capable of entraining river plumes and resuspended shelf sediments towards the shelf edge, as shown in the MODIS image of 4 May 2013 (Fig. 2.12b), taken after an enhancement in the discharge of Nalón River (Fig. 2.9a). The same wind forcing then builds a westward coastal jet, which originates onshore transport at the bottom of the Ekman layer and thus favours the retention of resuspended sediments over the shelf. Similarly, in the nearby continental shelf of the Basque country to the east, Jouanneau et al. (2008) reported that prevailing winds and surface currents also redistribute preferentially suspended sediment river plumes, with particle settling occurring during periods of calm.

The relation between increases in river discharge (Fig. 2.9a) and TMFs in the Avilés Canyon and the western open slope (Fig. 2.10a and b) is an interesting point of discussion. Our dataset seems to suggest a connection between sustained high river discharge conditions from January to February 2013 and the increases of TMFs in near-bottom traps AC2000B and, AC4700 although the later being less clear and somewhat delayed (Fig. 2.10a-c). However, this connection is not apparent neither for AC2000T and WS1200 nor for other shorter events of enhanced river discharge, such as the one in April 2012, which apparently had no effect on TMFs in the shallower stations, as shown by high TMFs occurring before the discharge peak (Figs. 2.9a and 2.10a, b).

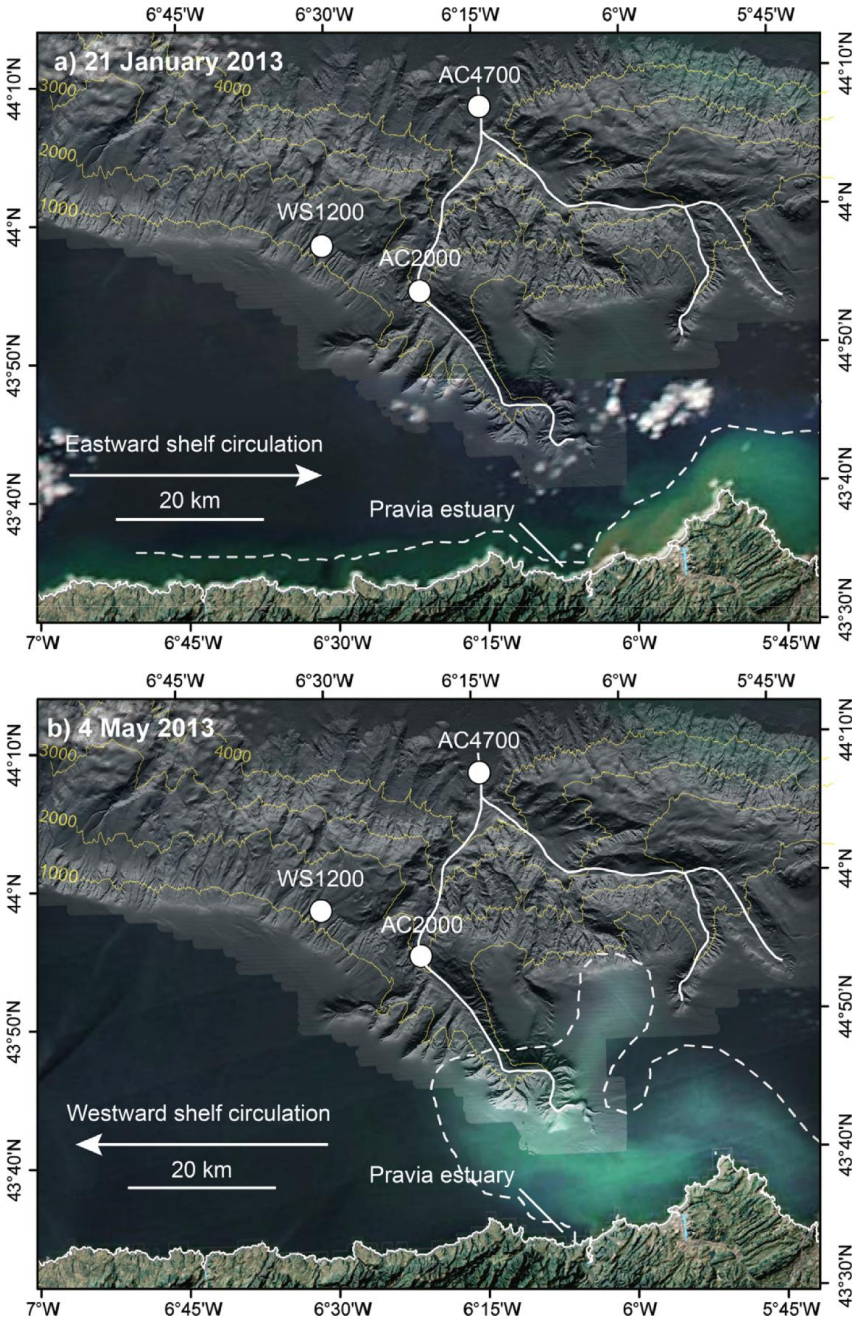

Fig. 2.12. Lance rapid response MODIS satellite true colour images from the NASA Earth Observing System Data and Information System (EOSDIS) with the shaded relief bathymetry of the Avilés Canyon and adjacent open slope as background layer. White dots indicate the mooring sites. Dashed white lines follow the outer limit of coast-derived sediment plumes at sea surface. (a) Image from 21 January 2013 illustrating plume dispersal under a westward surface circulation. (b) Image from 4 May 2013 illustrating plume dispersal under an eastward surface circulation. (For interpretation of the references to colour in this figure legend, the reader is referred to the web version of this article.)

Without totally precluding some direct connection between the river and the submarine canyon under specific conditions, it is worth considering other dispersion mechanisms that may act either by themselves or in combination with a more direct connection and among themselves. The normal winter mixed layer in the region hardly exceeds the depth of the shelf-break, as it is only about 250 m thick (González-Pola et al., 2007). Therefore, a direct influence of winter convective mixing events on sedimentary particle dynamics at depths where the moorings were deployed should not be expected and, at the most, can only be indirect and likely minor. Only exceptionally the mixed layer reaches larger depths (e.g. in 2005; Somavilla et al., 2009), thus increasing the chances to directly imprint sedimentary processes in the canyon. During winters 2012 and 2013 atmospheric forcings were not exceptionally strong and the mixed layer did not reach unusual depths (R. Somavilla, personal communication). Below the maximum winter mixed layer, the density gradient characteristic of the local permanent pycnocline (van Aken, 2001) may hinder the vertical transport of particulate matter, especially of the lighter fractions. In this context, processes favouring lateral advection of sediments from the shelf become good candidates for triggering major arrivals of river-sourced particles into the canyon. Our hypothesis is that river-sourced particles temporarily accumulate on the shelf until high-energy forcing conditions (see Section 2.2.6.2) capable to resuspend and lead to bottom Ekman layer transport carry them into the canyon. This involves a critical assessment of the bottom transport against the surface transport to avoid misleading interpretations (see Section 2.2.6.2.1). A similar mechanism of delayed transfer to the continental slope and submarine canyons has been described in other margin settings, such as the Gulf of Lion and the North Catalan margin, where dense shelf water cascading and eastern storms provide such high-energy conditions (Canals et al., 2006; Ulses et al., 2008a; Sanchez-Vidal et al., 2012).

Marine primary production is the second main source of sinking particles in the study area. In the shelf and offshore waters of the Cantabrian margin there is a seasonal succession of phytoplankton species that relates directly to the hydrographical variability (Fernández and Bode, 1994). In winter and spring, intense vertical mixing leads to a homogenized, nutrient-rich water column and noticeable diatom-dominated phytoplanktonic blooms (Fernández and Bode, 1994), as shown in March-April 2012 and April-May 2013 (Figs. 2.9b and 2.13). In contrast, in summer and autumn, reduced vertical mixing accompanied by enhanced solar heating leads to a nutrient-depleted stratified upper layer and low

primary production. Under these conditions, dinoflagellates, which are able to migrate towards nutrient-rich layers, dominate the phytoplanktonic community (Fernández and Bode, 1994). Occasionally, upwelling alters the above-described hydrographic pattern by reinforcing vertical mixing, injecting extra inputs of inorganic nutrients to the surface layers and increasing primary production (González-Quirós et al., 2003). Upwelling events can be traced as intermittent cold-water tongues close to the coast, often nearby Cabo Peñas promontory, where topographic effects enhance this process (Botas et al., 1989). During the studied period, the spring primary production bloom in 2012 occurred mostly off-shore in the central part of the Bay of Biscay, while in 2013 the bloom maximum was observed closer to the Cantabrian coast (Fig. 2.13). More persistent upwelling favourable conditions in 2013 than in 2012, especially from mid March to late April (Fig. 2.14), likely led to a higher supply of new nutrients close to the shoreline along the entire Cantabrian margin, thus resulting in a pronounced coast-parallel phytoplankton bloom (Fig. 2.13). A stronger and more constant river discharge during 2013 (Fig. 2.9a), also contributing new nutrients to the coastal area, could have also enhanced the coast-parallel primary production. It should be noted, however, that the algorithms used to estimate primary production are susceptible to interference caused by the complex optical properties of the constituents commonly found in coastal waters, where the influence of river outflows, riverine suspended sediments and dissolved OM may confuse the interpretation of satellite-based ocean colour data (Moreno-Madriñán and Fischer, 2013). Further elaboration on this aspect is hampered by the closure of the last collecting cup before the 2013 phytoplanktonic bloom.

The composition of settling particles allows defining two settling regimes. First, the record of the shallower sediment traps both on the open slope (WS1200, near-bottom) and the canyon middle course (AC2000T, mid-water) was markedly seasonal and showed relatively high contents of OM and opal, which most likely resulted from pelagic settling of biogenic particles. Second, the record of the near-bottom traps at the canyon middle and lowermost course AC2000B and AC4700 did not show any evidence of seasonality because of the dilution of biogenic components amidst more abundant, laterally advected lithogenic material.

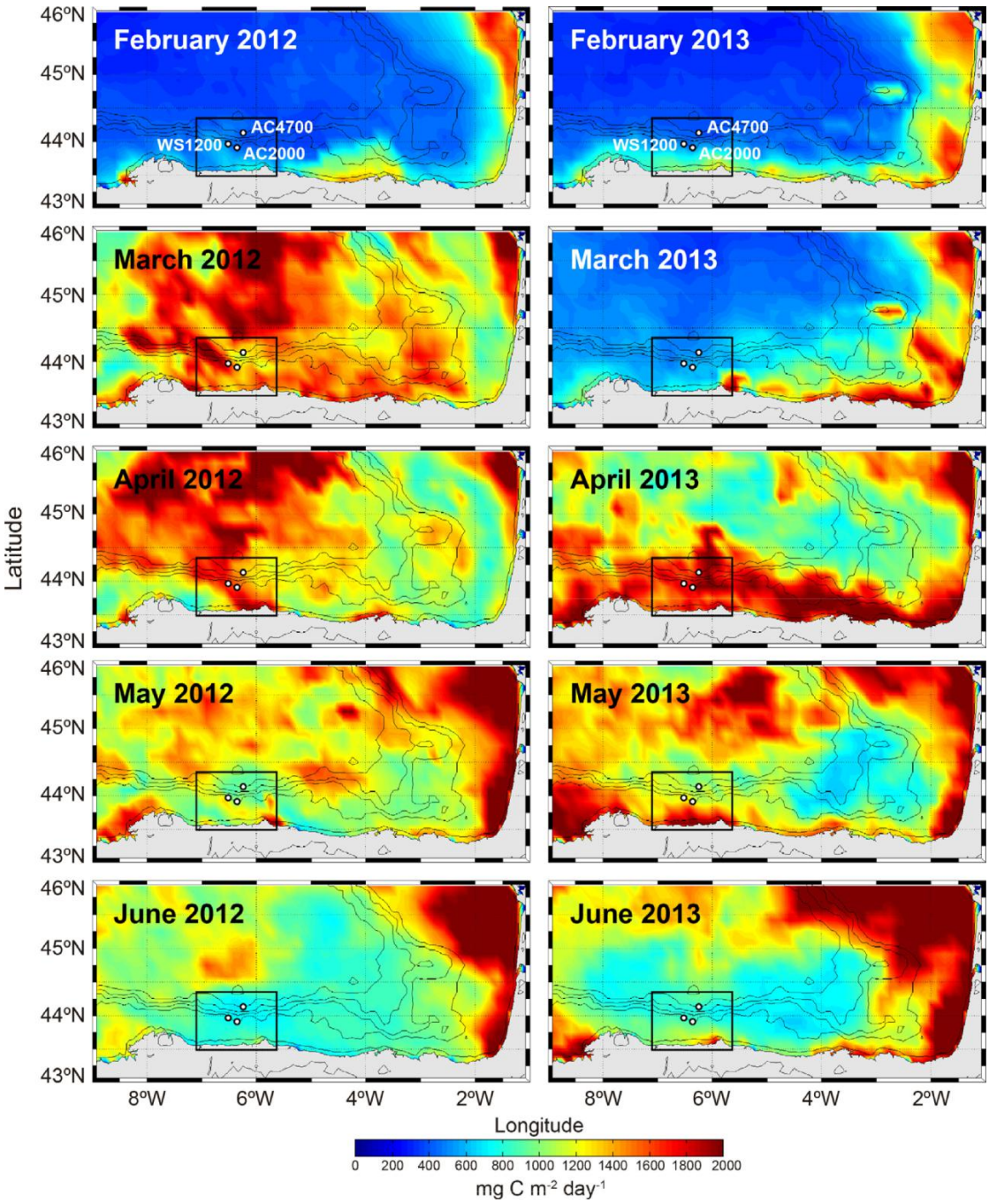

Fig. 2.13. MODIS-based net primary production maps (mg C m^{-2} d^{-1}) showing the development of phytoplanktonic blooms that occurred in spring 2012 and 2013. Black squares correspond to the area shown in Fig. 2.7 and white dots indicate mooring locations. (For interpretation of the references to colour in this figure legend, the reader is referred to the web version of this article.).

In the shallower environment including the mid-water AC2000T and the near-bottom WS1200 sediment traps, relatively high opal abundance (>12%) found in

March 2012 (Fig. 2.11d) can be directly related to the pelagic settling of material derived from blooms dominated by oceanic tychoplanktonic diatoms and chrysophyceans with siliceous skeletons and/or cysts. It is noteworthy that in April 2012, 16-30 days after the opal peak at AC2000T, an increase is also observed at AC2000B (Fig. 2.11d). This suggests that particles settling at 1200 m of water depth most probably reached the seafloor. The 800 m of depth difference between AC2000T and AC2000B, and the 30 days of delay result in a siliceous skeletons and/or cysts sinking speed of about 26 m d^{-1}, which is within the range published by Asper (1987) for sinking diatom aggregates.

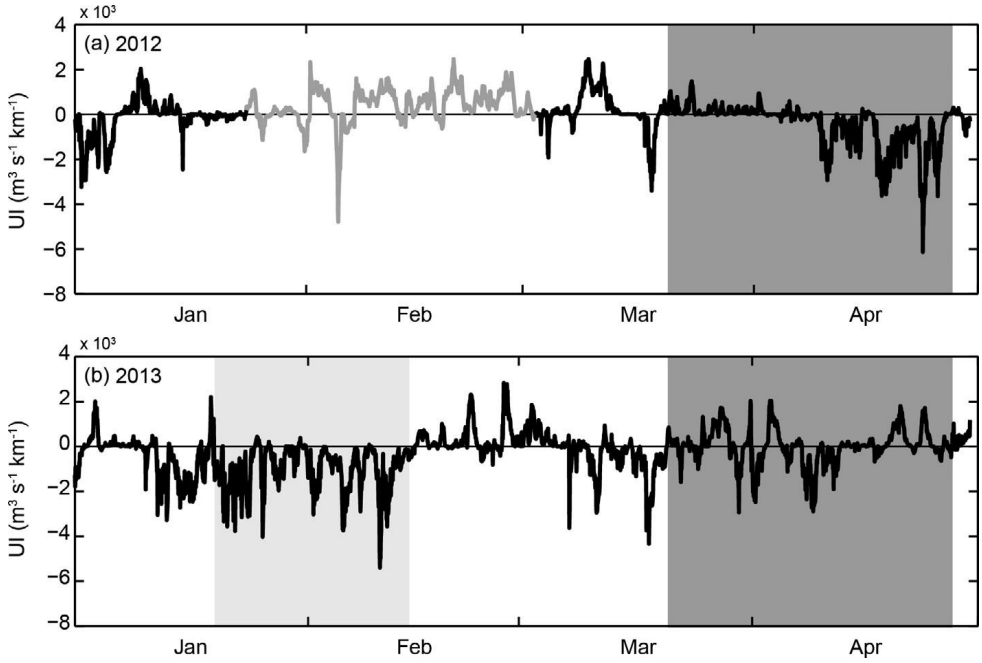

Fig. 2.14. Time series of upwelling index (UI) during (a) January to April 2012, and (b) January to April 2013. The grey line represents data from the WANA point 1053075. Shaded areas highlight specific events discussed in the text. Note that albeit we do not have particle flux data during January and February 2012, data on UI during such months have been included to note the more persistent upwelling favourable conditions during winter 2013 than during the previous winter.

Following the opal peak in March 2012, an increase in OM relative abundance was also detected in May 2012 in the shallower WS1200 (near-bottom) and AC2000T (mid-water) traps. The OM peak following that in opal relative abundance can be explained by a growth response of consumers (zooplankton) after an increase in phytoplankton, which is in agreement with Stenseth et al. (2006). During this period, in the same two traps N:OC ratios were slightly higher than during most of

the following fall and winter months, which according to the high N content of marine OM (N:OC > 0.12), might be a direct signal of the arrival of OM from marine algae. Slightly higher OM relative abundances were recorded from October to December 2012 at both WS1200 and AC2000T, which might be connected to an autumn phytoplankton bloom that may occur in the region during the transitional stage from stratification to mixing (Fernández and Bode, 1991). In September 2012, prevailing easterly winds and accompanying westward surface currents (Fig. 2.9c and g) led to a prolonged upwelling-favourable situation. This situation, jointly with some short-lived easterly wind episodes in October and November, might have favoured the nutrient replenishment of the surface layer and thus, phytoplankton growth. Bottom-up processes, driven ultimately by meteorological and hydrodynamic forcings, have been widely recognized as key factors in modulating phytoplankton growth and population dynamics (Margalef, 1978).

About the similarities in the evolution of OM relative contents of WS1200 (near-bottom) and AC2000T (mid-water), located at about the same depth (1150-1200 m) below the surface (see Section 2.2.5.4), it must be pointed out that both traps lie within the background flow of the slope currents (e.g. Pingree and Le Cann, 1990), which may help homogenizing OM relative contents because of along slope transport. The persistently high relative abundance of lithogenics in the near-bottom AC2000B trap (Fig. 2.11a) suggests a dilution effect of OM and opal biogenic particles. Higher opal relative abundance in AC4700 than in AC2000B and, for most of the time, the shallower traps (Fig. 2.11d), suggests a distinct behaviour of the lower canyon course, that seems to be more influenced by pelagic settling and less by advective transport from the inner continental margin. OM relative abundance is also slightly higher at AC4700 than at AC2000B during most of the time (Fig. 2.11c).

The lowermost canyon trap AC4700 is the one showing the highest relative content of $CaCO_3$ (Fig. 2.11b and Table 2.1), with the most prominent peak occurring in June 2012. The fact that this $CaCO_3$ peak is synchronous with OM and opal peaks (Fig. 2.11b-d) following three months of rather high primary production (Fig. 2.13) points to pelagic sedimentation of material derived from the spring phytoplanktonic bloom. This view is further supported by relatively high presence of foraminifera and pteropod shells in trap samples, which evidences a significant contribution of biogenic carbonate particles. Berner and Honjo (1981)

reported a 12% contribution of pteropod shells to the total carbonate flux in open ocean sites of the Atlantic Ocean. Given that labile organic material can be degraded while being transported to lower canyon environments (de Stigter et al., 2007; Pasqual et al., 2011), the higher $CaCO_3$ relative abundance at AC4700 probably results from a good preservation of pelagic carbonate shells. Furthermore, N:OC ratios also point to a marine, pelagic origin. It is to be noted that the calcium carbonate compensation depth (CCD) in the region is several hundred meters deeper (5200 m) than the deployment depth of our deeper trap AC4700 (Biscaye et al., 1976), which prevents significant dissolution of $CaCO_3$ particles. Also some contribution of terrestrial, river-sourced $CaCO_3$ cannot be totally discarded, as Nalón River drains from limestone formations and advection processes might bring light carbonate particles to the outer continental margin.

Compared to other locations in the Bay of Biscay, peaks in TMFs in the upper open slope west of the Avilés Canyon (WS1200) are higher than, for instance, those recorded by Schmidt et al. (2009) in the western slope adjacent to the nearby Cap Ferret submarine canyon. Similarly, TMFs peaks in AC2000T and AC2000B are also higher than those recorded both in the water column (1350 m water depth, 950 m above the bottom) and near-bottom (at 2250 m water depth, 50 m above the bottom) by Heussner et al. (1999) in the mid Cap Ferret Canyon at 2300 m of water depth, where neither variability in river discharge nor in wind dynamics (see Section 2.2.6.2.1) seem to be related to the observed rapid changes (e.g. from 57 mg m^{-2} d^{-1} to 2630 mg m^{-2} d^{-1}) in particulate fluxes. Instead, variability in particle fluxes in the mid Cap Ferret Canyon seems to be mainly controlled by oceanographic forcing, namely short-term fluctuations of the along-slope current (Heussner et al., 1999). The links of atmospheric, oceanographic and other forcings with particle fluxes in the Avilés Canyon area are discussed in the next chapter.

2.2.6.2 PHYSICAL CONTROLS ON PARTICLE FLUXES

2.2.6.2.1 STORMS

Increased wave height due to storms and their effects on the water column and on the resuspension of seabed sediments seem to be the main driver of TMFs temporal variability in the Avilés submarine canyon. This is supported by the good correlation coefficients (0.6-0.7) of TMFs with wave height and wind speed at time

lag 1 (15 days) for AC2000T and AC2000B (see Section 2.2.5.3), which also indicates that in terms of sediment dynamics the middle reaches of the Avilés Canyon respond relatively quick (15 days) to external forcings such as waves and wind. Given its shallower depth, it is to be supposed that the upper canyon reaches respond even faster. Such relationship is in agreement with observations made by several authors who have shown that submarine canyons ease the transport of particulate matter from coastal and shelf environments to the deep sea, often during storms associated to large wave heights and subsequent current intensification (Guillén et al., 2006; Palanques et al., 2008, 2009; Ulses et al., 2008b; Sanchez-Vidal et al., 2012). Other authors have also pointed out that in some continental margins, particles from the shelf reach the deep margin and basin after experiencing several cycles of deposition and resuspension (e.g. Palanques et al., 2012; Rumín-Caparrós et al., 2013).

The good correlation (0.7) of both levels of AC2000 with total river discharge means that riverine inputs have a clear impact on TMFs in the Avilés Canyon mid course, although with some delay as this coefficient corresponds to time lag 3 (45 days). Several storm events occurred during the monitoring period. The first event took place in early March 2012 after a February increase in riverine discharge up to almost 1100 m^3 s^{-1} (Fig. 2.9a), which likely resulted in the arrival of large amounts of particulate matter to the shelf. During this event, easterly winds up to 12 m s^{-1} (Fig. 2.9c and d) coexisted with up to 6 m Hs swell waves from the NW-N quadrant reaching the study area (dark grey shaded area in Fig. 2.9e and f). The combination of easterly winds and high swell waves led to a surface westward shelf current peaking at 37 cm s^{-1} (dark grey shaded areas in Fig. 2.9g and h), involving a westwards and offshore transport of particles in the surface Ekman layer. This situation favoured the surface advection and subsequent settling of particulate matter originating from the shelf into the Avilés Canyon down to depths of at least 2000 m eventually reaching also the open slope to the west towards La Vallina branches (Figs. 2.7, 2.8 and 2.10a). However, the transport in the bottom Ekman layer, should favour a shoreward flow thus hampering the bottom nepheloid layer to reach the shelf edge and beyond. The opposite situation occurred during the April 2012 and the late January-early February 2013 storm (see further down). This supports the relative importance of surface nepheloid layer transport vs. bottom nepheloid layer transport under different situations. The scenario described above explains why no significant LFs were recorded in AC2000B and WS12000 in March 2012 (Fig. 2.10d and e). It is worth

referring here to the discrepancies between sediment trap-based vertical mass TMFs and turbidity sensor-based LFs (Fig. 2.10). This topic has been discussed often in the literature where discrepancies are attributed to the inefficiency of sediment traps to collect laterally advected particulate matter under high current speeds, and also to the presence of coarse particles that settle rapidly and give low turbidity readings (e.g. Gardner, 1989; Gardner and Walsh, 1990; Walsh and Gardner, 1992; Bonnin et al., 2008). The lack of data on the sizes of suspended sedimentary particles in our study area prevents us to further discuss this aspect.

The weaker correlation (0.4-0.5) of TMFs during the studied period and the three variables considered in Table 2.3 for the near-bottom, western open slope trap WS1200, together with its fit with time lag 2 (30 days) for wave height and wind speed and time lag 4 (60 days) for total river discharge points to a different behaviour of the canyon and the upper open slope west of it. This also implies that, if affected by advection from the shelf, the open upper slope west of the Avilés Canyon will be impacted with a noticeable delay (eventually involving shifts in the meteoceanic conditions) and to a lesser extent than the Avilés Canyon mid (and probably upper) course.

A second, more severe storm was recorded in late April 2012, which was practically concomitant with a >600 m^3 s^{-1} peak in riverine discharge (Fig. 2.9a) bringing river-sourced particles to the shelf. During this storm, western wind bursts of 17.1 m s^{-1} (Fig. 2.9c and d) were accompanied by an 8-day period of waves from the northwest (light grey shaded areas in Fig. 2.9e) exceeding 8 m of Hs (Fig. 2.9f) that may have caused again shelf sediment resuspension adding to river-sourced inputs. Prevailing wind-driven surficial eastward shelf currents (light grey shaded areas in Fig. 2.9g and h) opposed to the arrival of shelf resuspended settling particles within the surface Ekman layer into the Avilés Canyon and its western open slope. It is noteworthy that during this storm an increase in raw near-bottom current speed up to 34 cm s^{-1} occurred at AC2000B (Fig. 2.15). Filtered current speed also increased in WS1200, reaching a peak value of 10.8 cm s^{-1}. However, filtered current speed in AC2000B remained greatly unchanged despite the large increment of the raw velocity data.

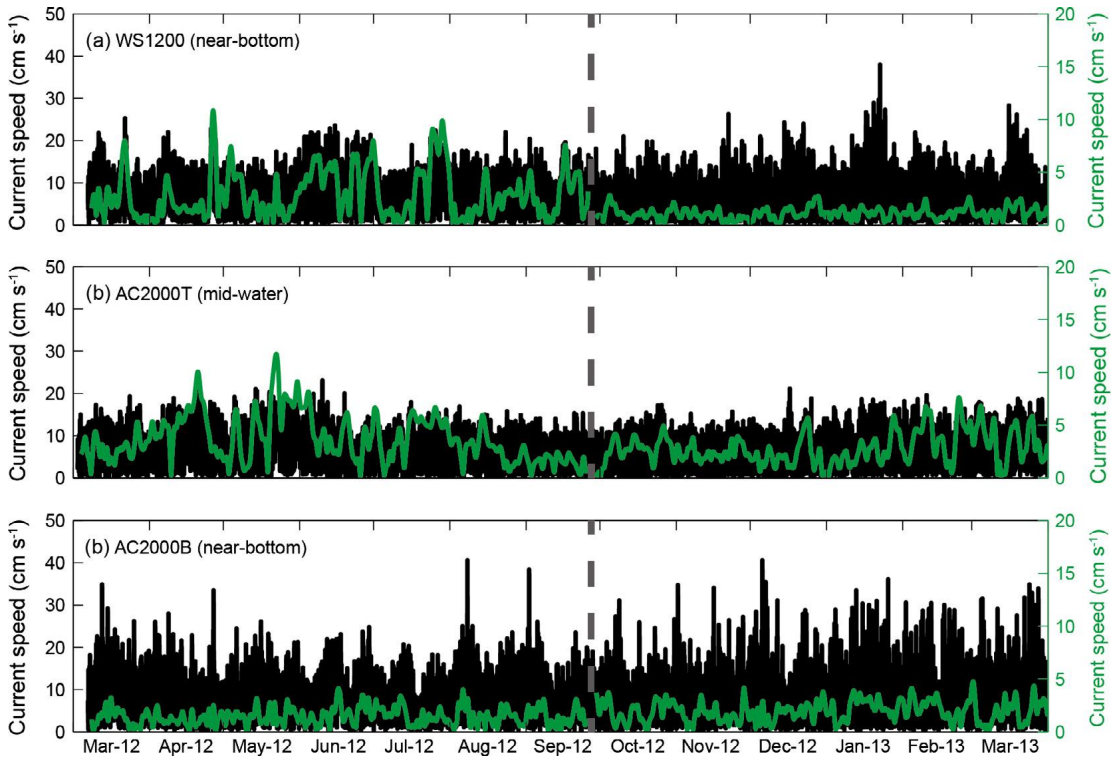

Fig. 2.15. Current speed (black line) and de-tided current speed (green line) over (a) the continental slope west of Avilés Canyon at 1200 m depth near-bottom (WS1200); (b) the Avilés Canyon middle course (AC2000T) at mid-water depth (1200 m); and (c) the Avilés Canyon (AC2000B) middle course near-bottom. The vertical grey dashed line marks the boundary between the two observational periods (see Section 2.2.4.3). (For interpretation of the references to colour in this figure legend, the reader is referred to the web version of this article.)

A possible supporting evidence of some near-bottom advection of particles during the April 2012 event is the small LFs spike in AC2000B. This suggests that part of the material supplied by the river and eventually resuspended from the shelf floor could have been transported offshore in the bottom Ekman layer having an impact initially restricted to the canyon upper and mid courses, which may explain the increase in LFs recorded in AC2000B (Fig. 2.10e). The lack of a concurrent increase in LFs in WS1200 is in agreement with the view of a different behaviour of the upper open slope compared to the canyon.

The concurrent though smaller peak of TMF in April 2012 at AC2000T (mid-water) is tentatively attributed to intermediate nepheloid layers detaching from the canyon head and upper course, or from the upper continental slope. Nepheloid layers spreading along isopycnal surfaces have been found at

intermediate depths over the continental slope of the nearby Celtic Sea, where near-bottom nepheloid layers have been identified too (e.g. McCave et al., 2001). Several studies demonstrate that such nepheloid layers mainly result from particle resuspension triggered by storms associated to high waves and increased bottom currents, with internal waves eventually playing a role in such particle loading (e.g. Biscaye and Andersson, 1994; Durrieu de Madron et al., 1999; Bonnin et al., 2002; Puig et al., 2004b).

In an attempt to asses if sedimentary particles could be carried from the mid to the lowermost canyon reaches we built the progressive vector diagram in Fig. 2.16 using near-bottom raw (non-filtered) currents recorded at the location of AC2000B (near-bottom). We selected the period of April-May 2012 as it corresponds to the highest TMFs in the canyon mid course and also includes a significant storm and river discharge event, so that it could be considered representative of enhanced transport along the canyon. We also assume that the overall circulation pattern in the upper-middle canyon course (as represented by station AC2000) could be extrapolated to the canyon lowermost course. The composition depicted in Fig. 2.16 therefore represents the horizontal displacement that a particle should follow if the horizontal current field was homogenous in the study area. The plot shows that particles which on the 1st of April 2012 were at 2000 m depth on the position of mooring AC2000 (AC2000B at 44 mab) could move horizontally roughly following the direction of the canyon from AC2000 to AC4700, and reach the position of AC4700 (still at 2000 m depth) around the 10th of May 2012. This scenario is in agreement with the pattern of increments in TMFs in both stations, first in AC2000 in April 2012, and 30 days later in AC4700 (Fig. 2.10b and c). However, these results and their interpretation have to be taken with care, as the characteristics of the near bottom transit of particles would depend on the deeper circulation of Avilés Canyon, not necessarily connected to the circulation at upper layers. The lack of significance of cross-correlation coefficients between AC4700 and the external forcings in Table 2.3 points towards a different behaviour of the lowermost canyon compared to the shallower canyon reaches and open upper slope.

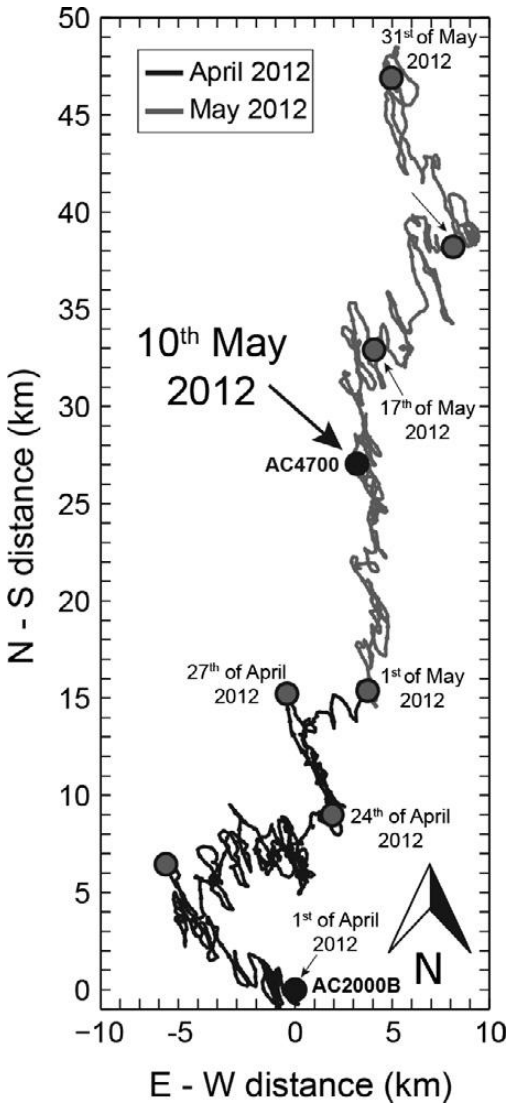

Fig. 2.16. Progressive vector diagram built after near-bottom raw (non-filtered) currents recorded at the location of AC2000B (near-bottom) in Avilés Canyon from 1 April 2012 to 31 May 2012. The position of the mooring stations in the middle canyon (AC2000) and the lowermost canyon (AC4700) is indicated with black dots.

The significance of residual currents that can be derived from the hodograph in Fig. 2.16 is discussed further down within Section 2.2.6.2.2 on tidal currents. A set of moderate storms with Hs never exceeding 5.4 m occurred from October to December 2012 (Fig. 2.9f). During this period, prevailing westerly winds (Fig. 2.9c) triggering eastward coastal currents (Fig. 2.9g) led to bottom Ekman transport directed offshore, likely contributing to the particle loading of bottom nepheloid layers in the mid and outer shelf and advecting particles in suspension towards the Avilés Canyon head, which were carried subsequently into the canyon upper

and middle sections, as recorded by the progressive increase in TMF at AC2000B (near-bottom) (Fig. 2.10b). The fact that a slight increase in TMF is also observed at AC2000T suggests that in addition to the bottom nepheloid layer, also intermediate nepheloids eventually detaching from the upper canyon and/or slope reached the location of AC2000 mooring station in the middle canyon (Fig. 2.10b). Durrieu de Madron et al. (1990) found that nepheloid structures extending seaward along isopycnals in the Gulf of Lion may increase the frequency of injection of sediment to the water column over the continental slope and sediment fluxes along submarine canyons.

The last stormy period with an impact on particle fluxes in the Avilés Canyon and the adjacent slope to the west lasted 27 days in January and February 2013. That event started synchronously with an increase in discharge of the Nalón River exceeding 800 m^3 s^{-1}, which likely resulted in the arrival of large amounts of material to the continental shelf (Fig. 2.9a). During this stormy period, westerly winds of about 18 m s^{-1} blowing along the Cantabrian coast raised waves up to 7.5 m of Hs arriving from the northwest (light grey shaded areas in Fig. 2.9c-f), induced downwelling pulses (Fig. 2.14) and promoted an eastward Ekman surface transport (Fig. 2.12a). However, the eastward coastal currents that these wind conditions generate along the shelf, might also lead to bottom Ekman transport directed offshore, potentially advecting sediments into the canyon head and slope as indicated by LF increases up to 1.97 and 0.61 g m^{-2} s^{-1} in AC2000B and WS1200, respectively (Fig. 2.10d and e).

Unlike the storm of late April 2012, this one was not accompanied by an increase in near-bottom filtered current speed in WS1200 (Fig. 2.15a), where the current meter provided negligible low-passed Godin $(A^2A_{25})/(24^225)$ currents (Godin, 1972), likely because it fell in a gully during the second deployment period from September 2012 to March 2013, thus lying in the shadow of along-slope currents. A 70 m deeper deployment depth during the second period compared to the first deployment period supports this view. Noticeably, raw near-bottom current speed (amplitude of tidal currents) reached the highest value (39 cm s^{-1}) in late January 2013 in WS1200. However, the location of the mooring obscures establishing the link between this increase and the passage of the stormy period here described.

Vertical TMFs also augmented in AC2000B during the occurrence of the January-February 2013 storm and shortly after up to a maximum of 5.24 g m^{-2} d^{-1} by mid-

February, following the above-mentioned increase in LFs in January (Fig. 2.10b and e). Within this stormy period, filtered currents were also rather low in AC2000B, similarly to WS1200, while raw near-bottom currents were fluctuating markedly around a mean value close to 22 cm s^{-1}, peaking at 37 cm s^{-1} (Fig. 2.15a and c). The increase in LFs and TMFs at AC2000B is interpreted as indicative of the arrival to the mid Avilés Canyon of bottom nepheloid layers triggered by the storm and increased river discharge, which further supports the offshore transport hypothesis in the bottom Ekman layer. Our observations also indicate that the nepheloid layers entering the canyon had practically no impact on TMFs in the open slope to the west (Fig. 2.10a). It is also plausible that the bottom nepheloid layer has been supplied by particles settling down from intermediate nepheloid layers. The peak values in TMFs recorded in early March 2013 at AC4700 could also be related to the transfer of the storm signal from AC2000B downcanyon (Fig. 2.10c). The higher contents of lithogenics at AC4700 during the second deployment period (September 2012 to March 2013) compared to the first one (March to September 2012) (Fig. 2.11a) support this view, as such higher values could be interpreted as a result of the set of moderate storms from October to December 2012 and the January-February 2013 storm, with concomitant increases of TMFs at AC2000B (Fig. 2.10b). The downcanyon propagation of bottom nepheloid layers, eventually leading to intermediate nepheloid layers too, has been noticed in other submarine canyons around Iberia, such as the Nazaré Canyon (van Weering et al., 2002; Martín et al., 2011).

The coastal downwelling conditions in early 2013, together with the concurrent increase in river discharge (Fig. 2.9a) and the phytoplankton bloom near Cabo Peñas and more generally along the coastal area, already visible in March 2013 (Fig. 2.13), help explaining the enrichment in OM and opal visible in all stations by March 2013 (Fig. 2.11c and d). In addition to the general meteorological and hydrological conditions in the Bay of Biscay, it is likely that the new nutrients brought by the sustained high river discharge from mid-January 2013 onwards by Nalón River (Fig. 2.9a) and also other Cantabrian rivers (data not shown) contributed to the coastal phytoplankton bloom starting in March 2013 and continuing for the following months (Fig. 2.13). The overall situation would have resulted in the formation of turbid layers enriched in biogenic constituents that were spreading over the margin at various levels, eventually eased by Ekman intermediate and bottom transport, including nepheloid layers detaching from the seabed at certain depths. The impact of the OM and opal-rich turbid layers

extending over the continental margin was, however, much larger at mid depths, both in the water column and near-bottom (i.e. 1200 m of water depth) and not restricted to the canyon, as shown by the records of traps AC2000T and WS1200. This impact was much lower, though it was still visible, in the deeper near-bottom traps AC2000B and AC4700 in the mid and lower canyon (Fig. 2.11c and d). The marine algal contribution to the particle load was especially remarkable at mid depths, as indicated by the prominent increases in the N:OC ratios at AC2000T and WS1200 traps, likely resulting from downwelling and pelagic settling. Such a signal, however, barely reached the deeper levels either because of consumption, dilution or retention at shallower levels (e.g. at density boundaries).

Overall, our set of observations indicates that the direction of wind, especially when it blows over a threshold of 12 m s^{-1} (Fig. 2.9d), and the wind-triggered currents determine whether river-contributed and resuspended shelf particulate matter reaches Avilés Canyon or not, and if this occurs mostly at surface, intermediate or near-bottom levels (Fig. 2.17). Clearly, there are two contrasting situations: (i) during westerly wind conditions an eastward shelf circulation is established and sea surface plumes tend to pile up along the coast while the Ekman bottom transport can carry sedimentary particles offshore; and (ii) during easterly wind conditions a westward shelf circulation is established and sea surface plumes can move over the canyon head and upper course while the bottom nepheloid layer would be pushed shoreward.

According to Ruiz-Villarreal et al. (2004), during the upwelling season eased by the prevailing easterly winds in spring-summer, mean westward flows would enhance upwelling over the head and upper reaches of the Avilés Canyon. This situation may enhance the westwards and seawards transport of particles in the surface Ekman Layer and thus, the advection and subsequent settling of particulate matter from the shelf into the Avilés Canyon and the open continental slope west of it (Fig. 2.17). Following the same authors, during the downwelling season induced by the prevailing westerly winds in autumn-winter, near-bottom flows in the upper reaches of the Avilés Canyon are variable but directed offshore, which would enhance the propagation of bottom nepheloid layers from the canyon head into the canyon upper and middle sections and possibly beyond.

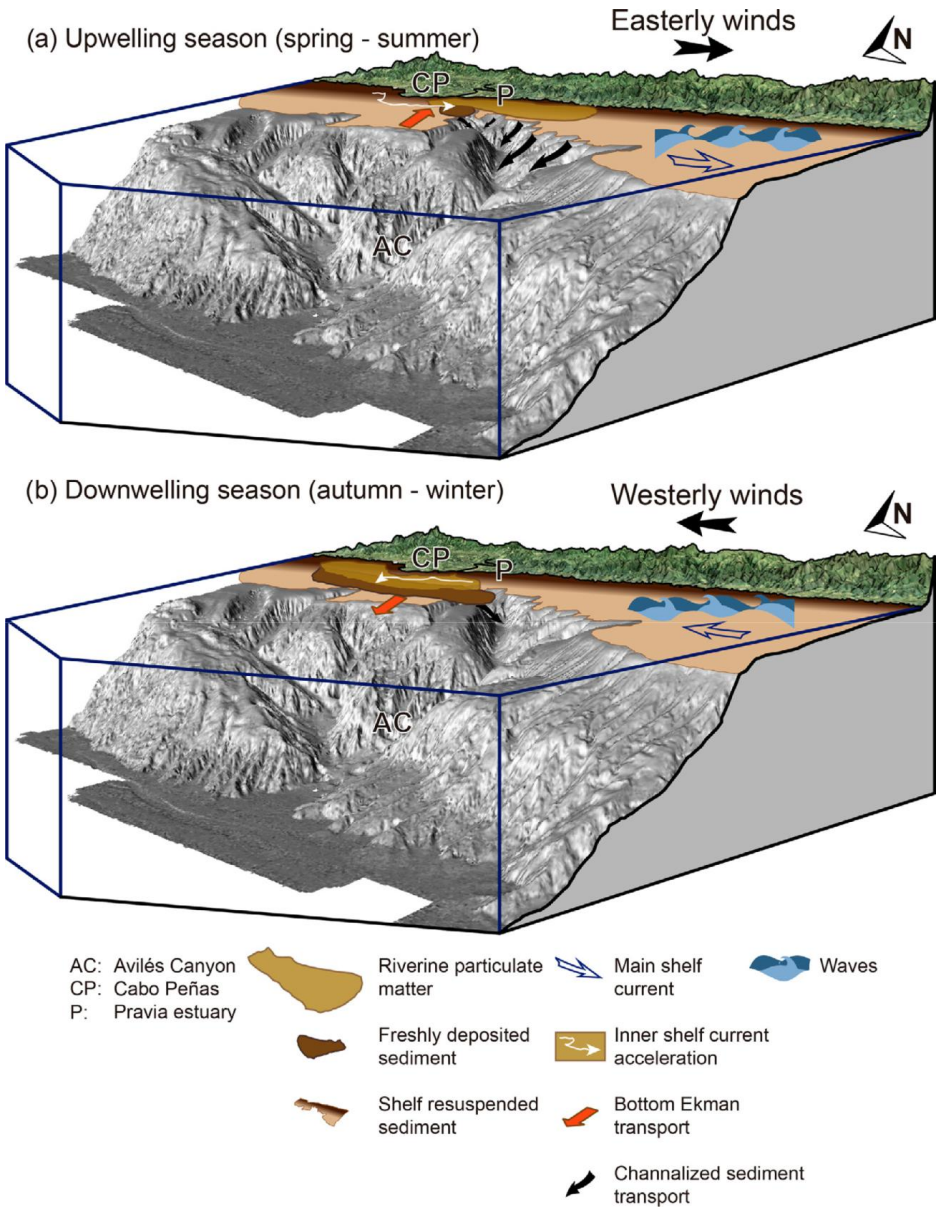

Fig. 2.17. Scheme illustrating wind regimes and associated processes including sediment transport (a) during spring and summer, when easterly winds induce a westward circulation and favour the advection of coast-derived sea surface sediment plumes towards Avilés Canyon and its adjacent open slope, and (b) during autumn and winter, when westerly winds induce and eastward circulation pushing sea surface sediment plumes against the shoreline, i.e. away from the canyon head and upper course. Note, however, that the bottom Ekman transport is directed offshore (see Section 2.2.6.1). (For interpretation to colour in this figure, the reader is referred to the web version of this article.)

2.2.6.2.2 TIDAL CURRENTS

The influence of tidal currents on sediment transport along submarine canyons has attracted since long the attention of researchers (e.g. Shepard et al., 1979 and references therein). Observations in the Baltimore Canyon showed how internal tides focussing in the upper and middle canyon course resulted in sediment resuspension and ultimately in a net down-canyon sediment transport (Gardner, 1989). In the Nazaré Canyon, off Portugal, de Stigter et al. (2007) demonstrated how 15-25 cm s^{-1} semidiurnal tidal currents in the upper and middle canyon course were able to trigger sudden increases in suspended particulate matter and to promote net down-canyon sediment transport.

The spectral analysis carried out in the near-bottom AC2000B and WS1200 current meters within the Avilés Canyon and on the adjacent open slope, respectively, reveals that the main tidal component is semidiurnal (M2) with frequencies of 0.0805 cycles per hour (cph) (12.42 h) (not shown). Other less energetic peaks are also present in the inertial frequency (f) of 0.0605 cph (16.52 h), as a mix of diurnal species (mostly K1) with 0.0410 cph (24.38 h), and as higher harmonic species M4 and M6 with 0.1621 cph (6.17 h) and 0.2441 cph (4.10 h), respectively. This underlines the relevance of tidal currents in the dynamics of the upper and middle Avilés Canyon and its adjacent slope. The Godin $(A^2A_{25})/(24^225)$ filter applied to obtain tidal period variations and extract subinertial series, shows that during the study period, tidal currents represented, at least, 60% in average of all currents recorded both at Avilés Canyon and on the open continental slope west of it.

One further aspect that can be derived from the currentmeter time series, and is well depicted in the hodograph of Fig. 2.16, is the existence of two directions of polarization of the residual current at AC2000B. In a first time the current measured at that depth consisted in a residual movement towards NW (hodograph ending at about 5 km North/5 km West), so suggesting the presence of a residual current coming downcanyon along the Avilés Canyon axis. Then the residual movement due to horizontal currents at AC2000B becomes directed towards NE (hodograph end at about 10 km North/3 km East). This would imply the presence at AC2000B, during this period, of a current coming from the slope southwest of the mooring position and directed towards NE roughly. This would be a residual current coming from La Vallina tributary branches located in the

westward flank of Avilés Canyon (Figs. 2.7 and 2.8). In evolution that follows, periods when this residual current was flowing down-canyon coming from the Avilés Canyon axis can be distinguished from periods (that seem to predominate) when the residual current came from La Vallina branches.

During the entire period there were also short-lived current fluctuations overprinted on these residual currents, which are apparently polarized along the Avilés Canyon axis. These short period fluctuations have periods from half a day (that would be the semidiurnal tidal currents) to one or two days and the particle excursions associated with these movements seem to align very well with the orientation of the Avilés Canyon axis no matter the orientation of the residual flow.

Tidal currents add, therefore, an extra amount of energy to the prevailing bottom currents, which may actively favour sediment transport along the Avilés submarine canyon system. Repeated cycles of semidiurnal tides shorten the intervals during which particles might settle, thus contributing to keep a permanent back-ground of suspended particles in near-bottom waters (Fig. 2.10d and e), which is about 0.04 g m^{-2} d^{-1}. De Stigter et al. (2007) noticed a similar situation in the Nazaré Canyon off the western Iberian margin. Also, during quiet summer conditions when the water column is stratified the turbulence associated to internal waves likely has the capability to resuspend and remobilize sedimentary deposits on the continental slope and possibly the outer and mid-shelf (e.g. Quaresma et al., 2007).

The above observations further suggest the important role being played by the La Vallina tributary branches, in the westward flank of Avilés Canyon. The significance of these tributaries is further discussed in the next section.

2.2.6.2.3 COASTAL AND SEAFLOOR PHYSIOGRAPHY

The interaction of the regional circulation with shoreline and seafloor morphological irregularities has been proven to influence the long-term sediment dispersal and accumulation in continental margins. In the study area, the interaction of the Cabo Peñas headland and the Avilés Canyon system topography with the wind-forced circulation adds complexity to the understanding of sediment transport.

As pointed out by DeGeest et al. (2008), headlands behave as sediment bypass areas where alongshore currents accelerate and deviate offshore. This is well illustrated, amongst other examples, by Cape Creus coastal promontory, in the Gulf of Lion, northwestern Mediterranean Sea, which accelerates and deviates shelf water flows offshore into the Cap de Creus Canyon (Canals et al., 2006; Lastras et al., 2007; Ulses et al., 2008a). Cabo Peñas headland (Fig. 2.7) might play a similar a role, i.e. deflecting and accelerating the regional along shelf circulation, thus conveying sediment off the nearshore belt into the Avilés Canyon. This would be associated with the specific interactions of Cabo Peñas promontory, and also the canyon head, with the prevailing westward and eastward shelf and slope surface circulation favouring coastal upwelling and downwelling, respectively (see Sections 2.2.3 and 2.2.6.2.1).

Based on morphological criteria, La Vallina tributary branches seem to play a relevant role in feeding the Avilés Canyon. After the canyon head, the heads of this set of tributaries are the most indented into the continental shelf west of Cabo Peñas (Fig. 2.7). Therefore, they might be able to capture sediment fluxes reaching the outer shelf. Interestingly, the main La Vallina branches but the westernmost one are markedly asymmetric with dominantly smoothened right flanks and gullied left flanks (Fig. 2.8a-c). The westernmost branch, which is the largest and most open one, displays a similar smoothening in both flanks (Fig. 2.8b). These features suggest preferential sediment deposition on the right flanks of the shelf-indented La Vallina branches, with a more widespread sedimentation over the larger westernmost branch. Furthermore, the dominant gullied character of the left flanks of La Vallina branches (Fig. 2.8c) points to erosion. Such features might be related not only to the location of La Vallina branches but also to recirculation induced by Cabo Peñas Promontory and topographic effects caused by the presence of the head of the Avilés Canyon under the two dominant wind regimes and the associated Ekman transport at various depths. The sedimented, smoothened character of the shelf-indented segments of the right (eastern) flank of several of the La Vallina branches points to a significant role of the bottom Ekman transport during periods of persistent eastward shelf circulation. Part of the sediment captured by La Vallina branches likely ends up into the Avilés Canyon main trunk up-course of the location of our AC2000 mid-canyon mooring. Therefore, this set of tributaries may constitute a relevant side sediment source opening directly into the Avilés Canyon mid-course.

In situ inspection with towed cameras have shown the rough, rocky and sediment-starved nature of the Avilés Canyon head (Sánchez-Delgado et al., 2014), which on one side indicates that sedimentary particles do not settle possibly due to the prevailing intense hydrodynamics occurring there and, on another side, reinforces the role of the La Vallina branches as significant sediment feeders of the canyon mid-course. This is supported by observations made by Sánchez et al. (2014) in the neighbouring La Gaviera Canyon (Fig. 2.7), where the intensification of hydrodynamic activity at the very canyon head is a consequence of the regional circulation, especially during high-energy events such as storms, and the semidiurnal tidal cycle causing bore-like structures and strong resuspension.

The two main directions of polarization depicted in Fig. 2.16 illustrate the swinging behaviour of residual currents at AC2000B, with periods of northwestward residual movement followed by periods of northeastward movement and so on (see Section 2.2.6.2.2). These directions correspond to residual currents flowing down the main trunk of the Avilés Canyon alternating with currents coming from La Vallina branches, and therefore further support the significant role of La Vallina tributaries in the dynamics and sediment fluxes of the Avilés Canyon system.

The smaller tributaries situated between la Vallina group and the main canyon head do not look particularly asymmetric in terms of flank smoothening and gullies appear only locally, without forming closely spaced sets as in some of the flanks of la Vallina branches (Fig. 2.7). Their overall appearance also suggests some sediment smoothening, although not as pronounced as in the shelf-indented segments of the (mostly right) flanks of La Vallina branches, which could be related to the shorter incision distance into the continental shelf of these smaller tributaries, subsequently resulting in a lessened ability to capture sediment escaping from the shelf, but also to an extended effect of the intense hydrodynamics in the main canyon head preventing particles to settle, as described above.

2.2.6.2.4 BOTTOM TRAWLING

The role of bottom trawling in resuspending sediments and inducing sediment gravity flows within submarine canyons has been documented by several authors, in particular in La Fonera Canyon, in the northwestern Mediterranean Sea

(Palanques et al., 2006b; Martín et al., 2008; Puig et al., 2012; Martín et al., 2014a, b). These authors have shown how the action of trawlers on the seabed triggers sharp near-bottom turbidity peaks associated with increases in downslope near-bottom currents. Amongst other authors, Pusceddu et al. (2014) and Martín et al. (2015) have investigated other far-reaching consequences of recurrent bottom trawling.

In the western slope adjacent to Avilés Canyon there is an active commercial bottom trawling fishery down to 600 m of water depth that mainly targets blue whiting (Sánchez-Delgado et al., 2014, their Fig. 8.2.5A). As shown by satellite-based vessel tracking data (Sánchez-Delgado et al., 2014), this fishery mainly operates during periods of fair weather by means of pair trawling, a highly aggressive fishing technique able to resuspend large amounts of unconsolidated bottom sediment. An impact of bottom trawling on the Avilés Canyon area, and especially on the canyon head and upper course but also on the adjacent upper open slope is, therefore, likely. This view is supported by the increase in LFs at WS1200 (near-bottom) (Fig. 2.10d, grey dashed lines) during the calm seas period extending from June to September 2012, when some prominent peaks were also noticed (Fig. 2.10d, black solid lines). Unfortunately, there are no TMF or LF data available that could help assessing the impact of bottom trawling in the canyon head and upper course. The bottom trawl triggered resuspension does not seem to reach the middle canyon where AC2000 was deployed (Fig. 2.10b).

2.2.7 CONCLUSIONS

The dominance of lithogenics (averaged annual values between 53.05% and 66.98% of TMFs) in settling particulate matter shows that riverine inputs represent the main source of particles arriving into the Avilés Canyon and its adjacent open slope. However, we did not detect a univocal direct control of river discharge on the temporal variability of TMFs neither in the middle and lower course of the Avilés Canyon, nor in the open upper slope west of the canyon, which suggests that other factors should control particle fluxes beyond the continental shelf edge. Indeed, certain hydrodynamic processes such as storms involve enough energy to enhance the transport of particles from coastal and shelf environments beyond that boundary.

Marine primary production is the second main source of sedimentary particles settling down in the study area. Biological components represented in average more than 30% in weight of the particles collected at all sediment traps during the monitoring period. In the lowermost canyon course (station AC4700) the $CaCO_3$ content of the biogenic fraction reaching the seabed is higher due to an enhanced flux of carbonate particles compared to siliceous ones. Furthermore, a CCD deeper (5200 m) than our deepest sediment traps prevents significant dissolution of $CaCO_3$ particles.

Two different particle settling regimes have been identified. The first involves the shallower sediment traps in the open slope to the west (WS1200, near-bottom) and in the middle canyon course (AC2000T, mid-water). This regime encompasses a clear seasonal signal with relatively high contents of biogenic particles. The second regime refers to the deeper, near-bottom traps in the canyon middle (AC2000B) and lowermost (AC4700) course, where no seasonal signal has been identified. Instead, resuspended, lithogenic-rich particulate matter diluting biogenic particles characterises this regime. The 16-30 days of delay in biogenic fraction increases recorded between the mid water AC2000T trap and the near-bottom AC2000B trap in the middle canyon course indicate some degree of connection through pelagic settling between different depth levels within the Avilés Canyon. Furthermore, the trajectory of particles between AC2000B in the middle canyon course and AC4700 in the lowermost canyon course points to an effective horizontal along canyon transport, at least at the depth level of AC2000B. However, this does not prove that the near-bottom circulation on Avilés Canyon is connected to the circulation at upper layers.

Storms are the main physical driver of particle fluxes in the Avilés Canyon area. Wind direction and wind-driven currents determine whether resuspended shelf particulate matter may reach the canyon, and if this will occur by surface or bottom transport. Winds blowing from the west induce an onshore surface Ekman transport that pushes river-sourced and shelf-resuspended sedimentary particles away from the Avilés canyon head and upper course. However, under the same situation, the bottom Ekman transport is directed offshore and, therefore, favours the injection of particles into the Avilés Canyon. In contrast, winds blowing from the east induce coastal upwelling and favour the advection in the surface layer of particulate matter towards the Avilés Canyon and the adjacent western open

slope. The same wind forcing triggers a bottom Ekman transport easing the retention of resuspended sediments on the shelf.

The Avilés Canyon head displays a very rough topography and a sediment-starved character. We suggest this to be caused, at least partly, by current deflection and turbulence induced by Cabo Peñas promontory. Such current deflection causes the bypass of suspended material over the Avilés Canyon head while steering the collection and funnelling of sediment fluxes into the main trunk of the canyon through La Vallina branches further west, as suggested by the smoothened nature of the shelf-incised segments in the right flanks of these set of tributaries, which could also respond to bottom trawling resuspension and subsequent setting there. The enhancement of hydrodynamic activity at the canyon head associated to high-energy events and tides likely plays a role too in making it sediment-starved.

Tidal currents actively contribute to sediment transport both in the upper-middle canyon course and over the western open slope. Repeated cycles of semidiurnal tides prevent particles to settle, thus resulting in a permanent background of suspended particles in near-bottom waters.

Increases in LFs occurring in summer months under calm sea conditions with no apparent relationship with meteoceanic external forcings are hypothesized to be also a consequence of commercial bottom trawling in the area. This anthropogenic disturbance may intensify the input of suspended matter all over the slope adjacent to the Avilés Canyon, and sporadically trigger shelf-slope sediment flows.

Finally, the specific physiography and orientation of the central Cantabrian margin, with a narrow continental shelf ahead of the Avilés Canyon and the presence of the nearby major coastal promontory of Cabo Peñas might help explaining its sensitivity to atmospheric and associated oceanographic forcings. The impact of these forcings on shallow waters would trigger a direct response propagating across the margin, which may explain the higher TMFs peaks in the Avilés Canyon compared to other canyons in the Bay of Biscay, such as Cap Ferret Canyon.

Acknowledgements. This research has been supported mainly by the DOS MARES Spanish project (CTM2010-21810-C03-01). Generalitat de Catalunya supported

GRC Geociències Marines through grant 2009 SGR 1305 (now 2014 SGR 1068). We thank the crew of R/V Sarmiento de Gamboa, Universitat de Barcelona and Instituto Español de Oceanografía staff involved in sampling at sea and in the maintenance of the mooring lines. We also thank the crew of R/V Miguel Oliver and the COCAN cruise shipboard party for multibeam bathymetry data acquisition and processing. R. Pedrosa-Pàmies and M. Guart were extremely helpful during sea going and laboratory work. M. Romero and R. Roca assisted us during ICP-AES and EA analyses. D.L. Jones provided the Fathom Toolbox for Matlab and made it freely available for download. The mission scientists and principal investigators from Giovanni system provided chlorophyll-a data. X. Rayo assisted us with the ArcGis software, X. Tubau contributed with valuable comments and L. D. Pena improved the English. ASV is supported by a Ramon y Cajal contract by the Spanish Ministry for Science and Innovation.

2.2.8 REFERENCES

Álvarez Fanjul, E., Alfonso, M., Ruiz, M.I., López, J.D., Rodríguez, I., 2003. Building the European capacity in operational oceanography. Proceedings of the third international conference on EuroGOOS. Elsevier Oceanography Series 69, 398-402.

Arzola, R.G., Wynn, R.B., Lastras, G., Masson, D.G., Weaver, P.P.E., 2008. Sedimentary features and processes in the Nazaré and Setúbal submarine canyons, west Iberian margin. Marine Geology 250, 64-88.

Asper, V.L., 1987. Measuring the flux and sinking speed of marine snow aggregates. Deep Sea Research Part A: Oceanographic Research Papers 34, 1-17.

Baines, P.G., 1982. On internal tide generation models. Deep Sea Research Part A: Oceanographic Research Papers 29, 307-338.

Baker, E.T., Milburn, H.B., Tennant, D.A., 1988. Field assessment of sediment trap efficiency under varying flow conditions. Journal of Marine Research 46, 573-592.

Bakun, A., 1973. Coastal Upwelling Indices, West Coast of North America, 1946-71. US. Dep. Comm. NOAA. Tech. Rep. NMFS-SSRF 671.

Behrenfeld, M.J., Falkowski, P.G., 1997. Photosynthetic rates derived from satellite-based chlorophyll concentration. Limnology and Oceanography 42, 1-20.

Berner, R.A., Honjo, S., 1981. Pelagic sedimentation of aragonite: its geochemical significance. Science 211, 940-942.

Biscaye, P.E., Kolla, V., Turekian, K.K., 1976. Distribution of calcium carbonate in surface sediments of the Atlantic Ocean. Journal of Geophysical Research 81, 2595-2603.

Biscaye, P.E., Andersson, R.F., 1994. Fluxes of particulate matter on the slope of the southern Middle Atlantic Bight: SEEP-II. Deep Sea Research Part II: Topical Studies in Oceanography 41, 459-509.

Bonnin, J., Van Raaphorst, W., Brummer, G.J., Van Haren, H., Malschaert, H., 2002. Intense mid-slope resuspension of particulate matter in the Faeroe-Shetland Channel: short-term deployment of near-bottom sediment traps. Deep Sea Research Part I: Oceanographic Research Papers 49, 1485-1505.

Bonnin, J., Heussner, S., Calafat, A., Fabrés, J., Palanques, A., Durrieu de Madron, X., Canals, M., Puig, P., Avril, J., Delsaut, N., 2008. Comparison of horizontal and downward particle fluxes across canyons of the Gulf of Lions (NW Mediterranean): meteorological and hydrodynamical forcing. Continental Shelf Research 28, 1957-1970.

Botas, J.A., Fernández, E., Bode, A., Anadón, R., 1989. Water masses off the central Cantabrian coast. Scientia Marina 53, 755-761.

Buesseler, K.O., Antia, A.N., Chen, M., Fowler, S.W., Gardner, W.D., Gustafsson, O., Harada, K., Michaels, A.F., Rutgers van der Loeff, M., Sarin, M., Steinberg, D.K., Trull, T., 2007. An assessment of the use of sediment traps for estimating upper ocean particle fluxes. Journal of Marine Research 65, 345-416.

Cacchione, D.A., Pratson, L.F., Ogston, A.S., 2002. The shaping of continental slopes by internal tides. Science 296, 724-727.

Canals, M., Puig, P., de Madron, X.D., Heussner, S., Palanques, A., Fabrés, J., 2006. Flushing submarine canyons. Nature 444, 354-357.

Canals, M., Company, J.B., Martín, D., Sanchez-Vidal, A., Ramírez-Llodra, E., 2013. Integrated study of Mediterranean deep canyons: novel results and future challenges. Progress in Oceanography 118, 1-27.

Charria, G., Lazure, P., Le Cann, B., Serpette, A., Reverdin, G., Louazel, S., Batifoulier, F., Dumas, F., Pichon, A., Morel, Y., 2013. Surface layer circulation derived from Lagrangian drifters in the Bay of Biscay. Journal of Marine Systems 109, S60-S76.

DeGeest, A.L., Mullenbach, B.L., Puig, P., Nittrouer, C.A., Drexler, T.M., Durrieu de Madron, X., Orange, D.L., 2008. Sediment accumulation in the western Gulf of Lions, France: the role of Cap de Creus canyon in linking shelf and slope sediment dispersal systems. Continental Shelf Research 28, 2031-2047.

De Leo, F.C., Smith, C.R., Rowden, A.A., Bowden, D.A., Clark, M.R., 2010. Submarine canyons: hotspots of benthic biomass and productivity in the deep sea. Proceedings of the Royal Society of London B: Biological Sciences 277, 2783-2792.

de Stigter, H.C., Boer, W., de Jesus Mendes, P.a., Jesus, C.C., Thomsen, L., van den Bergh, G.D., van Weering, T.C.E., 2007. Recent sediment transport and deposition in the Nazaré Canyon, Portuguese continental margin. Marine Geology 246, 144-164.

de Stigter, H.C., Jesus, C.C., Boer, W., Richter, T.O., Costa, A., van Weering, T.C.E., 2011. Recent sediment transport and deposition in the Lisbon-Setúbal and Cascais submarine canyons, Portuguese continental margin. Deep Sea Research Part II: Topical Studies in Oceanography 58, 2321-2344.

Díaz del Río, G., González, N., Marcote, D., 1998. The intermediate Mediterranean water inflow along the northern slope of the Iberian Peninsula. Oceanologica Acta 21, 157-163.

Dickson, R.R., Gould, W.J., Müller, T.J., Maillard, C., 1985. Estimates of the mean circulation in the deep (>2,000 m) layer of the Eastern North Atlantic. Progress in Oceanography 14, 103-127.

Drake, D.E., Gorsline, D.S., 1973. Distribution and transport of suspended particulate matter in Hueneme, Redondo, Newport and La Jolla submarine canyons. Geological Society of America Bulletin 84, 3949-3968.

Durrieu de Madron, X., Nyffeler, F., Godet, C.H.C., 1990. Hydrographic structure and nepheloid spatial distribution in the Gulf of Lions continental margin. Continental Shelf Research 10, 915-929.

Durrieu de Madron, X., 1994. Hydrography and nepheloid structures in the Grand-Rhône canyon. Continental Shelf Research 14, 457-477.

Durrieu De Madron, X., Castaing, P., Nyffeler, F., Courp, T., 1999. Slope transport of suspended particulate matter on the Aquitanian margin of the Bay of Biscay. Deep-Sea Research Part II 46, 2003-2027.

Fabrés, J., Calafat, A., Sanchez-Vidal, A., Canals, M., Heussner, S., 2002. Composition and spatio-temporal variability of particle fluxes in the Western Alboran Gyre, Mediterranean Sea. Journal of Marine Systems 34, 431-456.

Fanjul, E.A., Gómez, B.P., Sánchez-Arévalo, I.R., 1997. A description of the tides in the Eastern North Atlantic. Progress in Oceanography 40, 217-244.

Fernández, E., Bode, A., 1991. Seasonal patterns of primary production in the Central Cantabrian Sea (Bay of Biscay). Scientia Marina 55, 629-636.

Fernández, E., Bode, A., 1994. Succession of phytoplankton assemblages in relation to the hydrography in the southern Bay of Biscay: a multivariate approach. Scientia Marina 58, 191-205.

Friocourt, Y., Levier, B., Speich, S., Blanke, B., Drijfhout, S.S., 2007. A regional numerical ocean model of the circulation in the Bay of Biscay. Journal of Geophysical Research: Oceans 112, 1-19.

Frouin, R., Fiúza, A.F.G., Ambar, I., Boyd, T.J., 1990. Observations of a poleward surface current off the coasts of Portugal and Spain during winter. Journal of Geophysical Research: Oceans 95, 679-691.
Gardner, W.D., 1985. The effect of tilt on sediment trap efficiency. Deep Sea Research Part A: Oceanographic Research Papers 32, 349-361.

Gardner, W.D., 1989. Baltimore Canyon as a modern conduit of sediment to the deep sea. Deep Sea Research Part A: Oceanographic Research Papers 36, 323-358.

Gardner, W.D., Walsh, I.D., 1990. Distribution of macroaggregates and fine-grained particles across a continental margin and their potential role in fluxes. Deep Sea Research Part A: Oceanographic Research Papers 37, 401-411.

Gardner, W.D., Biscaye, P.E., Richardson, M.J., 1997. A sediment trap experiment in the Vema Channel to evaluate the effect of horizontal particle fluxes on measured vertical fluxes. Journal of Marine Research 55, 995-1028.

Gil, J., Gomis, D., 2008. The secondary ageostrophic circulation in the Iberian Poleward Current along the Cantabrian Sea (Bay of Biscay). Journal of Marine Systems 74, 60-73.

Gili, J., Bouillon, J., Palanques, A., Puig, P., 1999. Submarine canyons as habitats of prolific plankton populations: three new deep-sea Hydroidomedusae in the western Mediterranean. Zoological Journal of the Linnean Society 125, 313-329.

Godin, G., 1972. The Analysis of Tides. Univ. Toronto, Toronto, Canada, 264pp. Gómez-Ballesteros, M., Druet, M., Muñoz, A., Arrese, B., Rivera, J., Sánchez, F.,

Cristobo, J., Parra, S., García-Alegre, A., González-Pola, C., Gallástegui, J., Acosta, J., 2013. Geomorphology of the Avilés Canyon System, Cantabrian Sea (Bay of Biscay). Deep Sea Research Part II: Topical Studies in Oceanography, 1-19.

González-Pola, C., Ruiz-Villarreal, M., Lavín, A., Cabanas, J.M., Álvarez-Fanjul, E., 2005. A subtropical water intrusion spring-event in the shelf-slope of the south-western Bay of Biscay after strong wind-forcing pulses. Journal of Atmospheric and Ocean Science 10, 343-359.

González-Pola, C., Fernández-Díaz, J.M., Lavín, A., 2007. Vertical structure of the upper ocean from profiles fitted to physically consistent functional forms. Deep Sea Research Part I: Oceanographic Research Papers 54, 1985-2004.

González-Quirós, R., Cabal, J., Álvarez-Marqués, F., Isla, A., 2003. Ichthyoplankton distribution and plankton production related to the shelf break front at the Avilés Canyon. ICES Journal of Marine Science 60, 198-210.

Guillén, J., Palanques, A., Puig, P., Durrieu de Madron, X., Nyffeler, F., 2000. Field calibration of optical sensors for measuring suspended sediment concentration in the western Mediterranean. Scientia Marina 64, 427-435.

Guillén, J., Bourrin, F., Palanques, A., Durrieu de Madron, X., Puig, P., Buscail, R., 2006. Sediment dynamics during wet and dry storm events on the Têt inner shelf (SW Gulf of Lions). Marine Geology 234, 129-142.

Haynes, R., Barton, E.D., 1990. A poleward flow along the Atlantic coast of the Iberian Peninsula. Journal of Geophysical Research: Oceans 95, 11425-11441.

Heussner, S., Ratti, C., Carbonne, J., 1990. The PPS 3 time-series sediment trap and the trap sample processing techniques used during the ECOMARGE experiment. Continental Shelf Research 10, 943-958.

Heussner, S., Durrieu de Madron, X., Radakovitch, O., Beaufort, L., Biscaye, P.E., Carbonne, J., Delsaut, N., Etcheber, H., Monaco, A., 1999. Spatial and temporal patterns of downward particle fluxes on the continental slope of the Bay of Biscay (northeastern Atlantic). Deep-Sea Research II 46, 2101-2146.

Heussner, S., Durrieu de Madron, X., Calafat, A., Canals, M., Carbonne, J., Delsaut, N., Saragoni, G., 2006. Spatial and temporal variability of downward particle fluxes on a continental slope: lessons from an 8-yr experiment in the Gulf of Lions (NW Mediterranean). Marine Geology 234, 63-92.

Hickey, B., Baker, E., Kachel, N., 1986. Suspended particle movement in and around Quinault submarine canyon. Marine Geology 71, 35-83.

Hung, J.-J., Lin, C.-S., Chung, Y.-C., Hung, G.-W., Liu, W.-S., 2003. Lateral fluxes of biogenic particles through the Mien-Hua canyon in the southern East China Sea slope. Continental Shelf Research 23, 935-955.

Iorga, M.C., Lozier, M.S., 1999a. Signatures of the Mediterranean outflow from a North Atlantic climatology: 1. Salinity and density fields. Journal of Geophysical Research 104, 25985-26009.

Iorga, M.C., Lozier, M.S., 1999b. Signatures of the Mediterranean outflow from a North Atlantic climatology: 2. Diagnostic velocity fields. Journal of Geophysical Research: Oceans 104, 26011-26029.

Jouanneau, J.-M., Weber, O., Champilou, N., Cirac, P., Muxika, I., Borja, A., Pascual, A., Rodríguez-Lázaro, J., Donard, O., 2008. Recent sedimentary study of the shelf of the Basque country. Journal of Marine Systems 72, 397-406.

Lastras, G., Canals, M., Urgelès, R., Amblas, D., Ivanov, M., Droz, L., Dennielou, B., Fabrés, J., Schoolmeester, T., Akhmetzhanov, A., Orange, D., García-García, A., 2007. A walk down the Cap de Creus canyon, northwestern Mediterranean Sea: recent processes inferred from morphology and sediment bedforms. Marine Geology 246, 176-192.

Lastras, G., Canals, M., Amblas, D., Calafat, A.M., Durán, R., Muñoz, A., Pedrosa-Pàmies, R., Sanchez-Vidal, A., Rayo, X., Rumin, A., Tubau, X., Veres, O., 2012. The Avilés submarine canyon drainage system, northern Iberian margin. The Deep-Sea and Sub-Seafloor Frontiers Conf. 11-14 March, Spain, Abstr., vol. P085.

Lavín, A., Valdés, L., Sénchez, F., Abaunza, P., Forest, A., Boucher, J., Lazure, P., Jegou, A.-M., 2006. The Bay of Biscay: the encountering of the ocean and the shelf. Seas Harvard Press 14, 933-1001.

Le Cann, B., Serpette, A., 2009. Intense warm and saline upper ocean inflow in the southern Bay of Biscay in autumn-winter 2006-2007. Continental Shelf Research 29, 1014-1025.

Margalef, R., 1978. Life-forms of phytoplankton as survival alternatives in an unstable environment. Oceanologica Acta 1, 493-509.

Martín, J., Palanques, A., Puig, P., 2006. Composition and variability of downward particulate matter fluxes in the Palamós submarine canyon (NW Mediterranean). Journal of Marine Systems 60, 75-97.

Martín, J., Puig, P., Palanques, A., Masqué, P., García-Orellana, J., 2008. Effect of commercial trawling on the deep sedimentation in a Mediterranean submarine canyon. Marine Geology 252, 150-155.

Martín, J., Palanques, A., Vitorino, J., Oliveira, A., de Stigter, H.C., 2011. Near-bottom particulate matter dynamics in the Nazaré submarine canyon under calm and stormy conditions. Deep Sea Research Part II: Topical Studies in Oceanography 58, 2388-2400.

Martín, J., Puig, P., Palanques, A., Ribó, M., 2014a. Trawling-induced daily sediment resuspension in the flank of a Mediterranean submarine canyon. Deep Sea Research Part II: Topical Studies in Oceanography 104, 174-183.

Martín, J., Puig, P., Masqué, P., Palanques, A., Sánchez-Gómez, A., 2014b. Impact of bottom trawling on deep-sea sediment properties along the flanks of a submarine canyon. PLoS ONE 9, e104536.

Martín, J., Puig, P., Palanques, A., Giamportone, A., 2015. Commercial bottom trawling as a driver of sediment dynamics and deep seascape evolution in the Anthropocene. Anthropocene 7, 1-15.

McCave, I.N., Hall, I.R., Antia, a.N., Chou, L., Dehairs, F., Lampitt, R.S., Thomsen, L., Van Weering, T.C.E., Wollast, R., 2001. Distribution, composition and flux of particulate material over the European margin at 47º-50ºN. Deep Sea Research Part II: Topical Studies in Oceanography 48, 3107-3139.

Miquel, J.C., Martín, J., Gasser, B., Rodríguez-y-Baena, A., Toubal, T., Fowler, S.W., 2011. Dynamics of particle flux and carbon export in the northwestern Mediterranean Sea: a two decade time-series study at the DYFAMED site. Progress in Oceanography 91, 461-481.

Moreno-Madriñán, M.J., Fischer, A.M., 2013. Performance of the MODIS FLH algorithm in estuarine waters: a multi-year (2003-2010) analysis from Tampa Bay, Florida (USA). International Journal of Remote Sensing 34, 6467-6483.

Mortlock, R.A., Froelich, P.N., 1989. A simple method for the rapid determination of biogenic opal in pelagic marine sediments. Deep Sea Research Part A: Oceanographic Research Papers 36, 1415-1426.

Mulder, T., Zaragosi, S., Garlan, T., Mavel, J., Cremer, M., Sottolichio, a., Sénéchal, N., Schmidt, S., 2012. Present deep-submarine canyons activity in the Bay of Biscay (NE Atlantic). Marine Geology 295-298, 113-127.

Nittrouer, C.A., Wright, L.D., 1994. Transport of particles across continental shelves. Reviews of Geophysics 32, 85-113.

Oliveira, A., Santos, A.I., Rodrigues, A., Vitorino, J., 2007. Sedimentary particle distribution and dynamics on the Nazaré canyon system and adjacent shelf (Portugal). Marine Geology 246, 105-122.

Paillet, J., Mercier, H., 1997. An inverse model of the eastern North Atlantic general circulation and thermocline ventilation. Deep Sea Research Part I: Oceanographic Research Papers 44, 1293-1328.

Palanques, A., El Khatab, M., Puig, P., Masqué, P., Sánchez-Cabeza, J.A., Isla, E., 2005. Downward particle fluxes in the Guadiaro submarine canyon depositional system (north-western Alboran Sea), a river flood dominated system. Marine Geology 220, 23-40.

Palanques, A., Durrieu de Madron, X., Puig, P., Fabrés, J., Guillén, J., Calafat, A., Canals, M., Heussner, S., Bonnin, J., 2006a. Suspended sediment fluxes and transport processes in the Gulf of Lions submarine canyons. The role of storms and dense water cascading. Marine Geology 234, 43-61.

Palanques, A., Martín, J., Puig, P., Guillén, J., Company, J.B., Sardà, F., 2006b. Evidence of sediment gravity flows induced by trawling in the Palamós (Fonera) submarine canyon (northwestern Mediterranean). Deep Sea Research Part I: Oceanographic Research Papers 53, 201-214.

Palanques, A., Guillén, J., Puig, P., Durrieu de Madron, X., 2008. Storm-driven shelf-to-canyon suspended sediment transport at the southwestern Gulf of Lions. Continental Shelf Research 28, 1947-1956.

Palanques, A., Puig, P., Latasa, M., Scharek, R., 2009. Deep sediment transport induced by storms and dense shelf-water cascading in the northwestern Mediterranean basin. Deep Sea Research Part I: Oceanographic Research Papers 56, 425-434.

Palanques, A., Puig, P., Durrieu de Madron, X., Sanchez-Vidal, A., Pasqual, C., Martín, J., Calafat, A., Heussner, S., Canals, M., 2012. Sediment transport to the deep canyons and open-slope of the western Gulf of Lions during the 2006 intense cascading and open-sea convection period. Progress in Oceanography 106, 1-15.

Pasqual, C., Lee, C., Goñi, M., Tesi, T., Sanchez-Vidal, A., Calafat, A., Canals, M., Heussner, S., 2011. Use of organic biomarkers to trace the transport of marine and terrigenous organic matter through the southwestern canyons of the Gulf of Lion. Marine Chemistry 126, 1-12.

Paull, C.K., Mitts, P., Ussler, W., Keaten, R., Greene, H.G., 2005. Trail of sand in upper Monterey Canyon: offshore California. Geological Society of America Bulletin 117, 1134-1145.

Pierau, R., Henrich, R., Preiß-Daimler, I., Krastel, S., Geersen, J., 2011. Sediment transport and turbidite architecture in the submarine Dakar Canyon off Senegal, NW-Africa. Journal of African Earth Sciences 60, 196-208.

Pingree, R.D., 1993. Flow of surface waters to the west of the British Isles and in the Bay of Biscay. Deep Sea Research Part II: Topical Studies in Oceanography 40, 369-388.

Pingree, R.D., Le Cann, B., 1990. Structure, strength and seasonality of the slope currents in the Bay of Biscay region. Journal of the Marine Biological Association of the United Kingdom 70, 857-885.

Pingree, R.D., Le Cann, B., 1992. Anticyclonic eddy X91 in the southern Bay of Biscay, May 1991 to February 1992. Journal of Geophysical Research: Oceans 97, 14353-14367.

Pingree, R.D., New, A.L., 1989. Downward propagation of internal tidal energy into the Bay of Biscay. Deep Sea Research Part A: Oceanographic Research Papers 36, 735-758.

Pollard, R.T., Pu, S., 1985. Structure and circulation of the Upper Atlantic Ocean northeast of the Azores. Progress in Oceanography 14, 443-462.

Pollard, R.T., Griffttths, M.J., Cunningham, S.A., Read, J.F., Pérez, F.F., Ríos, A.F., 1996. Vivaldi 1991 -a study of the formation, circulation and ventilation of Eastern North Atlantic Central Water. Progress in Oceanography 37, 167-192.

Prego, R., Boi, P., Cobelo-García, A., 2008. The contribution of total suspended solids to the Bay of Biscay by Cantabrian Rivers (northern coast of the Iberian Peninsula). Journal of Marine Systems 72, 342-349.

Puig, P., Palanques, A., 1998. Temporal variability and composition of settling particle fluxes on the Barcelona continental margin (Northwestern Mediterranean). Journal of Marine Research 56, 639-654.

Puig, P., Ogston, A.S., Mullenbach, B.L., Nittrouer, C.A., Parsons, J.D., Sternberg, R.W., 2004a. Storm-induced sediment gravity flows at the head of the Eel submarine canyon, northern California margin. Journal of Geophysical Research 109, C03019.

Puig, P., Palanques, a., Guillén, J., El Khatab, M., 2004b. Role of internal waves in the generation of nepheloid layers on the northwestern Alboran slope: implications for continental margin shaping. Journal of Geophysical Research: Oceans C109, 1-11.

Puig, P., Canals, M., Company, J.B., Martín, J., Amblas, D., Lastras, G., Palanques, A., Calafat, A.M., 2012. Ploughing the deep sea floor. Nature 489, 286-289.

Pusceddu, A., Bianchelli, S., Martín, J., Puig, P., Palanques, A., Masqué, P., Danovaro, R., 2014. Chronic and intensive bottom trawling impairs deep-sea biodiversity and ecosystem functioning. Proceedings of the National Academy of Sciences 111 (24), 8861-8866.

Quaresma, L.S., Vitorino, J., Oliveira, A., da Silva, J., 2007. Evidence of sediment resuspension by nonlinear internal waves on the western Portuguese mid-shelf. Marine Geology 246, 123-143.

Ríos, A.F., Pérez, F.F., Fraga, F., 1992. Water masses in the upper and middle North Atlantic Ocean east of the Azores. Deep Sea Research Part A: Oceanographic Research Papers 39, 645-658.

Ruiz-Villarreal, M., Coelho, H., Díaz del Río, G., Nogueira, J., 2004. Slope Current in the Cantabrian: Observations and Modeling of Seasonal Variability and Interaction with Aviles Canyon. ICES CM 2004/N:12, 23pp.

Rumín-Caparrós, A., Sanchez-Vidal, A., Calafat, A., Canals, M., Martín, J., Puig, P., Pedrosa-Pàmies, R., 2013. External forcings, oceanographic processes and particle flux dynamics in Cap de Creus submarine canyon, NW Mediterranean Sea. Biogeosciences 10, 3493-3505.

Sánchez, F., González-Pola, C., Druet, M., García-Alegre, A., Acosta, J., Cristobo, J., Parra, S., Ríos, P., Altuna, Á., Gómez-Ballesteros, M., Muñoz-Recio, A., Rivera, J., del Río, G.D., 2014. Habitat characterization of deep-water coral reefs in La Gaviera Canyon (Avilés Canyon System, Cantabrian Sea). Deep Sea Research Part II: Topical Studies in Oceanography 106, 118-140.

Sánchez-Delgado, F., Gómez-Ballesteros, M., Parra-Descalzo, S., Cristobo, J., Serrano-López, A., Druet-Vélez, M., García-Alegre-Garralda, A., Rodríguez-Cabello-Ródenas, M.C., Preciado-Ramírez, M.I., Tello-Antón, M.O., Punzón-Merino, A. M., Blanco-Giner, M.Á., Ríos, P., Frutos-Parralejo, M.I., González-Pola, C., Acosta-Yepes, J., Rivera, J., 2014. Caracterización ecológica del área marina del sistema de cañones submarinos de Avilés. Informe final área LIFE+ INDEMARES (LIFE07/ NAT/E/000732). Instituto Español de Oceanografía. Coordinación: Fundación Biodiversidad, Madrid, 243pp.

Sanchez-Vidal, A., Canals, M., Calafat, A.M., Lastras, G., Pedrosa-Pàmies, R., Menéndez, M., Medina, R., Company, J.B., Hereu, B., Romero, J., Alcoverro, T., 2012. Impacts on the deep-sea ecosystem by a severe coastal storm. PLoS ONE 7, e30395.

Schmidt, S., Howa, H., Mouret, A., Lombard, F., Anschutz, P., Labeyrie, L., 2009. Particle fluxes and recent sediment accumulation on the Aquitanian margin of Bay of Biscay. Continental Shelf Research 29, 1044-1052.

Schmidt, S., Howa, H., Diallo, A., Martín, J., Cremer, M., Duros, P., Fontanier, C., Deflandre, B., Metzger, E., Mulder, T., 2014. Recent sediment transport and deposition in the Cap-Ferret Canyon, South-East margin of Bay of Biscay. Deep Sea Research Part II: Topical Studies in Oceanography 104, 134-144.

Serpette, A., Le Cann, B., Colas, F., 2006. Lagrangian circulation of the North Atlantic Central Water over the abyssal plain and continental slopes of the Bay of Biscay: description of selected mesoscale features. Scientia Marina 70, 27-42.

Shepard, F.P., 1981. Submarine canyons: multiple causes and long-time persistence. American Association of Petroleum Geologists Bulletin 65, 1062-1077.

Shepard, F.P., Marshall, N.F., McLoughlin, P.A., Sullivan, G.G., 1979. Currents in submarine canyons and other seavalleys. AAPG Studies in Geology 8, 173.

Smith, S.D., 1988. Coefficients for sea surface wind stress, heat flux, and wind profiles as a function of wind speed and temperature. Journal of Geophysical Research 93, 15467-15472.

Somavilla, R., González-Pola, C., Rodríguez, C., Josey, S.A., Sánchez, R.F., Lavín, A., 2009. Large changes in the hydrographic structure of the Bay of Biscay after the extreme mixing of winter 2005. Journal of Geophysical Research 114, 1-14.

Stabholz, M., Durrieu de Madron, X., Canals, M., Khripounoff, A., Taupier-Letage, I., Testor, P., Heussner, S., Kerhervé, P., Delsaut, N., Houpert, L., Lastras, G., Dennielou, B., 2013. Impact of open-ocean convection on particle fluxes and

sediment dynamics in the deep margin of the Gulf of Lions. Biogeosciences 10, 1097-1116.

Stenseth, N.C., Llope, M., Anadón, R., Ciannelli, L., Chan, K.-S., Hjermann, D.Ø., Bagøien, E., Ottersen, G., 2006. Seasonal plankton dynamics along a cross-shelf gradient. Proceedings of the Royal Society of London B: Biological Sciences 273, 2831-2838.

Taylor, J.R., Sarkar, S., 2008. Stratification effects in a bottom Ekman layer. Journal of Physical Oceanography 38, 2535-2555.

Tyler, P., Amaro, T., Arzola, R., Cunha, M.R., de Stigter, H., Gooday, A., Huvenne, V., Ingels, J., Kiriakoulakis, K., Lastras, G., Masson, D., Oliveira, A., Pattenden, A., Vanreusel, A., Van Weering, T., Vitorino, J., Witte, U., Wolff, G., 2009. Europe's grand canyon: Nazaré submarine canyon. Oceanography 22, 46-57.

Ulses, C., Estournel, C., Bonnin, J., Durrieu de Madron, X., Marsaleix, P., 2008a. Impact of storms and dense water cascading on shelf-slope exchanges in the Gulf of Lion (NW Mediterranean). Journal of Geophysical Research 113, 1-18.

Ulses, C., Estournel, C., Durrieu de Madron, X., Palanques, A., 2008b. Suspended sediment transport in the Gulf of Lions (NW Mediterranean): impact of extreme storms and floods. Continental Shelf Research 28, 2048-2070.

van Aken, H.M., 2000a. The hydrography of the mid-latitude Northeast Atlantic Ocean. I: the deep water masses. Deep Sea Research Part I: Oceanographic Research Papers 47, 757-788.

van Aken, H.M., 2000b. The hydrography of the mid-latitude Northeast Atlantic Ocean. II: the intermediate water masses. Deep Sea Research Part I: Oceanographic Research Papers 47, 789-824.

van Aken, H.M., 2001. The hydrography of the mid-latitude Northeast Atlantic Ocean -part III: the subducted thermocline water mass. Deep Sea Research Part I: Oceanographic Research Papers 48, 237-267.

van Weering, T.C.E., de Stigter, H.C., Boer, W., de Haas, H., 2002. Recent sediment transport and accumulation on the NW Iberian margin. Progress in Oceanography 52, 349-371.

Vetter, E.W., 1994. Hotspots of benthic production. Nature 372, 47.

Vetter, E.W., Dayton, P.K., 1998. Macrofaunal communities within and adjacent to a detritus-rich submarine canyon system. Deep Sea Research Part II: Topical Studies in Oceanography 45, 25-54.

Vetter, E.W., Smith, C.R., De Leo, F.C., 2010. Hawaiian hotspots: enhanced megafaunal abundance and diversity in submarine canyons on the oceanic islands of Hawaii. Marine Ecology 31, 183-199.

Walsh, I.D., Gardner, W.D., 1992. A comparison of aggregate profiles with sediment trap fluxes. Deep Sea Research Part A: Oceanographic Research Papers 39, 1817-1834.

Xu, J., Noble, M., Eittreim, S.L., Rosenfeld, L.K., Schwing, F.B., Pilskaln, C.H., 2002. Distribution and transport of suspended particulate matter in Monterey Canyon, California. Marine Geology 181, 215-234.
Xu, J.P., Swarzenski, P.W., Noble, M., Li, A.-C., 2010. Event-driven sediment flux in Hueneme and Mugu submarine canyons, southern California. Marine Geology 269, 74-88.

2.3 OCEAN SYSTEM RESPONSE TO ATMOSPHERIC FORCING AND SYNCHRONOUS EXTREME EVENTS OVER MID-LATITUDES: THE CANTABRIAN SEA AND THE GULF OF LION CASE STUDY

A. Rumín-Caparrós[a], C. González-Pola[b], R. Somavilla[b], A. Sanchez-Vidal[a], K. Schroeder[c], J. Chiggiato[c], X. Durrieu de Madron[d], M. Canals[a]*

[a]GRC Geociències Marines, Departament de Dinàmica de la Terra i de l'Oceà, Universitat de Barcelona, Barcelona, Spain
[b]Instituto Español de Oceanografía, C.O. Gijón, Gijón, Spain
[c]Consiglio Nazionale delle Ricerche, Istituto di Scienze Marine, CNR-ISMAR, Venezia, Italy
[d]CEFREM, CNRS-Université de Perpignan, Perpignan, France

Submitted to Progress in Oceanography. Januray 2017.

2.3.1 ABSTRACT

The present work aims at understanding the ocean system response to atmospheric forcing and the occurrence of synchronous extreme events in the Cantabrian Sea and the Gulf of Lion, i.e. the CASGOL region. Both areas are located in the 42º-43º N latitudinal fringe and are separated by the 425 km long Pyrenees mountain range. The Cantabrian Sea extends along the north Iberian margin and occupies the southern Bay of Biscay, while the Gulf of Lion is in the NW Mediterranean Sea. A retrospective analysis of air temperature, heat and buoyancy fluxes, and sea-water temperature allowed detecting the formation of dense water in the Gulf of Lion, both on the continental shelf and offshore, which led to cascading and open sea convection, respectively. During some intense events, these processes were synchronous with the deepening of the mixed layer depth in the Cantabrian Sea. The parallel occurrence of such processes may ultimately enhance the role of submarine canyons incised along both continental margins as preferential vectors for the transfer of the teleconnected signal to the deep margin and basin. In turn, this is indicative of the relevance of the atmospheric connectivity in between the two areas, which highly depends on the prevalent location of an anomalous high-pressure center during winter. This

center controls the penetration of cold and dry air masses to the latitude of the CASGOL region and determines ocean-atmosphere heat exchanges. The co-occurrence of major spring blooms in both areas after the above-referred synchronous oceanographic events highlights the relevance of the atmospheric connection and its impacts on the marine ecosystem. Increases in primary productivity are related to the intensification of vertical mixing events, which transfer nutrients from deeper layers into surface waters. Such increases may spread to the entire food web, starting by organisms feeding on phytoplankton and ultimately benefiting the most relevant target species for fisheries in the CASGOL region. Finally, atmospheric forcing over the CASGOL region likely lies behind the resemblance of the intra-annual variability of total mass fluxes found off each end of the Pyrenees.

2.3.2 INTRODUCTION

The pronounced interannual variability of wintertime upper ocean mixing and deep-water formation has grabbed the attention of numerous researchers all over the world (e.g. Lacombe et al., 1985; Alekseev et al., 1995, 2001; Mertens and Schott, 1998; Avsic et al., 2006; González-Pola et al., 2007; Herrmann et al., 2010; Våge et al., 2011; Kolodziejczyk et al., 2015; Somot et al., 2016). In areas of dense water formation, either intermediate or deep water, strong winds triggering large ocean to atmosphere heat losses constitute the principal mechanism for cooling, evaporating and mixing of the surface layer. This results in the homogenization of the thermohaline structure of the upper water column and, eventually, in the formation of modal waters (see Tomczak and Godfrey, 1994, for a detailed explanation of modal water formation). The newly formed water masses are then transported and mixed with intermediate and/or deep waters by a number of mechanisms.

The two study areas, the Cantabrian Sea (CAS) in the southern Gulf of Biscay and the Gulf of Lion (GoL) in the NW Mediterranean Sea (hereinafter referred to as the "CASGOL region"), are located in the 42º-43º N latitudinal fringe and are separated by landmass of the Pyrenees mountain range, that is only 425 km long (Fig. 2.18).

In the GoL, winter transformation of shelf water into dense water occurs mainly over its broad continental shelf (Fig. 2.18) due to atmosphere-driven evaporation

and heat losses that diminish water buoyancy (Durrieu de Madron et al., 2005). The overall flow of newly formed dense shelf water, which cascades off the shelf and eventually spreads down to more than 2000 m in depth, experiences significant interannual variability (Béthoux et al., 2002; Canals et al., 2006; Heussner et al., 2006). The annual average formation rate of dense shelf water in severe winters is estimated to be around 0.07 Sv (Ulses et al., 2008b). Cascading dense shelf water flows downslope at high speed over the bottom (up to 1.3 cm s^{-1}; Durrieu de Madron et al., 2013), while carrying large amounts of sediment, organic matter and pollutants, which are subsequently injected into the deep-sea environment (Canals et al., 2006; Sànchez-Vidal et al., 2008; Palanques et al., 2009; Pasqual et al., 2010; Salvadó et al., 2012; Sànchez-Vidal et al., 2015).

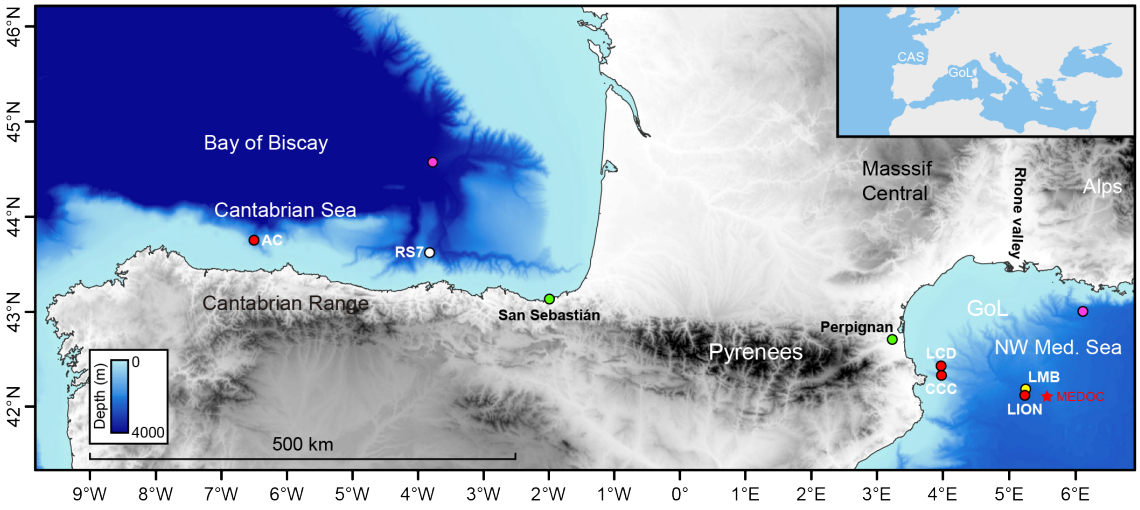

Figure 2.18. Topo-bathymetric map of the northern Iberian Peninsula and adjacent landmasses and seas showing the location of the Cantabrian Sea within the Bay of Biscay the Gulf of Lion in the NW Mediterranean Sea. The continental shelf and upper slope appear in light blue. Red star: location of the center of the MEDOC convection area. Red dots: location of moorings in the submarine canyons of Cap de Creus (CCC) and Lacaze-Duthiers (LCD), in the MEDOC convection area (LION) and in the Avilés canyon system (AC). Yellow dot: metoceanic buoy (LMB). White dot: "Radiales" hydrographic station 7 (RS7, Santander). Green dots: meteorological stations (San Sebastian and Perpignan). Pink dots: NCEP/NCAR grid points where heat and buoyancy forcings have been calculated. Bathymetry from GEBCO 2014 Grid version 20150318, (http://www.gebco.net).

Dense shelf water formation and cascading are commonly coupled with open-sea intermediate or deep convection involving the deepening of the mixed layer (MEDOC Group, 1970). In years with severe atmospheric forcing, the Mixed Layer Depth (MLD) in the GoL can extend down to the seabed at bathyal depths (L'Hévéder et al., 2013; Houpert et al., 2016). Offshore convection in the GoL is the main mechanism for the renewal of the Western Mediterranean Deep Water (WMDW), with yearly formation rates that exceed 1 Sv in years with strong convection (Herrmann et al., 2010; Somot et al., 2016). Recent investigations have shown that open-sea convection may also play a role in sediment transfer and benthic ecology dynamics (Martín et al., 2010; Palanques et al., 2012; Stabholz et al., 2013).

The Cantabrian Sea extends for 800 km along the northern Iberian continental margin, occupying the southern part of the Bay of Biscay (Fig. 2.18). Winter convection events modulate the thickness and depth of the mixed layer (González-Pola et al., 2007). Phytoplankton blooms are largely controlled by the supply of nutrients from mid-depths to the photic layer by winter convection (Somavilla et al., 2009; Hartman et al., 2014). This highlights how interannual variability in the MLD and in the areal extension of a given mixing depth have relevant consequences for the ecosystem.

Studies conducted in the CASGOL region showed that its hydrography was significantly altered during the 2004-05 extremely cold and dry winter, suggesting a teleconnection pattern (Somavilla et al., 2009). The term "teleconnection" refers to the tendency for atmospheric variables to directly or inversely relate over spatially non-contiguous areas, thus showing synchronous or correlated patterns of variation. In the Cantabrian Sea, the mixed layer reached unprecedented depths directly affecting the depth of local modal waters that are usually unconnected to air-sea interactions (Somavilla et al., 2009). In the GoL, exceptionally intense dense shelf water cascading (DSWC) and open-sea convection events occurred (López-Jurado et al., 2005; Canals et al., 2006; Font et al., 2007; Herrmann et al., 2010; Schroeder et al., 2010 and 2016). The DSWC event triggered a massive transfer of matter and energy to the deep basin while the interplay between dense shelf and open-sea convection waters resulted in denser than usual, newly formed WMDW (Font et al., 2007).

The co-occurrence of an anomalous situation both in the Cantabrian Sea and the Gulf of Lion in winter 2004-05 showed that while physically non-connected, and with different physiography and water masses, these two areas are teleconnected. According to its geographical location, the water column structure in the Cantabrian Sea, corresponds to the Northeast Atlantic one (Lavín et al., 2006), i.e.: (1) surface waters which extend down to the winter maximum depth (~250 m) of the mixed layer (González-Pola et al., 2007) and present a pronounced inter-annual variability related to seasonal cycles; (2) the East North Atlantic Central Waters (ENACW), which extend from the base of the mixed layer down to 400-600 m and result from winter mixing over the area surrounded by the North Atlantic Current and the Azores Current (Pollard and Pu, 1985; Pollard et al., 1996); (3) the Mediterranean Outflow Waters (MW), located just below the ENACW, extending down to 500-1500 m depth (Iorga and Lozier, 1999) and resulting from the outflow of Mediterranean dense water into the Atlantic Ocean through the Strait of Gibraltar mixed with local modal waters; and finally (4) the Bottom Waters (BW), which extend from the base of the MW to the seafloor and consist of a deep water mass formed after the mixing of several water masses including the North Atlantic Deep Water (NADW), the Lowered Deep Water (LDW) and the Antarctic Bottom Water (ABW) (Botas et al., 1989; van Aken, 2000).

The water mass distribution in the NW Mediterranean Sea, and in the GoL in particular, also comprises several layers. In the upper part of the water column and under normal conditions these are the following: (1) surface waters, which are directly affected by weather seasonal cycles, and (2) the Atlantic Waters (AW) (e.g. Lacombe and Tchernia, 1960), which extend from the base of the mixed layer down to 150 m depth and originate in the Atlantic inflow through the Strait of Gibraltar. Below, and mainly during wintertime, cold lenses of (3) Winter Intermediate Water (WIW) formed in the NW Mediterranean Sea by the transformation of shelf water into dense water can be found centered between 150-200 m depth (Salat and Font, 1987). Then, between 200 m and 1000 m depth warmer and saltier (4) Levantine Intermediate Waters (LIW) are found (e.g. Lacombe and Tchernia, 1972; Guibout, 1987). This water mass is formed by intermediate convection in the eastern Mediterranean basin and propagates into the western basin through the Sicily Channel. Finally, below the LIW, the (5) WMDW (Lacombe et al., 1985), formed by open-sea convection in the GoL beyond the continental shelf, fills the NW Mediterranean basin. It should be noted that in

winter the average depth of the mixed layer in the open GoL is ~425 m (Houpert el al., 2015).

Numerous submarine canyons incising the continental slope and shelf occur in the CASGOL margin. These canyons connect shallower environments with base of slope and basin environments. However, the shape and width of the continental shelf in both areas is markedly different, with a straight and narrow continental shelf (with segments that are only ~12 km wide) in the Cantabrian Sea, and a crescent-shaped and rather wide (~70 km) shelf in the GoL (Fig. 2.18).

In this work we investigate the synchronicity of atmospheric forcings and the resulting ocean system responses in the Cantabrian Sea and the GoL. With this aim we analyze both hydrographical records from 1995 to 2014 and the available historical and modeled data from 1956 to 2014 of winter mixing in the Cantabrian Sea and of cascading and deep convection in the GoL and frame them within large-scale atmospheric patterns. We also consider how atmospheric forcings and the resulting ocean system responses translate to downward particle fluxes fueling the deep ecosystem in both areas of the CASGOL region.

2.3.3 METHODS AND DATASET

The dataset needed for this study has been obtained from: (i) open databases; (ii) in situ ocean observing and sampling systems deployed both at the GoL and the Cantabrian Sea (Table 2.4); and (ii) the literature. Ad hoc laboratory analytical methods and data analysis techniques have been applied as described below.

Air temperature and precipitation data were collected from the San Sebastian and Perpignan meteorological stations (Fig. 2.18), which are the reference stations closest to our study areas at sea. Meteorological data were downloaded from the NOAA National Climatic Data Center (http://www.ncdc.noaa.gov/cdo-web/datasets). MODIS-based net primary production data were downloaded from the Ocean Productivity site (http://www.science.oregonstate.edu/ocean.productivity/).

Heat and water exchanges between the atmosphere and the ocean trigger modifications of the thermohaline properties of the upper ocean layer, which affect its density and buoyancy (Cronin and Sprintall, 2001). The variables needed

to calculate ocean surface heat fluxes and buoyancy have been estimated from the NCEP/NCAR atmospheric model reanalysis of the NOAA Earth System Research Laboratory (Kalnay et al., 1996). According to Josey (2003), the net heat exchange Q_{Net} through the ocean surface is given by the sum of four components:

$$Q_{Net} = Q_E + Q_H + Q_{LW} + Q_{SW} \quad (2.8)$$

Where Q_E and Q_H are the latent and sensible heat fluxes, respectively, i.e. the two components comprising the turbulent (non-radiative) heat fluxes. The other components are the longwave flux, Q_{LW}, and the shortwave flux, Q_{SW}, which determine the radiative heat flux. 1981-2010 monthly mean net air-sea heat fluxes have been used to calculate winter heat flux anomalies between the ocean and the atmosphere in both areas of the CASGOL region. The sign convention adopted in this work attributes positive net heat flux values to losses from the ocean to the atmosphere.

The ratio of the energy available for sensible heating to energy available for latent heating is defined by the Bowen ratio (B_o) (Bowen, 1926), as given by equation:

$$B_o = \frac{Q_H}{Q_E} \quad (2.9)$$

As Q_E and Q_H depend, besides wind speed, on air-sea moisture and temperature difference, respectively, B_o can be used as a proxy for the arrival of very cold air masses increasing sensible heat fluxes to a greater extent than latent fluxes (Renfrew and Moore, 1999).

The surface buoyancy flux, which depends on the heat and freshwater fluxes at the sea surface, can be expressed as:

$$B = -\frac{g}{\rho}\left(\frac{\alpha}{C_p}Q_{Net} + \rho\beta S\frac{E-P}{\left(1-\frac{S}{1000}\right)}\right) \quad (2.10)$$

where g is the acceleration due to gravity, ρ the density of sea surface water, α and β the thermal expansion and haline contraction coefficients, C_p the heat capacity of water, Q_{net} the surface heat loss, S the sea surface salinity and $E - P$ the net freshwater flux.

º	Observing system	Location	Instrument/sensor type	Nominal depths (m)	Sampling interval	Initial / final deployment dates	Operating institution
Gulf of Lion	Mooring line (CC1000)	Cap de Creus canyon 42º18.7'N 3º 33.2'E	Currentmeter (Nortek Aquadopp)	1000	15 min.	Oct. 2005-present	UB
			Sediment trap (PPS3)		15 days		
	Mooring line (LCD)	Lacaze-Duthiers canyon 42°25.1N 3°32.1E	Currentmeter (Aanderaa RCM 7/8/9) (Nortek Aquadopp)	500-1000	60 min.	Oct. 1993-present	CNRS-UPVD
	Mooring line (LION)	Deep basin (MEDOC site) 42º02.4'N 4º40.9'E	CTD (Microcat SBE37-SMP)	From Sep. 2007/Mar. 2008: 170-700-1500-2300 From Mar. 2008/Sep. 2008: 170-300-500-700-1500-2300 From Sep. 2008/onwards: 170-300-500- 700-850-1100-1300-1500-1750-2000-2300	3/6 min.	Nov. 2007-present	CNRS-UPVD
			Currentmeters (Aandera RCM9 from Sep. 2007/Sep. 2008 Nortek Aquadopp from Sep. 2008/onwards)	From Sep. 2007/Mar. 2008: 1000-2300 From Mar. 2008/Sep.2008: 1000 From Sep. 2008/onwards: 150-250-500-1000-2300	30 min.		
			Temperature sensors (TR1050/60 from Sep. 2007/Jun. 2011 SBE56 Jun. 2011/onwards)	From Sep. 2007/Mar. 2008: 250-350-500-600 From Mar. 2008/onwards: 150-200-230- 250-350-400-450-550-600-650	15 sec.		
	Meteoceanic buoy (LMB)	Deep basin (MEDOC site) 42º03.8'N 4º38.9'E	CTD (SeaBird SBE37)	2	10 sec.	Dec. 2001 (CTD since Sept. 2011)-present	MF
			Temperature sensors (NKE SP2T)	From Nov. 2008/Mar 2010: 10-20-50-100-200 From Mar. 2010/Nov. 2010: 10-200	5 min.		

				From Nov. 2010/onwards: 5-10-15-20-25-30-35-40- 50-60-70-75-80-90-100-120-150-175-200-250			
	Perpignan meteorological station	Perpignan 42º44,20'N 2º52.38'E	Data not available	N.A	60 min.	1981-present	NOAA
	Gridded ocean heat flux data	Close to MEDOC site 42°51'23.04"N 5°37'30"E	Reanalysis	Surface	Daily	1948-present	NCEP/NCAR
Cantabrian Sea	Repeated hydrographic surveys (Radiales station 7)	Deep slope in front of Santander 43º48'N 03º47'W	CTD (SBE 11)	0-2850	1 month	Aug. 1994-presentt	IEO
	Mooring line (AC)	Avilés canyon 43º54.6'N; 6º20.9'W	Currentmeter (Nortek Aquadopp)	2000	30 min.	March 2012-April2013	UB
			Sediment trap (PPS3)		15 days		
	San Sebastian meteorological station	43º18.48'N 2º23.4'W	Data no available	N.A	60 min.	1981-present	NOAA
	Gridded ocean heat flux data	Close to Radiales station 7 44°45'39.96"N 3°45'0"W	Reanalysis	Surface	Daily	1948-present	NCEP/NCAR

Table 2.4. Metadata of the observing and sampling systems deployed in the Cantabrian Sea and the Gulf of Lion, and in adjacent land areas, contributing to the dataset analyzed in this study.

Heat and buoyancy fluxes in the CASGOL region were also obtained from the grid points close to our two study areas that are available from the NOAA National Center for Environmental Prediction (http://www.esrl.noaa.gov/psd/).

In the GoL we used hydrographic and metoceanic data from the long-term LION mooring line and the nearby LION metoceanic buoy (LMB) too, located at ~2400 m depth in the center of the MEDOC area (Fig. 2.18). The LION line supports 5 currentmeters, 11 CTD sensors and 10 temperature sensors that extend from the sea floor to 150 m below the sea surface. The LMB includes a CTD sensor just below the sea surface and a thermistor string of temperature sensors extending from 5 m down to 200 m of water depth. The LION mooring is managed by CEFREM from CNRS-University of Perpignan, and the LMB is operated by Météo-France (http://www.meteofrance.com/accueil). The regular monitoring of the water column above the deep basin beyond the continental slope in the GoL started in the 2000s.

Given the unavailability of continuous and homogeneous hydrographic records in the GoL, years of intense convection and MLD time series have been compiled from previously published studies:

- The interannual variability of convection for the 1970-1994 period has been derived from Mertens and Schott (1998), who applied a one-dimensional mixed layer model to typical early winter preconditioning profiles and forced it with the heat flux variations of each winter.
- Years with intense winter convection leading to bottom-reaching mixing during the 1971-2000 period have been obtained from the analysis of potential temperature/salinity (θ/S) diagram shapes in the deep water performed by Béthoux et al. (2002), who identified years of convection down to the bottom after anomalous θ/S values in the bottom layer.
- The MLD for the 2007-2013 period has been obtained from Houpert et al. (2016), who computed it after merging and linearly interpolating the data from the permanent LMB and LION deep mooring line (cf. Section 2), using a ΔT=0.1°C criterion and a reference level at 10 m depth.
- Complementary data on convection and MLD from years 1986-2012 have been extracted from Somot et al. (2016), who after comparing the characteristics of bottom water masses before and after winter were able to

identify years of bottom reaching convection from the occurrence of a θ/S anomaly in the bottom layer. From the same source, we also obtained MLDs from computations applied to vertical profiles during the winter months (January, February, March) of years 1982 to 2013.

Other relevant sources of information on deep oceanographic conditions in the GoL have been the papers by Canals et al. (2006), Herrmann et al. (2010), Martín et al. (2010), Palanques et al. (2012), Durrieu de Madron et al. (2013), Puig et al. (2013), Rumín-Caparrós et al. (2013).

Hydrographic records from the Cantabrian Sea were obtained from the Santander standard section (also known as station 7) of the permanent monitoring program "Radiales" of *Instituto Español de Oceanografía* (Valdés et al., 2002; Bode et al., 2012; http://www.seriestemporales-ieo.com) (Fig. 2.18). This is the only oceanic station (2580 m) in the Cantabrian Sea that has been sampled on a monthly basis since the 90's and it is currently being used as a regional reference for ocean climate variations (Larsen et al., 2016).

The variability of the MLD in the Cantabrian Sea has been obtained from simulations using the one-dimensional General Ocean Turbulence Model (GOTM) developed by Burchard et al. (1999), which is available at www.gotm.net. The MLD long-term reconstruction in the Cantabrian Sea is based on the GOTM run forced by NCEP air-sea fluxes also using the mean seasonal evolution of the water column structure as initial and relaxing conditions. The output is an update of the simulations presented in Somavilla et al. (2011).

Data from two mooring lines located in the middle reaches (~1000 m depth) of Cap de Creus (CCC) and Lacaze-Duthiers (LCD) submarine canyons in the western GoL were also utilized (Fig. 2.18). The CCC mooring line was equipped with a currentmeter and an automated sequential sampling sediment trap at ~30 m above seafloor (asf). The LCD line held two currentmeters, one at ~30 m asf and another at mid-water (i.e. 480 m asf). Samples from sediment traps allowed calculating the total mass fluxes (TMFs) of particulate matter. The CCC1000 and the LDC1000 mooring lines are operated and maintained by *GRC Geociències Marines* of the University of Barcelona, and CEFREM from CNRS-University of Perpignan, respectively, with the two teams working in close collaboration. The

systematic monitoring of the water column above submarine canyons in the GoL, with special attention to the near-bottom layer, started in the 1980s.

The Cantabrian Sea dataset also includes data from a mooring line deployed from January 2012 to March 2013 in the middle reaches of the Avilés canyon (Fig. 2.18). This mooring line was equipped with a sequential sampling sediment trap and a currentmeter at ~45 m asf and jointly with those deployed also in middle reaches of CCC and LDC allowed monitoring TMFs simultaneously for the first time in submarine canyons of the two study areas (Table 2.4).

The sediment traps used in the two study areas were the Technicap PPS3 and PPS4 models, with collecting areas of 0.125 m^2 and 0.05 m^2, respectively. These traps have a cylindro-conical collection funnel and 12 polypropylene collecting cups (Heussner et al., 1990), which were set to rotate every 15 days. The only exception were two periods of 7-8 opening days in November 2012 and February 2013 in the Cap de Creus canyon and in Avilés canyon, respectively, which were needed to adjust the total sampling interval to the scheduled recovery dates. Before the deployment the cups were cleaned with 0.5 N HCl, rinsed with ultrapure water and filled with buffered 5% (v/v) formaldehyde solution in 0.45 μm filtered seawater to prevent degradation of trapped particles and limit the disruption of swimming organisms. After recovery, the cups were stored in the dark at 2–4 °C until they could be processed in the laboratory. Sediment trap sample processing followed a modified version of the methodology of Heussner et al. (1990). Swimming organisms were removed in two steps according to their size: large swimming organisms were removed by wet sieving through a 1 mm nylon mesh, and organisms of less than 1 mm were handpicked under a microscope with fine tweezers. A high-precision peristaltic pump robot was used to split samples into aliquots through repeated division of the sample. Samples were then rinsed repeatedly with Milli-Q water, centrifuged to remove formaldehyde and salt, and freeze-dried. The dried fraction was weighted to obtain the total mass flux as follows:

$$TMF\ (g\ m^{-2}\ d^{-1}) = \frac{Sample\ dry\ weight\ (g)}{Collecting\ area\ (m^2) \cdot Sampling\ interval\ (days)} \qquad (2.11)$$

2.3.4 RESULTS

2.3.4.1 ATMOSPHERIC FORCINGS

Time series of atmospheric forcings have been calculated for the reference period 1981-2010 in order to be consistent with NOAA published data (Arguez et al., 2012). Monthly long-term mean air temperature in the easternmost Cantabrian Sea (San Sebastian station) and the westernmost GoL (Perpignan station) responds to the typical seasonal cycle of temperate latitudes (Fig. 2.19a). However, the amplitude of temperature variations differs in both basins, with a range from 24.32ºC to 8.33ºC in Perpignan centered around 16ºC, and a range from 19.48ºC to 8.44ºC in San Sebastian centered around 11ºC. Monthly mean precipitation records exhibit a similar pattern in both locations, with fall and spring peaks and a drier summer (Fig. 2.19b). However, precipitation in San Sebastian station more than doubles the one in Perpignan station (Figs. 2.18 and 2.19b).

Winter averaged air temperature anomalies for the period 1950-2014 between San Sebastian and Perpignan stations result in a linear correlation coefficient r = 0.83 following calculations using the current reference period 1981-2010 for climatic studies (Fig. 2.20a). Windowed cross-correlations have also been computed to check how correlation varies over time (Fig. 2.20). This technique, which is particularly useful to highlight teleconnected events, requires calculating the Pearson product moment for a given time series (Boker et al., 2002). This yields a vector, or “window”, of sequential measurements sampled from the time series. Grey bars in Figure 2.20a show the result of the windowed cross correlation for the winter averaged air temperature anomalies using a time window of 3 years. Most values are between 0.5 and 0.7, which underscores the similarities and synchronic character of winter air temperature anomalies at the two stations situated at both ends of the Pyrenees Cordillera.

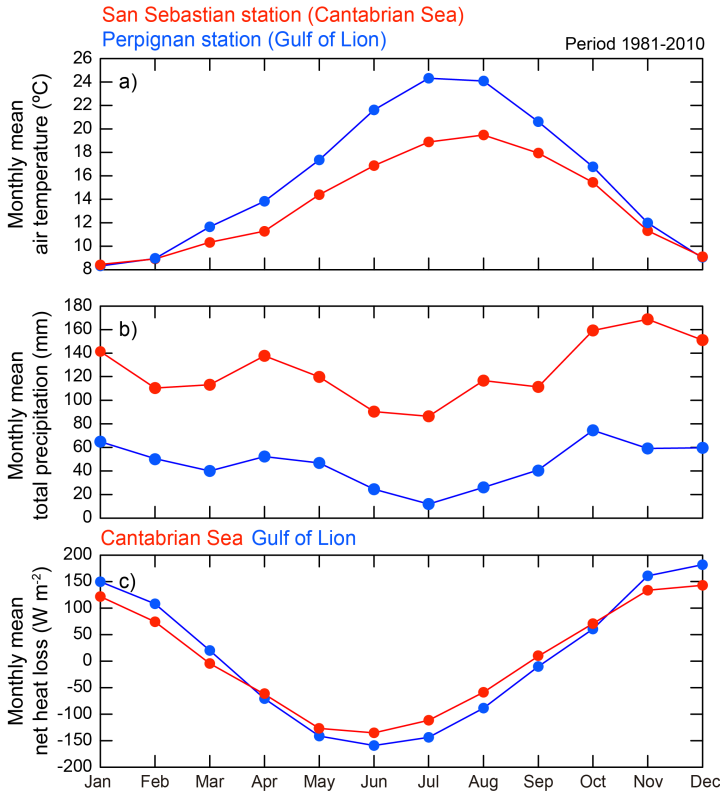

Figure 2.19. Monthly mean (a) air temperature, (b) total precipitation and (c) ocean surface net heat losses for the 1981-2010 period from meteorological stations in San Sebastian, as representative of the Cantabrian Sea (red curves) and Perpignan, as representative of the Gulf of Lion (blue lines). Net heat fluxes are extracted from the NCEP/NCAR grid points shown in Figure 2.18. Note that the grid points are close to the "Radiales" hydrographic station 7 (Santander) and the MEDOC convection area in order to be representative of heat fluxes in the two study areas.

On the contrary, winter averaged total precipitation anomalies for the very same period, also calculated from the reference period 1981-2010, show no linear correlation (r = 0.06) between the two stations, and the windowed cross-correlation lacks of consistency, with highly variable values (0.6 to -0.6) (Fig. 2.20b).

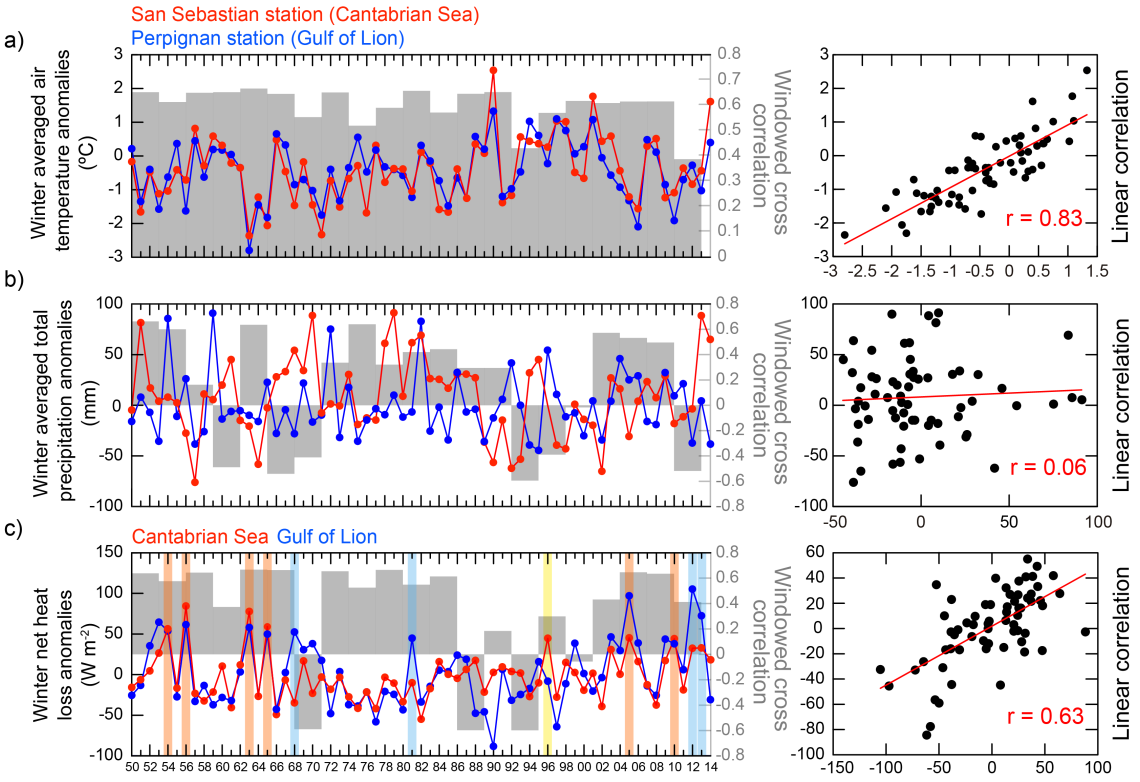

Figure 2.20. (a) Left: 1950-2014 time series of winter averaged air temperature anomalies in San Sebastian and Perpignan meteorological stations, as representative of the Cantabrian Sea and the Gulf of Lion (GoL), respectively. Grey bars represent the result of the windowed cross correlation of winter averaged air temperature anomalies using a time window of 3 years. Right: linear correlation plot of winter averaged air temperature anomalies in the two stations. (b) Left: 1950-2014 time series of winter averaged total precipitation anomalies in San Sebastian and Perpignan meteorological stations. Grey bars as in (a). Right: linear correlation plot of winter averaged total precipitation anomalies in the two stations. (c) Left: 1950-2014 time series of winter net heat loss anomalies in grid points of the Cantabrian Sea and the GoL (see Fig. 2.18 for location). Grey bars as in (a). Orange vertical stripes show winters with high concomitant net heat loss over the Cantabrian Sea and the GoL. Light blue stripes indicate winters presenting anomalous ocean-atmosphere heat losses especially over the GoL. The yellow stripe indicates winter presenting anomalous ocean-atmosphere heat losses only over the Cantabrian Sea. Right: linear correlation plot of winter net heat loss anomalies in the two grid points.

2.3.4.2 ATMOSPHERE-OCEAN INTERACTIONS

Air-sea interactions at both study areas are reflected by heat exchanges, whereas their eventual synchronous character might be an expression of an atmospheric teleconnection. Monthly mean net heat losses in the Cantabrian Sea and the GoL follow a similar seasonal evolution. The Cantabrian Sea yearlong curve displays a smoother profile than the GoL one, which indicates a strongest contrast in terms of air-ocean heat exchanges between summer and winter in the later (Fig. .2.19c). Winter net heat loss anomalies in both marine areas show a rather good linear correlation ($r = 0.63$), with a number of synchronous periods and remarkable events along the 1950-2014 record (Fig. 2.20c). The windowed cross correlation is always positive except for three periods, with most years around or above 0.5. The most noticeable concurrent events with pronounced neat heat loss anomalies correspond to 1954 (i.e. from December 1953 to March 1954), 1956, 1963, 1965, 2005 and 2010 winters. In winter 1968, 1981, 2012 and 2013 prominent anomalies were observed mostly or only in the GoL, whereas in 1996 severe anomalies were observed only in the Cantabrian Sea (Fig. 2.20c). However, periods of poor correlation and inverse correlation also occur (e.g. 1968 and 1970).

Winter averaged Bowen ratios, expressing the ratio of the energy available for sensible heating to energy available for latent heating, also show good correlation between the two marine areas along most of the 1950-2014 time series. The two records match particularly well or follow similar trends within the periods 1950-60, 1962-68, 1972-78, 1981-83, 1984-92, 1994-96, 1998-02 and 2004-14, i.e. for 85% of the 65 year long time series (Fig. 2.21). It should be also noted that the windowed cross correlation is always positive except for two short periods, with most years around or above 0.5.

Winter averaged buoyancy losses have been calculated to further investigate the impacts of ocean-atmosphere heat exchanges on the density of surface waters, also paying attention to synchrony patterns between the Cantabrian Sea and the GoL. Overall, the buoyancy loss records present a similar evolution along the 1950-2014 period (Fig. 2.22). Specific winters show large buoyancy losses in both areas (e.g. 1954, 1956, 1963, 1965, 2005 and 2010, indicated by orange bands in Fig. 2.22), but there are also buoyancy loss peaks that are particularly prominent in one area only (e.g. 1968, 1981, 2012 or 2013 in the GoL, and 1996

compared with the average value of the Cantabrian Sea, as indicated by blue and yellow bands in Fig. 2.22).

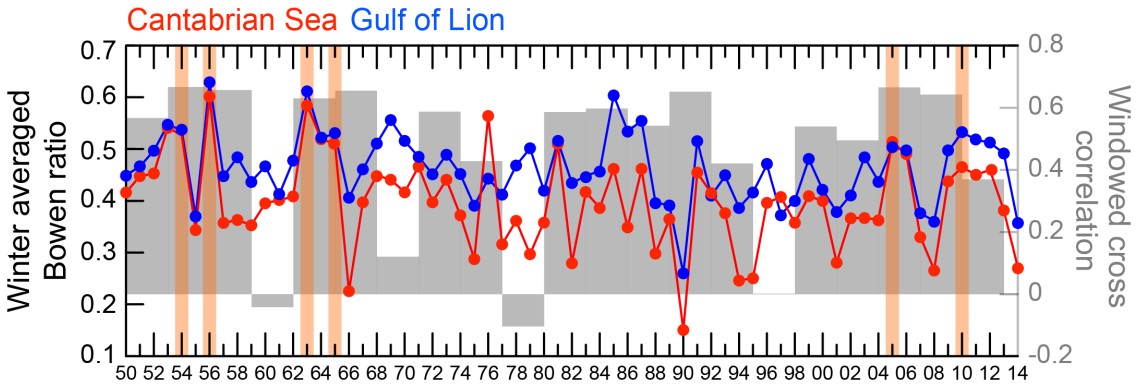

Figure 2.21. Winter averaged Bowen ratios from the grid points close to the "Radiales" hydrographic station 7 (in red, Santander) and the MEDOC convection area (in blue), as representative of heat fluxes in the Cantabrian Sea and the Gulf of Lion (see grid point locations in Figure 2.18). Grey bars correspond to windowed cross correlations between both curves. Orange vertical stripes highlight winters with concomitant severe surface forcings in both studied areas (also shown in Figure 2.20c).

2.3.4.3 OCEAN RESPONSE: DENSE SHELF WATER CASCADING AND DEEP CONVECTION

Net heat losses directly relate to winter convective mixing events both in the Cantabrian Sea and the GoL. Computing the MLD brings light on such relationship (Fig. 2.23). Temperature records for the 1995-2014 period illustrate the interannual variability of the MLD, including some years were large depths were reached during winter open-ocean convection episodes (i.e. 2005, 2006, 2009 and 2010 in the Cantabrian Sea; and 1999, 2000, 2003, 2005, 2006, 2009, 2010, 2011, 2012 and 2013 in the GoL). Large depths were reached synchronously in the two areas in 2005, 2006, 2009 and 2010 (Fig. 2.23a, b).

Time series of near bottom (30 m asf) and mid-water depth (480 m asf) temperature records from the CCC and LDC are also shown as a proxy of cascading of cooled dense waters escaping from the wide GoL shelf (Fig. 2.23b) (cf. Section 1). Time series show pronounced water temperature drops (i.e. >3ºC in 2012 in CCC) due to the arrival of cooled dense shelf waters at the 1000 m

deep mooring locations (cf. Section 2) within submarine canyons in 1999, 2005, 2006, 2010, 2012 and 2013 (Figs. 2.18 and Fig. 2.23b).

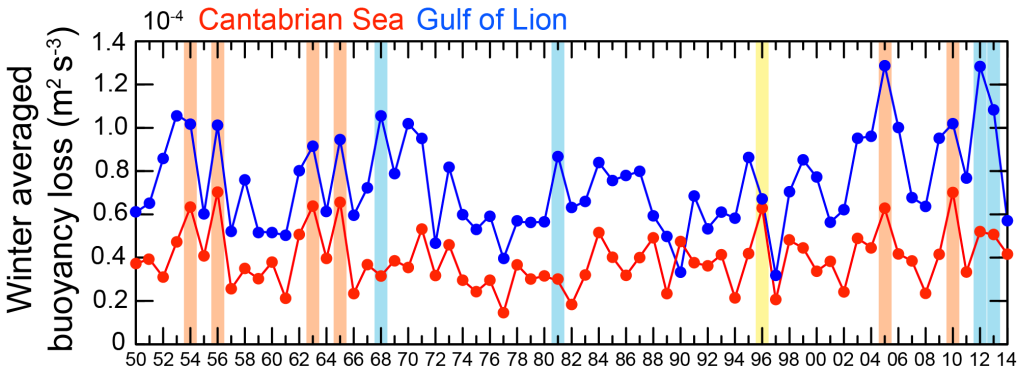

Figure 2.22. Time evolution of winter averaged buoyancy losses for the 1950-2014 period in the Cantabrian Sea (in red) and the Gulf of Lion (GoL, in blue) extracted from the grid points close to the "Radiales" hydrographic station 7 (Santander) and the MEDOC convection area, respectively (see grid point locations in Figure 2.18). Orange bands highlight winters with enhanced synchronous surface buoyancy losses in the entire CASGOL region (also pointed out in Figures 2.20 and 2.21 for presenting concomitant severe surface heat forcings and Bowen ratios in both study areas). The light yellow band indicates the 1996 winter when buoyancy loss was particularly prominent in the Cantabrian Sea (red curve). Light blue bands highlight winters with significant buoyancy losses affecting mostly the GoL (also underlined in Figure 2.20 for presenting anomalous ocean-atmosphere heat losses specially over the GoL).

The records in Figure 2.23 highlight the high interannual variability of the MLD both in the Cantabrian Sea and the GoL. Three particularly intense events appear as synchronous in all records within the 20 yearlong time series from 1995 to 2014, namely those from the winter months of 2005, 2006 and 2010. Other still pronounced events recorded only in the Cantabrian Sea occurred in 2001, 2003, 2004 and 2011. On the contrary, the events of years 1999, 2012 and 2013 were significantly more intense in the GoL, as also shown by the submarine canyon records.

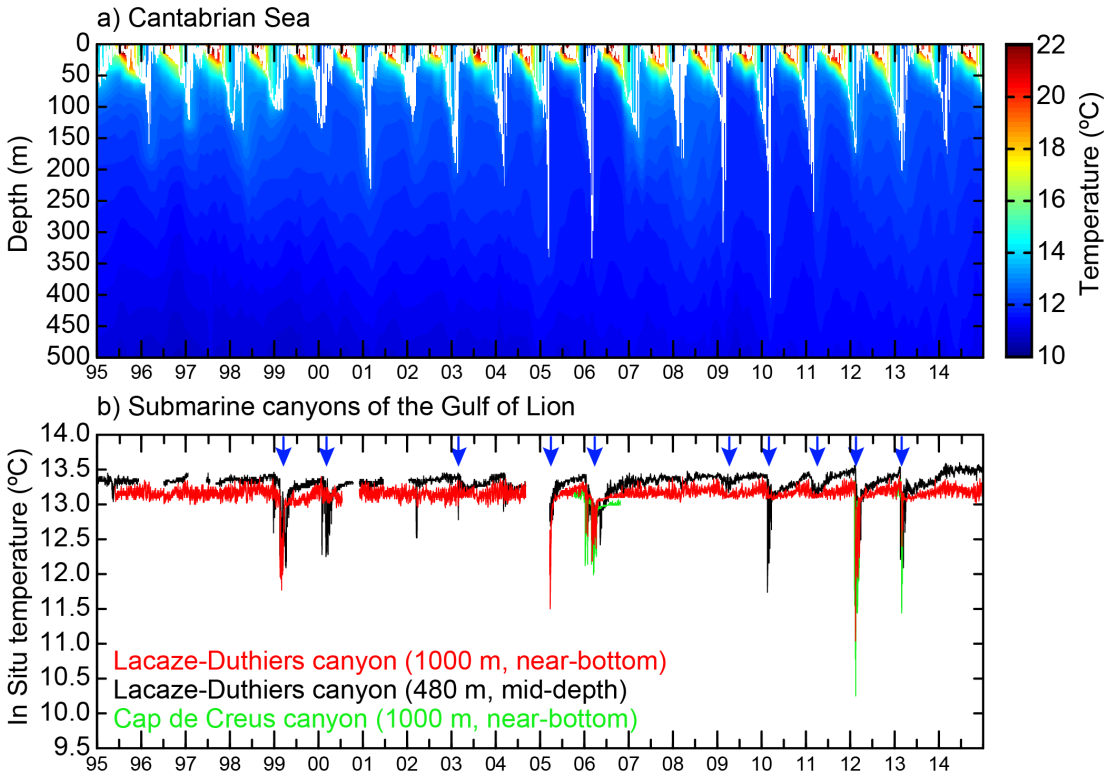

Figure 2.23. (a) Upper water layer temperature evolution at the "Radiales" hydrographic station 7 (Santander) in the Cantabrian Sea. Vertical white lines show the Mixed Layer Depth (MLD) after the General Ocean Turbulence Model (GOTM) model as the depth of the turbulent surface layer. (b) Near-bottom (~30 m above seafloor, asf, in red) and mid-water (480 m asf, in black) temperature time series measured in the Lacaze-Duthiers canyon (LDC) at 1000 m depth. Green lines indicate near-bottom temperature at 1000 m depth during winters 2006, 2012 and 2013 as measured ~30 m asf in the Cap de Creus canyon. Note that the LDC records are mostly continuous, while the CCC ones refer to specific winters only. CCC is the main escape route for dense shelf water in the GoL and displays larger temperature drops than the LDC (e.g. 2006, 2012 and 2013). Blue arrows indicate years with severe convection according to Béthoux et al. (2002), Houpert (2013) and Somot et al. (2016).

2.3.4.4 TMF AND ECOSYSTEM RESPONSE

TMFs obtained simultaneously in the Avilés canyon and CCC within the January 2012 to March 2013 period show similar variability patterns off each end of the Pyrenees. TMFs peaked in winter and early spring, with peak flux magnitudes being much higher in the CCC than in the Avilés Canyon (70 g m^{-2} d^{-1} in February at CCC vs. 16 g m^{-2} d^{-1} in April in the Avilés canyon) (Fig. 2.24).

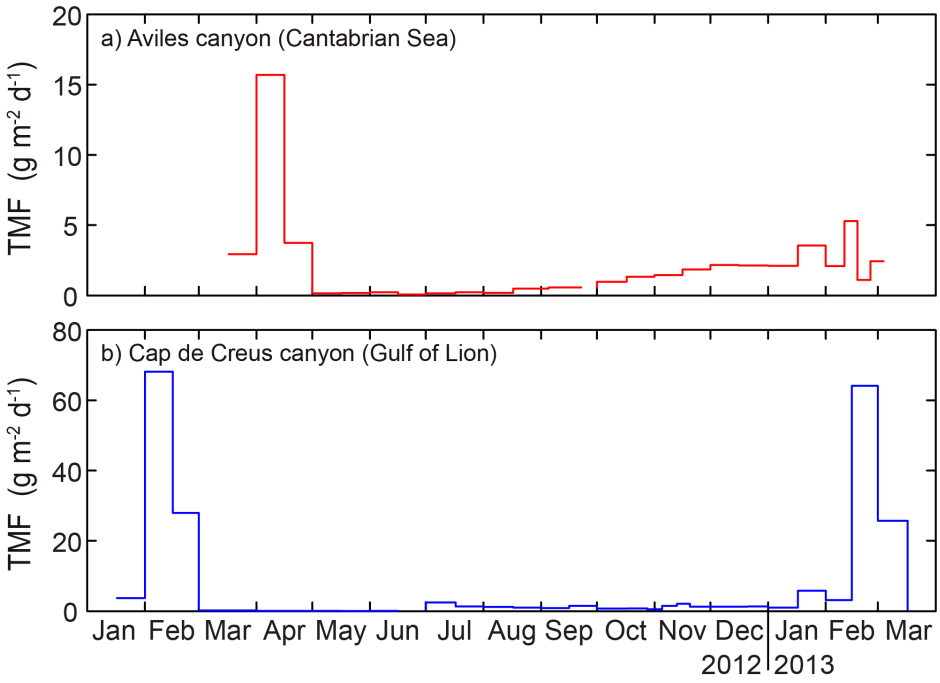

Figure 2.24. Total mass fluxes (TMF) from two near-bottom sediment traps in mooring stations deployed simultaneously from January 2012 to March 2013 at the middle course of (a) the Avilés canyon (2000 m, red stepped line) and (b) the Cap de Creus canyon (1000 m, blue stepped line). Vertical scales in (a) and (b) differ.

Winter convective mixing events have an impact on the intensity of spring blooms in the entire CASGOL region, as illustrated by the net primary production maps (mg C m^{-2} d^{-1}) in Figure 2.25. MODIS-based composites show concomitant high net primary production in the Bay of Biscay and the NW Mediterranean Sea in springs (i.e. averaged from March to April) that follow winters where abnormal convection took place simultaneously in both areas forming the CASGOL region, such as in years 2005, 2006, 2010 (together with intense DSWC in the GoL) and 2011.

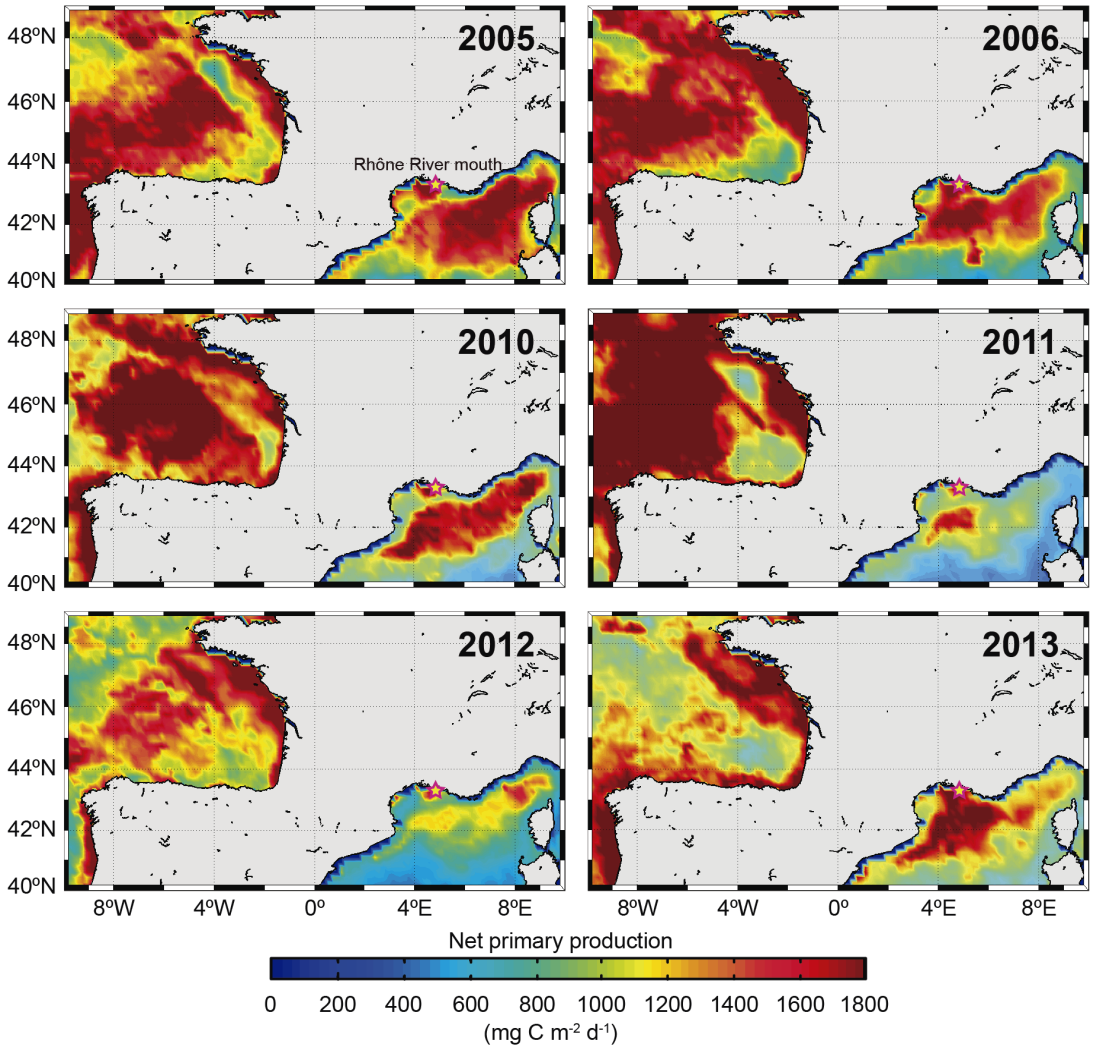

Figure 2.25. Net primary production maps (mg C m^{-2} d^{-1}) from MODIS data showing the development of phytoplanktonic blooms in spring (averaged April and May) 2005, 2006, 2010, 2011, 2012 and 2013. Net primary production data have been downloaded from the Ocean Productivity site (http://www.science.oregonstate.edu/ocean.productivity/) and calculated using the Vertically Generalized Production Model (VGPM) (Behrenfeld and Falkowski, 1997). For the VGPM, net primary production is a function of chlorophyll, available light, and photosynthetic efficiency. Note the local net primary production high immediately offshore the Rhône River mouth (red star with yellow core).

2.3.5 DISCUSSION

2.3.5.1 CONCURRENT ATMOSPHERIC FORCING OVER THE CASGOL REGION AND ITS CONSEQUENCES

The atmospheric circulation over the NE Atlantic Ocean and Western Europe is mainly driven by the interaction between the Iceland Low and the Azores High. This large-scale atmospheric pattern presents a marked seasonality and its variability determines weather anomalies and climate variability in the entire region. During winter, the Iceland Low strengthens and the Azores High weakens and migrates south-eastward towards the Canary Islands. The situation reverses during summer, when the Azores High reinforces and the Iceland Low weakens. In the Cantabrian Sea, this leads to a season with N and NE prevailing winds from April to September and a season with NW prevailing winds from October to March. During the latter period, the Cantabrian area is frequently impacted by severe storms linked to the passage of Atlantic atmospheric fronts. The E-W oriented Cantabrian Range to the south (Fig. 2.18) opposes to the flow of humid marine air masses from the Atlantic, which are forced to raise, subsequently enhancing precipitation (orographic rainfalls). This is the main cause of the high precipitation rates of the Cantabrian area (Fig. 2.19b). The Atlantic atmospheric fronts weaken while crossing the Iberian Peninsula and the Pyrenees from west to east after having released most of their moisture over western Iberia and the Cantabrian watershed.

Conversely, in the NW Mediterranean Sea, eastern storms occurring occasionally in winter transfer humid marine air towards the coast, where air masses are forced to ascend by the Catalan Coastal Ranges and the eastern Pyrenees, which normally results in short (hours to few days) but often very intense orographic rainfalls. These storms do not penetrate much into the Iberian Peninsula and, therefore, do not reach the Cantabrian watershed. The differences in precipitation regimes between the Cantabrian and the NW Mediterranean regions is well depicted by the lack of correlation ($r = 0.06$) of winter averaged precipitation anomalies over the 1950-2014 period using again San Sebastian and Perpignan as reference meteorological stations (Fig. 2.20b). The windowed cross-correlation also lacks of consistency, with highly variable values with r between 0.6 and -0.6.

The Mediterranean Basin has a warmer (and drier) climate than the Cantabrian region (Fig. 2.19a, b), largely due to warm air intrusions from North Africa. Despite this, winter averaged air temperature anomalies parallel each other during most of the 1950-2014 time series, as illustrated by the records of San Sebastian and Perpignan (Fig. 2.20a), with most values in the windowed cross-correlations analysis between 0.5 and 0.7. This highlights the view of a winter atmospheric teleconnection between the Cantabrian area and the GoL, as reflected by air temperature patterns.

Given that air temperature is a key parameter in water mass formation processes, teleconnection maps of winter averaged surface air temperature anomalies are particularly useful to evaluate the spatial structure and the consequences of teleconnections leading to synchronous winter climate variability patterns. For this reason, we have computed a "teleconnection map" of winter averaged surface air temperature anomalies referring the dataset from the Perpignan meteorological station to 2.5° latitude x 2.5° longitude global grid (144x73) points from 90°N to 90°S and 0°E to 357.5°E (Fig. 2.26).

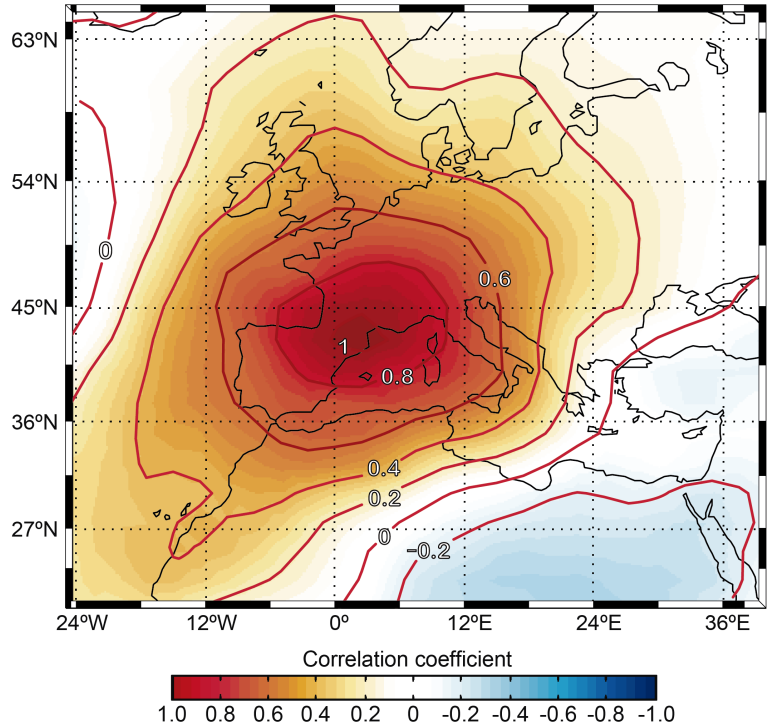

Figure 2.26. Correlation map of surface air temperature anomalies between the Gulf of Lion and the NCEP/NCAR grid points existing worldwide.

This map expresses the correlation between winter averaged air temperature anomalies in the GoL and elsewhere, and highlights that a large part of the computed air temperature anomalies vary in parallel ($r \geq 0.8$) within a radius of about 1,000 km from the Perpignan station base point. Such a correlation distance, which encompasses the Cantabrian Sea and the GoL in one single domain (Fig. 2.26), is much smaller than the thousands of kilometers of large-scale teleconnection patterns. The above suggests that the fluctuations of the atmosphere temperature forcings occurring over the CASGOL region, and their eventual synchrony, could be viewed as a short-range teleconnection owed to the rather close geographic location of the Cantabrian Sea and the GoL.

Such short-range teleconnections are often neglected and, more importantly, the ocean system responses they trigger and their ecosystemic impacts over marine areas separated by landmasses ignored. Several major consequences result from the atmospheric forcing acting concurrently over the Cantabrian Sea and the GoL. First, it causes the annual cycle of net ocean surface heat flux to oscillate almost in parallel (Fig. 2.19c) with the windowed cross correlation coefficient being always positive, with most years around or above 0.5, except for rare periods (four) (Fig. 2.20c). Second, it determines extreme net heat loss to occur during certain winters, eventually in synchrony in the two areas (Fig. 2.20c). Somavilla et al. (2009) noticed abnormally high net heat losses in the Cantabrian Sea in 1963, 1965, 2005 and 2006 winters. Similarly, Schroeder et al. (2010) and Durrieu de Madron et al. (2013) highlighted abnormally high ocean-atmosphere heat losses in the GoL in winters 2005 and 2012, respectively.

Our 1950-2014 records show that abnormal heat losses occurred in synchrony over both the Cantabrian Sea and the GoL during the winters of 1954, 1956, 1963, 1965, 2005, and, to a lesser extent, 2010 (orange bands in Fig. 2.20c). Exceptional winters in terms of ocean heat transfer to the atmosphere in both areas have been attributed to sensible heat fluxes contributing to net heat losses well over “normal” winters (Somavilla et al., 2009; Schroeder et al., 2010). High sensible heat fluxes, which are linearly proportional to the air-sea temperature difference, give rise to high Bowen ratios, which in turn are related to the presence of cold air masses (Renfrew and Moore, 1999). The synchronous character of the winter atmospheric forcing over the CASGOL region is further evidenced by the good correlation of winter averaged net heat loss anomalies and Bowen ratios, with the most pronounced events presenting concomitant increases of the two

variables in both areas (Figs. 2.20c and 2.21). Indeed, correlations are r = 0.6 both for winter averaged net heat loss in the GoL vs. Bowen ratio in the Cantabrian Sea, and for winter averaged net heat loss in the Cantabrian Sea vs. Bowen ratio in the GoL (not shown).

2.3.5.2 ATMOSPHERIC VARIABILITY AND THEIR IMPACT OVER THE STUDY AREAS

The main modes of atmospheric variability over the NE Atlantic region, including the CASGOL region, are the North Atlantic Oscillation (NAO) and the East Atlantic Pattern (EAP), as discussed by Rogers (1990), Josey (2001), Josey and Marsh (2005), Cassou et al. (2011) and Tréguer et al. (2014), amongst other. However, according to Thompson and Wallace (1998), during winter monts the Arctic Oscillation (AO) accounts for a substantially larger fraction of the variance of the northern hemisphere surface air temperature than the NAO.

Several authors have referred to the links between atmospheric circulation patterns and the strengthening of vertical convective mixing in the Cantabrian Sea, and open-sea and dense shelf water formation events in the GoL (López-Jurado et al., 2005; Somavilla et al., 2009; Schroeder et al., 2010; Durrieu de Madron et al., 2013). Wintertime extreme oceanographic events relate to a high-pressure anomaly located west of Ireland, which results from long-lasting anticyclones subsequently leading to pervasive, cold and dry north-easterly winds over southwestern Europe. Some authors, such as Somavilla et al. (2009) and Schroeder et al. (2010), identify this atmospheric pattern as the negative phase of the EAP from Rogers (1990), which would be the mode with the greater impact on heat exchanges over the GoL (Josey et al., 2011). However, the northward displacement of the center of such high-pressure anomaly has also lead to identify it as the negative phase of the AO (Thompson and Wallace, 1998).

One critical question is to understand whether or not this atmospheric configuration consisting of a high-pressure anomaly over the NE Atlantic is a recurrent driver of synchronous shifts over both study areas, independently of the principal mode of atmospheric variability, either the EAP or the AO. A retrospective analysis of the principal modes of atmospheric variability over the latitudinal range of the CASGOL region brings light to that point (Fig. 2.27a, b).

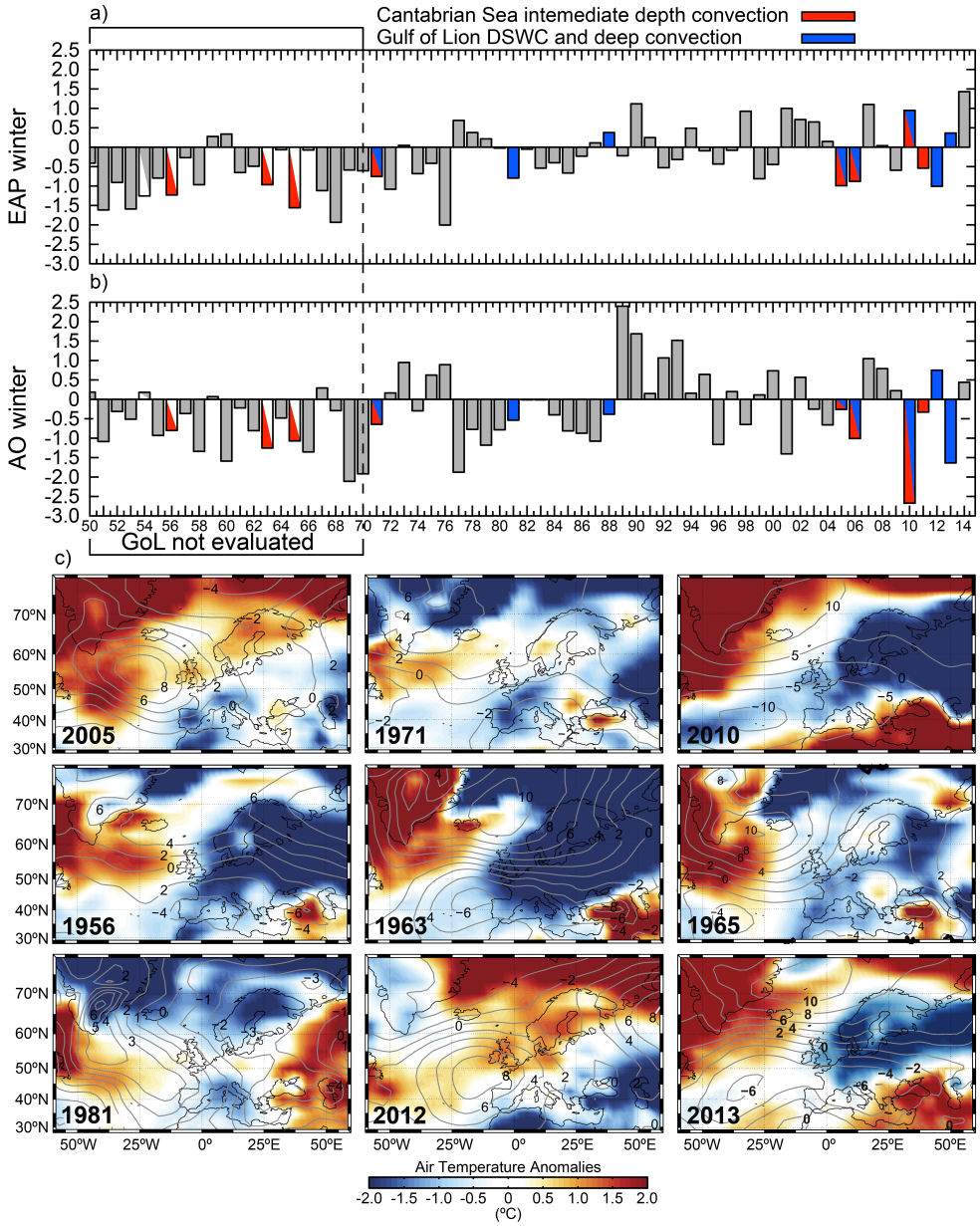

Figure 2.27. Time series of 1950-2014 winter averaged (a) East Atlantic Pattern (EAP) and (b) Arctic Oscillation (AO) indexes from the NOAA National Climatic Data Center. Years with intense convection in the Cantabrian Sea and DSWC and intense convection in the Gulf of Lion (GoL) are shown in red and blue, respectively. It must be noted that it has not been possible to evaluate GoL events prior to 1970 due to the lack of hydrographic data (white bars indicate that no data is available for the GoL). (c) Large-scale fields of sea level pressure (millibars) and air temperature (ºC) winter averaged anomalies over the NE Atlantic and the Mediterranean region during some illustrative winters presenting severe anomalies over at least one (1981, 2012 and 2013) or the two study areas (1971, 2005 and 2010). Whereas for winters 1956, 1963 and 1965 only evaluations for the Cantabrian Sea are available, it cannot be excluded that DSWC and deep convection co-occurred in the GoL

Years with enhanced mixing in the Cantabrian Sea and/or intense DSWC and open-sea deep convection in the GoL generally show winter averaged (i.e. from December to March) negative EAP and AO indexes (Fig. 2.27a, b). However, some exceptions can be observed along the time series. This is illustrated by the EAP, which was found to be positive in DSWC and deep convection years 1998 and 2013 in the GoL and in DSWC and convection year 2012 both in the GoL and the Cantabrian Sea. The AO index was positive only once, in the GoL, in DSWC and deep convection year 2012. On the other hand, there are several years showing pronounced negative EAP and AO indexes in absence of intense DSWC and open-sea deep convection in the GoL and/or enhanced mixing in the Cantabrian Sea. This opens the question about the reliability of modes of atmospheric variability to capture particular atmospheric configurations.

To address this issue, maps of winter (i.e. December to March) Sea Level Pressure (SLP) anomalies leading to the arrival of cold air masses over southwestern Europe have been computed for some representative years (Fig. 2.27c). They show first that simultaneous convection in the Cantabrian Sea, and DSWC and convection in the GoL (Fig. 2.27a, b), can occur both due to the blowing of continental cold easterly winds (e.g. 1971 and 2010) and of cold and dry north-easterly winds (e.g. 2005). The situation in 2005, with the anticyclonic anomaly west of the British Islands, closely resembles the negative state of the EAP as given by SLP, which is similar to the one shown by the SLP anomaly maps (Fig. 2.27c). This is confirmed by a negative winter averaged EAP index (Fig. 2.27a), but also by an AO index indicating a concurrent negative phase of the AO (Fig. 2.27b). In 1971 and 2010 the anticyclonic anomaly was shifted north or north-westwards in conjunction with negative EAP and AO indexes (1971), or only with a strong negative AO index while the EAP index was positive (2010) (Fig. 2.27a-c). Temperature and MLD records from 1995 onwards further highlight the sinking of dense water in both convection areas and the cascading of dense shelf water along the submarine canyons of the GoL in years 2005 and 2010, and in other years too (Fig. 2.23).

The SLP anomaly maps also illustrate years where there was convection in only one of the two study areas, either the Cantabrian Sea or the GoL, in the latter associated with DSWC. Years 1956, 1963 and 1965 were all characterized by the flow of continental cold easterly winds along a corridor between the anticyclonic anomaly located nearby Iceland and a pressure low over Iberia or west of it (Fig.

2.27c). Both indexes, EAP and AO, were negative during these winters (Fig. 2.27a, b). The ESE-WNW orientation of the Pyrenees Range (Fig. 2.18), with elevations in excess of 3000 m, may have helped channelizing the easterly winds towards the Cantabrian Sea, thus triggering there the highest net heat loss anomalies and some of the highest buoyancy losses in the 1950-2014 time series (Figs. 2.20c and 2.22), which eased convection. Significant net heat loss anomalies and buoyancy losses might have occurred during these winters also in the GoL (Figs. 2.20c and 2.22), eventually triggering intense DSWC and open-sea convection processes, but the data prior to 1970 did not allow evaluating winter EPA and AO indexes there (Fig. 2.27a, b).

In years 1981 and 2012 the anomalous high-pressure centre was closer or directly above the Cantabrian Sea, which pushed eastwards (i.e. directly over the GoL) the north-easterly flow of cold and dry continental air (Fig. 2.27c), subsequently triggering DSWC and open-sea convection in the GoL, whereas no intense convection occurred in the Cantabrian Sea. The atmospheric configuration in 2012, when the high-pressure centre was directly over the Bay of Biscay, resulted in the highest net heat loss anomalies and buoyancy losses (jointly with 2005) in the GoL along the entire 1950-2015 period (Figs. 2.20c and 2.22). This corresponds to the largest near-bottom temperature drop in the submarine canyons of the western GoL, namely 3ºC in CCC at 1000 m depth occurring jointly with intense convection reaching the basin floor (Durrieu de Madron et al., 2013). In 1981, both the EAP and AO indexes were slightly negative, while in 2012 the EAP was negative and the AO positive.

In winter 2013, the anomalous high-pressure centre was shifted to the north, i.e. similar to 2010, with the low-pressure centre west of the Cantabrian Sea. The EAP was positive and the AO negative during that winter (Fig. 2.27a, b). Such situation led to cold air masses to reach only the GoL, where they triggered DSWC and open-sea convection whereas no intermediate convection took place in the Cantabrian Sea. (Fig. 2.27a, b).

The above observations suggest that the synchronic character of the ocean response to extreme winter atmospheric forcing in the CASGOL region is strictly dependent on the prevailing winter regional atmospheric configuration, which is captured only partly by atmospheric variability modes. The occurrence or co-occurrence of intense, abnormal convection processes in both study areas, and

DWSC in the GoL, ultimately depends on the prevalent location of the high-pressure anomaly during winter, which determines the penetration, provenance and persistence of cold air masses over the CASGOL region, also controlling ocean to atmosphere heat exchanges.

In absence of hydrographic evidence, the Bowen ratio has been explored as proxy for the arrival to the CASGOL region of cold air masses able to steepen the ocean-atmosphere temperature gradient and enhance both heat losses through the ocean surface and surface water density, eventually leading to abnormal convection in the CASGOL region and DSWC in the GoL only (Figs. 2.19c, 2.20 and 2.21). This is the case, for instance, of winters 1954, 1956, 1963 and 1965, characterized by very deep MLD as highlighted in the reconstruction of the MLD variability for the last 60 years in the southern Bay of Biscay by Somavilla et al. (2011). Winter 1954 stands out for presenting anomalously high and well correlated Bowen ratios (shaded areas in Fig. 2.21), high and also well correlated net heat anomalies and buoyancy losses in both basins ($r > 0.5$ for both Bowen ratios and net heat anomalies), and negative EAP but slightly positive AO indexes (Figs. 2.20c, 2.22 and 2.27a, b). This highlights the occurrence of concomitant severe atmospheric forcing over the Cantabrian Sea and the GoL, which may have resulted in synchronous ocean system response and extreme events. However, the above-mentioned lack of hydrographic evidence in the GoL prior to 1970, and also the limitations of reproducing the MLD in the Cantabrian Sea so back in time with the GOTM model (Somavilla et al., 2011), prevents us to firmly state that intense convection (and deep DSWC in the GoL) extended to the entire CASGOL area in winter 1954.

The analysis of SLP and air temperature anomalies shows that during the winters of 1956, 1963 and 1965 cold air masses reached the CASGOL latitudes and extended well over the entire region (Fig. 2.27c). The winters of 1956 and 1963 stand out for presenting high and well correlated Bowen ratios (Fig. 2.21), net heat anomalies ($r > 0.6$ both for Bowen ratios and net heat anomalies) and buoyancy losses amongst the two study areas, and negative EAP and AO indexes (Figs. 2.20c, 2.22 and 2.27a, b). The Bowen ratio of winter 1965 is not particular high, but this winter is also prominent as it presents high net heat anomalies and buoyancy losses ($r > 0.6$) in both areas, and negative EAP and AO indexes. As for 1954, the evidences above and the MLD analysis by Somavilla et al. (2011) support a severe surface forcing during these three winters over the entire

CASGOL region, which likely resulted in extreme and synchronous oceanographic responses.

However, using the Bowen ratio as proxy for the arrival of cold air masses to the CASGOL region must be done with caution. This is illustrated, for instance, by the 1985-87 period, when high Bowen ratios were recorded in the GoL (Fig. 2.21) in parallel with low net heat loss anomalies (Fig. 2.20c) and moderate buoyancy losses (Fig. 2.22) associated to strong convection but not to DSWC (Mertens and Schott, 1998; Béthoux et al., 2002). Indeed, only during particularly severe winters the cooling and evaporation of coastal surface waters is strong enough to lead to an increase of its density up to values larger than that the waters below, thus overcoming the buoyancy increase effect of freshwater inputs that oppose to dense water formation over the shelf. When formed, dense shelf water overflows the shelf edge down to the basin (Canals et al., 2006; Durrieu de Madron et al., 2013; Puig et al., 2013) while progressively mixing with intermediate and deep ambient waters. Clearly, this was not the case in the 1985-87 period, no matter the high winter Bowen ratio recorded. It is important noticing that in this triennium the high Bowen ratios were due to the higher proportion of sensible heat fluxes (numerator) compared to latent heat fluxes (denominator) rather than to the arrival of cold air masses increasing Q_H. And this occurred despite the relative low magnitude of sensible vs. latent heat fluxes (not shown).

Another interesting case is the 1976 one, when high Bowen ratios were recorded in the Cantabrian Sea in absence of significant net heat loss anomalies and buoyancy losses (Figs. 2.20c and 2.22). A noticeable oceanic response was also lacking in 1976 (Fig. 2.27a, b) (Somavilla et al., 2011). The higher proportion of sensible heat fluxes compared to latent heat fluxes (see Figure 3 in Somavilla et al., 2009) was also the reason behind the high Bowen ratio recorded in 1976. Also, whereas high Bowen ratios were recorded concomitantly in both the Cantabrian Sea and the GoL in 1981, 1991 and 2010-2012, extreme oceanographic responses were triggered only in the GoL in winters 1981 and 2010-2012. In these years r was close to 0.6 in 1981, > 0.6 in 1991 and almost 0.4 in 2010-2012). Overall, the examples above demonstrate that the Bowen ratio should not be used alone to detect situations that could lead to intense convection in the CASGOL region, with DSWC in the GoL, but together with other variables such as net heat and density losses. Actually, DSWC is nothing else than the result

of convection over the continental shelf followed by shelf edge spillover of the newly formed dense waters (Canals et al., 2013, their Figure 5).

2.3.5.3 THE 2005-2006 SHIFT AND OTHER RECENT EVENTS

According to observations, intense convection, with DSWC in the GoL, in one or both areas of the CASGOL region normally occurs in single winters, with only two times in records where it took place in two or more successive years: 2005-2006 and 2010-2013 (Fig. 2.27a, b). Of these, only in 2005 and 2006 abnormal convection took place simultaneously in the Cantabrian Sea and the GoL, where intense DSWC also occurred (see Somavilla et al., 2009 and 2011 for the Cantabrian Sea; and López-Jurado et al., 2005; Canals et al., 2006; Font et al., 2007; Puig et al., 2008; Schroeder et al., 2008, 2010 and 2016 for the GoL). In the 2010-14 four-year period abnormal convection took place synchronously only in 2010 both in the Cantabrian Sea and, jointly with DSWC, in the GoL, while recurrence in successive years involved only the Cantabrian Sea (2011) or the GoL (2012 and 2013). An update of the simulations of Somavilla et al. (2011) for the Cantabrian Sea is presented in Figure 2.23a, while a parallel update of Houpert (2013) Rumín-Caparrós et al. (2013) and Somot et al. (2016) for the GoL is shown in Figure 2.23b. Considering only the two first biennia 2005-2006 and 2010-11, the net heat loss anomaly and buoyancy loss curves follow a parallel pattern in each of them, with peak values in the two study areas in the first year (i.e. 97 W m^{-2} and 45 W m^{-2} net heat loss anomalies and 1.3 m^2 s^{-3} and 0.6 m^2 s^{-3} buoyancy loss in the GoL and the Cantabrian Sea, respectively). The second year is punctuated by a marked descend in both net heat loss and buoyancy loss (i.e. 39 W m^{-2} and 16 W m^{-2} net heat loss and 1.0 m^2 s^{-3} and 0.4 m^2 s^{-3} buoyancy loss in the GoL and the Cantabrian Sea, respectively). In 2012 and 2013, heat loss anomalies and buoyancy losses peaked significantly in the GoL only, with 105 W m^{-2} and 73 W m^{-2}, and 1.3 m^2 s^{-3} and 1.1 m^2 s^{-3}, respectively (Fig. 2.20c, 2.22). Actually, given that no deep convection took place in winter 2011 in the GoL but in the Cantabrian Sea, it would make sense splitting the 2010-2014 period into two separate biennia, the 2010-11 and the 2012-2013 ones (Fig. 2.27a, b). In the second of these biennia enhanced convection took place in the GoL but not in the Cantabrian Sea (see below).

Interestingly, smaller net heat and buoyancy losses during the second year of the 2005-06 and 2010-11 biennia (Fig. 2.20c, 2.22) led for a second winter to

abnormally large mixed layer depths both in the Cantabrian Sea and the GoL, although DSWC did not go deep in 2011 (Fig. 2.23a, b). Such a situation has been attributed to a "reemergence mechanism" (Smith et al., 2008; Somavilla et al., 2009). The concept of reemergence mechanism (also referred to as "recurrence") refers to a phenomenon in which ocean thermal anomalies created over the deep mixed layer during a given winter reappear next winter within the newly formed mixed layer, being the loss of the stratification acquired the previous year the cause of and easy reproduction of a deep and cold mixed layer. Whereas in the GoL this phenomenon is documented in the work of Béthoux et al. (2002), the winters of 2005 and 2006 were the first time such phenomena was observed in the Bay of Biscay. Somavilla et al. (2009) inferred that this situation may have been more frequent in the early 1960s, and possibly earlier, when large net heat and buoyancy losses occurred in the area (Figs. 2.20c and 2.22).

Another interesting situation to address is the one of winter 1996 in the Cantabrian Sea only, when relatively high heat loss (reaching almost 50 W m^{-2}) and buoyancy loss (0.6 m^2 s^{-3}) (Figs. 2.20c and 2.22) were unable to trigger any significant hydrographic response (Fig. 2.23a). According to Somavilla et al. (2011), the contribution of Q_h to the total heat loss in winter 1996 was much lower than, for instance, during winter 2005 (see low Bowen ratio during winter 1996 in Fig. 2.21). Winter 1996 was characterised by relatively high sea surface temperature and large amounts of heat exchanged by evaporation, being the high sea surface temperatures partly caused by the milder conditions of the previous autumn. In addition, in 1996 the NCEP/NCAR reanalysis provides substantially higher values than other data sets (i.e. the ERA40 from the European Center for Medium Range Weather Forecasting, available from 1957 to 2002) (Somavilla et al., 2011). This may have led to overestimating the 1996 heat and buoyancy losses, and thus the density flux in this year might be smaller than, for instance, in 2005.

Synchronous intense convection events, and DSWC in the GoL, had important consequences for both areas forming the CASGOL region. In the Cantabrian Sea and, more generally, in the Bay of Biscay, the unusual depth of the mixed layer in 2005 and 2006 (Fig. 2.23a) allowed it reaching and ventilating the ENACW, which are not involved in air-sea interactions under normal conditions (Somavilla et al., 2009). The mixing of warmer and saltier upper waters with colder and fresher modal ENACW made the upper waters colder and transformed the ENACW into a

saltier, warmer and thus denser variety (Somavilla et al., 2009). Somavilla et al. (2016) have recently described the implications of such shift on the North Atlantic heat budget. The 2005 and 2006 events also resulted in a dramatic reduction of the stratification of the upper permanent thermocline triggering a cold low stratification anomaly with a large spatial extent that remained for the two years below the seasonal thermocline.

Similarly, Schroeder et al. (2010) found that extreme surface forcings acting over the NW Mediterranean Sea during winters 2005 and 2006 were related to a major renewal of the WMDW. López-Jurado et al. (2005) documented how after winter 2005 the deep water masses in the Western Mediterranean Basin presented higher heat and salt contents, which according to Font et al. (2007) partly resulted from the mixing of dense waters generated by open-sea convection and DSWC in the GoL. In the Mediterranean Sea, winter 2005 was the onset of the so called "Western Mediterranean Transition" (WMT), which involved a significant shift in the physical properties of the water masses, with temperature and salinity decreases in intermediate waters and sudden increases in deep waters (CIESM, 2009; Schroeder et al., 2016).

However, other factors likely played a role in the exceptional character of winter 2005 in the GoL and, by extension, the Western Mediterranean Basin, which was also followed by reemergence in 2006, and also in the Bay of Biscay. These included a progressive increase of heat and salt contents in the intermediate and bottom layers due to the westward propagation of the Eastern Mediterranean Transient (EMT) (Roether et al., 2007), which would have eased an unusual production of dense deep water. In the Cantabrian area, the pronounced air temperature anomaly in 2004 and 2005, also observed in the GoL, combined with a precipitation low (Fig. 2.20a, b). These two factors likely reinforced each other subsequently modifying the thermohaline properties of surface waters, which would tend to gain density not only because of cooling but also as a consequence of enhanced evaporation due to wind action and of reduced precipitation and runoff. A similar situation in the Cantabrian Sea, with a strong air temperature anomaly and at least one year of marked precipitation deficit, and a relevant buoyancy loss, occurred only in the 1963-65 period, with year 2014 representing a milder interval (Figs. 2.20a, b and 2.22). Puig et al. (2008) pointed to reduced river discharge, with no floods, as a factor contributing to decrease the buoyancy

of coastal waters and to enhance dense shelf water formation and the intensity of DSWC in the Gulf of Lion.

Overall, the above suggests that the occurrence of exceptional winters, such as 2005, eventually associated to reemergence phenomena, as in 2006, depends on the interplay amongst factors ultimately driven by atmospheric configurations over much larger areas than the CASGOL region itself. These include (i) the weakening of the Bermudas-Azores high-pressure center regulating the atmosphere-ocean heat exchanges through air subsidence and moderate winds; (ii) the shift of the high-pressure center to the west of the British Islands, as in 2005, or further north, leading to extremely cold north-easterly and easterly winds to blow directly over the CASGOL region; and (iii) changes in the precipitation (and river-discharge) vs. evaporation budgets. There are also factors specific of only one of the two study areas, such as the propagation towards the Western Mediterranean Basin of the property changes linked to the EMT.

According to a model based on the IPPC-A2 scenario, the effect of temperature augmentation will dominate over the effect of salinity increase in the GoL during the 21st century. This will lead to a severe reduction of the MLD in the GoL, from 2280 m for the 1961-99 control period to 550 m by the end of the century, and to a major decrease in deep water formation (Somot et al., 2006, 2007; Herrmann et al., 2014). Therefore, assuming that the current warming trend will continue in the near future (e.g. Mann et al., 1999; Mann and Jones 2003; Moberg et al., 2005), it is to be expected that DSWC and deep open-sea convection become progressively less frequent and intense in the GoL. However, the occurrence of shortly spaced and particularly intense events in 2005-06, but also in 2010-11 and 2012-13, eventually affecting the Bay of Biscay, after a long period with less frequent events (1966-2004) including a 16 years interval (1989-2004) when no events occurred in any of the two areas, may rise doubts about model predictions. Continued observation and in situ monitoring are therefore critical to better understand the triggers and development of intense convection and DSWC events in the CASGOL region, and to adjust model predictions.

2.3.5.4 IMPACTS ON ECOSYSTEM AND LIVING RESOURCES

Abnormally strong winter convective mixing and DSWC, and related hydrographic changes and dynamic processes, are likely to significantly impact the marine

ecosystem. This is illustrated by the reinforcement effect of intense mixing events over spring blooms in the North Atlantic (Follows and Dutkiewicz, 2001; Pelegrí et al., 2006; Williams et al., 2006). In the Bay of Biscay winter vertical mixing dominates the supply of nutrients to the euphotic layer and modulates its interannual variability (Puillat et al., 2004; Llope et al., 2006, 2007). Likewise, in the GoL winter convection plays a major role in nutrient fueling from deep to shallower environments by uplifting deep, nutrient rich waters to the photic layer (Severin et al., 2014). DSWC also plays a relevant role mainly by enhancing horizontal transfers over the continental margin, with near-bottom downslope flows triggering a surface return circulation towards the shelf (Canals et al., 2006; Palanques et al., 2006; Sànchez-Vidal et al., 2008; Pasqual et al., 2010). Following the influx of nutrients to the surface layer due to winter mixing, phytoplankton blooms generally occur in late winter and spring (Sverdrup, 1953; Chiswell, 2011), at the onset of the stratification period (Pingree et al., 1976; Estrada, 1996; Waniek, 2003).

MODIS-based composites show high net primary production in both the Bay of Biscay and the NW Mediterranean Sea during the springs that follow anomalous winters, such as those discussed in the previous section (Fig. 2.25). Those images can be viewed as the ultimate expression of the atmospheric connection and event synchrony between both areas. It is to be noted that net primary production may also be enhanced locally by river discharge, as is observed offshore the Rhône River mouth (Fig. 2.25). A priori, enhanced mixing events may steer the transfer of carbon and particulate matter from the shallow to the deep ecosystem. In the Cantabrian Sea, the normal winter MLD hardly exceeds the depth of the shelf break, as it is less than 250 m (Fig. 2.23a). Therefore, a major direct imprint of winter convection on sedimentary particle fluxes over the continental slope and deeper should not be expected in this area. Only exceptionally the mixed layer reaches substantially greater depths (e.g. 400 m in 2010, and 350 m in 2005 and 2006) (Fig. 2.23a), thus increasing the chances to directly influence particle fluxes over the upper continental slope. Below the maximum winter MLD, the density gradient associated to the local permanent pycnocline (van Aken, 2001) may prevent the vertical transport of particulate matter to deeper locations.

Lateral advection is then left as the only possible main pathway for major transfers of particles towards the deep slope and basin (e.g. Heussner et al., 1999). In the Cantabrian Sea, advection is eased by extensive submarine canyon

systems cut into the continental shelf and slope, which open to the Biscay abyssal plain. One of them is the Avilés canyon system (Fig. 2.18), which extends from the mid-Cantabrian shelf, with its head at less than 15 km from the coastline, to a depth of about 5000 m. Its ability to convey sedimentary particles from the continental shelf to the deep has been shown by Rumín-Caparrós et al. (2016). However, particulate matter is not directly and immediately funneled down canyon from the shelf. Instead, particulate matter accumulates on the shelf until the occurrence of high-energy conditions capable to resuspend and trigger bottom Ekman transport subsequently carrying it into the canyon. Such high-energy conditions may develop at the occasion of large northern sea storms that usually occur in wintertime in the Cantabrian Sea, eventually combined with strong mid-depth convection. A similar mechanism of stepped advective sediment transfer to submarine canyons and to the continental slope has been described in the GoL, where DSWC and eastern storms hitting the coastline provide the required high-energy conditions (Canals et al., 2006; Ulses et al., 2008a; Sànchez-Vidal et al., 2012). Winter northern sea storms are also common in the GoL but since they push water seawards and raise high waves far from the coast their effect on sediment transfer from shallow to deep is lessened.

For the first time, total mass fluxes (TMFs) were monitored simultaneously from January 2012 to March 2013 in submarine canyons of the Cantabrian Sea and the GoL. Moorings were places in the middle reaches (2000 m depth) of the Avilés canyon in the Cantabrian Sea, and in the mid-course of the CCC (1000 m depth) in the GoL (Figs. 2.18, 2.24 and Table 2.4) (cf. Section 2). In winters 2012 and 2013 DSWC and open-sea convection occurred in the GoL, while normal, mild conditions prevailed in the Cantabrian Sea (Fig. 2.23a, b). This was caused by an atmospheric configuration discussed and illustrated earlier (cf. Section 5.2 and Fig. 2.27c). Despite differences in hydrological situation, TMFs at each side of the Pyrenees presented similar intra-annual variability patterns, peaking in winter-early spring (Fig. 2.24). Atmospheric forcing over the entire CASGOL region likely lies behind such a resemblance. Atmospheric conditions in winter 2012 and 2013 triggered high heat and buoyancy losses and DSWC events in the GoL, which led to high peak TMFs (i.e. 70 g m^{-2} d^{-1} in February 2012 and 64 g m^{-2} d^{-1} in February 2013). In the Cantabrian Sea, western and northwestern wind bursts associated to high waves triggered shelf sediment resuspension and led to a bottom Ekman transport directed offshore, thus favoring the near-bottom advection of particles down into the Avilés canyon (Rumín-Caparrós et al., 2016), with peak TMFs of 16

g m^{-2} d^{-1} in April 2013 (Fig. 2.24), i.e. significantly lower than those observed in the CCC. Unfortunately, no in situ TMF data is available from a year with enhanced convection in the Cantabrian margin, which prevents assessing the role of other relevant factors such as margin configuration and MLD as related to atmospheric forcing and water mass structure in each area.

The finding of similarly higher TMFs in the comparatively milder 2013 than in the more severe 2012 in the CCC can be attributed to dynamic processes (e.g. eastern storms), unrelated to DSWC and open-sea convection, that enhanced down canyon particle transfer, as previously pointed out by Palanques et al. (2009) and Sànchez-Vidal et al. (2012). It is also plausible that, in addition to storms, a sort of reemergence mechanism applies to TMFs too, involving the delayed export of significant amounts of sedimentary material left behind in the previous year, when intense convection and DSWC occurred. Such a delay would be of about one year, as candidate triggering processes such as severe storms will normally occur in winter next year. This may help explaining the 2012 early spring peak in Avilés canyon, as there was convection in winter 2011 in the Cantabrian Sea (and also in 2010), and the winter peak in winter 2013 in the GoL following DSWC and strong convection there in 2012 (Figs. 2.27a, b and 2.24). The much smaller winter 2013 TMF relative maxima (3 g m^{-2} d^{-1}) in the Avilés canyon might reflect the background situation for winters that have not been preceded by intense convection and related steering of particle remobilization in the previous year. An additional, multi-annual in situ monitoring effort in both areas would be required to test these hypotheses.

Our results also show that most TMFs occur during short time periods within a year, and that they follow a seasonal pattern. TMFs during most of the year are extremely low, representing background levels. This pattern reflects the TMFs response to the equally short-lived character of the ocean system conditions leading to larger fluxes, which take place only occasionally, mainly during wintertime and early spring.

The difference in deployment depth of sediment traps in the Avilés canyon (2000 m) and the CCC (1000) is also a relevant variable that may help explaining the contrasting magnitudes of TMFs in both canyons. Average TMFs in the CCC along the 2012-13 monitoring period was more than 3 times higher than in Avilés canyon (~7 g m^{-2} d^{-1} vs. ~2 g m^{-2} d^{-1}) (Fig. 2.24). Average TMFs at ~1900 m depth

in the CCC have been reported to be about 3 g m^{-2} d^{-1} (Pasqual et al., 2010), which is close to the average reported for Avilés canyon. However, it must be noted that in the CCC this depth corresponds to the canyon mouth, while in the Avilés canyon still corresponds to its deeply entrenched middle reach. At its mouth, the CCC loses the constriction effect of the canyon walls and, subsequently, its funneling capacity decreases causing mass fluxes to decrease too. In the mesotidal environment of the Cantabrian Sea tidal currents may help sustaining a background level of suspended particulate matter over the Avilés canyon, while also contributing to the regular remobilization of sedimentary particles. The tidal contribution to TMFs would add to the one of severe storms mentioned above. Tidal effects would be much smaller in the microtidal Mediterranean Sea. Previous observations in the GoL and elsewhere support the view that submarine canyons connecting shelf environments with base of slope and basin environments constitute preferential pathways for the transfer to the deep seafloor of mass and energy fluxes ultimately resulting from the ocean system response to atmospheric forcing (e.g. Hickey et al., 1986; Durrieu de Madron, 1994; Durrieu de Madron et al., 2005; Palanques et al., 2006; Canals et al. 2009; Xu et al., 2010; Puig et al., 2013). Similarly to other submarine canyons, the Avilés canyon meets the conditions to behave as a prime vector for the transfer of the shallow ocean signal to the deep ocean's interior in the Cantabrian Sea, as it is incised in a narrow continental shelf and is affected by high energy processes driving particle loads to its head and upper reaches, from where they could be transferred down course (Rumín-Caparrós et al., 2016).

The impacts of eventually synchronous convection and DSWC events on the pelagic and benthic ecosystems and on individual species, including some of high commercial interest, have been investigated mostly in the GoL. According to Severin et al. (2014), open-sea convection plays a critical role as it steers nutritional support to phytoplankton communities in the GoL. Increases in primary productivity are related to mixing events, which vertically transfer nutrients from deeper layers into surface waters as a result of the intensification of vertical mixing. Figure 2.25 illustrates high primary productivity associated to convection events in the GoL. Increases in primary productivity spread to the rest of the food web, starting by organisms feeding on phytoplankton. According to Company et al. (2008), DSWC during the winters of 2005 and 2006 led to a temporary collapse of the valuable bottom-trawling fishery of the deep-sea shrimp *Aristeus antennatus*. Following this initial negative effect over the fishery, major DSWC events help

improving the recruitment process of *A. antennatus*, as demonstrated by a 30 years long time series that shows major increases in the catches of juveniles two to three years after each event, and peaking adult landings three to five years after each event. This suggests a sort of regeneration mechanism following an initial negative impact over the local fishery, which mitigates a general trend towards overexploitation and prevents the depletion of the stocks of this highly priced deep-sea species.

To our best knowledge, first-order consequences of the enhanced vertical mixing in 2005 on the pelagic marine ecosystem of the Bay of Biscay, which includes populations of valuable species from the commercial viewpoint, still remains unknown. As in the GoL, intense winter mixing events in the Cantabrian Sea promote the ascent of nutrients from deeper layers into the upper ocean, which enhances net primary production (Fig. 2.25 and Somavilla et al., 2009). Pelagic fishing is particularly important in the Cantabrian Sea, and it is to be expected that the most relevant target species for fisheries, such as sardine (*Sardine pilchardus*), anchovy (*Engraulis encrasicolus*) and Atlantic blue tuna (*Thunnuns thynnus*) ultimately benefit from events of high primary productivity as a result of a cascading process through the food web (Sánchez and Olaso, 2004). However, so far no direct link has been established between the occurrence of enhanced vertical mixing and the yield of commercially relevant species in the Cantabrian Sea. Stock depletion of valuable fish species in the Cantabrian Sea, such as hake (*Merluccius merluccius*), has led to long-term recovery programs. The hake one was implemented in 2006 over the entire Iberian margin of the Bay of Biscay, and involved a large number of fishing regulatory measures (ICES, 2009). One of the main challenges that remains is disentangling the individual and cumulative short to long-term effects over the resource of the modulation of the fishing effort, short-lived oceanographic events driven by atmospheric forcing, and climate change and its consequences over the ocean system in the long run, all acting in parallel.

Consequently with the lines set up in this paper, mid to long-term (i.e. seasonal) meteorological forecasts could be used to anticipate the occurrence of convection and DSWC in the CASGOL region so that a comprehensive research effort could be focused in specific time windows, such as winter and spring. Including the continuous collection of fisheries data, the cross-analysis of results should lead to an improved understanding of the links between physical processes and resource

variability to the point that, ideally, management plans could fully integrate such knowledge. This would require strengthening in situ data collection and remote observations, long time series on fisheries and a devoted modeling effort. Finally, given the occurrence of synchronous events in the Cantabrian Sea and the GoL, it may be convenient considering management components to be applied in parallel in both areas, located in two different ocean basins, at both ends of the Pyrenees Range.

2.3.6 CONCLUDING REMARKS

In this paper, we have investigated the causes and consequences of atmospheric forcing over the Cantabrian Sea and the GoL, including the synchronous occurrence of ocean system responses and extreme events. These two areas form the CASGOL region that extends offshore within the same latitude range beyond both ends of the Pyrenees, in the NE Atlantic and the Mediterranean Sea, respectively. Their geographic closeness (about 450 km in straight line) promotes atmospheric forcing to act simultaneously over the two areas, which could be viewed as an otherwise common short-range teleconnection.

In addition of sea storms, which are not treated in detail in this paper, the main oceanographic events in the study areas are intermediate depth convection in the Cantabrian Sea and deep open-sea convection and DSWC in the GoL. When atmospheric forcing involving the arrival of cold air masses is severe enough and spreads over the two areas, which occurs in some winters, all these processes tend to take place simultaneously with high intensity. Alternatively, they may occur in only one of the two areas.

The synchrony between both areas has been found to be strictly dependent on the atmospheric pressure distribution. The prevalence of a high-pressure anomaly cell over the North Atlantic, which results from the recurrence of long-lasting anticyclones, and its prevailing location during winter appear to be the key factors determining, first, whether intense convection and cascading is likely to occur in any of the two areas and, second, whether oceanographic responses in the Cantabrian Sea and the GoL will be synchronous. Factors such as margin configuration and riverine discharge may also have an effect on such responses.

Two exceptional situations occurred in the last years. In winter 2005 synchronous intense mixing events took place in the Cantabrian Sea and the GoL, with reemergence in winter 2006. Unprecedented MLDs were reached these years in the Cantabrian Sea (~350 m) and in the GoL (>2500 m), were near bottom DSWC flows involving a temperature drop of up to 1.7ºC were recorded at 1000 m depth in the Cap de Creus and Lacaze-Duthiers submarine canyons. In winters 2010 and 2011, synchronous intense mixing events took place again in both areas, together with DSWC in the GoL only in 2010. DSWC and deep convection resumed in the GoL alone in winter 2012 and 2013. In 2010 the MLD in the Cantabrian Sea reached even deeper levels (~400 m) than in 2005, while in the GoL it was again >2500 m. In winter 2012, DSWC flows in the GoL led to a near-bottom temperature drop in excess of 3ºC at 1000 m depth in CCC.

TMF peaks in submarine canyons occur in winter and early spring all over the CASGOL region according to data obtained simultaneously for the first time in the Avilés canyon, Cantabrian Sea, and CCC, in the GoL) in 2012-2013. Peak flux magnitudes were much higher in CCC. However, these results must be taken with caution as in winters 2012 and 2013 there was intense convection and DSWC only in the GoL, and also because the deployment depth of the sediment traps within the canyons was substantially different. A reemergence mechanism affecting TMFs is suggested, eventually assisted by the action of eastern storms that are common in the area. Jointly with results in the published literature, our results further support the view of submarine canyons as preferential conduits for the transfer of the shallow ocean signal to the deep under the steering of short-lived processes.

The view of two physically non-connected marine areas responding in parallel when the ocean system gets highly perturbed by atmospheric forcing is novel, contributes to a better understanding of oceanographic and ecosystem dynamics, and has the potential to facilitate a better management of priced living resources sensitive to physical forcing through the integration of meteorological and oceanographic observations, and devoted modeling.

Acknowledgements. This research has been carried out within the framework of the DOS MARES Spanish project (CTM2010-21810-C03-01). Generalitat de Catalunya supported GRC Geociències Marines through grant 2014 SGR 1068. We thank Dr. Luis Valdés, coordinator of the Spanish Oceanographic Institute

(IEO) “Radiales” time series program during most of the period of the data collection, for supporting the Santander Section. We also thank the IEO staff involved in *in situ* measurements, which were often carried out in rough seas. We kindly thank the University of Barcelona “GRC Geociències Marines” and the CNRS-University of Perpignan CEFREM staff involved in the servicing of the various mooring stations in the Gulf of Lion. We acknowledge NOAA for providing climate data through http://www.esrl.noaa.gov/psd/. X. Rayo assisted us when using the ArcGis software. ASV is supported by a Ramon y Cajal contract by the Spanish Ministry for Science and Innovation (now Ministry of Economy and Competitiveness). JC and KS acknowledge support from EU FP7 Ocean-Certain (GA # 603773), EU FP7 COMMON SENSE (GA #228344) and the Italian Flagship Project RITMARE, supported by the Ministry of Education, University and Research (MIUR).

2.3.7 REFERENCES

Alekseev, G. V., Ivanov, V. V., Korablyev, A. A., 1995. Interannual variability of deep convection in the Greenland Sea. Oceanology 35, 40-47.

Alekseev, G. V., Kovalevsky, D. V., Johannessen, O.M., Korablev, A. A., Ivanov, V. V., 2001. Interannual variability in water masses in the Greenland Sea and adjacent areas. Polar Research 20, 201-208.

Arguez, A., Durre, I., Applequist, S., Vose, R. S., Squires, M. F., Yin, X., Heim Jr., R. R., Owen, T. W., 2012. NOAA's 1981-2010 U.S. Climate Normals: An Overview. Bull. American Meteor Society 93, 1687-1697.

Avsic, T., Karstensen, J., Send, U., Fischer, J., 2006. Interannual variability of newly formed Labrador Sea water from 1994 to 2005. Geophysical Research Letters 33, L21S02.

Behrenfeld, M.J., Falkowski, P.G., 1997. Photosynthetic rates derived from satellitebased chlorophyll concentration. Limnology and Oceanography 42, 1-20.

Bethoux, J.P., Durieu de Madron, X., Nyffeler, F., Tailliez, D., 2002. Deep water in the western Mediterranean: Peculiar 1999 and 2000 characteristics, shelf

formation hypothesis, variability since 1970 and geochemical inferences. Journal of Marine Systems 33-34, 117-131.

Bode, A., Valdés, L., Lavín, A., 2012. Cambio climático y oceanográfico en el Atlántico del norte de España. Instituto Español de Oceanografía, Madrid, 280 pp.

Boker, S.M., Xu, M., Rotondo, J.L., King, K., 2002. Windowed cross-correlation and peak picking for the analysis of variability in the association between behavioral time series. Psychological Methods 7, 338-355.

Botas, J.A., Fernández, E., Bode, A., Anadón, R., 1989. Water masses off the central Cantabrian coast. Scientia Marina 53, 755-761.

Bowen, I.S., 1926. The ratio of heat losses by conduction and by evaporation from any water surface. Physical Review 27, 779-787.

Burchard, H., Bolding, K., Villarreal, R.M., 1999. GOTM, a general ocean turblence model: theory, implementation and test cases, Rep. EUR18745, European Commission, 103 pp.

Canals, M., Puig, P., de Madron, X.D., Heussner, S., Palanques, A., Fabrés, J., 2006. Flushing submarine canyons. Nature 444, 354-357.

Canals, M., Danovaro, R., Heussner, S., Lykousis, V., Puig, P., Trincardi, F., Calafat, A.M., Durrieu de Madron, X., Palanques, A., Sanchez-Vidal, A., 2009. Cascades in Mediterranean submarine grand canyons. Oceanography 22, 26-43.

Chiswell, S.M., 2011. Annual cycles and spring blooms in phytoplankton: Don't abandon Sverdrup completely. Marine Ecology Progress Series 443, 39-50.

CIESM, 2009. Dynamics of Mediterranean deep waters. CIESM Workshop Monographs, vol. 38, CIESM Publisher, Monaco, 132 pp.

Company, J.B., Puig, P., Sardà, F., Palanques, A., Latasa, M., Scharek, R., 2008. Climate influence on deep sea populations. PLoS One 3, e1431.

Cronin, M. F., Sprintall, J., 2001. Wind and buoyancy-forced upper ocean, in Encyclopedia of Ocean Sciences, vol. 6, Academic, San Diego, California, 3219-3227 pp.

Durrieu de Madron, X., 1994. Hydrography and nepheloid structures in the Grand-Rhône canyon. Continental Shelf Research 14, 457-477.

Durrieu de Madron, X. Zervakis, V., Theocharis, A., Georgopoulos, D., 2005. Comments on "Cascades of dense water around the world ocean." Progress in Oceanography 64, 83-90.

Durrieu de Madron, X., Houpert, L., Puig, P., Sanchez-Vidal, A., Testor, P., Bosse, A., Estournel, C., Somot, S., Bourrin, F., Bouin, M.N., Beauverger, M., Beguery, L., Calafat, A., Canals, M., Cassou, C., Coppola, L., Dausse, D., D'Ortenzio, F., Font, J., Heussner, S., Kunesch, S., Lefevre, D., Le Goff, H., Martín, J., Mortier, L., Palanques, A., Raimbault, P., 2013. Interaction of dense shelf water cascading and open-sea convection in the northwestern Mediterranean during winter 2012. Geophysical Research Letters 40, 1379-1385.

Estrada, M., 1996. Primary production in the northwestern Mediterranean. Scientia Marina 60, 55-64.

Follows, M., Dutkiewicz, S., 2001. Meterological modulation of the North Atlantic spring bloom. Deep Sea Research Part II: Topical Studies in Oceanography 49, 321-344.

Font, J., Puig, P., Salat, J., Palanques, A., 2007. Sequence of hydrographic changes in NW Mediterranean deep water due to the exceptional winter of 2005. Scientia Marina 71, 339-346.

González-Pola, C., Fernández-Díaz, J.M., Lavín, A., 2007. Vertical structure of the upper ocean from profiles fitted to physically consistent functional forms. Deep Sea Research Part I: Oceanographic Research Papers 54, 1985-2004.

Guibout, P., 1987. Atlas hydrologique de la Méditerranée. Laboratoire d'Océanographie Physique du Museum, Paris, 174 pp.

Hartman, S.E., Hartman, M.C., Hydes, D. J., Jiang, Z. P., Smythe-Wright, D., González-Pola, C., 2014. Seasonal and inter-annual variability in nutrient supply in relation to mixing in the Bay of Biscay, Deep Sea Research Part II: Topical Studies in Oceanography 106, 68-75.

Herrmann, M., Sevault, F., Beuvier, J., Somot, S., 2010. What induced the exceptional 2005 convection event in the northwestern Mediterranean basin? Answers from a modeling study. Journal of Geophysical Research 115, 1-19.

Herrmann, M., Estournel, C., Adloff, F., Diaz, F., 2014. Impact of climate change on the northwestern Mediterranean Sea pelagic planktonic ecosystem and associated carbon cycle, Journal of Geophysical Research - Oceans 119, 5815-5836.

Heussner, S., Ratti, C., Carbonne, J., 1990. The PPS 3 time-series sediment trap and the trap sample processing techniques used during the ECOMARGE experiment. Continental Shelf Research 10, 943-958.

Heussner, S., Durrieu de Madron, X., Radakovitch, O., Beaufort, L., Biscaye, P. E., Carbonne, J., Delsaut, N., Etcheber, H., Monaco, A., 1999. Spatial and temporal patterns of downward particle fluxes on the continental slope of the Bay of Biscay (northeastern Atlantic). Deep Sea Research Part II: Topical Studies in Oceanography 46, 2101-2146.

Heussner, S., Durrieu de Madron, X., Calafat, A., Canals, M., Carbonne, J., Delsaut, N., Saragoni, G., 2006. Spatial and temporal variability of downward particle fluxes on a continental slope: Lessons from an 8-yr experiment in the Gulf of Lions (NW Mediterranean). Marine Geology 234, 63-92.

Hickey, B., Baker, E., Kachel, N., 1986. Suspended particle movement in and around Quinault submarine canyon. Marine Geology 71, 35-83.

Houpert, L., Testor, P., Durrieu de Madron, X., Somot, S., D'Ortenzio, F., Estournel, C., Lavigne, H,. 2015 Seasonal cycle of the mixed layer, the seasonal thermocline and the upper-ocean heat storage rate in the Mediterranean Sea derived from observations. Progress in Oceanography 132, 333-352.

Houpert L., Durrieu de Madron, X., Testor, P., Bosse, A., D'Ortenzio, F., Bouin, M. N., Dausse, D., Le Goff, H., Kunesch, S., Labaste, M., Coppola, L., Mortier, L., Raimbault, P., 2016. Observations of open-ocean deep convection in the Northwestern Mediterranean Sea seasonal and interannual variability of mixing and deep water masses for the 2007-2013 period. J Journal of Geophysical Research - Oceans 1-21.

ICES. 2009. Report of the ICES Advisory Committee, 2009. ICES Advice, 2009. Books 1-11. 1, 420 pp.

Iorga, M.C., Lozier, M.S., 1999. Signatures of the Mediterranean outflow from a North Atlantic climatology: 1. Salinity and density fields. Journal of Geophysical Research 104, 25985-26009.

Josey, S.A., 2003. Changes in the heat and freshwater forcing of the eastern Mediterranean and their influence on Deep Water Formation, Journal of Geophysical Research 108, 32-37.

Josey, S. A., Somot, S., Tsimplis, M., 2011. Impacts of atmospheric modes of variability on Mediterranean Sea surface heat exchange. Journal of Geophysical Research 116, 1-15.

Kalnay, E., Kanamitsu, M., Kistler, R., Collins, W., Deaven, D., Gandin, L., Iredell, M., Saha, S., White, G., Woollen, J., Zhu, Y., Chelliah, M., Ebisuzaki, W., Higgins, W., Janowiak, J.E., Mo, K.C., Ropelewski, C., Wang, J., Leetmaa, A., Reynolds, R.W., Jenne, R., Joseph, D., 1996. The NCEP/NCAR 40-year reanalysis project. Bulletin of the American Meteorological Society 77, 437-471.

Kolodziejczyk, N., Reverdin, G., Lazar, A., 2015. Interannual Variability of the Mixed Layer Winter Convection and Spice Injection in the Eastern Subtropical North Atlantic. Journal of Physical Oceanography 45, 504-525.

L'Hévéder, B., Li, L., Sevault, F., Somot, S., 2013. Interannual variability of deep convection in the Northwestern Mediterranean simulated with a coupled AORCM. Climate Dynamics 41, 937-960.

Lacombe, H., Tchernia, P., 1960. Quelques traits généraux de l'hydrologie Méditerranéenne. Cahiers Océanographiques XII (8), 527-547.

Lacombe, H., Tchernia, P., 1972. Caractères hydrologiques et circulation des eaux en Méditerranée. In: The Mediterranean Sea, Stanley, D.J (Ed.), Dowden Hutchinson and Ross, Stroudsburg, pp. 25-36.

Lacombe, H., Tchernia, P., Gamberoni, L., 1985. Variable bottom water in the Western Mediterranean basin. Progress in Oceanography 14, 319-338.

Larsen, K. M. H., Gonzalez-Pola, C., Fratantoni, P., Beszczynska-Möller, A., Hughes, S. L. (Eds.), 2016. ICES Report on Ocean Climate 2014, ICES Cooperative Research Report No. 329, 139 pp.

Lavín, A., Valdés, L., Sénchez, F., Abaunza, P., Forest, A., Boucher, J., Lazure, P., Jegou, A.-M., 2006. The Bay of Biscay: the encountering of the ocean and the shelf. Seas Harvard Press 14, 933-1001.

Llope, M., Anadón, R., Viesca, L., Quevedo, M., González-Quirós, R., Stenseth, N.C., 2006. Hydrography of the southern Bay of Biscay shelf-break region: Integrating the multiscale physical variability over the period 1993-2003. Journal of Geophysical Research, C09021.

Llope, M., Anadón, R., Sostres, J.Á., Viesca, L., 2007. Nutrients dynamics in the southern Bay of Biscay (19932003): Winter supply, stoichiometry, long-term trends, and their effects on the phytoplankton community. Journal of Geophysical Research 112, C07029.

López-Jurado, J.-L., González-Pola, C., Vélez-Belchí, P., 2005. Observation of an abrupt disruption of the long-term warming trend at the Balearic Sea, western Mediterranean Sea, in summer 2005. Geophysical Research Letters 32, L24606.

Martín, J., Miquel, J.-C., Khripounoff, A., 2010. Impact of open sea deep convection on sediment remobilization in the western Mediterranean. Geophysical Research Letters 37, L13604.

MEDOC Group, 1970. Observation of Formation of Deep Water in the Mediterranean Sea, 1969. Nature 227, 1037-1040.

Mann, M. E., Bradley, R. S., Hughes., M. K., 1999. Northern Hemisphere temperatures during the past millennium: inferences, uncertainties, and limitations. Geophysical Research Letters 26, 759-762.

Mann, M.E., Jones., P.D., 2003. Global surface temperatures over the past two millennia. Geophysical Research Letters 30, 1820.

Mertens, C., Schott, F., 1998. Interannual variability of deep-water formation in the Northwestern Mediterranean. Journal of Physical Oceanography 28, 1410-1424.

Moberg, A., Sonechkin, D. M., Holmgren, K., Datsenko, N. M., Karlen, W., 2005. Highly variable Northern Hemisphere temperatures reconstructed from low- and high-resolution proxy data. Nature 433, 613-617.

Palanques, A., Durrieu de Madron, X., Puig, P., Fabrés, J., Guillén, J., Calafat, A., Canals, M., Heussner, S., Bonnin, J., 2006. Suspended sediment fluxes and transport processes in the Gulf of Lions submarine canyons. The role of storms and dense water cascading. Marine Geology 234, 43-61.

Palanques, A., Puig, P., Latasa, M., Scharek, R., 2009. Deep sediment transport induced by storms and dense shelf-water cascading in the northwestern Mediterranean basin. Deep Sea Research Part I: Oceanographic Research Papers 56, 425-434.

Palanques, A., Puig, P., Durrieu de Madron, X., Sanchez-Vidal, A., Pasqual, C., Martín, J., Calafat, A., Heussner, S., Canals, M., 2012. Sediment transport to the deep canyons and open-slope of the western Gulf of Lions during the 2006 intense cascading and open-sea convection period. Progress in Oceanography 106, 1-15.

Pasqual, C., Sanchez-Vidal, A., Zúñiga, D., Calafat, A., Canals, M., Durrieu de Madron, X., Puig, P., Heussner, S., Palanques, A., Delsaut, N., 2010. Flux and composition of settling particles across the continental margin of the Gulf of Lion: the role of dense shelf water cascading. Biogeosciences 7, 217-231.

Pelegrí, J.L., Marrero-Díaz, A., Ratsimandresy, A.W., 2006. Nutrient irrigation of the North Atlantic. Progress in Oceanography 70, 366-406.

Pingree, R.D., Holligan, P.M., Mardell, G.T., Head, R.N., 1976. The influence of physical stability on spring, summer and autumn phytoplankton blooms in the Celtic Sea. Journal of the Marine Biological Association of the United Kingdom 56, 845-873.

Pollard, R.T., Pu, S., 1985. Structure and circulation of the Upper Atlantic Ocean northeast of the Azores. Progress in Oceanography 14, 443-462.

Pollard, R.T., Griffttths, M.J., Cunningham, S.A., Read, J.F., Pérez, F.F., Ríos, A.F., 1996. Vivaldi 1991 a study of the formation, circulation and ventilation of Eastern North Atlantic Central Water. Progress in Oceanography 37, 167-192.

Puig, P., Palanques, A., Orange, D.L., Lastras, G., Canals, M., 2008. Dense shelf water cascades and sedimentary furrow formation in the Cap de Creus Canyon, northwestern Mediterranean Sea. Continental Shelf Research 28, 2017-2030.

Puig, P., Durrieu de Madron, X., Salat, J., Schroeder, K., Martín, J., Karageorgis, A.P., Palanques, A., Roullier, F., López-Jurado, J.L., Emelianov, M., Moutin, T., Houpert, L., 2013. Thick bottom nepheloid layers in the western Mediterranean generated by deep dense shelf water cascading. Progress in Oceanography 111, 1-23.

Puillat, I., Lazure, P., Jégou, A.M., Lampert, L., Miller, P.I., 2004. Hydrographical variability on the French continental shelf in the Bay of Biscay, during the 1990s. Continental Shelf Research 24, 1143-1163.

Renfrew, I.A., Moore, G.W.K., 1999. An extreme cold-air outbreak over the Labrador Sea: roll vortices and airsea interaction. Monthly Weather Review 127, 2379-2394.

Roether, W., Klein, B., Manca, B.B., Theocharis, A., Kioroglou, S., 2007. Transient Eastern Mediterranean deep waters in response to the massive dense-water output of the Aegean Sea in the 1990s. Progress in Oceanography 74, 540-571.

Rogers, J.C., 1990. Patterns of low-frequency monthly sea level pressure variability (1899-1986) and associated wave cyclone frequencies. Journal of Climate 3, 1364-1379.

Rumín-Caparrós, A., Sanchez-Vidal, A., Calafat, A., Canals, M., Martín, J., Puig, P., Pedrosa-Pàmies, R., 2013. External forcings, oceanographic processes and particle flux dynamics in Cap de Creus submarine canyon, NW Mediterranean Sea. Biogeosciences 10, 3493-3505.

Rumín-Caparrós, A., Sanchez-Vidal, A., González-Pola, C., Lastras, G., Calafat, A., Canals, M., 2016. Particle fluxes and their drivers in the Avilés submarine canyon and adjacent slope, central Cantabrian margin, Bay of Biscay. Progress in Oceanography 144, 39-61.

Salat, J., Font, J., 1987. Water mass structure near and offshore the Catalan coast during the winter of 1982 and 1983. Annales Geophysicae 5, 49-54.

Salvadó, J.A., Grimalt, J.O., López, J.F., Palanques, A., Heussner, S., Pasqual, C., Sánchez-Vidal, A., Canals, M., 2013. The role of dense shelf water cascading in the transfer of organochlorine compounds to open marine waters. International Journal of Environmental Science and Technology 46, 2624-2632.

Sánchez, F., Olaso, I., 2004. Effects of fisheries on the Cantabrian Sea shelf ecosystem. Ecological Modelling 172, 151-174.

Sanchez-Vidal, A., Pasqual, C., Kerhervé, P., Calafat, A., Heussner, S., Palanques, A., Durrieu de Madron, X., Canals, M., Puig, P., 2008. Impact of dense shelf water cascading on the transfer of organic matter to the deep western Mediterranean basin. Geophysical Research Letters 35, L05605.

Sanchez-Vidal, A., Canals, M., Calafat, A.M., Lastras, G., Pedrosa-Pàmies, R., Menéndez, M., Medina, R., Company, J.B., Hereu, B., Romero, J., Alcoverro, T., 2012. Impacts on the deep-sea ecosystem by a severe coastal storm. PLoS One 7, e30395.

Sanchez-Vidal, A., Llorca, M., Farré, M., Canals, M., Barceló, D., Puig, P., Calafat, A., 2015. Delivery of unprecedented amounts of perfluoroalkyl substances towards the deep-sea. Science of the Total Environment 526, 41-48.

Schroeder, K., Ribotti, A., Borghini, M., Sorgente, R., Perilli, A., Gasparini, G.P., 2008. An extensive western Mediterranean deep water renewal between 2004 and 2006. Geophysical Research Letters 35, L18605.

Schroeder, K., Josey, S. A., Herrmann, M., Grignon, L., Gasparini, G. P., Bryden, H. L., 2010. Abrupt warming and salting of the Western Mediterranean Deep Water after 2005: Atmospheric forcings and lateral advection. Journal of Geophysical Research 115, 118.

Schroeder, K., Chiggiato, J., Bryden, H. L., Borghini, M., Ben Ismail, S., 2016. Abrupt climate shift in the Western Mediterranean Sea. Scientific Reports 6, 23009.

Severin, T., Conan, P., Durrieu de Madron, X., Houpert, L., Oliver, M. J., Oriol, L., Caparros, J., Ghiglione, J. F., Pujo-Pay, M., 2014. Impact of open-ocean convection on nutrients, phytoplankton biomass and activity, Deep Sea Research Part I: Oceanographic Research Papers 94, 62-71.

Smith, R. O., Bryden, H. L., Stansfield, K., 2008. Observations of new western Mediterranean deep water formation using Argo floats 2004-2006, Ocean Science 4, 133-149.

Somavilla, R., González-Pola, C., Rodriguez, C., Josey, S.A., Sánchez, R.F., Lavín, A., 2009. Large changes in the hydrographic structure of the Bay of Biscay after the extreme mixing of winter 2005. Journal of Geophysical Research 114, C01001.

Somavilla, R., González-Pola, C., Ruiz-Villarreal, M., Montero, A.L., Lavín, A., 2011. Mixed layer depth (MLD) variability in the southern Bay of Biscay. Deepening of winter MLDs concurrent with generalized upper water warming trends? Ocean Dynamics 61, 1215-1235.

Somavilla, R., González-Pola, C., Schauer, U., Budéus, G., 2016. Mid-2000s North Atlantic shift: Heat budget and circulation changes. Geophysical Research Letters 43, 2059-2068.

Somot, S., Sevault, F., Déqué, M., 2006. Transient climate change scenario simulation of the Mediterranean Sea for the twenty-first century using a high-resolution ocean circulation model. Climate Dynamics 27, 851-879.

Somot, S., Sevault, F., Déqué, M., 2007. Climate change scenario for the Mediterranean Sea. HERMES 2nd Annual Meeting, Carvoeiro, Portugal. Abstr. Vol.

Somot, S., Houpert, L., Sevault, F., Testor, P., Bosse, A., Taupier-Letage, I., Bouin, M.-N., Waldman, R., Cassou, C., Sánchez-Gómez, E., Durrieu de Madron, X., Adloff, F., Nabat, P., Herrmann, M., 2016. Characterizing, modelling and understanding the climate variability of the deep water formation in the North-Western Mediterranean Sea. Climate Dynamics, 1-32.

Stabholz, M., Durrieu de Madron, X., Canals, M., Khripounoff, A., Taupier-Letage, I., Testor, P., Heussner, S., Kerhervé, P., Delsaut, N., Houpert, L., Lastras, G., Dennielou, B., 2013. Impact of open-ocean convection on particle fluxes and sediment dynamics in the deep margin of the Gulf of Lions. Biogeosciences 10, 1097-1116.

Sverdrup, H., 1953. On conditions for the vernal blooming of phytoplankton. Journal du Conseil International pour l'Exploration de la Mer 18, 287-295.

Thompson, D.W.J., Wallace, J.M., 1998. The Arctic oscillation signature in the wintertime geopotential height and temperature fields. Geophysical Research Letters 25, 1297-1300.

Tomczak, M., Godfrey, S., 1994. Adjacent seas of the Atlantic Ocean, In Regional Oceanography: An introduction. Pergamon, Amsterdam, pp. 297-327.

Ulses, C., Estournel, C., Bonnin, J., Durrieu de Madron, X., Marsaleix, P., 2008a. Impact of storms and dense water cascading on shelf-slope exchanges in the Gulf of Lion (NW Mediterranean). Journal of Geophysical Research 113, 1-18.

Ulses, C., Estournel, C., Puig, P., Durrieu de Madron, X., Marsaleix, P., 2008b. Dense shelf water cascading in the northwestern Mediterranean during the cold winter

2005: Quantification of the export through the Gulf of Lion and the Catalan margin. Geophysical Research Letters 35, L07610.

Våge, K., Pickart, R.S., Sarafanov, A., Knutsen, Ø., Mercier, H., Lherminier, P., van Aken, H.M., Meincke, J., Quadfasel, D., Bacon, S., 2011. The Irminger Gyre: Circulation, convection, and interannual variability. Deep Sea Research Part I: Oceanographic Research Papers 58, 590-614.

Valdés, L., Lavín, A., Fernández de Puelles, M.L, Varela, M., Anadón, R., Miranda, A., Camiñas, J., Mas, J., 2002. Spanish Ocean Observation System: IEO Core Project: Studies on time series of oceanographic data, in: Operational Oceanography: Implementation at the European and Regional Scales, Elsevier, New York, pp. 99-105.

van Aken, H.M., 2000. The hydrography of the mid-latitude Northeast Atlantic Ocean. I: the deep water masses. Deep Sea Research Part I: Oceanographic Research Papers 47, 757-788.

van Aken, H.M., 2001. The hydrography of the mid-latitude Northeast Atlantic Ocean part III: the subducted thermocline water mass. Deep Sea Research Part I: Oceanographic Research Papers 48, 237-267.

Waniek, J.J., 2003. The role of physical forcing in initiation of spring blooms in the northeast Atlantic. Journal of Marine Systems 39, 57-82.

Williams, R.G., Roussenov, V., Follows, M.J., 2006. Nutrient streams and their induction into the mixed layer. Global Biogeochemical Cycles 20, GB1016.

Xu, J.P., Swarzenski, P. W., Noble, M., Li, A.C., 2010. Event-driven sediment flux in Hueneme and Mugu submarine canyons, southern California. Marine Geology. 269, 74-88.

2.4 RESUM DE RESULTATS

En aquesta Tesi hom ha investigat l'origen i la variabilitat espaciotemporal dels fluxos de matèria particulada al canyó submarí del cap de Creus, a la Mediterrània nord-occidental, i al canyó d'Avilés, a la mar Cantàbrica. Les mostres obtingudes mitjançant trampes de sediment instal·lades en ancoratges instrumentats desplegats durant períodes llargs de temps han estat analitzades per tal de quantificar els fluxos totals de massa i determinar l'abundància relativa dels constituents principals d'aquests fluxos (partícules terrígenes, sílice biogènica (òpal), carbonat de calci ($CaCO_3$) i MOP). També hem emprat dades obtingudes in situ i en paral·lel per mitjà de correntòmetres igualment muntats en els mateixos ancoratges instrumentats. Hom concebí aquesta recerca amb l'objectiu d'entendre els efectes sobre els ecosistemes marins de les teleconnexions entre les mars Mediterrània nord-occidental i Cantàbrica. Aquest treball ha donat lloc a dos articles científics publicats en revistes indexades, i a un article sotmès. A continuació es presenta un resum dels resultats obtinguts (per una descripció més complerta, vegeu els apartats 2.1 a 2.4).

Canyó del cap de Creus. En l'estudi del canyó del Cap de Creus hom ha investigat l'efecte de forçaments externs (vent, pèrdues de calor, onatge) intensos en els fluxos de matèria particulada durant els hiverns de 2009-10 i 2010-11, marcadament diferents entre ells. L'hivern de 2009-10 fou fred, força sec, amb ventades del nord fortes i freqüents, i amb pèrdues de calor molt pronunciades (Fig. 2.3). L'hivern de 2010-11 fou més càlid, amb episodis de vents del nord i pèrdues de calor ser molt més moderades, però amb una descàrrega fluvial més gran que l'hivern anterior (Fig. 2.3). Les diferències en la intensitat i la persistència dels forçaments externs en un hivern i l'altre induïren respostes oceanogràfiques diferenciades. Mentre que al primer hivern hom va enregistrar fortes caigudes de la temperatura de l'aigua acompanyades d'increments sobtats de la velocitat del corrent i la terbolesa prop del fons, i d'increments dels fluxos totals de massa (TMF, de l'anglès *Total Mass Flux*) al curs alt i mig del canyó, el segon hivern presentà condicions oceanogràfiques relativament més estables, sense grans canvis en la temperatura de l'aigua, la velocitat del corrent i la terbolesa a prop del fons (Fig. 2.2d-f). Semblantment, els increments en els TMFs foren molt inferiors als enregistrats l'hivern anterior, sobretot al curs mig del canyó (Fig. 2.2d-f).

La component terrígena representà la contribució principal, d'aproximadament el 70%, als TMFs en l'ambient investigat. Les contribucions mitjanes del $CaCO_3$ l'òpal i la MOP foren del 30%, el 4% i menys del 5% respectivament (Fig. 2.5 i Taula 3.1). Els continguts en òpal i MOP i mostraren una estacionalitat marcada, amb valors màxims els mesos de març i abril, coincidint amb el conegut *bloom* fitoplanctònic primaveral propi de l'àrea (Estrada *et al*., 1996) (Fig. 2.4).

Canyó d'Avilés. L'estudi del canyó d'Avilés i el talús adjacent es basa en el monitoratge continu al llarg d'un any, entre març de 2012 i abril de 2013,. La integració de dades metoceàniques i dades de satèl·lit ha estat de gran ajuda per identificar i traçar les fonts de matèria particulada, i per a l'estudi dels forçaments atmosfèrics que en darrera instància determinen el seu transport. Com en el cas del canyó del cap de Creus, la variabilitat dels TMFs fins al curs mig del canyó està estretament relacionada amb el règim de vents i la seva variabilitat. Així, els fluxos de partícules màxims han estat enregistrats després de temporals amb vent i onatge forts Al curs baix del canyó els TMFs foren molt inferiors als dels trams menys profuns, i sense relació directa amb els canvis en el règim de vents. Al canyó d'Avilés, els increments de TMFs mesurats mitjançant les trampes de sediment i els augments de terbolesa dels turbidímetres no estan massa ben correlacionats. Les anàlisis espectrals realitzades sobre les dades dels diferents correntòmetres revelen fluctuacions de curta durada superposades als corrents residuals, amb cicles de 12,42 h que corresponen a la variació semidiürna de la marea.

L'anàlisi de la composició dels fluxos revela un elevat contingut de partícules terrígenes, amb mitjanes anuals del 53% al 67% (Taula 3.1). Aquest fet posa de manifest que la font principal de matèria particulada cap al canyó d'Avilés és fluvial. Les partícules biogèniques, per la seva banda, també tenen un paper rellevant en els TMFs i mostren una clara estacionalitat, amb pics de primavera coincidents amb *blooms* fitoplanctònics. Les abundàncies relatives varien entre el 25% i el 35% dels TMFs pel $CaCO_3$, el 7% i el 10% per la MOP, i el 3% i el 4% per l'òpal (Fig. 2.5 i Taula 3.1). Al canyó, però, hom va detectar una certa diferència en la composició relativa dels TMFs segons corresponguessin a profunditats intermèdies dins la columna d'aigua o a les proximitats del fons en els cursos mig i baix del canyó. Mentre a profunditats intermèdies hom observà una variabilitat temporal era ben marcada, amb màxims entre març i maig, coincidint amb el

bloom primaveral, als nivells més propers al fons els TMFs es mostraren, en general, més constants.

Les teleconnexions atmosfèriques entre les mars del nord de la península Ibèrica. El repte principal d'aquest treball és l'estudi de la possible sincronia entre processos oceanogràfics a la Mediterrània nord-occidental, especialment al golf de Lleó, i a la mar Cantàbrica, així com la seva afectació sobre els fluxos de matèria particulada, tot plegat de resultes dels forçaments atmosfèrics. A la Mediterrània nord-occidental hom ha pogut detectar els episodis de formació d'aigua densa mercès a l'anàlisi retrospectiva de variables ambientals, com la temperatura de l'aire; variables calculades a partir de dades de satèl·lit, com les pèrdues de calor i la flotabilitat; i variables oceanogràfiques, com la temperatura de l'aigua, la velocitat i direcció dels corrents, i la concentració de partícules en suspensió. Aquests episodis desencadenaren DSWCs a la plataforma continental, les quals es propagaren talús avall, i situacions de convecció profunda a mar oberta. Ocasionalment, aquests fenòmens van ocórrer de forma sincrònica amb un aprofundiment anòmal de la capa de mescla a la mar Cantàbrica. El monitoratge simultani dels fluxos de matèria particulada als canyons del cap de Creus i d'Avilés palesa notables semblances pel que fa a la variabilitat estacional dels fluxos de partícules, amb màxims cap a finals d'hivern i mínims estivals.

Capítol 3
Discussió

S'exposa a continuació una discussió conjunta dels resultats dels articles del capítol 2. En primer lloc, confrontarem l'origen i la variabilitat espaciotemporal dels fluxos de matèria particulada en els ambients del canyó del cap de Creus, al golf de Lleó, i del canyó d'Avilés, a la mar Cantàbrica. Pel que fa a la variabilitat temporal, l'anàlisi fa especial èmfasi en els efectes dels forçaments externs (vents, pèrdues de calor, aportacions fluvials, onatge) sobre la hidrografia i els fluxos de matèria particulada prop del fons en ambdós ambients. En segon lloc, incidirem en les condicions atmosfèriques que donen lloc a respostes oceanogràfiques extremes i concomitants en dues mars geogràficament desconnectades.

3.1 ORIGEN I MECANISMES DE TRANSPORT DE LA MATÈRIA PARTICULADA A LES MARS DEL NORD DE LA PENÍNSULA IBÈRICA

Els marges cantàbric i mediterrani nord-occidental són marcadament diferents pel que fa a llur fisiografia, estructura i dinàmica de les masses d'aigua, i processos d'erosió, transport i acumulació sedimentària, responsables de l'afaiçonament, entre altres, dels seus canyons submarins.

A la Mediterrània nord-occidental, els marges català del nord (*sensu* Amblas *et al.,* 2006, i Amblas, 2012) i golflleonès, estan solcats per nombrosos canyons submarins de dimensions més que notables (Berné *et al*., 2004; Amblas *et al*., 2006; Lastras *et al.,* 2011). Alguns d'aquests canyons, sobretot el del cap de Creus, són afectats alguns hiverns i primaveres per episodis de DSWC altament energètics. Les DSWCs són un tipus de flux d'aigua ràpid (>1 m s^{-1}) i turbulent carregat de matèria particulada. S'originen per l'enfonsament d'aigües superficials de la plataforma continental densificades per l'efecte de forçaments externs. Les condicions més propícies per a l'ocurrència de DSWCs es donen després de períodes perllongats de vents del nord intensos, freds i secs, en hiverns amb poca precipitació. La intensitat i la persistència dels forçaments atmosfèrics durant l'hivern determinen el grau de modificació de les propietats termohalines de la capa superficial de l'oceà i, en conseqüència llur densitat. Al seu torn, aquesta determina el desencadenament dels moviments verticals damunt la plataforma i la fondària a que seran transportades les aigües durant els episodis de cascades.

En hiverns especialment severs, com el de 2009-10, amb reiteració de períodes de vents freds del nord, es produeixen transferències de calor oceà-atmosfera molt acusades (Fig. 2.3), amb la conseqüent evaporació i refredament de les aigües superficials, que van guanyant en densitat. Quan es traspassa un llindar de densitat, que pot variar d'un any a l'altre, s'inicien els moviments verticals d'enfonsament de les aigües superficials, en realitat una convecció de plataforma (Canals *et al*., 2013). Un cop assoleixen el fons de la plataforma continental, les aigües denses es desplacen per la seva pròpia dinàmica i per l'efecte de la combinació d'un seguit de factors, com la circulació regional o de mesoescala (*i.e.* el Corrent del Nord), el pendent de la mateixa plataforma, i la presència d'elements fisiogràfics singulars com el promontori del cap de Creus. Tot plegat fa que les aigües denses acabin vessant per la vora de plataforma tot i descendint talús avall en forma de cascades que es canalitzen pels canyons submarins que travessen el talús, i en especial pel canyó del cap de Creus. El paper predominant d'aquest canyó es degut a la seva situació a l'extrem sud del golf de Lleó, cap on es dirigeixen la deriva litoral dominant i la circulació de mesoscala; al fet d'estar encaixonat fortament a la plataforma continental; i a l'efecte d'obstacle del promontori del cap de Creus, que desvia la circulació litoral i de plataforma cap a la capçalera del canyó (Canals *et al*., 2006, 2013).

La intensitat de les DSWCs varia d'un hivern a l'altre, des d'inexistents o molt lleugeres fins altament intenses, circumstància que es tradueix en la menor o major profunditat assolida per les aigües de plataforma densificades. A més, en un mateix episodi de cascades se solen produir polsos d'intensitat variable (Canals *et al*., 2006). És especialment els hiverns en que les DSWCs tenen una gran intensitat quan es produeix una transferència ràpida de grans volums d'aigua des de la plataforma continental cap al marge pregon i la conca, fins assolir fondàries de més de 2000 m (Canals *et al*., 2006; Font *et al*., 2007). Les altes velocitats (> 1 $m \cdot s^{-1}$ a 30 m sobre el fons en certs intervals) i la turbulència associades a les cascades afavoreixen la incorporació de grans quantitats de partícules sedimentàries resuspeses del fons, amb concentracions molt elevades de fracció arena (e.g. fins al 65% a 30 m sobre el fons) en els polsos més intensos (Canals *et al*., 2006; Puig *et al*., 2008; Durrieu de Madron *et al*., 2013). La seva càrrega sedimentària grollera, de grans de mida llim i arena, confereix a les DSWCs una gran capacitat abrasiva i, per tant, un gran poder d'erosió. El pas de les DSWCs és fàcilment identificable mitjançant la instrumentació instal·lada als ancoratges, doncs correspon a forts augments de la velocitat del corrent i a

descensos marcats de la temperatura de l'aigua prop del fons (Fig. 2.2d, e). Els grans volums de sediment que s'erosionen i resuspenen per l'acció de les DSWCs acaben sent transportats cap al curs baix dels canyons, on s'acumulen. La mitjana ponderada en el temps dels fluxos totals de massa mesurats al canyó del cap de Creus en hiverns amb DSWCs intenses ascendeixen a gairebé 17 g m^{-2} d^{-1} a 1000 m de fondària (Taula 3.1), amb màxims puntuals de 85 g m^{-2} d^{-1} (Fig. 2.2g). De tota manera, hom pot considerar aquest xifres com valors mínims, doncs el transport enganxat al fons, sobretot de grollers, no és capturat per les trampes de sediment. Per tant, els valors reals han de ser molt més elevats. Semblantment, durant DSWC intenses la concentració de partícules en suspensió pot arribar pràcticament als 35 mg L^{-1}.

Codi ancoratge	TWF (g m^{-2} d^{-1})	Terrígens %	$CaCO_3$ %	MOP %	Òpal %
CC300	10,34 (11,42)	69,57 (69,61)	26,25 (25,70)	3,10 (3,49)	1,30 (1,21)
CC1000	16,79 (5,17)	69,74 (66,38)	26,25 (29,11)	2,63 (2,74)	1,24 (1,77)
AC2000T	0,43	61,32	24,93	10,25	3,00
AC2000B	1,98	66,98	24,42	6,52	2,20
AC4700	0.33	53,05	35,19	7,42	4,36

Taula 3.1. Fluxos anuals mitjans i contribució relativa de cadascun dels constituents principals de la matèria particulada als canyons del cap de Creus (CC) i d'Avilés (AC). En el cas del canyó del Cap de Creus, els valors fora de parèntesi corresponen a l'hivern de 2009-10 en que hi hagueren DSWCs intenses, mentre que els valors dins de parèntesi corresponen a l'any 2010-11 en que no hi hagueren DSWC intenses. Cal notar que els valors dels constituents principals són en percentatge. L'acrònim TWF fa referència a la mitjana ponderada en el temps dels fluxos totals de massa (de l'anglès *Time Weighted Flux*). Cal notar que l'hivern amb cascades intenses els TWFs es multiplicaren per tres a l'ancoratge situat a 1000 de fondària dins el canyó del Cap de Creus respecte l'hivern sense cascades intenses.

En canvi, als hiverns suaus, amb vent del nord moderat i poc persistent i amb refredament escàs de les capes superficials, l'exportació de matèria particulada cap al marge i la conca profunds es produeix principalment per l'acció de

temporals de l'est (llevantades). Això no vol pas dir que en hiverns crus els temporals no tinguin efecte sobre la transferència de matèria particulada sinó que el seu efecte queda empetitit o, si més no, es barreja amb el de les DSWCs (Palanques *et al*., 2009) (vegeu més avall). Abans d'arribar a les nostres costes, els vents de llevant tenen un gran recorregut sobre la superfície lliure del mar, o *fetch*, la qual cosa provoca un augment progressiu de l'alçada de les ones, més grans com més properes a la costa, que queda situada cara al vent. A títol il·lustratiu, a la gran llevantada de finals de desembre de 2008, a la costa gironina es produïren onades de més de 14 m d'alt (Sanchez-Vidal *et al*., 2012). Aquestes grans onades tenen, conseqüentment, una base de l'onatge força profunda que causa la resuspensió massiva dels sediments de la plataforma continental interna. A més, els vents de llevant transfereixen humitat de mar cap a terra, on els relleus costaners obstaculitzen el seu pas i provoquen el seu ascens, fet que afavoreix l'aparició de precipitacions orogràfiques i l'augment de la descàrrega fluvial, sovint en forma de riuades.

Al golf de Lleó les llevantades reforcen també la circulació ciclònica damunt la plataforma. Tot plegat provoca la convergència i l'apilament massiu d'aigua carregada de sediments a l'extrem sud-oest del golf. D'acord amb les observacions efectuades, el petit diferencial de densitat degut a l'increment en la càrrega particulada de les aigües de plataforma és suficient per desencadenar episodis d'enfonsament curts però intensos cap al talús superior (Ulses *et al*., 2008). De tota manera, l'augment de la densitat de l'aigua degut a l'elevada concentració de matèria particulada en suspensió que contenen i els processos d'enfonsament associats als temporals no basten per a que les aigües involucrades assoleixen el curs mig del canyó del cap de Creus. Això implica que a la majoria de llevantades l'exportació de matèria particulada des de la plataforma resta limitada pel que fa al seu abast. Així ho mostrà, per exemple, la llevantada de mitjans de març del 2011 (Fig. 2.2a, b). En aquest temporal, onades de més de 4,5 m d'alçada anaren acompanyades d'un augment pronunciat de la descàrrega per part dels rius que drenen el massís Central i els Pirineus (Fig. 2.2c). Els corrents de fons al curs superior del canyó del cap de Creus (ancoratge CC300) s'incrementaren fins gairebé 0,7 m s^{-1}, els TMFs fins uns 10 g m^{-2} d^{-1}, i la concentració de sediments en suspensió va superar els 7 mg L^{-1} (Fig. 2.2e-g). El fet que no es detectés cap augment en paral·lel dels TMFs a l'ancoratge profund CC1000, evidencia que el plomall d'aigua tèrbola provinent de la plataforma no penetrà fins les fondàries on se situa el curs mig del canyó (Fig. 2.2g). Per tant, en

llevantades similars a la citada, que són les majoritàries, l'exportació de partícules per enfonsament d'aigües de plataforma no va més enllà de la capçalera i el curs superior del canyó.

La coexistència de DSWCs i llevantades provoca situacions més complexes. Per exemple, a finals de gener del 2011 i després d'un seguit de polsos de DSWCs (posats de manifest per forts increments en la velocitat del corrent associats amb descensos pronunciats de la temperatura de l'aigua), la presència d'aigua densa damunt la plataforma va facilitar l'enfonsament d'aigua i sediments induït inicialment per una llevantada (Fig. 2.2a, d, e). L'aigua freda i densa carregada de sediments en suspensió sobreeixí per la vora de la plataforma continental, canalitzant-se principalment cap a l'interior del canyó del cap de Creus, com ho mostrem els descensos de temperatura i els augments de velocitat del corrent de fons, els fluxos totals i la concentració de sediments en suspensió enregistrats al curs superior del canyó (Fig. 2.2d-g).

El marge Atlàntic de de la península Ibèrica conté un seguit de canyons submarins notablement grans d'acord amb els estàndards mundials. Ho són els canyons de Nazaré, Lisboa-Setubal i Cascais, al marge de Portugal (Arzola *et al*., 2008; Tyler *et al*., 2009; Martín *et al*., 2011; de Stigter *et al*., 2007, 2011). mateixa Al marge cantàbric i, més àmpliament, al golf de Biscaia, també hi ha alguns canyons submarins molt grans, especialment els de cap Breton, Llanes i Lastres (Canals *et al*., 2004; Mulder *et al*., 2012) i, també, el canyó d'Avilés, objecte d'aquest estudi (Fig. 2.7).

A diferència de la Mediterrània i del canyó del cap de Creus, on l'efecte de les marees és pràcticament imperceptible, al canyó d'Avilés els corrents de marea, amb una marcada component semidiürna d'aproximadament 12 hores, són un factor altament rellevant (veure punt 2.2.6.2.2 del capítol 2.2). Dins del canyó, les fluctuacions del corrent estan fortament condicionades per la direcció del seu eix (Fig. 2.16), amb variacions d'alta freqüència lligades a les marees, amb períodes que van des de mig dia, com la marea semidiürna, fins un o dos dies. Els filtres aplicats per extraure les variacions periòdiques de les marees permeten discernir que les variacions d'alta freqüència representen almenys el 60% de mitjana de tots els corrents enregistrats en aquest canyó. Els cicles mareals escurcen els intervals de calma en que les partícules podrien sedimentar, contribuint així a mantenir un nivell de fons permanentment d'aproximadament 0.5 mg L^{-1} de

partícules en suspensió prop del fons (Fig. 2.10e) i afavorint activament la remobilització i al transport de sediment amunt i avall dins el canyó.

Al canyó d'Avilés els temporals són el principal dinamitzador físic dels fluxos de matèria particulada. La direcció del vent i els corrents associats determinen si els sediments resuspesos a la plataforma o provinents de les descàrregues fluvials assoleixen, o no, el canyó, i si això succeeix en superfície o per transport de fons. Com al canyó del cap de Creus, es donen també dues situacions ben diferenciades.

Sota condicions de vent de ponent s'estableix damunt la plataforma una circulació cap a l'est i un transport d'Ekman que empeny cap a la costa els plomalls superficials carregats de sediment, amb independència de llur procedència (resuspensió per l'acció de l'onatge o descàrrega fluvial) (Fig. 2.12a). Il·lustren aquesta situació el conjunt de tempestes moderades que tingueren lloc des d'octubre fins a desembre de 2012 (Fig. 2.9c, d). Tot i així, en aquesta situació el transport d'Ekman de fons és cap a mar i, per tant, afavoreix la càrrega de partícules de la capa nefeloide de fons i la seva advecció cap a la capçalera i el curs alt i mig del canyó d'Avilés. L'augment progressiu dels TMFs al curs mig del canyó, tant a prop del fons com a profunditats intermèdies, palesa el transport des de la plataforma mitjançant capes nefeloides de fons i intermèdies (Fig. 2.10b).

Sota condicions de vents de llevant s'estableixen sobre la plataforma una circulació superficial cap a l'oest i un transport d'Ekman de superfície que empenyen els plomalls superficials carregats de partícules en suspensió cap a la capçalera i el curs superior del canyó (Fig. 2.12b). Il·lustra aquesta situació el temporal de principis de març del 2012 (ombrejat a la Fig. 2.9c, d), el qual es desencadenà després d'un augment molt pronunciat de la descàrrega fluvial durant el mes anterior que amb tota probabilitat injectà grans quantitats de matèria particulada a la plataforma (Fig. 2.12). La combinació de vents de llevant de fins a 12 m s^{-1} i mar de fons amb onades de fins a 6 m, acompanyats de corrents superficials dirigides cap a l'oest (Fig. 2.9a, c, d), afavorí el transport matèria particulada en aquesta direcció i també cap a mar a la capa superficial d'Ekman. Aquesta matèria sedimentà més tard al canyó d'Avilés, a profunditats de com a mínim 2000 m, com ho mostra l'increment dels TMFs a la Figura 2.10b, tant a prop del fons com a nivells intermedis. En aquestes condicions, el transport

d'Ekman de fons és dirigeix cap a la costa i, per tant, no afavoreix la injecció a nivell de fons de matèria particulada des de la plataforma cap al canyó. Ho fa palès l'absència d'augment de la concentració de partícules en suspensió durant l'esdeveniment citat (Fig. 2.10e). Això és indicatiu que les capes nefeloides de fons quedaren retingudes a la plataforma.

Les dades obtingudes indiquen que el curs superior i mig del canyó d'Avilés estan connectats des del punt de vista de la dinàmica sedimentària, si més no de la matèria particulada. En això tots dos canyons, el del cap de Creus i el d'Avilés, s'assemblen, tot i les diferències en els rangs batimètrics implicats, i també en l'estructura de la columna d'aigua i la manera en que els forçaments externs l'afecten (125-1600 m i 130-2200 m, respectivament (Lastras et al., 2007; 2012).

Més avall del curs mig, nombroses evidències mostren que sota certes condicions (*e.g.* DSWCs intenses), el material resuspès a la plataforma del golf de Lleó pot assolir el curs baix del canyó i arribar a la conca pregona (López-Jurado *et al.,* 2005; Canals *et al*., 2006; Lastras *et al.,* 2007; Sanchez-Vidal *et al*., 2008; Palanques *et al*., 2009; Puig *et al.,* 2013). En el del canyó d'Avilés, també hi ha indicis que apunten en el mateix sentit, tot i que per mecanismes diferents. Tant la direcció de l'hodògrama[7] construït a partir de les dades sense filtrar dels corrents de fons del curs mig del canyó des de l'1 d'abril fins al 31 de maig de 2012 (Fig. 2.16), com la seqüència d'increments dels TMFs primer al curs mig i després al curs inferior (Fig. 2.10d, e), suggereixen que el canyó d'Avilés en el seu conjunt podria actuar també com a vector preferent dels fluxos de matèria particulada fins al talús inferior i la conca profunda, a més de 4.000 m. Convé assenyalar que el període esmentat (1 d'abril a 31 de maig de 2012) comprèn un temporal i una riuada, i correspon als TMFs més grans enregistrats al curs mig del canyó. Aquest fluxos, doncs, serien una expressió de la transferència del senyal dels forçaments externs, com les riuades i temporals, fins grans fondàries.

Hi ha, però, diferències molt significatives entre tots dos canyons pel que fa a les magnituds dels fluxos al curs mig i prop del fons. De mitjana, els fluxos totals al curs mig i prop del fons al canyó d'Avilés són d'uns 2 g m^{-2} d^{-1}, és a dir aproximadament una vuitena part dels TWFs al curs mig del canyó del cap de Creus en hiverns amb DSWCs intenses (Taula 3.1). És clar que, degut a la diferent

[7] Diagrama que dóna una representació vectorial del moviment d'un fluid.

fisiografia dels marges i a les diferències en els rangs batimètrics esmentades adés, en el cas del canyó d'Avilés les mesures han estat fetes a 2000 m mentre que al canyó del cap de Creus ho han estat a 1000, i a distàncies de la costa més propera de ~40 km i ~20 km, respectivament. En les condicions actuals d'alt nivell del mar, els processos implicats en les transferències sedimentàries al canyó d'Avilés tampoc semblen tenir, ni de lluny, la capacitat erosiva de les DSWCs, que erosionen activament tant la plataforma continental com el talús i els vessants i l'eix del canyó del cap de Creus (Canals *et al*., 2006, 2012; Lastras *et al*., 2007).

Composició i origen del fluxos de partícules. El predomini de la fracció terrígena en els fluxos de matèria particulada (Taula 3.1), apunta inequívocament a les aportacions fluvials com a font principal de les partícules que arriben als canyons submarins investigats. Tot i així, i com ja s'ha dit anteriorment, en cap dels dos canyons hi ha un control directe de la descàrrega fluvial sobre la variabilitat temporal dels TMFs, sinó que en tots dos indrets es necessita una aportació d'energia suficient, mitjançant processos com els temporals o les DSWCs, per desencadenar la resuspensió i el transport de partícules, i eventualment l'erosió del fons marí, des de la plataforma cap al marge i la conca pregons.

La segona font, en termes quantitatius, de les partícules que sedimenten als canyons estudiats és la producció primària marina. La seva variabilitat està relacionada amb l'ocurrència estacional i la intensitat dels *blooms* fitoplanctònics, tot i que en alguns episodis també hi poden haver contribucions bentòniques i fins i tot terrestres significatives (e.g. Sanchez-Vidal *et al*., 2012). Els camins seguits per la matèria particulada biogènica (fonamentalment carbonat de calci, MOP i òpal) fins ésser injectada als ambients de canyó són també canviants d'un episodi a un altre i, de vegades, fins i tot incerts. Aquesta injecció pot produir-se per via de la sedimentació pelàgica alimentada directament pels *blooms* superficials allunyats de la cosa, o pot provenir de *blooms* més costaners amb transportat per corrents de fons. Al canyó d'Avilés, la connexió entre els nivells intermedis de la columna d'aigua i el fons es posa de manifest per l'augment en l'abundància relativa d'òpal que experimentà la trampa de fons del curs mig del canyó AC2000B l'abril de 2012 entre 16 i 30 dies més tard que la trampa intermèdia AC2000T, situada 800 m per sobre de l'anterior. Aquest fet, que tingué lloc en un context d'elevada producció primària (Fig. 2.11), evidencia clarament que moltes partícules d'origen biogènic arriben per via pelàgica fins

nivells intermedis i fins el mateix fons del canyó d'Avilés. Els terminis de temps involucrats s'adiuen amb el rang publicat per Asper (1987) en relació amb la sedimentació d'agregats de diatomees. A més, la major abundància relativa d'òpal als fluxos de la trampa profunda AC4700 situada a la gola del canyó d'Avilés que a la trampa de fons AC2000B (Fig. 2.11 i Taula 3.1), situada aproximadament a 2000 m menys de fondària, indica que el curs inferior del canyó rep directament partícules biogènics per decantació pelàgica. (i Alhora, evidencia l'escassa o nul·la rellevància sobre les aportacions biogèniques del transport advectiu des del marge continental.

A més, la trajectòria de les partícules entre AC2000B al curs mig del canyó i AC4700 al curs inferior, ja comentada, posa de manifest un transport horitzontal de matèria particulada seguint l'eix canyó, si més no a la profunditat d'AC2000B (Fig. 2.16). De fet, l'enriquiment en MOP i òpal del març de 2013, visible a totes les estacions (Fig. 2.11), hom explicar-lo per la situació d'enfonsament costaner que es produïren a principis de 2013 (Fig. 2.14), combinades amb un augment de la descàrrega fluvial (Fig. 2.9a) i un *bloom* fitoplanctònic costaner el mateix mes de març de 2013 (Fig. 2.13). En aquestes condicions s'haurien format capes nefeloides enriquides en components biogènics, les quals s'haurien estès per tot el marge a diferents profunditats, impulsades també pel transport d'Ekman intermedi i de fons.

Tot i no neguar l'existència d'una aportació pelàgica de MOP i d'òpal durant o després del desenvolupament dels *blooms* fitoplanctònics, al canyó del cap de Creus, diversos estudis han conclòs que l'arribada de quantitats altes de MOP fresca i d'òpal es produeix majoritàriament per l'advecció de matèria particulada fina, amb la mediació de capes nefeloides, sobretot després d'episodis moderats de DSWC (Sanchez-Vidal *et al*., 2008; Tesi *et al*., 2010; Pasqual *et al*., 2011). Les nostres dades mostren que l'any 2010, la variabilitat més gran en el senyal biològic al canyó del cap de Creus es produí els mesos de març i abril (Fig. 2.5), coincidint amb el relaxament de les condicions hidrodinàmiques del final de la temporada de DSWC (Fig. 2.2d).

En resum, tot i que amb característiques diferents i amb la intervenció de processos peculiars, com les DSWCs, en el cas del golf de Lleó, a les mars del nord de la península Ibèrica l'advecció lateral es revela com el principal mecanisme de control dels fluxos de partícules i de l'intercanvi de material

biogènic entre els ambients soms de plataforma i els canyons submarins encaixonats als talussos adjacents. L'advecció lateral té un paper preponderant tant a les DSWCs com en el transport d'Ekman.

Atès que tant la MO com l'òpal són làbils i poden degradar-se durant el seu transport canyó avall (de Stigter *et al*., 2007; Pasqual *et al*., 2011), el $CaCO_3$, més resistent a la degradació, sol ésser present amb major abundància relativa a les estacions més profundes de tots dos canyons (Taula 3.1). A l'estació més profunda del canyó d'Avilés (AC4700), els registres de $CaCO_3$ presenten un cert patró estacional, doncs per la seva localització i pel règim hidrodinàmic que li és propi, aquesta estació és molt poc afectada pels processos d'advecció que transporten partícules terrígenes des de la plataforma tot i diluint els carbonats i partícules la resta de constituents biogèniques dins la matriu de partícules terrígenes, com també ocorre en el cas de les DSWCs. En aquesta estació profunda del canyó d'Avilés, el pic de $CaCO_3$ més destacable ocorregué el juny de 2012, simultàniament amb pics de MOP i òpal (Fig. 2.11), després de tres mesos consecutius amb una elevada producció primària (Fig. 2.13) i sense cap tempesta destacable i, per tant, en absència de transport advectius intens. Al canyó del cap de Creus, els registres de $CaCO_3$ també presenten una certa estacionalitat, recognoscible sempre i quan l'advecció de matèria particulada no sigui massa potent. Així, durant el suau hivern de 2010-11, els registres de $CaCO_3$ a l'estació més profunda presentaren un patró estacional prou clar. Donat que aquesta estació fou poc impactada per les DSWCs, els constituents biogènics no quedaren diluïts dins la matriu terrígena que sota condicions hidrodinàmiques severes hauria estat resuspesa i transportada des de la plataforma continental tot i barrejant-se amb i emmascarant possibles aportacions biogèniques pelàgiques (Fig. 2.5).

3.2 RESPOSTA OCEANOGRÀFICA ALS FORÇAMENTS ATMOSFÈRICS SINCRÒNICS A LES MARS DEL NORD DE LA PENÍNSULA IBÈRICA

Com s'ha vist a l'apartat anterior, els fluxos de partícules recollits a les trampes de sediment situades als canyons submarins del cap de Creus i d'Avilés, presenten una elevada variabilitat temporal tant en la seva magnitud com en la seva

composició. En això, els forçaments atmosfèrics hi juguen un paper fonamental. A banda, el cru hivern de 2005, extremadament fred i sec, va alterar dràsticament i en paral·lel la hidrografia de la Mediterrània nord-occidental i de la mar Cantàbrica, palesant l'existència d'algun tipus de connectivitat atmosfèrica, o patró de teleconnexió, entre les mars del nord de la península Ibèrica (Somavilla *et al*., 2009).

La correlació de les anomalies hivernals (*i.e.* de desembre a març) de la temperatura de l'aire superficial entre el golf de Lleó, prenent com a punt base l'estació meteorològica de Perpinyà, i qualsevol punt d'una malla global de 2,5º de latitud x 2,5º de longitud (144x73), entre 90ºN i 90ºS, i 0ºE i 357.5ºE, mostra que gran part de les anomalies varien en paral·lel ($r \geq 0{,}8$) dins d'un radi d'aproximadament 1000 km (Fig. 2.26). Les dimensions d'aquesta correlació, que situa el golf de Lleó i la mar Cantàbrica en un mateix domini, confirma l'existència d'una teleconnexió de curt abast entre les dues àrees. Aquesta teleconnexió fa que els cicles de pèrdues netes de calor superficial des de l'oceà cap a l'atmosfera oscil·lin gairebé de la mateixa manera a tots dos indrets (Fig. 2.19c), alhora que controla l'ocurrència d'episodis extrems alguns hiverns, amb una clara tendència a la sincronia (Fig. 2.20c).

La resposta oceanogràfica a aquests forçaments "teleconnectats" i, per tant, els intercanvis de massa i energia entre els ambients soms i profunds difereixen d'un marge a l'altre, doncs també depenen de l'estructura i el gruix total de les columnes d'aigua respectives, que són ben diferents (Figs. 1.10 i 1.11). A la Mediterrània nord-occidental, les màximes expressions dels forçaments atmosfèrics teleconnectats són els episodis de DSWC originats a la plataforma i els episodis de convecció a mar oberta que, en casos extrems, poden arribar a produir la desestratificació i l'homogeneïtzació completes de la columna d'aigua, de més de 2000 m de gruix. És comú, sobretot en hiverns ben crus, que les DSWCs i la convecció de mar oberta al golf de Lleó siguin sincròniques. A la mar Cantàbrica, però, la pertorbació de l'estructura hidrogràfica per causa dels forçaments teleconnectats arriba com a molt a 400 m de fondària (Fig. 2.23a). En condicions normals, la capa de mescla hivernal cantàbrica amb prou feines ultrapassa la profunditat a que està situada la vora de plataforma (~250 m) (González-Pola *et al*., 2007).

Els episodis més extrems de mescla convectiva (i DSWC al golf de Lleó) en una o a les dues àrees estudiades ocorren només en hiverns singulars, que poden anar acompanyats del fenomen de la "reemergència" (Smith *et al*., 2008). El concepte de "reemergència" es refereix a la reiteració d'una barreja vertical extrema o molt significativa l'hivern següent (vegeu detalls més avall). Al llarg dels últims 44 anys (1970-2014) de la sèrie temporal estudiada destaquen pel seu caràcter extrem els biennis corresponents als hiverns de 2005 i 2006, i de 2010 i 2011 (Fig. 2.23a, b). Els hiverns de 2005 i 2006, entesos com els primers mesos d'aquests anys, hom enregistrà aprofundiments excepcionals de la capa de mescla a la mar Cantàbrica (350 m) i al golf de Lleó (2500 m), on també es produïren DSWCs intenses evidenciades per forts descensos de la temperatura de l'aigua (~2ºC) de fons a 1000 m de fondària al canyó submarí del cap de Creus (Canals *et al*., 2006; Font *et al*., 2007; Schroeder *et al*., 2008; Puig *et al*., 2013).

Els hiverns de 2010 i 2011 va tornar a produir-se una mescla convectiva extrema a les dues àrees. A la mar Cantàbrica, l'any 2010 s'assolí un valor rècord d'aprofundiment de la capa de mescla (400 m), ment re que l'any 2011 arribà pràcticament a 300 m de fondària. Al golf de Lleó, tant l'hivern de 2010, juntament amb DSWC intens, com el de 2011, de nou la mescla convectiva tornà a desestratificar per complet la columna d'aigua (*i.e.* capa de mescla fins 2500 m) (Fig. 2.23a, b).

Tot i que les pèrdues de calor i de flotabilitat de les aigües superficials foren força més baixes el segon any que el primer any d'ambdós biennis 2005-06 i 2010-11, foren suficients per a que es repetís una mescla profunda a totes dues àrees, acompanyada per DSWCs al golf de Lleó, excepte l'hivern de 2011. A diferència del 2006, l'hivern de 2011 les DSWCs no "reemergiren" al golf de Lleó degut a que les aigües superficials de damunt la plataforma veieren augmentada la seva flotabilitat per la influència d'una descàrrega fluvial molt elevada, la qual inhibí la formació d'aigües denses de plataforma i, lògicament, llur penetració talús avall (Martín *et al.,* 2013) (Fig. 2.23a, b). Aquesta influència fluvial no arribà a mar oberta on sí que es produí una convecció profunda. Naturalment, la recurrència observada els biennis 2005-06 i 2010-11 correspon al fenomen de la reemergència esmentat més amunt. Per a que es produeixi reemergència cal que les anomalies tèrmiques formades dins la capa de mescla l'hivern anterior persisteixin durant mesos, fins al proper hivern, aprofitant la gran capacitat calorífica de l'aigua de mar. Nomes així podran reaparèixer l'hivern següents,

quan es desenvolupi una nova capa de mescla. La desestratificació de la columna d'aigua del primer hivern facilita, doncs, que l'hivern següent es torni a formar una capa de mescla que pot ser tan profunda com la precedent. També podríem dir que, d'alguna manera, les condicions extremes del primer hivern precondicionen les aigües de sota la termoclina estacional per a la seva reemergència l'hivern següent.

L'estudi de la situació atmosfèrica d'aquests hiverns revela que l'ocurrència d'esdeveniments extrems sincrònics al golf de Lleó i a la mar Cantàbrica depèn de la distribució dels camps de pressió atmosfèrica (Fig. 2.27c). L'aparició d'una anomalia d'altes pressions a l'Atlàntic nord i la seva localització predominant al llarg de l'hivern regulen la penetració de les masses d'aire continental fredes i seques fins la latitud de les nostres dues àrees d'estudi (cf. Cap. 2.3). La penetració i la presència més o menys persistent d'aquestes masses d'aire fred determinen els intercanvis de calor entre l'oceà i l'atmosfera, que és el factor del qual depèn, en última instància, el desencadenament dels episodis intensos de convecció de mar oberta en una o a a totes dues àrees, i de DSWC al golf de Lleó. També en depèn la sincronia dels processos oceanogràfics relacionats.

Tot plegat ja fa esperar que l'impacte de les teleconnexions sobre la dinàmica dels fluxos de matèria particulada als canyons estudiats sigui ben diferent, de la mateixa manera que ho és la resposta oceanogràfica de la qual en depenen els fluxos. Al golf de Lleó, aquesta resposta es manifesta en forma de convecció profunda de mar oberta i de DSWCs, les quals són responsables de que els TMFs del canyó del cap de Creus siguin molt més grans que al canyó d'Avilés, on la resposta oceanogràfica es manifesta en forma de convecció intermèdia. Per tant, la influència de la convecció sobre la dinàmica dels fluxos al canyó d'Avilés no hauria d'anar més enllà de la seva capçalera o, com a molt, el seu curs superior. Aquest segon supòsit només als anys en que la capa de mescla assoleix profunditats anòmalament grans, com als biennis esmentats (Fig. 2.23a). Malauradament, no es disposa d'un registre de TMFs del canyó d'Avilés durant un any amb convecció reforçada, per la qual cosa aquesta possibilitat resta en el terreny de les hipòtesis, si més no per ara. Cal assenyalar, però, que a més de la variabilitat intrínseca als forçaments atmosfèrics, factors com les diferents fondàries a que es van fondejar els ancoratges als canyons estudiats, condicionades per les característiques de cadascun d'ells,, i les especificitats dels processos causants del transport sedimentari (DSWC i llevantades al golf de Lleó, i

temporals del nord a la mar Cantàbrica), també podrien tenir una influència sobre les magnituds dels TMF, tan diferents, d'un canyó i l'altre.

Tot i aquestes diferències, els hiverns amb episodis sincrònics d'aprofundiment extraordinari de la capa de mescla comporten, justament per causa de la intensificació de la mescla vertical, la transferència de nutrients des de les capes més profundes cap a les aigües superficials, situació que desencadena l'aparició sincrònica de grans *blooms* fitoplanctònics a totes dues àrees (Fig. 2.25). Aquests *blooms*, que són els principals responsables de la contribució biogènica als TMFs, representen l'última expressió de l'efecte sincrònics de les teleconnexions atmosfèriques entre les dues àrees, i en realcen encara més la seva rellevància llur impacte sobre els ecosistemes marins de la Mediterrània nord-occidental i la mar Cantàbrica.

Capítol 4
Conclusions i línies de treball futures

En aquesta Tesi hom ha integrat dades metoceàniques, de satèl·lit, de mesures amb instruments instal·lats en ancoratges submergits i d'anàlisis biogeoquímiques de la matèria particulada, amb la finalitat última d'escatir la influència dels forçaments atmosfèrics i llur variabilitat intra- i interanual sobre el transport i la composició d'aquesta matèria particulada. En referir-nos als forçaments atmosfèrics considerem primordialment la temperatura i el vent, els quals determinen directament les pèrdues de calor per la superfície del mar, l'onatge i els corrents, i també la precipitació i les descàrregues fluvials associades. En situacions específiques aquests processos accentuen el seu paper, com quan es desencadenen temporals. Hi ha també altres factors no relacionats amb els forçaments atmosfèrics, com les marees, que poden tenir un rol altament rellevant. Per assolir els objectius plantejats vàrem escollir dos canyons submarins i el seu entorn més proper, partint de la base que els canyons submarins són vectors preferents per a l'exportació de la matèria particulada des de la plataforma continental cap al marge i la conca pregons, com han palesat manta estudis. Aquests canyons han estat el del cap de Creus, al golf de Lleó, a la Mediterrània nord-occidental, i el d'Avilés, a la mar Cantàbrica. El context de cadascun d'ells, ben diferent des de diversos punts de vista, dona sentit a aquesta tria. Una segona, i no pas menor, hipòtesi de l'experiment que en realitat és aquesta Tesi, és que els forçaments atmosfèrics més intensos en una i altra àrea estan teleconnectats, de manera que actuen sincrònicament tot i desencadenant les respostes oceanogràfiques de nivell energètic més alt conegudes en ambdues àrees, marees a banda.

L'estudi de la variabilitat espaciotemporal dels fluxos de partícules i de la seva composició als canyons del cap de Creus i d'Avilés, demostra que tots dos ambients responen ràpidament als forçaments atmosfèrics. A l'hivern, al golf de Lleó el desencadenament, la intensitat i la persistència de processos oceanogràfics d'alt nivell energètic depenen directament dels forçaments atmosfèrics. Quan aquests són molt severs, la pèrdua de calor per la superfície del mar i el refredament i l'augment de la densitat de les aigües superficials de damunt de la plataforma continental s'accentuen. Aquesta situació condueix a l'enfonsament de les aigües superficials en forma de corrents de fons altament energètiques que cauen en cascada talús avall i cap a l'interior dels canyons submarins. Les cascades d'aigües denses de plataforma assoleixen velocitats molt elevades (>1 m s^{-1}) i tenen caràcter turbulent, la qual cosa facilitat la resuspensió dels sediments solts dels fons de la plataforma i del talús i la seva incorporació a

la massa d'aigua densa. Els sediments que s'incorporen a les cascades poden contenir proporcions elevades (>50%) de mida llim i arena, la quals les hi confereix una gran capacitat abrasiva i erosiva. Per tot plegat, aquestes cascades, al golf de Lleó, i al canyó del cap de Creus en concret, són el principal procés determinant de la sedimentació al talús continental i més enllà. Els hiverns més suaus en termes de situacions persistents de vent del nord i de refredament de la capa superficial, l'exportació de matèria particulada cap al marge i la conca profunds es produeix principalment durant les llevantades. També és donen situacions en que les cascades i les llevantades coincideixen en el temps, circumstància afavorida pel fet que les cascades d'aigües denses, un cop activades, poden persistir durant setmanes. Són situacions complexes en que preval l'efecte de les cascades, sobretot perquè les llevantades duren només unes hores o uns pocs dies.

Al canyó d'Avilés els forçaments atmosfèrics i, concretament, els temporals són el principal agent dinamitzador dels fluxos de matèria particulada cap a l'interior de l'oceà. La direcció del vent i dels corrents que impulsa controlen la possible transferència cap al canyó tant dels sediments aportats pels rius i dels resuspesos a la plataforma, i si aital transferència es produirà en superfície o per transport de fons. Com és comú a la majoria de marges continentals, i com ocorre també en el cas del canyó del cap de Creus, el transport de matèria particulada es produeix predominantment per advecció lateral. En lloc de ser canalitzades directament cap al canyó i els seus tributaris també endentats a la plataforma, les partícules sedimentàries s'acumulen inicialment a la pròpia plataforma fins l'aparició de condicions d'alta energia amb capacitat de resuspendre-les i desencadenar un transport d'Ekman cap al canyó. La plataforma continental actua, doncs, com a reservori temporal de sediment, en el sentit més ampli del terme, és a dir incloent-li les fraccions terrígena i biogènica. De fet, el concepte de reservori temporal de sediment per part de la plataforma continental també és perfectament vàlid en el cas del golf de Lleó, on les cascades i, en menor mesura, les llevantades, remobilitzen el sediment acumulat temporalment a la plataforma.

Aquesta Tesi confirma el rol dels canyons del cap de Creus i d'Avilés com a vectors preferents per a la transferència del senyal dels forçaments externs des de la plataforma cap al talús i la conca profunda. Les DSWCs tenen, però, una capacitat molt més gran que el transport d'Ekman per erosionar i transportar sediment de la plataforma continental cap al marge extern i la conca, doncs, de

mitjana, els TMFs enregistrats al curs mig del canyó d'Avilés són vuit vegades inferiors als mesurats al curs mig del canyó del cap de Creus els hiverns amb DSWCs intenses. Cal pensar, que en anys sense DSWCs i de DSWCs suaus els TMFs en un i altre canyó siguin molt més semblants.

El predomini de la fracció terrígena en els fluxos de matèria particulada apunta inequívocament a les aportacions fluvials com a font principal, tant a la Mediterrània nord-occidental com a la mar Cantàbrica. Una petita porció de la fracció terrígena pot arribar directament als canyons per decantació pelàgica i per transport de fons, però la major part s'acumula a la plataforma, des d'on serà remobilitzada massivament sota l'acció dels processos oceanogràfics d'alta energia esmentats adés.

La producció primària és la segona font de matèria particulada, a la qual hi contribueix fonamentalment amb carbonat de calci, MOP i òpal. Presenta una clara variabilitat estacional relacionada amb els *blooms* fitoplanctònics, els quals al seu torn responen a les condicions hidrodinàmiques i, per tant, als forçaments externs, de manera que hi ha un paral·lelisme clar en el grau de desenvolupament que assoleixen a cadascuna de les àrees estudiades. A totes dues, l'advecció lateral, especialment quan és intensa, té una efecte de dilució dels constituents biogènics. En general, a les estacions més profundes dels dos canyons estudiats, hom sol trobar majors abundàncies relatives de $CaCO_3$ que de MOP i òpal, degut al caràcter làbil d'aquest darrers, que es degraden durant el seu transport cap a nivells més pregons.

A més dels temporals, que són comuns a totes dues àrees tot i que amb característiques diferents, els processos oceanogràfics més rellevants són la convecció intermèdia (i.e. fins 400 m) a la mar Cantàbrica i les DSWCs i la convecció profunda (i.e. fins 2500 m) al golf de Lleó. Quan els forçaments atmosfèrics que comporten l'arribada de masses d'aire fredes i seques a les latituds on són situades les dues àrees d'estudi són prou intensos i persistents, cosa que succeeix certs hiverns, tots els processos oceanogràfics esmentats tendeixen a ocórrer sincrònicament i amb gran vigor, palesant així l'existència de teleconnexions atmosfèriques entre la Mediterrània nord-occidental i la mar Cantàbrica. La situació atmosfèrica que determina aital sincronia depèn de la configuració dels camps de pressió atmosfèrica sobre l'Atlàntic nord i Europa. La formació i la localització d'un centre hivernal d'altes pressions sobre l'Atlàntic

nord, que hom podria qualificar d'anòmal, és clau per a l'ocurrència d'episodis intensos de convecció, i DSWC al golf de Lleó, a qualsevol de les dues regions, i també per a la sincronia entre la Mediterrània nord-occidental i la mar Cantàbrica.

Les teleconnexions atmosfèriques, el paral·lelisme en les respostes oceanogràfiques en una i altra àrea i, ocasionalment, llur sincronia contribueixen a les similituds dels patrons de variabilitat estacional dels fluxos de partícules i, conseqüentment, afecten la dinàmica dels ecosistemes mediterranis nord-occidentals i cantàbrics.

Els resultats assolits en aquesta Tesi plantegen, com és natural, noves qüestions. Així es fa la Ciència, per increments acumulatius. La idea de que dues àrees marines no connectades físicament puguin respondre de manera sincrònica quan les seves aigües són fortament pertorbades pels mateixos forçaments externs d'origen atmosfèric és innovadora, si més no pel que fa a les mars que envolten la península Ibèrica, i té un enorme potencial de desenvolupament en diferents direccions. Així, hom podria donar un nou enfoc a l'estudi de la dinàmica oceànica i els ecosistemes marins de totes dues àrees. La integració de dades meteorològiques i oceanogràfiques, la incorporació de la modelització numèrica i la inclusió de dades de pesqueries té un enorme potencial per ajudar a entendre millor el funcionament dels ecosistemes marins de les mars del nord la península Ibèrica i per fonamentar el desenvolupament de capacitats predictives i crear un nou, i segurament millor, model de gestió dels recursos vius que hom extreu d'aquests ecosistemes.

Per aconseguir-ho ens permetem suggerir les següents línies d'actuació:

- Disposar de sèries temporals llargues i paral·leles de variables oceanogràfiques, inclosa la mesura dels fluxos de matèria particulada, per poder caracteritzar els episodis extrems i detectar tendències a llarg termini tot i situant-les, si fos possible, en el context del canvi climàtic global (vegeu més avall). Hom duu a terme la monitorització hidrosedimentària del canyó del cap de Creus des de l'hivern de 2004-05, la qual cosa ha permès detectar i fer mesures in situ els hiverns en que tenen lloc les DSWCs i establir, així, un sèrie temporal de referència a la Mediterrània nord-occidental. La sèrie del canyó del cap de Creus està acompanyada per una sèrie del canyó veí de Lacaze-Duthiers iniciada els anys 80 del segle passat, tot i que aquest canyó juga un paper molt menys rellevant que el del cap de Creus com a via preferents per les DSWCs. Ni al

canyó d'Avilés ni a cap altre gran canyó submarí de la mar Cantàbrica no es compta amb un seguiment semblant. Mantenir amb caràcter continu, si més no els hiverns, un ancoratge instrumentar al canyó d'Avilés permetria obtenir una sèrie temporal cada cop més llarga i de referència per la mar Cantàbrica, cosa que permetria continuar investigant de manera adequada l'exportació de matèria particulada en aquest ambient i aprofundir en l'anàlisi de les relacions amb els forçaments externs.

- Intentar predir l'impacte del canvi climàtic sobre les condicions atmosfèriques que desencadenen respostes oceanogràfiques sincròniques al golf de Lleó i la mar Cantàbrica, dotant-se així de millors eines per avaluar els seus efectes sobre els recursos vius.

- Investigar les relacions entre forçaments externs, i atmosfèrics especialment, i la injecció de contaminants, en fase dissolta i particulada, per convecció oceànica en ambdues àrees estudiades i per DSWCs (al golf de Lleó. Hi ha base per pensar que aquest transport no és regular sinó que també està governat pels forçaments atmosfèrics i que segueix un patró estacional, amb una variabilitat interanual notable. Òbviament, també podria ser altament interessant intentar escatir les possibles relacions entre la injecció de contaminants i la seva presència a les espècies explotades, en funció dels seus hàbits i del seu cicle vital.

L'anàlisi creuada dels resultats que s'obtinguessin permetria, sens dubte, comprendre molt millor els vincles entre processos físics i la variabilitat i qualitat dels recursos vius, fent així possible, si més o idealment, que els plans de gestió de les mars del nord la península Ibèrica integressin plenament tal coneixement.

Capítol 5
Bibliografia

Albérola, C., Millot, C., Font, J., 1995. On the seasonal and mesoscale variabilities of the Northern Current during the PRIMO-0 experiment in the western Mediterranean Sea. Oceanologica Acta 18, 163-192.

Álvarez Fanjul, E., Alfonso, M., Ruiz, M.I., López, J.D., Rodríguez, I., 2003. Building the European capacity in operational oceanography. Proceedings of the third international conference on EuroGOOS. Elsevier Oceanography Series 69, 398-402.

Amblas, D., M. Canals, R. Urgeles, G. Lastras, C. Liquete, J.E. Hughes-Clarke, J.L. Casamor, and A.M. Calafat, 2006. Morphogenetic mesoscaleanalysis of the northeastern Iberian margin, NW Mediterranean Basin, Marine Geology 234, 3-20.

Amblas, A., 2012. Morfodinàmica sedimentària de marges continentals passius silicoclàstics. Memòria de Tesi Doctoral, Universitat de Barcelona, 181 pp.

Arístegui, J., Barton, E.D., Álvarez-Salgado, X.A., Santos, A.M.P., Figueiras, F.G., Kifani, S., Hernández-León, S., Mason, E., Machú, E., Demarcq, H., 2009. Subregional ecosystem variability in the Canary Current upwelling. Progress in Oceanography 83, 33-48.

Armstrong, R.A., Lee, C., Hedges, J.I., Honjo, S., Wakeham, S.G., 2002. A new, mechanistic model for organic carbon fluxes in the ocean based on the quantitative association of POC with ballast minerals. Deep-Sea Research Part II: Topical Studies in Oceanography 49, 219-236.

Arzola, R.G., Wynn, R.B., Lastras, G., Masson, D.G., Weaver, P.P.E., 2008. Sedimentary features and processes in the Nazaré and Setúbal submarine canyons, west Iberian margin. Marine Geology 250, 64-88.

Asper, V.L., 1987. Measuring the flux and sinking speed of marine snow aggregates. Deep-Sea Research Part A: Oceanographic Research Papers 34, 1-17.

Bader, R.G., Hood, D.W., Smith, J.B., 1960. Recovery of dissolved organic matter in sea-water and organic sorption by particulate material. Geochimica et Cosmochimica Acta 19, 236-243.

Balguerías, E., Quintero, M.E., Hernández-González, C.L., 2000. The origin of the Saharan Bank cephalopod fishery. ICES Journal of Marine Science 57, 15-23.

Baker, E.T. Lavelle, J.W., 1984. The effect of particle size on the light attenuation coefficient of natural suspensions Journal of Geophysical Research 89, 8197-8203.

Berné, S., Carré, B., Loubrieu, B., Mazé, J.P., Morvan, L., Normand, A., 2004. Le Golfe du Lion, Carte morpho-bathymétrique. Ifremer, Brest.

Bethoux, J.P., Durieu de Madron, X., Nyffeler, F., Tailliez, D., 2002. Deep water in the western Mediterranean: Peculiar 1999 and 2000 characteristics, shelf formation hypothesis, variability since 1970 and geochemical inferences. Journal of Marine Systems 33-34, 117-131.

Bishop, J.K.B., 1986. The correction of suspended particulate matter calibration of Sea Tech transmissometer data. Deep-Sea Research 33, 121-134.

Bode, A., Valdés, L., Lavín, A., 2012. Cambio climático y oceanográfico en el Atlántico del norte de España. Instituto Español de Oceanografía, Madrid, 280 pp.

Bonnin, J., Heussner, S., Calafat, A., Fabrés, J., Palanques, A., Durrieu de Madron, X., Canals, M., Puig, P., Avril, J., Delsaut, N., 2008. Comparison of horizontal and downward particle fluxes across canyons of the Gulf of Lions (NW Mediterranean): meteorological and hydrodynamical forcing. Continental Shelf Research 28, 1957-1970.

Botas, J.A., Fernández, E., Bode, A., Anadón, R., 1989. Water masses off the central Cantabrian coast. Scientia Marina 53, 755-761.

Bourillet J-F., Augris C., Cirac P., Mazé J.-P., Normand A., Loubrieu B., Crusson A., Gaudin M., Poirier D., Satra C., Simplet L., 2007. Le canyon de Capbreton. Cartes morpho-bathymétriques, Ifremer (Ed.) i Université Bordeaux 1.

Broecker, W.S., 1987. The biggest chill. Natural History 96, 74-82.

Broecker, W.S., Denton, G.H., 1989. The role of ocean-atmosphere reorganizations in glacial cicles. Geochimica et Cosmochimica Acta 53, 2465-2501.

Canals, M., 1985. Estructura sedimentaria y evolución morfológica del talud y el glacis continentales del Golfo de León: fenómenos de desestabilización de la cobertera sedimentaria Plio-Cuaternaria. PhD Thesis, Universitat de Barcelona, Spain, 618 pp.

Canals, M., Casamor, J.L., Lastras, G., Monaco, A., Acosta, J., Berné, S., Loubrieu, B., Weaver, P. P. E., Grehan, A., Dennielou, B., 2004. The role of canyons in strata formation. Oceanography 17, 80-91.

Canals, M., Puig, P., Durrieu de Madron, X., Heussner, S., Palanques, A., Fabrés, J., 2006. Flushing submarine canyons. Nature 444, 354-357.

Canals, M., Amblas, D., Lastras, G., Sanchez-Vidal, A., Calafat, A. M., Rayo, X., Casamor, J.L., 2012. Els canyons submarins. A: Enciclopèdia Catalana (Eds.), Suplement de la Història Natural dels Països Catalans. La terra a l'univers: astronomia. Addenda geològica. Institut d'Estudis Catalans, Barcelona, 251–272.

Canals, M., Company, J.B., Martin, D., Sanchez-Vidal, A., Ramírez-Llodra, E., 2013. Integrated study of Mediterranean deep canyons: Novel results and future challenges. Progress in Oceanography 118, 1-27.

Colas, F., 2003. Circulation et dispersion lagrangiennes en Atlantique Nord-Est, Tesis Doctoral, Universitat de Bretanya Occidental, Brest, França 259 pp.

Cooley, S.R., Doney, S.C., 2009. Ocean acidification's impact on fisheries and societies: a U.S. perspective. Current, the Journal of Marine Education 25, 15-19.

Company, J.B., Puig, P., Sardà, F., Palanques, A., Latasa, M., Scharek, R., 2008. Climate influence on deep sea populations. PLoS ONE 3 (1), e1431.

Conan, P., Millot, C., 1995. Variability of the Northern Current off Marseilles, western Mediterranean Sea, from February to June 1992. Oceanologica Acta 18, 193-205.

de Stigter, H.C., Boer, W., de Jesus Mendes, P.A., Jesus, C.C., Thomsen, L., van den Bergh, G.D., van Weering, T.C.E., 2007. Recent sediment transport and deposition in the Nazaré Canyon, Portuguese continental margin. Marine Geology 246, 144-164.

de Stigter, H.C., Jesus, C.C., Boer, W., Richter, T.O., Costa, A., van Weering, T.C.E., 2011. Recent sediment transport and deposition in the Lisbon-Setúbal and Cascais submarine canyons, Portuguese continental margin. Deep-Sea Research Part II: Topical Studies in Oceanography 58, 2321-2344.

Dickson, R.R., Gould, W.J., Müller, T.J., Maillard, C., 1985. Estimates of the mean circulation in the deep (>2,000 m) layer of the Eastern North Atlantic. Progress in Oceanography 14, 103-127.

Ding, X., Henrichs, S. M., 2002. Adsorption and desorption of proteins and polyamino acids by clay minerals and marine sediments. Marine Chemistry 77, 225-237.

Divins, D.L., 2003. Total Sediment Thickness of the World's Oceans & Marginal Seas. NOAA National Geophysical Data Center, Boulder, CO. Vegeu la informació digital a: <www.ngdc.noaa.gov/mgg/sedthick/sedthick.html>.

Doney, S.C., Mahowald, N., Lima, I., Feely, R. A., Mackenzie, F.T., Lamarque, J.F., Rasch, P.J., 2007. Impact of anthropogenic atmospheric nitrogen and sulfur deposition on ocean acidification and the inorganic carbon system. Proceedings of the National Academy of Sciences 104, 14580-14585.

Dufau-Julliand, C., Marsaleix, P., Petrenko, A., Dekeyser, I., 2004. Three-dimensional modeling of the Gulf of Lion's hydrodynamics (northwest Mediterranean) during January 1999 (MOOGLI3 Experiment) and late winter 1999: Western Mediterranean Intermediate Water's (WIW's) formation and its cascading over the shelf break. Journal of Geophysical Research 109, C11002.

Durrieu de Madron, X., Houpert, L., Puig, P., Sanchez-Vidal, A., Testor, P., Bosse, A., Estournel, C., Somot, S., Bourrin, F., Bouin, M.N., Beauverger, M., Beguery, L., Calafat, A., Canals, M., Coppola, L., Dausse, D., D'Ortenzio, F., Font, J., Heussner, S., Kunesch, S., Le Goff, H., Martín, J., Mortier, L., Palanques, A., Raimbault, P., 2013.

Interaction of dense shelf water cascading and open-sea convection in the northwestern Mediterranean during winter 2012. Geophysical Research Letters 40, 1379-1385.

Fabrés, J., Calafat, A., Sanchez-Vidal, A., Canals, M., Heussner, S., 2002. Composition and spatio-temporal variability of particle fluxes in the Western Alboran Gyre, Mediterranean Sea. Journal of Marine Systems 34, 431-456.

Font, J., Puig, P., Salat, J., Palanques, A., 2007. Sequence of hydrographic changes in NW Mediterranean deep water due to the exceptional winter of 2005. Scientia Marina 71, 339-346.

Fraga, F. 1981. Upwelling off the Galician coast, northwest Spain. Coastal Upwelling, American Geophysical Union, Washington, DC., 176-182.

François, R., Honjo, S., Krishfield, R., Manganini, S., 2002. Factors controlling the flux of organic carbon to the bathypelagic zone of the ocean. Global Biogeochemical Cycles 16, 1087.

Frouin, R., Fiúza, A.F.G., Ambar, I., Boyd, T.J., 1990. Observations of a poleward surface current off the coasts of Portugal and Spain during winter. Journal of Geophysical Research: Oceans 95, 679-691.

Gardner, W.D., 1985. The effect of tilt on sediment trap efficiency. Deep-Sea Research Part A: Oceanographic Research Papers 32, 349-361.

Gardner, W.D., 1989. Baltimore Canyon as a modern conduit of sediment to the deep sea. Deep-Sea Research Part A: Oceanographic Research Papers 36, 323-358.

Gardner, W.D., Walsh,I.D., 1990. Distribution of macroaggregates and fine-grained particles across a continental margin and their potential role in fluxes. Deep-Sea Research Part A: Oceanographic Research Papers 37, 401-411.

Garrison, T. 1993. Oceanography: An Invitation to Marine Science. Wadsworth Publishing Company, Belmont, 540 pp.

Gattuso, J.P., Hansson, L., 2011. Ocean acidification: history and background. Ocean Acidification, Oxford University Press, New York, 1-20.

Gill, A.E., 1982. Atmosphere-Ocean Dynamics, International Geophysics Series 30, Academic Press, New York, London, 680 pp.

Gómez-Ballesteros, M., Druet, M., Muñoz, A., Arrese, B., Rivera, J., Sánchez, F., Cristobo, J., Parra, S., García-Alegre, A., González-Pola, C., Gallástegui, J., Acosta, J., 2013. Geomorphology of the Avilés Canyon System, Cantabrian Sea (Bay of Biscay). Deep-Sea Research Part II: Topical Studies in Oceanography, 1-19.

Gomez-Gesteira, M., Moreira, C., Álvarez, I., deCastro, M., 2006. Ekman transport along the Galician coast (NW, Spain) calculated from forecasted winds. Journal of Geophysical Research 111, C10005.

González-Pola, C., Fernández-Díaz, J.M., Lavín, A., 2007. Vertical structure of the upper ocean from profiles fitted to physically consistent functional forms. Deep-Sea Research Part I: Oceanographic Research Papers 54, 1985-2004.

Gross, M.G., Gross, E., 1996. Oceanography: A View of Earth. Prentice Hall, Upper Saddle River, New Jersey, 472 pp.

Guibout, P., 1987. Atlas Hydrologique de le Méditerranée. Laboratoire d'Oceanographie physique du Museum, Paris, 174 pp.

Guillén, J., Palanques, A., Puig, P., Durrieu de Madron, X., Nyffeler, F., 2000. Field calibration of optical sensors for measuring suspended sediment concentration in the western Mediterranean. Scientia Marina 64, 427-435.

Haynes, R., Barton, E. D., 1990. A poleward flow along the Atlantic coast of the Iberian Peninsula. Journal of Geophysical Research - Oceans 95, 11425-11441.

Heussner, S., Ratti, C., Carbonne, J., 1990. The PPS 3 time-series sediment trap and the trap sample processing techniques used during the ECOMARGE experiment. Continental Shelf Research 10, 943-958.

Heussner, S., Durrieu de Madron, X., Radakovitch, O., Beaufort, L., Biscaye, P. E., Carbonne, J., Delsaut, N., Etcheber, H., Monaco, A., 1999. Spatial and temporal patterns of downward particle fluxes on the continental slope of the Bay of Biscay (northeastern Atlantic). Deep-Sea Research II 46, 2101-2146.

Held, I.M., Soden, B J., 2000. Water vapor feedback and global warming. Annual Review of Energy Environment 25, 441-475.

Hickey, B., Baker, E., Kachel, N., 1986. Suspended particle movement in and around Quinault submarine canyon. Marine Geology 71, 35-83.

Honjo, S., Manganini, S.J., Cole, J.J., 1982. Sedimentation of biogenic matter in the deep ocean. Deep-Sea Research Part A: Oceanographic Research Papers 29, 609-625.

Honjo, S., 1996. Fluxes of particles to the interior of the open oceans. Particle Fluxes in the Ocean- John Wiley and Sons Ltd., New York, 91-154.

Hung, J.-J., Lin, C.-S., Chung, Y.-C., Hung, G.-W., Liu, W. S., 2003. Lateral fluxes of biogenic particles through the Mien-Hua canyon in the southern East China Sea slope. Continental Shelf Research 23, 935-955.

Iorga, M.C., Lozier, M.S., 1999a. Signatures of the Mediterranean outflow from a North Atlantic climatology: 1. Salinity and density fields. Journal of Geophysical Research 104, 25985-26009.

Iorga, M.C., Lozier, M.S., 1999b. Signatures of the Mediterranean outflow from a North Atlantic climatology: 2. Diagnostic velocity fields. Journal of Geophysical Research: Oceans 104, 26011-26029.

Kalnay, E., Kanamitsu, M., Kistler, R., Collins, W., Deaven, D., Gandin, L., Iredell, M., Saha, S., White, G., Woollen, J., Zhu, Y., Chelliah, M., Ebisuzaki, W., Higgins, W., Janowiak, J.E., Mo, K.C., Ropelewski, C., Wang, J., Leetmaa, A., Reynolds, R.W., Jenne, R., Joseph, D., 1996. The NCEP/NCAR 40-year reanalysis project. Bulletin of the American Meteorological Society 77, 437-471.

Kearey, P., Klepeis, K.A., Vine, F.J., 2009. Global tectonics. Wiley-Blackwell, Chichester, Regne Unit, 482 pp.

Kennedy MJ, Pevear DR, Hill RJ, 2002. Mineral surface control of organic carbon in black shale. Science 295, 657-660.

Kiehl J.T., Trenberth K.E., 1997. Earth's Annual Global Mean Energy Budget. Bulletin of the American Meteorological Society. American Meteorological Society 78, 197-208.

Klaas, C., Archer D.E., 2002. Association of sinking organic matter with various types of mineral ballast in the deep sea: Implications for the rain ratio. Global Biogeochemical Cycles 16, 1116.

Kump L.R., 1989. Chemical stability of the atmosphere and ocean. Global and Planetary Change 1, 123-36.

L'Hévéder, B., Li, L., Sevault, F., Somot, S., 2013. Interannual variability of deep convection in the Northwestern Mediterranean simulated with a coupled AORCM. Climate Dynamics. 41, 937-960.

Lacombe, H., Tchernia, P., 1972. Caractères hydrologiques et circulation des eaux en Méditerranée. The Mediterranean Sea: A Natural Sedimentation Laboratory, Dowden Hutchinson and Ross, Stroudsburg, 25-36.

Lacombe, H., Tchernia, P., Gamberoni, L., 1985. Variable Bottom Water in the Western Mediterranean Basin. Progress in Oceanography 14, 319-338.

Lastras, G., Canals, M., Urgeles, R., Amblas, D., Ivanov, M., Droz, L., Dennielou, B., Fabrés, J., Schoolmeester, T., Akhmetzhanov, A., Orange, D., García-García, A., 2007. A walk down the Cap de Creus canyon, northwestern Mediterranean Sea: Recent processes inferred from morphology and sediment bedforms. Marine Geology 246, 176-192.

Lastras, G., Canals, M., Amblas, D., Lavoie, C., Church, I., De Mol, B., Duran, R., Calafat, A.M., Hughes-Clarke, J.E., Smith, C., Heussner, S., Euroleón cruise shipboard party, 2011. Understanding sediment dynamics of two large submarine

valleys from seafloor data: Blanes and La Fonera canyons, northwestern Mediterranean Sea. Marine Geology 280, 20-39.

Lastras, G., Canals, M., Amblas, D., Calafat, A.M., Durán, R., Muñoz, A., Pedrosa-Pàmies, R., Sanchez-Vidal, A., Rayo, X., Rumin, A., Tubau, X., Veres, O., 2012. The Avilés submarine canyon drainage system, northern Iberian margin. The Deep-Sea and Sub-Seafloor Frontiers Conf. 11–14 March, Spain, Abstract, volume P085.

Lavín, A., Valdés, L., Sánchez, F., Abaunza, P., Forest, A., Boucher, J., Lazure, P., Jegou, A.M., 2006. The Bay of Biscay: the encountering of the Ocean and the Shelf. The Sea 14, Part B. Harvard University Press, Cambridge, 935–1002.

Llope, M., Anadón, R., Viesca, L., Quevedo, M., González-Quirós, R., Stenseth, N.C., 2006. Hydrography of the southern Bay of Biscay shelf-break region: Integrating the multiscale physical variability over the period 1993-2003. Journal of Geophysical Research 111, C09021.

Llope, M., Anadón, R., Sostres, J.Á., Viesca, L., 2007. Nutrients dynamics in the southern Bay of Biscay (19932003): Winter supply, stoichiometry, long-term trends, and their effects on the phytoplankton community. Journal of Geophysical Research 112, C07029.

López-Jurado, J.L., González-Pola, C., Vélez-Belchi, P., 2005. Observation of an abrupt disruption of the long-term warming trend at the Balearic Sea, western Mediterranean Sea, in summer 2005. Geophysical Research Letters 32, L24606.

Margalef, R., 1978. Life-forms of phytoplankton as survival alternatives in an unstable environment. Oceanologica Acta 1, 493-509.

Martin, J.H., Knauer, G.A., Karl, D.M., Broenkow, W.W., 1987. VERTEX: carbon cycling in the northeast Pacific. Deep-Sea Research Part A: Oceanographic Research Papers 34, 267-285.

Martín, J., Palanques, A., Vitorino, J., Oliveira, A., de Stigter, H.C., 2011. Near-bottom particulate matter dynamics in the Nazaré submarine canyon under calm and stormy conditions. Deep-Sea Research Part II: Topical Studies in Oceanography 58, 2388-2400.

Martín, J., Durrieu de Madron, X., Puig, P., Bourrin, F., Palanques, A., Houpert, L., Higueras, M., Sanchez-Vidal, A., Calafat, A. M., Canals, M., Heussner, S., 2013. Sediment transport along the Cap de Creus Canyon flank during a mild, wet winter, Biogeosciences 10, 2013, 3221-3239.

MEDOC Group, 1970. Observation of formation of deep water in the Mediterranean Sea, 1969. Nature 227, 1037-1040.

Mellor, G.L., 1996. Introduction to Physical Oceanography. Princeton University, New Jersey, 260 pp.

Mertens, C., Schott, F., 1998. Interannual variability of deep-water formation in the Northwestern Mediterranean. Journal of Physical Oceanography 28, 1410-1424.

Middleton, G.V., Hampton, M.A., 1973. Part I. Sediment gravity flows: Mechanics of Flow and Deposition. In Turbidites and Deep Water Sedimentation, Soc. Econ. Pal. Miner., Pacific Section Short Course Lecture Notes, 1-38.

Millot, C., 1999. Circulation in the Western Mediterranean Sea. Journal of Marine Systems 20, 423-442.

Millot, C., Taupier-Letage, I., 2005. Circulation in the Mediterranean Sea. Handbook of Environmental Chemistry 5/K, 29-66.

Monaco, A., Courp, T., Heussner, S., Carbonne, J., Fowler, S.W., Deniaux, B., 1990. Seasonality and composition of particulate fluxes during ECOMARGE-I, western Gulf of Lions. Continental Shelf Research 10, 959-987.

Morgenstern, N.R., 1967. Submarine slumping and the initiation of turbidity currents. In A.F. Richards (Ed.): Marine geotechnique. University of Illinois Press, Urbana, Estats Units d'Amèrica, 189-220.

Mortlock, R.A., Froelich, P.N., 1989. A simple method for the rapid determination of biogenic opal in pelagic marine sediments. Deep-Sea Research Part A: Oceanographic Research Papers 36, 1415-1426.

Mulder, T., Zaragosi, S., Garlan, T., Mavel, J., Cremer, M., Sottolichio, A., Sénéchal, N., Schmidt, S., 2012. Present deep-submarine canyons activity in the Bay of Biscay (NE Atlantic). Marine Geology 295-298, 113-127.

Navarro-Pérez, E., Barton, E. D., 2001. Seasonal and interannual variability of the Canary Current, Scientia Marina 65, 205-213.

Nieuwenhuize, J., Maas, Y.E.M., Middelburg, J.J., 1994. Rapid analysis of organic carbon and nitrogen in particulate materials. Marine Chemistry 45, 217-224.

Ohman, M.D., K. Barbeau, P.J.S. Franks, R. Goericke, M.R. Landry, and A.J. Miller. 2013. Ecological transitions in a coastal upwelling ecosystem. Oceanography 26, 210-219.

Olbers, D. J., Willebrand, J., Eden, C., 2012. Ocean Dynamics, Springer, Berlin, 704 pp.

Orvik, K.A., Niiler, P., 2002. Major pathways of Atlantic water in the northern North Atlantic and Nordic Seas toward Arctic. Geophysical Research Letters 29, 1896-1900.

Paillet, J., Mercier, H., 1997. An inverse model of the eastern North Atlantic general circulation and thermocline ventilation. Deep-Sea Research Part I: Oceanographic Research Papers 44, 1293-1328.

Palanques, A., El Khatab, M., Puig, P., Masqué, P., Sánchez-Cabeza, J.A., Isla, E., 2005. Downward particle fluxes in the Guadiaro submarine canyon depositional system (north-western Alboran Sea), a river flood dominated system. Marine Geology 220, 23-40.

Palanques, A., Durrieu de Madron, X., Puig, P., Fabrés, J., Guillén, J., Calafat, A., Canals, M., Heussner, S., Bonnin, J., 2006. Suspended sediment fluxes and transport processes in the Gulf of Lions submarine canyons. The role of storms and dense water cascading. Marine Geology 234, 43-61.

Palanques, A., Puig, P., Latasa, M., Scharek, R., 2009. Deep sediment transport induced by storms and dense shelf-water cascading in the northwestern

Mediterranean basin. Deep-Sea Research Part I: Oceanographic Research Papers 56, 425-434.

Pasqual, C., Lee, C., Goñi, M., Tesi, T., Sanchez-Vidal, A., Calafat, A., Canals, M., Heussner, S., 2011. Use of organic biomarkers to trace the transport of marine and terrigenous organic matter through the southwestern canyons of the Gulf of Lion. Marine Chemistry 126, 1-12.

Pelegrí, J.L., Marrero-Díaz, A., Ratsimandresy, A.W., Antoranz, A., Cisneros-Aguirre, J., Gordo, C., Grisolía, D., Hernández-Guerra, A., Láiz, I., Martínez, A., Parrilla, G., Pérez-Rodríguez, P., Rodríguez-Santana, A., Sangrà, P., 2005. Hydrographic cruises off northwest Africa: the Canary Current and the Cape Ghir filament. Journal of Marine Systems 54, 39-63.

Pingree, R.D., Le Cann, B., 1992. Anticyclonic eddy X91 in the southern Bay of Biscay, May 1991 to February 1992. Journal of Geophysical Research - Oceans 97, 14353-14367.

Pollard, R.T., Pu, S., 1985. Structure and circulation of the Upper Atlantic Ocean northeast of the Azores. Progress in Oceanography 14, 443-462.

Pollard, R.T., Griffiths, M.J., Cunningham, S.A., Read, J.F., Pérez, F.F., Ríos, A.F., 1996. Vivaldi 1991 a study of the formation, circulation and ventilation of Eastern North Atlantic Central Water. Progress in Oceanography 37, 167-192.

Prego, R., Dale, A.W., deCastro, M., Gomez-Gesteira, M., Taboada, J.J., Montero, P., Villareal, M.R., Pérez-Villar, V., 2001. Hydrography of the Pontevedra Ria: Intra-annual spatial and temporal variability in a Galician coastal system (NW Spain). Journal of Geophysical Research 106, 19845-19857.

Puig, P., Palanques, A., 1998. Temporal variability and composition of settling particle fluxes on the Barcelona continental margin (Northwestern Mediterranean). Journal of Marine Research 56, 639-654.

Puig, P., Palanques, A., Orange, D.L., Lastras, G., Canals, M., 2008. Dense shelf wáter cascades and sedimentary furrow formation in the Cap de Creus Canyon, northwestern Mediterranean Sea. Continental Shelf Research 28, 2017-2030.

Puig, P., Durrieu de Madron, X., Salat, J., Schroeder, K., Martín, J., Karageorgis, A.P., Palanques, A., Roullier, F., Lopez-Jurado, J.L., Emelianov, M., Moutin, T., Houpert L., 2013. Thick bottom nepheloid layers in the western Mediterranean generated by deep dense shelf wáter cascading. Progress in Oceanography 111, 1-23.

Puillat, I., Lazure, P., Jégou, A.M., Lampert, L., Miller, P.I., 2004. Hydrographical variability on the French continental shelf in the Bay of Biscay, during the 1990s. Continental Shelf Research 24, 1143-1163.

Pusceddu, A., Mea, M., Gambi, C., Bianchelli, S., Canals, M., Sanchez-Vidal, A., Calafat, A., Heussner, S., Durrieu de Madron, X., Avril, J., Thomsen, L., Garcìa, R., Danovaro, R., 2010. Ecosystem effects of dense water formation on deep Mediterranean Sea ecosystems: an overview. Advances in Oceanography and Limnology 1, 67-83.

Ribó, M., Puig, P., Palanques, A., Lo Iacono, C., 2011. Dense shelf water cascades in the Cap de Creus and Palamós submarine canyons during winters 2007 and 2008. Marine Geology 284, 175188.

Salat, J., Font, J., 1987. Water mass structure near and offshore the Catalan coast during the winter of 1982 and 1983. Annales Geophysicae 5, 49-54.

Salvadó, J.A., Grimalt, J.O., López, J.F., Palanques, A., Heussner, S., Pasqual, C., Sanchez-Vidal, A, Canals, M., 2012a. The role of dense shelf water cascading in the transfer of organochlorine compounds to open marine waters. Environmental Science & Technology 46, 2624-2632.

Salvadó, J.A., Grimalt, J.O., López, J.F., Durrieu de Madron, X., Heussner, S., Canals, M., 2012b. Transformation of PBDE mixtures during sediment transport and resuspension in marine environments (Gulf of Lion, NW Mediterranean Sea). Environmental Pollution 168, 87-95.

Salvadó, J.A., Grimalt, J.O., López, J.F., Durrieu de Madron, X., Pasqual, C., Canals, M., 2013. Distribution of organochlorine compounds in superficial sediments from the Gulf of Lion, northwestern Mediterranean Sea. Progress in Oceanography 118, 235-248.

Sammari, C., Millot, C., Prieur, L., 1995. Aspects of the seasonal and mesoscale variabilities of the Northern Current in the western Mediterranean Sea inferred from the PROLIG-2 and PROS-6 experiments. Deep-Sea Research Part I: Oceanographic Research Papers 42, 893-917.

Sanchez-Vidal, A., Pascual, C., Kerhervé, P.A., Calafat, A., Heussner, S., Palanques, A., Durrieu de Madron, X., Canals, M., Puig. P., 2008. Impact of dense shelf water cascading on the transfer of organic matter to the deep Western Mediterranean Basin. Geophysical Research Letters 35, L05605.

Sanchez-Vidal, A., Canals, M., Calafat A.M., Lastras, G., Pedrosa-Pàmies, R., Menéndez, M., Medina, R., Company, J.B., Hereu, B., Romero, J., Alcoverro T., 2012. Impacts on the Deep-Sea Ecosystem by a Severe Coastal Storm. PLoS ONE 7(1), e30395.

Satterberg, J., Arnarson, T.S., Lessard, E.J., Keil, R.G., 2003. Sorption of organic matter from four phytoplankton species to montmorillonite, chlorite and kaolinite in seawater. Marine Chemistry 81, 11-18.

Schroeder, K., Ribotti, A., Borghini, M., Sorgente, R., Perilli, A., Gasparini, G.P., 2008. An extensive Western Mediterranean deep water renewal between 2004 and 2006. Geophysical Research Letters 35, L18605.

Schroeder, K., Josey, S.A., Herrmann, M., Grignon, L., Gasparini, G.P., Bryden, H.L., 2010. Abrupt warming and salting of the Western Mediterranean Deep Water after 2005: Atmospheric forcings and lateral advection. Journal of Geophysical Research 115, 1-18.

Segar D.A., 1998. Introduction to ocean sciences. Wadsworth Publishing xxiii, BelmontCA, USA, 497, 489 pp.

Seibold, E., Berger, W.H., 1993. The Sea Floor: An Introduction to Marine Geology (2nd Ed.). Springer Verlag, Berlin, 356 pp.

Severin, T., Conan, P., Durrieu de Madron, X., Houpert, L., Oliver, M.J., Oriol, L., Caparros, J., Ghiglione, J.F., Pujo-Pay, M., 2014. Impact of open-ocean convection

on nutrients, phytoplankton biomass and activity. Deep-Sea Research Part I: Oceanographic Research Papers 94, 62-71.

Shanmugam, G., 2002. Ten turbidite myths. Earth-Science Reviews 58, 311341.

Smith, R.O., Bryden, H.L., Stansfield, K., 2008. Observations of new western Mediterranean deep water formation using Argo floats 2004-2006, Ocean Science 4, 133-149.

Somavilla, R., González-Pola, C., Rodríguez, C., Josey, S.A., Sánchez, R.F., Lavín, A., 2009. Large changes in the hydrographic structure of the Bay of Biscay after the extreme mixing of winter 2005. Journal of Geophysical Research 114, 1-14.

Somavilla, R., González-Pola, C., Ruiz-Villarreal, M., Montero, A.L., Lavín, A., 2011. Mixed layer depth (MLD) variability in the southern Bay of Biscay. Deepening of winter MLDs concurrent with generalized upper water warming trends?. Ocean Dynamics 61, 1215-1235.

Somot, S., Houpert, L., Sevault, F., Testor, P., Bosse, A., Taupier-Letage, I., Bouin, M.-N., Waldman, R., Cassou, C., Sánchez-Gómez, E., Durrieu de Madron, X., Adloff, F., Nabat, P., Herrmann, M., 2016. Characterizing, modelling and understanding the climate variability of the deep water formation in the North-Western Mediterranean Sea. Climate Dynamics, 1-32.

Stewart, R.H., 2008. Introduction to Physical Oceanography. Texas A&M University, 345 pp.

Stommel, H., 1958. The Gulf Stream, A Physical and Dynamical Description. University of California Press, Berkley i Los Angeles, Estats Units d'Amèrica, 202 pp.

Syvitski, J.P.M., Vörösmarty, C.J., Kettner, A.J., Green, P., 2005. Impact of humans on the flux of terrestrial sediment to the global coastal ocean. Science 308, 376-380.

Talling, P.J., Masson, D.G., Sumner, E.J., Malgesini, G., 2012. Subaqueous sediment density flows: Depositional processes and deposit types. Sedimentology 59, 1937-2003.

Tarazona J, Arntz W., 2001. The Peruvian Coastal Upwelling System. Coastal Marine Ecosystems of Latin America. Ecological Studies 144, Springer, Berlin, 229-244.

Tesi, T., Puig, P., Palanques, A., Goñi, M.A., 2010. Lateral advection of organic matter in cascading-dominated submarine canyons. Progress in Oceanography 84, 185-203.

Thompson, D.W.J., Wallace, J.M., 1998. The Arctic oscillation signature in the wintertime geopotential height and temperature fields. Geophysical Research Letters 25, 1297.

Tyler, P., Amaro, T., Arzola, R., Cunha, M.R., de Stigter, H., Gooday, A., Huvenne, V., Ingels, J., Kiriakoulakis, K., Lastras, G., Masson, D., Oliveira, A., Pattenden, A., Vanreusel, A., Van Weering, T., Vitorino, J., Witte, U., Wolff, G., 2009. Europe's grand canyon: Nazaré submarine canyon. Oceanography 22, 46-57.

Ulses, C., Estournel, C., Bonnin, J., Durrieu de Madron, X., Marsaleix, P., 2008. Impact of storms and dense water cascading on shelf-slope exchanges in the Gulf of Lion (NW Mediterranean). Journal of Geophysical Research 113, 1-18.

Valdés, L., Lavín, A., Fernández de Puelles, M.L, Varela, M., Anadón, R., Miranda, A., Camiñas, J., Mas, J., 2002. Spanish Ocean Observation System: IEO Core Project: Studies on time series of oceanographic data, in: Operational Oceanography: Implementation at the European and Regional Scales, Elsevier, Nova York, pp. 99-105.

Vallis, G.K., 2006. Atmospheric and oceanic fluid dynamics: fundamentals and large-scale circulation. Cambridge University Press, Regne Unit, 745 pp.

van Aken, H.M., 2000a. The hydrography of the mid-latitude Northeast Atlantic Ocean. I: the deep water masses. Deep-Sea Research Part I: Oceanographic Research Papers 47, 757-788.

van Aken, H.M., 2000b. The hydrography of the mid-latitude Northeast Atlantic Ocean. II: the intermediate water masses. Deep-Sea Research Part I: Oceanographic Research Papers 47, 789-824.

van Aken, H.M., 2001. The hydrography of the mid-latitude Northeast Atlantic Ocean - Part III: the subducted thermocline water mass. Deep-Sea Research Part I: Oceanographic Research Papers 48, 237-267.

Wallace, J.M., Gutzier, D.S., 1981. Teleconnections in the geopotential height field during the northern hemisphere winter. Monthly Weather Review 109, 784-812.

Walsh, I.D., Gardner, W.D., 1992. A comparison of aggregate profiles with sediment trap fluxes. Deep-Sea Research Part A: Oceanographic Research Papers 39, 1817-1834.

Zeebe, R.E., 2012. History of Seawater Carbonate Chemistry, Atmospheric CO2, and Ocean Acidification. Annual Review of Earth and Planetary Sciences 40, 141-165.

Annex

Biogeosciences, 10, 3493–3505, 2013
www.biogeosciences.net/10/3493/2013/
doi:10.5194/bg-10-3493-2013

Biogeosciences Open Access

External forcings, oceanographic processes and particle flux dynamics in Cap de Creus submarine canyon, NW Mediterranean Sea

A. Rumín-Caparrós[1], A. Sanchez-Vidal[1], A. Calafat[1], M. Canals[1], J. Martín[2], P. Puig[2], and R. Pedrosa-Pàmies[1]

[1]GRC Geociències Marines, Dept. d'Estratigrafia, Paleontologia i Geociències Marines, Universitat de Barcelona, 08028 Barcelona, Spain
[2]Institut de Ciències del Mar (CSIC), Passeig Marítim de la Barceloneta 37–49, 08003, Barcelona, Spain

Correspondence to: A. Sanchez-Vidal (anna.sanchez@ub.edu)

Received: 29 November 2012 – Published in Biogeosciences Discuss.: 18 December 2012
Revised: 12 March 2013 – Accepted: 23 April 2013 – Published: 3 June 2013

Abstract. Particle fluxes (including major components and grain size), and oceanographic parameters (near-bottom water temperature, current speed and suspended sediment concentration) were measured along the Cap de Creus submarine canyon in the Gulf of Lions (GoL; NW Mediterranean Sea) during two consecutive winter-spring periods (2009–2010 and 2010–2011). The comparison of data obtained with the measurements of meteorological and hydrological parameters (wind speed, turbulent heat flux, river discharge) have shown the important role of atmospheric forcings in transporting particulate matter through the submarine canyon and towards the deep sea.

Indeed, atmospheric forcing during 2009–2010 and 2010–2011 winter months showed differences in both intensity and persistence that led to distinct oceanographic responses. Persistent dry northern winds caused strong heat losses ($14.2 \times 10^3\,W\,m^{-2}$) in winter 2009–2010 that triggered a pronounced sea surface cooling compared to winter 2010–2011 ($1.6 \times 10^3\,W\,m^{-2}$ lower). As a consequence, a large volume of dense shelf water formed in winter 2009–2010, which cascaded at high speed (up to $\sim 1\,m\,s^{-1}$) down Cap de Creus Canyon as measured by a current-meter in the head of the canyon. The lower heat losses recorded in winter 2010–2011, together with an increased river discharge, resulted in lowered density waters over the shelf, thus preventing the formation and downslope transport of dense shelf water.

High total mass fluxes (up to $84.9\,g\,m^{-2}\,d^{-1}$) recorded in winter-spring 2009–2010 indicate that dense shelf water cascading resuspended and transported sediments at least down to the middle canyon. Sediment fluxes were lower ($28.9\,g\,m^{-2}\,d^{-1}$) under the quieter conditions of winter 2010–2011. The dominance of the lithogenic fraction in mass fluxes during the two winter-spring periods points to a resuspension origin for most of the particles transported down canyon. The variability in organic matter and opal contents relates to seasonally controlled inputs associated with the plankton spring bloom during March and April of both years.

1 Introduction

Atmospheric–ocean interactions play a key role in the modification of oceanographic processes. Shifts in wind regime and air temperature are among the most important forcing variables in the atmosphere, triggering modifications in thermohaline properties of water, and therefore, in the hydrographic configuration of the upper part of the water column. There are several mechanisms that can transport and mix these atmospheric-modified shallow waters with intermediate or even deep waters. For example, cooling, evaporation or freezing in the surface layer of shallow areas of the continental shelf trigger the formation of dense water that eventually spills over the shelf edge onto the continental slope (see Ivanov et al., 2004, for a review). This causes the transmission of the atmospheric signal from shallow to deep waters within a short time range.

In the Gulf of Lions (GoL) there are three major mechanisms by which superficial waters are modified and transported from the surface to deep sea regions.

The first is storm-induced downwelling. This is related to the occurrence of E–SE winds that cause increased wave height and shelf sediment resuspension. The excess of water and suspended sediment piled in the inner shelf of the GoL, together with the reinforcement of the coastal current, forces shelf waters to flow towards the southwest and sink mainly through the Cap de Creus Canyon (Palanques et al., 2008). Furthermore, E–SE winds transfer humid marine air towards the coastal relief, where the air is obstructed and results in orographic rainfall and an increase in river discharge. The delivery of riverine particles and the increased shelf sediment resuspension during E–SE storms augments the export of suspended sediments towards the deep sea (Palanques et al., 2006, 2008; Guillén et al., 2006; Sanchez-Vidal et al., 2012).

The second mechanism is dense shelf water cascading (DSWC). This is linked to cold, dry, and persistent N–NW winds that induce sea-atmosphere heat losses and mixing of shelf waters (Millot, 1990). As a result, shelf waters become dense and sink, overflowing the shelf edge, and cascade downslope (preferentially through submarine canyons) until they reach their equilibrium depth (Durrieu de Madron et al., 2005).

Both mechanisms (i.e., E–SE storms and DSWC) can occur separately or in parallel, and are responsible for the remobilization and transport of sediments to the deep sea (Canals et al., 2006; Heussner et al., 2006; Palanques et al., 2006, 2008; Puig et al., 2008) and the variability in the biogeochemical composition of settling particles (Sanchez-Vidal et al., 2009; Pasqual et al., 2010). The occurrence of these events represents an important source of food to the deep ecosystems and influences the ecology of its deep-sea populations, as described, for instance, by Company et al. (2008) and Pusceddu et al. (2010). Furthermore, these events contribute to the transport and dispersion of persistent organic pollutants in the marine continental GoL shelf and open seawaters (Salvadó et al., 2012).

The third mechanism is deep-intermediate convection (MEDOC Group, 1970), which is caused again by the occurrence of cold, dry, and persistent N–NW winds that induce a heat and buoyancy loss of offshore waters in the Gulf of Lions, the Ligurian Sea and the Catalan Sea (Schroeder et al., 2010). This leads to mixing at great depths and homogenization of the water column in open sea regions. Recent studies have also documented the potential of such atmospheric-driven phenomena to remobilize sediments at depths below 2000 m in the northwestern Mediterranean basin (Martín et al., 2010).

With the aim of investigating the relationship between atmospheric forcings and the oceanographic processes and near-bottom particle fluxes, two mooring lines were deployed during two consecutive winter-spring periods (2009–2010 and 2010–2011) in the Cap de Creus Canyon at 300 m and 1000 m water depths. After three decades of year-round continuous monitoring of hydrosedimentary processes in the western GoL, and after considering several studies from both in situ observations (e.g. Canals et al., 2006; Heussner et al., 2006; Palanques et al., 2008; Puig et al., 2008) and numerical modeling (e.g. Ulses et al., 2008a, b), it appears that the most dynamic period in terms of water, sediment and organic matter export are the winter and early spring months. This is the time when dense shelf water forms and cascades downslope, occasional eastern storms occur, and the most prominent yearly planktonic bloom takes place (Fabres et al., 2008; Pasqual et al., 2010). For these reasons, the experiment described here focuses on these months and combines atmospheric data (wind speed and direction, air temperature and heat fluxes) with measured physical parameters (near-bottom temperature and current speed) and particle fluxes (total mass and main components) to assess the atmospheric variables that govern sediment transport to the deep sea floor during these two winter-spring periods. The manuscript is structured as follows: in Sect. 2 the hydrological and oceanographic settings of study area are presented. Material and methods are presented in Sect. 3. Section 4 describes data on the external forcings during the studied period (atmospheric conditions, river discharge, wave height and chlorophyll *a* concentration), and particle flux and oceanographic data obtained with the sediment traps and the current meters. Section 5 compares all data obtained and discusses the role of atmospheric forcing in the transport of particulate matter through the Cap de Creus submarine canyon. Finally, Sect. 6 contains the main conclusions of the study.

2 Study area

The GoL is a river-dominated micro-tidal continental margin that extends from the Cap Croisette, in the northeastern corner of the GoL, to the Cap de Creus at its southwestern limit (Fig. 1). The main morphological characteristic of its sea floor is its crescent-shaped shelf and the numerous submarine canyons incising the slope and shelf-break. The sea surface circulation in the GoL is linked to the Northern Current (NC), which in the study area manifests itself as a geostrophic jet flowing cyclonically along the slope over the 1000–2000 isobaths (Millot, 1999). The NC is associated with a permanent shelf-slope density front which separates shelf fresh coastal waters, directly influenced by the discharge of the Rhône River, from open-sea waters. Seasonal variations of the structure and intensity of the NC have been observed, with the current being narrower, deeper and more intense during winter (Millot, 1999).

Fresh water inputs into the GoL are mainly from three different hydrographic basins: the Alps in the northern part of the GoL (Rhône River), the Massif Central mountains (Hérault and Orb) and the Pyrenees mountains (Agly, Aude,

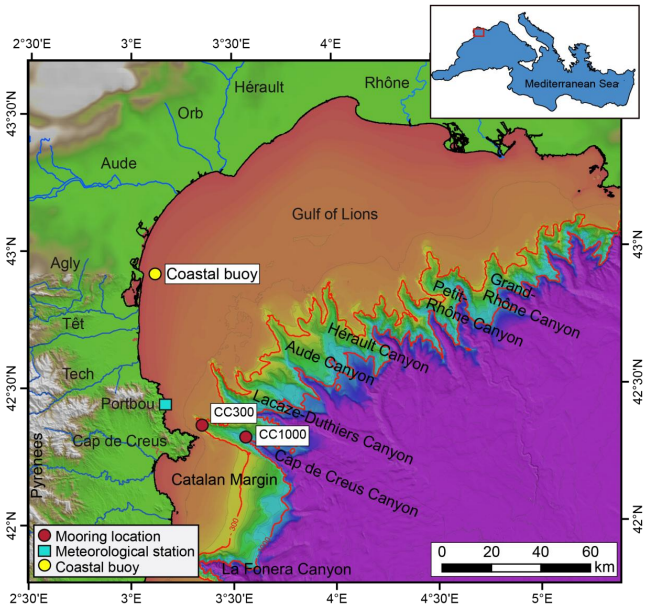

Fig. 1. Topo-bathymetric map of the Cap de Creus Canyon and neighboring areas: the northern Catalan margin at the South and the Gulf of Lions (northwestern Mediterranean) at the North. Locations of moorings (red dots), the meteorological station in Portbou (light blue square) and the Leucate coastal buoy (yellow dot) are shown. Top-right red square indicates where the heat fluxes and Chl *a* concentration maps have been obtained. Bathymetric data published by Canals et al. (2004).

Tech and Têt rivers). The Rhône River drains much of the water coming from the snowmelt of the Alps and its inputs represent more than the 90 % of the total annual freshwater inputs of the GoL (Bourrin et al., 2006). On the other hand, the Hérault and Orb rivers, and the Agly, Aude, Tech and Têt rivers, drain the Massif Central and the Pyrenees mountains respectively and, unlike the Rhône River, they are mainly controlled by a Mediterranean climatic regime, with short and intense flash flood events (Serrat et al., 2001).

The absence of significant tidal motions makes the combination of the atmospheric forcings (as the prevailing wind fields), the internal dynamics of the currents (and their interaction with the bathymetry) and the main river discharges the major source of variability in the oceanographic parameters of the GoL.

3 Material and methods

3.1 Sample collection and preparation

Two mooring lines were deployed from November 2009 to May 2010 and from December 2010 to June 2011 along the axis of the Cap de Creus submarine canyon (Fig. 1). Moorings were deployed at the canyon head and upper canyon course (as described by Lastras et al., 2007) at 300 m and 1000 m depth, respectively, and were defined as CC300 and CC1000 according to the deployment depth. Each moored line was equipped with a PPS3 Technicap sequential sampling sediment trap with a 0.125 m^2 collecting surface and a 2.5 height/diameter ratio in its cylindrical part (Heussner et al., 1990). Each trap was equipped with 12 receiving cups and was deployed at 25 m above the bottom with sampling intervals of 15 days. The collecting cups were filled with a buffered 5 % (v/v) formaldehyde solution in 0.45 μ filtered seawater. Each moored line included an Aanderaa RCM9 current meter deployed at 5 m above the bottom (CC300) and 23 m above the bottom (CC1000) equipped with a turbidimeter with a sampling interval of 30 min. Turbidity units, recorded in Formazin Turbidity Units (FTU), were transformed into suspended sediment concentrations (SSC) (mg L^{-1}) using the general calibration of Guillén et al. (2000). A technical failure of the current meter deployed at 1000 m in both years resulted in the complete absence of data at this water depth.

3.2 Analytical methods

After recovery, samples were processed according to a modified version of Heussner et al. (1990). Large swimming organisms were removed by wet sieving through a 1 mm nylon mesh, and organisms of less than 1 mm were handpicked under a microscope with fine tweezers. Samples were split into aliquots using a high-precision peristaltic pump robot and freeze-dried prior to chemical analysis.

Total carbon, organic carbon, and nitrogen contents were analyzed at "Centres Científics i Tecnològics" of the "Universitat de Barcelona" using an elemental organic analyzer Thermo EA Flash 1112 (Thermo Scientific, Milan, Italy) working in standard conditions recommended by the supplier of the instrument. For the organic carbon analysis, samples were first decarbonated with repeated additions of 100 μL of 25 % HCl until no effervescence was observed. Between each acidification step a 60 °C drying lapse of 8 h was carried out. Organic matter (OM) content was calculated as twice the organic carbon content. The inorganic carbon content was calculated as total carbon minus organic carbon and the carbonate content was calculated assuming that all the inorganic carbon is contained within calcium carbonate ($CaCO_3$), using the molecular mass ratio of 100/12.

Biogenic silica was analyzed using a two-step 2.5 h extraction with 0.5 M Na_2CO_3 separated by filtration of the leachates. Si and Al contents of both leachates were analyzed with an Inductive Coupled Plasma Atomic Emission Spectroscopy (ICP-AES), correcting the Si content of the first leachate by the Si/Al ratio of the second one. Once corrected, Si concentrations were transformed to opal by multiplying by a factor of 2.4 (Mortlock and Froelich, 1989).

The siliciclastic fraction was obtained by subtracting from the total mass the part corresponding to the major biogenic

components, assuming that the amount of siliciclastics (%) was = 100 – (% OM + % $CaCO_3$ + % Opal).

Grain size analyses were performed on a Coulter LS 230 Laser Particle Size Analyzer after organic matter oxidation with 10 % H_2O_2.

3.3 Meteorological, hydrological and oceanographic data

The exchange of energy between the atmosphere and the sea surface takes place through turbulent and radiative energy fluxes. Mathematically, the net air-sea heat exchange (Q_{net}) is the sum of four components:

$$Q_{net} = Q_{sh} + Q_{lh} + Q_{sw} + Q_{lw}, \quad (1)$$

where Q_{sh} is the sensible heat flux (SHF), Q_{lh} is the latent heat flux (LHF), Q_{sw} is the short-wave flux, and Q_{lw} is the long-wave flux. The sum of the sensible and latent heat fluxes ($Q_{sh}+Q_{lh}$, named turbulent heat flux) is linearly proportional to the wind speed and the air-sea temperature or humidity difference, while the sum of the short-wave and long-wave fluxes ($Q_{sw} + Q_{lw}$, named radiative flux) is function of air temperature, humidity, and cloudiness (Deser et al., 2010).

According to Josey (2003) and Schroeder et al. (2010), LHF, and to a lesser extent SHF, control anomalies in the winter net heat exchanges in the GoL. Both parameters are calculated as follows:

$$Q_{sh} = \rho c_p C_h u [T_s - (T_a + \gamma z)] \quad (2)$$

$$Q_{lh} = \rho L C_e u (q_s - q_a), \quad (3)$$

where ρ is the air density at observation level, c_p the specific heat capacity of the air at constant pressure, L is the latent heat of evaporation of water, C_h is the transfer coefficient for the SHF, u is the wind speed, T_s and T_a are the sea surface temperature and the surface air temperature corrected for the adiabatic lapse rate respectively, γz is the height at which the air temperature is measured, C_e is the transfer coefficient for the LHF, and q_s and q_a are the specific humidity at the sea surface and the atmospheric specific humidity at the reference level, respectively (Josey et al., 1999). LHF and SHF in the study area have been acquired as part of the activities of NASA's Science Mission Directorate, archived and distributed by the Goddard Earth Sciences (GES) Data and Information Services Center (DISC). The source used has been the Modern Era Retrospective-analysis for Research and Applications (MERRA), which uses the GEOS-5 Data Assimilation System with the adoption of a joint analysis with the National Centers for Environmental Prediction (NCEP) and of a set of physics packages for the atmospheric general circulation model. The study of the sea-atmosphere interactions has been gridded from 42.1° N to 43.4° N; and from 3.1° E to 5° E (Fig. 1).

Significant wave height (Hs) data have been obtained from the Leucate coastal buoy (Fig. 1), provided by the "Centre d'Études Techniques Maritimes Et Fluviales" ("Ministère de l'Ecologie, de l'Energie, du Développement durable et de la Mer", CANDHIS, France).

Wind speed and direction have been acquired from the automatic meteorological station in Portbou (see location in Fig. 1), maintained by "Servei Meteorològic de Catalunya" ("Generalitat de Catalunya").

Riverine discharges have been obtained from the "Laboratoire Hydraulique et Mesures" from the Compagnie Nationale du Rhône. The rivers considered are the Rhône River, because it is the main contributor of freshwater inputs of the GoL, and the Hérault, Orb, Agly, Aude, Tech and Têt rivers, in order to consider the freshwater inputs from most of the small rivers discharging into the GoL.

Data on concentration of the photosynthetic pigment Chlorophyll *a* (Chl *a*) have been obtained from the Goddard Earth Sciences (GES) Data and Information Services Center (DISC), using as a source the Moderate Resolution Imaging Spectoradiometer (MODIS) onboard the Aqua satellite. Chl *a* concentration is calculated using remotely sensed observations of the ocean surface with visible wavelength data. For our study, Chl *a* concentration has been gridded, including the mooring location and most of the GoL area (Fig. 1).

4 Results

4.1 External forcings

Winter 2009–2010 in the Cap de Creus area (northern Catalonia) was characterized by very low temperatures. Air temperatures were approximately 2 °C lower than the average climatic values registered in the climatic atlas of Catalonia (Martín-Vide and Raso Nadal, 2008). Several wind episodes with severe N–NW winds were recorded during late December 2009 (with speeds reaching up to 40 m s^{-1}), mid-January 2010 (up to 47 m s^{-1}), and mid-February 2010 (up to 44 m s^{-1}) (Fig. 2a). At the same time the cumulative turbulent heat losses (LHF and SHF) reached values of 14.2×10^3 W m^{-2} through the entire winter, from November 2009 until the end of March 2010.

The second winter studied was on average 1 °C warmer than the previous one. N–NW velocities reached speeds of up to 45 m s^{-1} during late December 2010, and up to 42 m s^{-1} in early February 2011 (Fig. 2a). Strong wind events were concentrated in the first half of the winter, so the cumulative turbulent heat loss for the whole winter (from November until the end of March), was 1.6×10^3 W m^{-2} lower than the previous winter.

Two very important increases in the discharge of rivers draining the Pyrenees and the Massif Central are well distinguished in October 2010 and in March 2011 (Fig. 2c, 3d). During both events the Hérault River reached 40 and 850 m^3 s^{-1}, the Orb River reached 91 and 899 m^3 s^{-1}, the Agly River reached 741 and 635 m^3 s^{-1}, the Aude

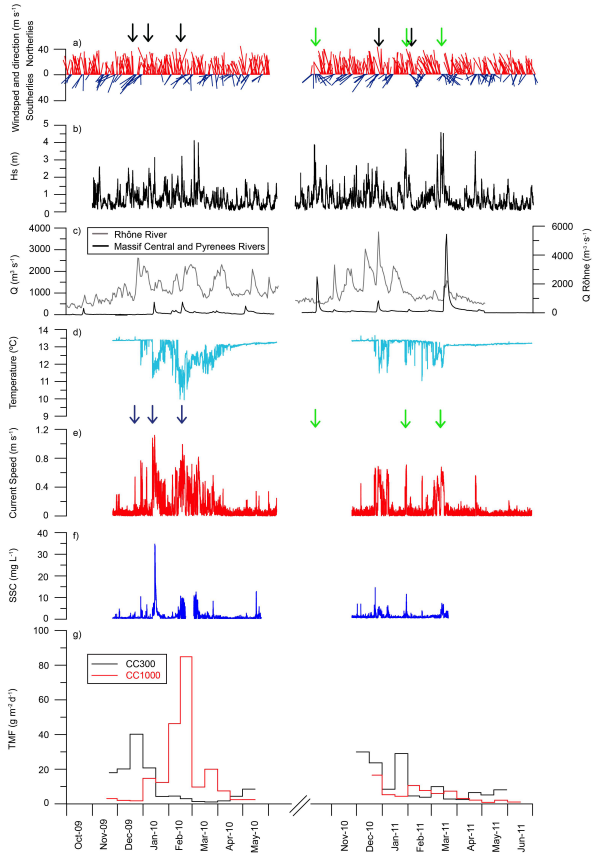

Fig. 2. **(a)** Temporal variability of northerly winds (red) and southerly winds (blue). Black arrows highlight severe N-NW wind episodes and green arrows the occurrence of eastern storms **(b)** Significant wave height (Hs); **(c)** Daily fluvial discharges of the Rhône River in grey and the sum of the main small rivers flowing to the Gulf of Lions (Hérault, Orb, Agly, Aude, Tech and Têt) in black; **(d)** near-bottom temperature recorded at CC300; **(e)** near-bottom current speed recorded at CC300, **(f)** suspended sediment concentration (SSC) as recorded by the currentmeter at 300 m of water depth; **(g)** total mass flux at 300 (black) and 1000 m (red) of water depth. Blue arrows show period of intense heat losses and DSWC event (as in Figs. 3 and 5), and green arrows the occurrence of eastern storms (as in Fig. 5).

River reached 399 and 561 $m^3 s^{-1}$, the Tech River 239 and 512 $m^3 s^{-1}$, and the Têt 245 and 366 $m^3 s^{-1}$, respectively. Considering that the Rhône river basin is not affected by the Mediterranean climate characterized by its limited rainfall regime (Ludwig et al., 2003), its basal discharge was always very high compared to the rest of the rivers, presenting a much more regular flow rate during the whole period of around 2,000 $m^3 s^{-1}$ (Figs. 2c, 3e). The higher water discharge in the whole time series was registered at the very end of December 2010, with 5,600 $m^3 s^{-1}$.

Maximum significant wave height (Hs) was recorded in March in both winters in the context of a reinforcement of easterly winds (Fig. 2a, b), in agreement with larger swell due to the longer fetch distance of E winds. During winter 2009–2010, the maximum Hs recorded was of 4 m, while during the next winter the maximum Hs was 4.6 m.

Chl *a* concentration images showed increased pigment concentrations during March, reflecting the well-known seasonal phytoplankton bloom in the region (e.g. Estrada et al., 2011) (Fig. 4).

4.2 Near-bottom current regime and downward particle fluxes

Time series of near-bottom water temperature, current speed, near-bottom suspended sediment concentration (SSC) at CC300, and downward total mass flux (TMF) at both CC300 and CC1000, are shown in Fig. 2d–g.

4.2.1 Winter 2009–2010

November 2009 was characterized by relatively stable oceanographic conditions at the CC300 station, with no major changes in near-bottom water temperature and current speeds below 0.29 $m s^{-1}$. At the very end of December 2009, a drop in near-bottom water temperature (to 11.98 °C) was recorded concomitantly with increased current speeds (0.77 $m s^{-1}$) and SSC (10.41 $mg L^{-1}$). This event lasted a couple of days. At the same time TMF reached 40.2 $g m^{-2} d^{-1}$ at CC300 while no significant increase was recorded at CC1000.

In mid-January 2010 near-bottom water temperature at CC300 decreased abruptly more than 2 °C (from 13.40 to 11.21 °C), and current speed and SSC increased up to 1.12 $m s^{-1}$ and 34.68 $mg L^{-1}$, respectively. The lower temperatures and high current speeds were maintained for approximately 16 days. Total mass flux (TMF) at CC300 reached only 20.1 $g m^{-2} d^{-1}$ and at CC1000 increased slightly up to 14.7 $g m^{-2} d^{-1}$ (Fig. 2g).

In February 2010 the longer event started, which lasted for one and a half months and was characterized by persistent low bottom water temperature (as low as 9.95 °C) and high velocities (up to 0.99 $m s^{-1}$). SSC also increased considerably but did not reach the levels of the previous month, being almost 4 times lower. While no variation in TMF was recorded at the CC300 station, TMF at CC1000 registered a sharp increase up to values of 84.9 $g m^{-2} d^{-1}$.

4.2.2 Winter 2010–2011

The second monitored winter presented smaller magnitude anomalies in near-bottom water temperature, current speed and SSC at the CC300 station. At the end of December 2010 water temperature dropped more than 1.5 °C (to 11.49 °C) and current speed increased up to 0.68 $m s^{-1}$ and SSC up to 14.57 $mg L^{-1}$. These anomalies lasted for 17 days. TMF values at the CC300 and CC1000 stations increased up to 23.7 $g m^{-2} d^{-1}$ and 16.6 $g m^{-2} d^{-1}$, respectively (Fig. 2g).

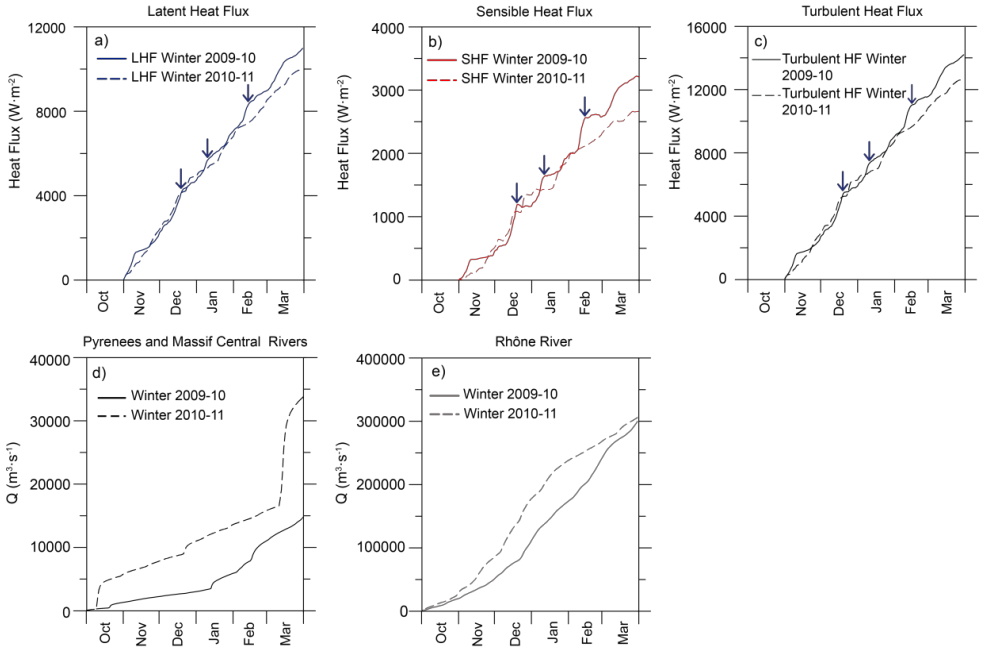

Fig. 3. (a) Cumulated Latent Heat Flux for winter-spring 2009–2010 (continuous line) and 2010–2011 (dashed line); **(b)** Cumulated Sensible Heat Flux for winter-spring 2009–2010 (continuous line) and 2010–2011 (dashed line); **(c)** Cumulated Turbulent Heat Flux for winter-spring 2009–2010 (continuous line) and 2010–2011 (dashed line); **(d)** Cumulated river discharge from the Hérault, Orb, Agly, Aude, Tech and Têt rivers for winters 2009–2010 (continuous line) and 2010–2011 (dashed line); **(e)** Cumulated river discharge from the Rhône river for winters 2009–2010 (continuous line) and 2010–2011 (dashed line). Blue arrows show period of intense heat losses (as in Figs. 2 and 5).

January and February 2011 were characterized by relatively stable conditions, except for a discrete (lasting less than 2 days) water temperature drop recorded concomitantly with increased current speeds (up to 0.71 m s^{-1}) recorded at the end of January 2011. At the same time, SSC peaked at 11.53 mg L^{-1} and TMF at CC300 reached values up to 28.9 g m^{-2} d^{-1}. No increased TMF was recorded at the CC1000 station.

In March 2011 slight temperature drops (to 11.07 °C), increased current speeds (0.68 m s^{-1}) and increased SSC (7.37 mg L^{-1}) were again recorded (Fig. 2g). TMF increased slightly at CC300 (up to 9.9 g m^{-2} d^{-1}) and after 15 days at CC1000 (up to 7.3 g m^{-2} d^{-1}) (Fig. 2g).

4.3 Main components of settling particles

The temporal variability of the main components (OM, $CaCO_3$, opal and siliciclastics) at the two stations during the winter-spring periods studied is shown in Fig. 5. As repeatedly observed in this region, the siliciclastic component is the main contributor to TMF at all stations and at all depths (Heussner et al., 2006; Pasqual et al., 2010), representing almost 70 % of the total flux. Furthermore, during the second monitored winter-spring 2010–2011, the siliciclastic relative abundance decreased with depth from CC300 to CC1000.

In general the OM relative abundance of TMF during both periods showed a clear temporal variability, displaying almost always higher concentrations at the CC300 station. During the first period maximum concentration values were recorded during the end of March 2010 at CC300 (up to 4.68 %) and during late April 2010 at CC1000 (up to 3.42 %). During the second monitored period, maximum peaks were reached in late February 2011 at CC300 (4.38 %) and late April 2011 in CC1000 (3.61 %).

$CaCO_3$ relative abundance during the first monitored winter-spring period peaked in late January and February 2010 in CC300 and late January 2010 in CC1000, and accounted for up to 30.49 % of the total flux. During the second period values were significantly lower at the CC300 station, increasing in March-April 2011 up to 28.23 and 30.54 % of the CC300 and CC1000 flux.

Opal represented always less than 4 % of the mass flux. During the first monitored winter-spring opal relative abundance increased in December 2009 (up to 1.99 %) and March–April 2010 (up to 2.01 %) at both stations. During the second period, the seasonal increase of opal was more evident, increasing in very late April 2011 up to values of 1.93 % at CC300, and 3.43 % at CC1000.

4.4 Grain size

During the two monitored periods, approximately 90 % of the particles were mainly silt-sized (between 4 and 63 μm)

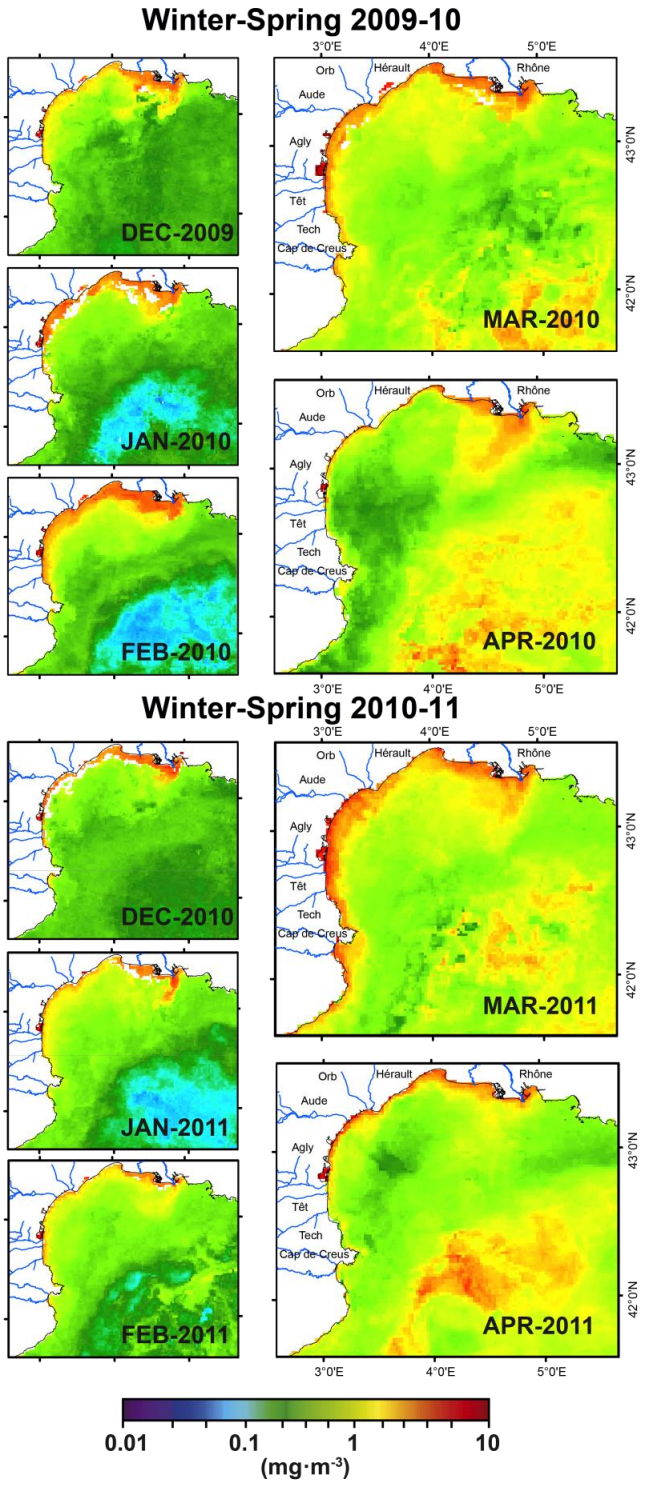

Fig. 4. Sequence of monthly mean Chlorophyll *a* concentration in the study area during both winter-spring periods.

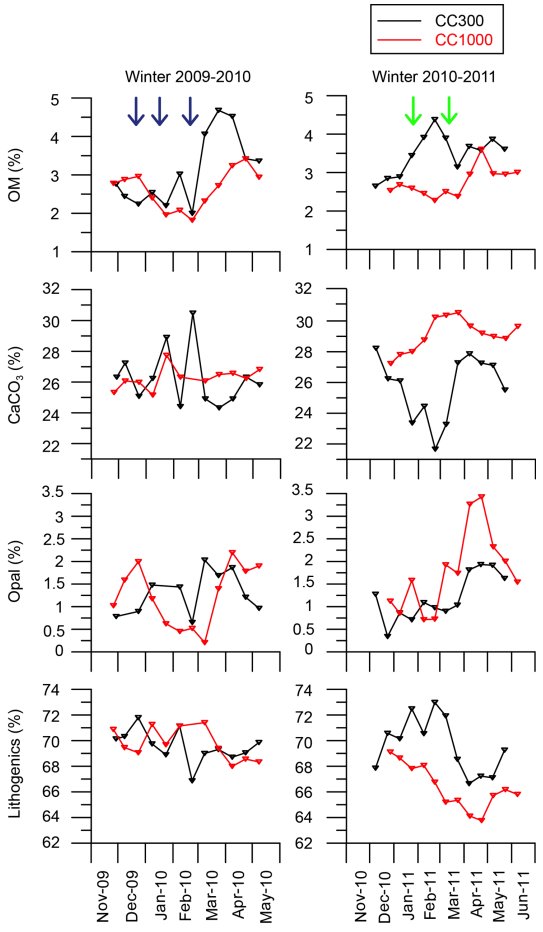

Fig. 5. Temporal variability of the main components of the settling particles ($CaCO_3$, Organic Mater (OM), opal and siliciclastics) of the two stations during the two winter-spring periods studied. Black line represents the CC300 station whereas the red line represents the CC1000. **(a)** Winter-spring 2009–2010. **(b)** Winter-spring 2010–2011. Blue arrows show periods of intense heat losses and DSWC event (as in Figs. 2 and 3), and green arrows show eastern storms events (as in Fig. 2).

whereas 10 % of the particles where clay-sized ($< 4\,\mu$m). A few samples included sand-sized particles ($> 63\,\mu$m).

The grain size distributions display many fluctuations (Fig. 6). During the first winter-spring, the low amount of mass obtained from the sediment cups at CC300 from mid-January to mid-April 2010 prevented grain size determination. However, the available data show coarsening of the sediments collected during the second half of December 2009 with respect to the samples collected at the beginning and at the end of the evaluated time series (very late November 2009 and early May 2010, respectively). Samples collected during February 2010 in CC1000 also displayed a clear coarsening with respect to the initial and final conditions (Fig. 6a).

During the second winter-spring, smaller changes in the grain size distribution of the sediments collected by the sediment traps were recorded. Nevertheless, the samples

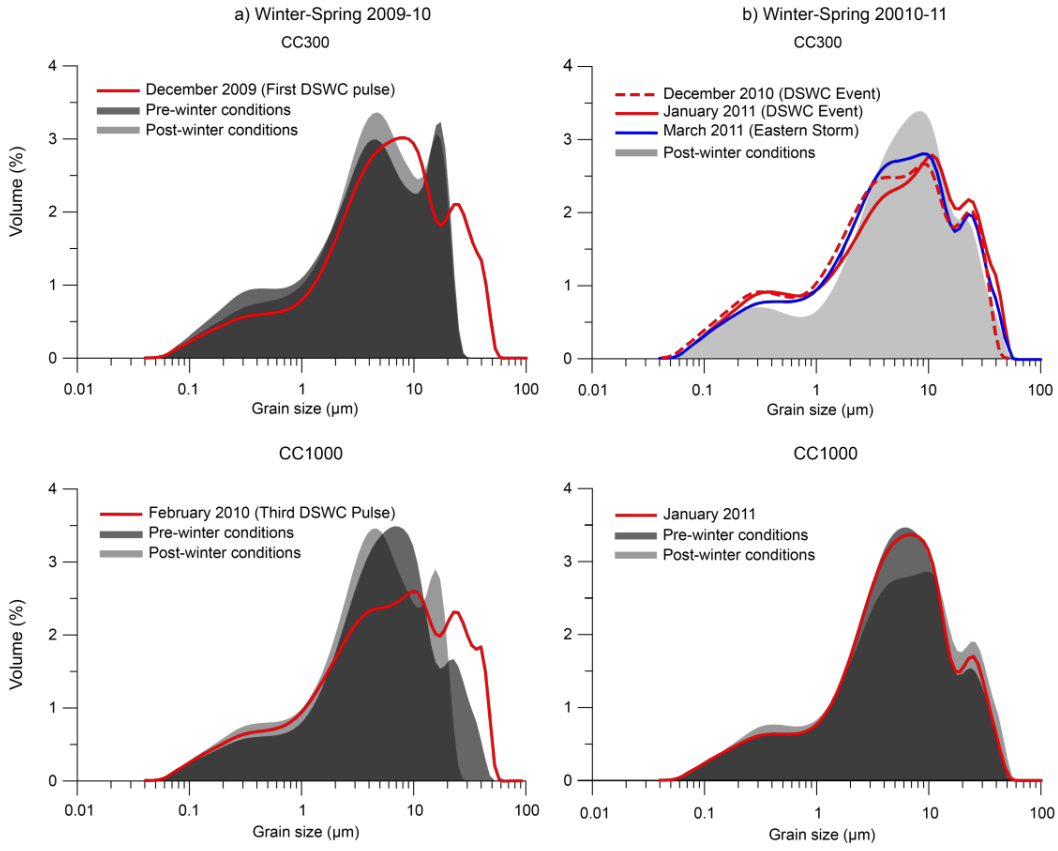

Fig. 6. Grain size distribution of sediment trap samples. Black represents the grain size distribution at the beginning of the winter (initial conditions) and gray the grain size distribution at the end of the winter (final conditions). Red and blue lines represent the grain size distribution during main transport events. **(a)** Grain size distribution at CC300 and CC1000 during winter 2009–2010. **(b)** Grain size distribution at CC300 (dashed line for December 2010 DSWC event and continuous line for January 2011 DSWC event) and CC1000 during winter 2010–2011.

collected at CC300 during mid–late January 2011 and during the first half of March 2011 displayed a clear coarsening with respect to the initial and final conditions (end of December 2010 and first half of June 2011, respectively) (Fig. 6b). No remarkable changes were recorded in CC1000 during the second winter-spring evaluated.

5 Discussion

5.1 Atmospheric forcing of particle fluxes in winter 2009–2010

Winter 2009–2010 was characterized by the occurrence of several wind storms that triggered important changes in the water column structure and the sediment transport downcanyon. The northern windstorms occurring in December 2009 resulted in strong sea–atmosphere heat losses in the studied area (Fig. 3a–c). Cumulated SHF increased 640 W m^{-2} in less than two weeks (Fig. 3b), which represents an average of sensible heat losses of 58 W m^{-2} per day. These values are higher than those reported by Schroeder et al. (2010) for "normal" winters in the nearby convection zone, where most extreme heat losses are believed to occur (42–43° N, 4–5° E). Consequently, at the end of December 2009 shelf waters lost temperature, became denser and sank, overflowing the shelf edge and cascading downslope through the Cap de Creus submarine canyon, as shown by the decrease in near-bottom water temperature at the upper canyon. This process, known as DSWC, has been recently studied in detail in several papers (e.g. Canals et al., 2006; Heussner et al., 2006; Palanques et al., 2006). The DSWC event started in December 2009, lasted for about 2 months and was formed by 3 main pulses of water.

The first DSWC pulse was recorded at the end of December 2009. This event increased down-canyon suspended sediment fluxes mainly by increasing the current speed up to 0.77 m s^{-1} and caused an increase in the TMF up to 40.2 g m^{-2} d^{-1} at CC300 (Fig. 2e, g). In addition, grain size distributions of the particles collected by the sediment trap display a clear coarsening during this pulse (Fig. 6a). This means that the cascading currents were strong enough

to resuspend and transport coarse particles in suspension from the shelf downwards to the basin. Nevertheless, currents were not strong enough to transport sediment deeper in the canyon, as suggested by the low TMF measured at CC1000. Overall, data suggest that the sediment eroded and transported by the dense water plume settled in somewhere between CC300 and CC1000.

From the end of December 2009 to mid-January 2010, several cold and dry northern windstorms with high wind speeds led to a continued period of heat losses. This sustained heat loss triggered a continued cooling of the surface waters and thus a loss of buoyancy. In consequence, DSWC was reactivated in mid-January, as confirmed by the decrease in the near-bottom water temperature and the sharp increase in the current speed and in the SSC at CC300. The strong intensification in current speed (up to $1.12\,m\,s^{-1}$) and in SSC (up to $34.68\,mg\,L^{-1}$) denoted a major escape of resuspendible fine sediments from the shelf and down the canyon. Furthermore, the TMF at both CC300 and CC1000 increased slightly, evidencing that, this time, cascading waters reached probably the middle canyon course. In addition, the coarsening of the samples collected during this event at CC1000 indicates that, effectively, the cascading waters flowed downcanyon, reaching depths of at least 1000 m.

The third DSWC pulse started February 2010. At this stage, the superficial waters of the GoL were probably completely unstratified as a result of the continued wind cooling and mixing processes that took place during the winter. Winter cumulated SHF in the beginning of February was higher than $520\,W\,m^{-2}$ (note the high slope of SHF in February 2010 Fig. 3b) and the cumulated turbulent heat losses were around $11 \times 10^3\,W\,m^{-2}$. This might have caused surface water temperature to decrease, resulting in pronounced buoyancy losses of the coastal waters of the GoL. This situation led shelf waters to cascade downslope continuously for a prolonged time period (from the beginning of February 2010 until the beginning of March 2010), as can be seen by the long and marked drop in near-bottom water temperature (of more than 3 °C) and the notable increase in the current speed at the upper canyon (Fig. 2d, e). However, this event resulted in a small increase in down-canyon suspended sediment fluxes at CC300. Guillén et al. (2006) suggested that the "memory" of the past events on the shelf plays a crucial role in sediment dynamics as the recurrence of the preceding storms reduces the availability of fresh shelf sediments that can be resuspended. This also suggests that those events in December 2009 and January 2010 cleaned erodible sediments in the upper canyon and thus cascading waters in February flowed without a significant suspended sediment transport to CC300 (Fig. 2g). However, cascading waters may have eroded part of the sediments trapped between the two moorings in the upper-middle canyon, thus triggering an increased arrival of particles, with the maximum fluxes recorded at the CC1000 station (Fig. 2g). This is also confirmed by the grain size distributions of particles settling during that event, which repeatedly show coarsening when compared to the pre- and post-winter conditions (Fig. 6a). Overall, the results demonstrate the multi-step sediment transport by cascading pulses, first from the shelf to the upper canyon, and then from the upper canyon to the middle canyon, as observed in winter 2006 by Pasqual et al. (2006) and Palanques et al. (2012). In addition, the arrival of resuspended particles through the southern flank of the canyon may have caused TMF to increase only at middle canyon depths and not at the canyon head (Canals et al., 2006; Martin et al., 2013). Even though with decreasing current speeds (and thus with decreasing capacity of eroding sediments), the DSWC pulse triggered another increase in TMF at the CC1000 station in the end of March 2010, at the very end of the cascading event.

5.2 Atmospheric forcing of particle fluxes in winter 2010–2011

An eastern windstorm with high E winds and Hs up to 3.9 m affected the Cap de Creus area in fall 2010. This episode was followed by increased river discharge in the rivers adjacent to the study area, which altogether reached $1{,}661\,m^3\,s^{-1}$ (Fig. 2c). As the mooring lines were not yet deployed, we cannot investigate the impact of this eastern storm on the sediment transport downcanyon.

The following months were characterized by the occurrence of cold and dry northern windstorms. Cumulative turbulent heat fluxes from the beginning of November 2010 to late December 2010 were about $400\,W\,m^{-2}$ higher than during the same months in the previous winter. Heat loss triggered a loss of buoyancy and the occurrence of DSWC along the submarine canyon. In fact, it seems that there is a certain heat loss threshold above which DSWC occurs, as can be seen when comparing the two winters evaluated (Fig 3a–b). During the first winter it was not until turbulent heat fluxes (Fig. 3c) reached values of about $6 \times 10^3\,W\,m^{-2}$ that the first DSWC event occurred. The same happened during winter 2010–2011 – the first dense shelf water pulse was recorded, as a near-bottom water temperature drop, when winter cumulative turbulent heat fluxes reached values of around $6 \times 10^3\,W\,m^{-2}$ (Fig. 3c).

The DSWC event of December 2010 lasted for 17 days and triggered increased current speeds. The consequences of this event were a rapid but discrete increase in the current speed, SSC and TMF in the canyon head (Fig. 2e–g). Furthermore, the newly formed water plume became dense enough to cascade along the canyon, reaching depths of at least 1000 m as the TMF of the CC1000 recorded values of approximately $16.6\,g\,m^{-2}\,d^{-1}$ (Fig. 2g).

Turbulent heat losses from the beginning of January until March 2011 were lower than the previous 2009–2010 winter. Furthermore, the increased river discharge recorded in the Rhône River throughout winter, together with the punctual discharge from the smaller rivers opening to the Gulf of Lions, suggest the presence of a large amount of light

freshwater in the shelf. This might have inhibited dense water formation through increased buoyancy of surface waters.

In late January 2011 a slight temperature drop indicates the arrival of dense shelf waters. The occurrence of a concomitant eastern storm with Hs of up to 3.6 m suggests that the eastern storm reactivated punctually DSWC, despite the freshwater inhibition. Indeed it is well known that eastern storms cause intense shelf sediment resuspension, which can decrease buoyancy and form a downcanyon flow (Palanques et al., 2006; Sanchez-Vidal et al., 2012). This is demonstrated by the increased current speed ($0.71\,m\,s^{-1}$), SSC ($11.02\,mg\,L^{-1}$) and TMF (up to $29.0\,g\,m^{-2}\,d^{-1}$) at the canyon head. The turbid flow might have stopped before reaching the CC1000 station as no significant TMF increase was recorded. The grain size of the samples collected during this event presented a clear coarsening at CC300 but not at CC1000 (Fig. 6b).

In mid-March 2011, another eastern storm occurred, with Hs of more than 4.5 m, which was accompanied by a significant increase in the Massif Central and Pyrenees rivers discharge (Figs. 2c, 3d). Increased current speeds (up to $0.68\,m\,s^{-1}$) and SSC (up to $7.37\,mg\,L^{-1}$) were recorded. The fact that flooding occurred several days after the main pulse of downcanyon sediment transport suggest again, that erosion from the adjacent shelf was the main source of particles introduced in the canyon during mid-March 2011 (Martín et al., 2013). The turbid flow did not penetrate into the canyon deeper than about 350 m. The coarsening of the grain size of the particles collected at CC300 suggest that near-bottom currents during this event where strong enough to resuspend and transport coarse particles in suspension from the shelf to the canyon head (Fig. 6b).

5.3 Variability in composition of the settling particles and Chl *a*

5.3.1 Principal variations in the composition of the settling particles of winter-spring 2009–2010

Winter 2009–2010 dense shelf water pulses caused TMF to increase and to be dominated by the siliciclastic fraction (more than 67 %) (Fig. 5). During December 2009, and January and February 2010, the composition of the settling particles was relatively constant, showing that DSWC pulses transported homogenized materials from the same origin (i.e. the shelf and upper slope) towards the basin (as reported before by Pasqual et al. (2010)). Furthermore, during these events, the non-siliciclastic fraction was close to the values reported by Heussner et al. (2006), with ∼ 20–30 % $CaCO_3$, 2–3 % OM, and opal was virtually absent. These values were also close to those reported by Roussiez et al. (2006) for the superficial sediments from the shelf and upper slope (31 % $CaCO_3$, 1-4 % OM and opal nearly absent or under detection limit).

In the end of the winter and beginning of spring, the changes in the composition of the settling particles responded to a seasonal control. The higher variability in the biological signal (i.e. OM and opal content) occurred in response to the biological spring bloom recorded during March and April 2010 (Fig. 4). The less severe hydrodynamic conditions (end of the major cascading pulse) also favored the reduction of the input of resuspended lithogenic particles.

The $CaCO_3$ relative abundance displayed an apparently random pattern with higher values in January and February 2010, which are not related to OM and opal peaks (Fig. 5). The resuspension and transport of carbonated shell remains from the shelf is the most plausible explanation, as suggested by Martín et al. (2006) in the nearby La Fonera submarine canyon (Fig. 1).

5.3.2 Composition variability of settling particles during winter-spring 2010–2011

In the context of a milder and wetter 2010–2011 winter-spring period, the high lithogenic fraction in settling particles suggests also a dominant resuspended origin, especially in the shallower station, which was the more affected by the main sediment transport events. However, primary production products (i.e. OM and opal) dilution due to increased lithogenic sediments resuspension was lower, most likely because of the weakened main transport events. This was also evident in the relative abundance of $CaCO_3$ and especially at the CC1000 station, which was impacted by less events than the preceding winter and spring. Nevertheless, at CC300 the $CaCO_3$ relative abundance decreased progressively until the end of February 2011. At the same time, an increase of OM and lithogenic contributions were recorded, which in absence of any primary production event suggests the arrival of OM-rich resuspended material. The occurrence of a weakened dense shelf water cascading may have triggered a selective winnowing of fine (and OC-rich, following Tesi et al., 2010 and Sanchez-Vidal et al., 2008) particles (Ferré et al., 2005; Bourrin et al., 2008) that sedimented in the head of the canyon. The development of the phytoplanktonic bloom in spring 2011 (Fig. 4) may have increased the contribution of $CaCO_3$, together with OM and opal to maximum levels (Fig. 5).

6 Conclusions

This study compares hydro-sedimentary processes and associated particle fluxes in the westernmost submarine canyon of the Gulf of Lions, at the outlet of the shelf and slope cyclonic circulation system of the area, during the winters and part of the springs of 2009–2010 and 2010–2011. During these periods, contrasting atmospheric forcings developed and led to unequal modifications of the thermohaline properties of the upper ocean layer.

A more pronounced ocean-to-atmosphere heat transfer (up to 14.2×10^3 W m^{-2}) occurred in winter 2009–2010, which triggered a stronger cooling of the water over the continental shelf, compared to winter 2010–2011. This situation resulted in an increase in the density of surface water, which sank and cascaded at higher velocities (up to 0.99 m s^{-1}) down the Cap de Creus canyon. The higher current speeds recorded during winter 2009–2010 caused higher erosion, resuspension and ultimately transport of sediment to the mid-canyon reach. In contrast, reduced heat losses were recorded (12.6×10^3 W m^{-2}) during winter 2010–2011, which, together with a high volume of cumulated freshwater over the shelf, inhibited the penetration of dense shelf water down to the middle canyon. A noticeable eastern storm that occurred during this winter-spring, resulted in peak near-bottom currents of 0.68 m s^{-1} at 300 m and the export of particles only down to the upper canyon reach.

The lithogenic fraction was dominant in the particle fluxes of the two winter-spring seasons, which point to a resuspension origin, despite the comparatively milder character of the 2010–2011 winter. The variability in OM and opal contents followed a seasonal pattern in response to the plankton spring bloom during March and April 2010 and 2011.

The $CaCO_3$ relative abundance also showed a noticeable variability both within each winter-spring and between the two winter-spring periods. Variability sources are, however, different. The apparently random pattern of $CaCO_3$ in 2009–2010 is attributed to the resuspension of relict carbonate shells during the multi-pulse, deep-penetrating DSWC of that winter. In contrast, the weakened transport events during winter-spring 2010–2011 triggered the resuspension of only fine (and OM-rich) particles. Furthermore, the lower advection of resuspended sediments favored an increase in the relative content of the biogenic components (OM, opal and $CaCO_3$) during the spring bloom.

These results confirm that DSWC plays a key role in governing the timing, composition and volumes of particle fluxes that are exported down Cap de Creus canyon, while eastern storms similar to the one recorded in winter-spring 2010–2011 can also contribute to enhance erosion, resuspension and the off-shelf transport of particles independently of the occurrence of DSWC.

Acknowledgements. This research has been supported by the EC-funded HERMIONE (FP7-ENV-2008-1-226354) and PERSEUS RTD projects (FP7 287600), and by the Spanish projects GRACCIE (CSD2007-00067) and DOS MARES (CTM2010-21810-C03-01). J. Martin was funded through a JAE-DOC contract within the Program "Junta Para la Ampliación de Estudios", granted by Consejo Superior de Investigaciones Científicas and co-financed by the European Social Fund. Generalitat de Catalunya is acknowledged for support to GRC Marine Geosciences through its Grups de Recerca Consolidats grant 2009 SGR 1305. We thank D. Amblas and the crew of the vessels *Lluerna* and *Felipe* for their dedication during mooring operations. We also thank M. Guart for helping with the laboratory work, X. Rayo for his technical assistance when using Geographic Information Systems, A. Micallef for improving the English, and two anonymous referees for their valuable comments.

Edited by: R. Danovaro

References

Bourrin, F. and Durrieu de Madron, X.: Contribution of the study of coastal rivers and associated prodeltas to sediment supply in north-western Mediterranean Sea (Gulf of Lions), Vie Milieu, 56, 307–314, 2006.

Bourrin, F., Durrieu de Madron, X., Heussner, S., and Estournel, C.: Impact of winter dense water formation on shelf sediment erosion (evidence from the Gulf of Lions, NW Mediterranean), Cont. Shelf Res., 28, 1984–1999, doi:10.1016/j.csr.2008.06.006, 2008.

Canals, M., Casamor, J. L., Urgeles, R., Farrán, M., Calafat, A. M., Amblas, D., Willmott, V., Estrada, F., Sánchez, A., Arnau, P., Frigola, J., and Colás, S.: Mapa del relleu submarí de Catalunya, 1:250 000; Institut Cartogràfic de Catalunya, Barcelona, Spain, 1 map, 2004.

Canals, M., Puig, P., Durrieu de Madron, X., Heussner, S., Palanques, A., and Fabres, J.: Flushing submarine canyons, Nature, 444, 354–357, doi:10.1038/nature05271, 2006.

Company, J. B., Puig, P., Sardà, F., Palanques, A., Latasa, M., and Scharek, R.: Climate influence on deep sea populations, PloS one, 3, e1431, doi:10.1371/journal.pone.0001431, 2008.

Deser, C., Alexander, M. A., Xie, S.-P., and Phillips, A. S.: Sea Surface Temperature Variability: Patterns and Mechanisms, Ann. Rev. Mar. Sci., 2, 115–143. doi:10.1146/annurev-marine-120408-151453, 2010.

Durrieu de Madron, X., Zervakis, V., Theocharis, A., and Georgopoulos, D.: Comments to "Cascades of dense water around the world ocean", Progr. Oceanogr., 64, 83–90, doi:10.1016/j.pocean.2004.08.004, 2005.

Estrada, M.: Primary production in the Northwestern Mediterranean, Sci. Mar. 60, 55–64, 1996.

Fabres, J., Tesi, T., Velez, J., Batista, F., Lee, C., Calafat, A., Heussner, S., Palanques, A., and Miserocchi, S.: Seasonal and event-controlled export of organic matter from the shelf towards the Gulf of Lions continental slope, Cont. Shelf Res., 28, 1971–1983, doi:10.1016/j.csr.2008.04.010, 2008.

Ferré, B., Guizien, K., Durrieu de Madron, X., Palanques, A., Guillén, J., and Grémare, A.: Fine-grained sediment dynamics during a strong storm event in the inner-shelf of the Gulf of Lion (NW Mediterranean), Cont. Shelf Res., 25, 2410–2427, doi:10.1016/j.csr.2005.08.017, 2005.

Guillén, J., Palanques, A., Puig, P., Durrieu de Madron, X., and Nyffeler, F.: Field calibration of optical sensors for measuring suspended sediment concentration in the Western Mediterranean, Sci. Mar., 64, 427–435, 2000.

Guillén, J., Bourrin, F., Palanques, a, Durrieu de Madron, X., Puig, P., and Buscail, R.: Sediment dynamics during wet and dry storm events on the Têt inner shelf (SW Gulf of Lions), Mar. Geol., 234, 129–142, doi:10.1016/j.margeo.2006.09.018, 2006.

Heussner, S., Ratti, C., and Carbonne, J.: The PPS 3 time-series sediment trap and the trap sample processing techniques used

during the ECOMARGE experiment, Cont. Shelf Res., 10, 943–958, doi:10.1016/0278-4343(90)90069-X, 1990.

Heussner, S., Durrieu de Madron, X., Calafat, A., Canals, M., Carbonne, J., Delsaut, N., and Saragoni, G.: Spatial and temporal variability of downward particle fluxes on a continental slope: Lessons from an 8-yr experiment in the Gulf of Lions (NW Mediterranean), Mar. Geol., 234, 63–92, doi:10.1016/j.margeo.2006.09.003, 2006.

Ivanov, V. V., Shapiro, G. I., Huthnance, J. M., Aleynik, D. L., and Golovin, P. N.: Cascades of dense water around the World Ocean. Progr. Oceanogr., 60, 47–98, doi:10.1016/j.pocean.2003.12.002, 2004.

Josey, S. A.: Changes in the heat and freshwater forcing of the eastern Mediterranean and their influence on Deep Water Formation, J. Geophys. Res., 108, 3237, doi:10.1029/2003JC001778, 2003.

Josey, S. A., Kent, E. C., and Taylor, P. K.: New insights into the ocean heat budget closure problem from analysis of the SOC air-sea flux climatology, J. Clim., 12, 2856–2880, doi:10.1175/1520-0442(1999)012<2856:NIITOH>2.0.CO;2, 1999.

Lastras, G., Canals, M., Urgeles, R., Amblas, D., Ivanov, M., Droz, L., Dennielou, B., Fabrés, J., Schoolmeester, T., Akhmetzhanov, A., Orange, A., and García-García, A.: A walk down the Cap de Creus canyon, Northwestern Mediterranean Sea: Recent processes inferred from morphology and sediment bedforms, Mar. Geol., 246, 176–192. doi:10.1016/j.margeo.2007.09.002, 2007.

Ludwig, W., Meybeck, M., and Abousamra, F.: Riverine transport of water, sediments, and pollutants to the Mediterranean Sea, UNEP MAP Technical report Series 141, UNEP/MAP Athens, 111 pp., 2003.

Martín, J., Palanques, A., and Puig, P.: Composition and variability of downward particulate matter fluxes in the Palamós submarine canyon (NW Mediterranean), J.Mar. Sys., 60, 75–97, 2006.

Martín, J., Miquel, J. C., and Khripounoff, A.: Impact of open sea deep convection on sediment remobilization in the western Mediterranean, Geophys. Res. Lett., 37, L13604, doi:10.1029/2010GL043704, 2010.

Martín, J., Durrieu de Madron, X., Puig, P., Bourrin, F., Palanques, A., Houpert, L., Higueras, M., Sanchez-Vidal, A., Calafat, A. M., Canals, M., Heussner, S., Delsaut, N., and Sotin, C.: Sediment transport along the Cap de Creus Canyon flank during a mild, wet winter, Biogeosciences, 10, 3221–3239, doi:10.5194/bg-10-3221-2013, 2013.

Martín-Vide, J. and Raso Nadal, J. M.: Atlas climàtic de Catalunya, Període 1961-1990, Institut Cartogràfic de Catalunya, Barcelona, 2008.

MEDOC Group: Observation of formation of deep water in the Mediterranean Sea, 1969, Nature, 227, 1037–1040, doi:10.1038/2271037a0, 1970.

Millot, C. A.: The Gulf of Lions' hydrodynamic. Cont. Shelf Res., 10, 885-894, 1990.Millot, C., Circulation in the Western Mediterranean Sea, J. Mar. Sys., 20, 423–442, 1999.

Mortlock, R. A. and Froelich, P. N.: A simple method for the rapid determination of biogenic opal in pelagic marine sediments, Deep-Sea Res., 36, 1415–1426, 1989.

Palanques, A., Durrieu de Madron, X., Puig, P., Fabres, J., Guillén, J., Calafat, A., Canals, M., Heussner, S., and Bonnin, J.: Suspended sediment fluxes and transport processes in the Gulf of Lions submarine canyons, The role of storms and dense water cascading, Mar. Geol., 234, 43–61. doi:10.1016/j.margeo.2006.09.002, 2006.

Palanques, A., Guillén, J., Puig, P., and Durrieu de Madron, X.: Storm-driven shelf-to-canyon suspended sediment transport at the southwestern Gulf of Lions, Cont. Shelf Res., 28, 1947–1956, doi:10.1016/j.csr.2008.03.020, 2008.

Palanques, A., Puig, P., Durrieu de Madron, X., Sanchez-Vidal, A., Pasqual, C., Martín, J., Calafat, A., Heussner, S., and Canals, M.: Sediment transport to the deep canyons and open-slope of the western Gulf of Lions during the 2006 intense cascading and open-sea convection period, Progr. Oceanogr., 106, 1–15, 2012.

Pasqual, C., Sanchez-Vidal, A., Zúñiga, D., Calafat, A., Canals, M., Durrieu de Madron, X., Puig, P., Heussner, S., Palanques, A., and Delsaut, N.: Flux and composition of settling particles across the continental margin of the Gulf of Lion: the role of dense shelf water cascading, Biogeosciences, 7, 217-231, doi:10.5194/bg-7-217-2010, 2010.

Puig, P., Palanques, A., Orange, D.L., Lastras, G., and Canals, M.: Dense shelf water cascading and furrows formation in the Cap de Creus Canyon, northwestern Mediterranean Sea, Cont. Shelf Res., 28, 2017–2030, 2008.

Pusceddu, A., Bianchelli, S., Canals, M., Sanchez-Vidal, A., Durrieu De Madron, X., Heussner, S., Lykousis, V., de Stigter, H., Trincardi, F., and Danovaro, R.:Organic matter in sediments of canyons and open slopes of the Portuguese, Catalan, Southern Adriatic and Cretan Sea margins, Deep-Sea Res., 57, 441-457, doi:10.1016/j.dsr.2009.11.008, 2010.

Roussiez, V., Ludwig, W., Monaco, A., Probst, J.L., Bouloubassi, I., Buscail, R., and Saragoni, G.: Sources and sinks of sediment-bound contaminants in the Gulf of Lions (NW Mediterranean Sea): A multi-tracer approach, Cont. Shelf Res., 26, 1843–1857, doi:10.1016/j.csr.2006.04.010, 2006.

Salvadó, J. A., Grimalt, J. O., López, J. F., Durrieu de Madron, X., Heussner, S., and Canals, M.: Transformation of PBDE mixtures during sediment transport and resuspension in marine environments (Gulf of Lion, NW Mediterranean Sea), Environ. Pollut., 168, 87–95, doi:10.1016/j.envpol.2012.04.019, 2012.

Sanchez-Vidal, A., Pascual, C., Kerhervé, P.A., Calafat, A., Heussner, S., Palanques, A., Durrieu de Madron, X., Canals, M., and Puig. P: Impact of dense shelf water cascading on the transfer of organic matter to the deep Western Mediterranean Basin, Geophys. Res. Lett., 35, L05605, doi:10.1029/2007GL032825, 2008.

Sanchez-Vidal, A., Pasqual, C., Kerhervé, P., Heussner, S., Calafat, A., Palanques, A., Durrieu de Madron, X., Canals, M., and Puig, P.: Across margin export of organic matter by cascading events traced by stable isotopes northwestern Mediterranean Sea, Limnol. Oceanogr., 54, 1488–1500, 2009.

Sanchez-Vidal, A., Canals, M., Calafat, A., Lastras, G., Pedrosa-Pàmies, R., Menéndez, M., Medina, R., Company, J. B., Hereu, B., Romero. J., and Alcoverro, T.: Impacts on the Deep-Sea Ecosystem by a Severe Coastal Storm, PLoS one, 7, e30395, doi:10.1371/journal.pone.0030395, 2012.

Schroeder, K., Josey, S. A., Herrmann, M., Grignon, L., Gasparini, G. P., and Bryden, H.L.: Abrupt warming and salting of the Western Mediterranean Deep Water: Atmospheric forcings and lateral advection, J. Geophys. Res., 115, C08029, doi:10.1029/2009JC005749, 2010.

Serrat, P., Ludwig, W., Navarro, B., and Blazi, J.L.: Variabilité spatio-temporelle des flux de matières en suspension d'un fleuve côtier méditerranéen: la Têt (France), Spatial and temporal

variability of sediment fluxes from a coastal Mediterranean river: the Têt (France), Cr. Acad. Sci. IIA, 333, 389–397, doi:10.1016/S1251-8050(01)01652-4, 2001.

Tesi, T., Puig, P., Palanques, A., and Goñi, M. A.: Lateral advection of organic matter in cascading-dominated submarine canyons, Progr. Oceanogr., 84, 185–203, doi:10.1016/j.pocean.2009.10.004, 2010.

Ulses, C., Estournel, C, Bonnin, J., Durrieu de Madron, X., and Marsaleix, P.: Impact of storms and dense water cascading on shelf-slope exchange in the Gulf of Lions (NW Mediterranean), J. Geophys. Res., 113, CO2010, doi:10.1029/2006JC003795, 2008a.

Ulses, C., Estournel, C., Durrieu de Madron, X., and Palanques, A.: Suspended sediment transport in the Gulf of Lion (NW Mediterranean): impact of extreme storms and floods, Cont. Shelf Res., 28, 2048–2070, doi:10.1016/j.csr.2008.01.015, 2008b.

Progress in Oceanography 144 (2016) 39–61

Contents lists available at ScienceDirect

Progress in Oceanography

journal homepage: www.elsevier.com/locate/pocean

Particle fluxes and their drivers in the Avilés submarine canyon and adjacent slope, central Cantabrian margin, Bay of Biscay

A. Rumín-Caparrós [a], A. Sanchez-Vidal [a], C. González-Pola [b], G. Lastras [a], A. Calafat [a], M. Canals [a,*]

[a] GRC Geociències Marines, Departament de Dinàmica de la Terra i de l'Oceà, Universitat de Barcelona, E-08028 Barcelona, Spain
[b] Instituto Español de Oceanografía, C.O. Gijón, Avda. Príncipe de Asturias 70 bis, E-33212 Gijón, Spain

ARTICLE INFO

Article history:
Received 4 June 2015
Received in revised form 17 March 2016
Accepted 20 March 2016
Available online 25 March 2016

ABSTRACT

The Avilés Canyon in the central Cantabrian margin is one of the largest submarine canyons in Europe, extending from the shelf edge at 130 m depth to 4765 m depth in the Biscay abyssal plain. In this paper we present the results of a year-round (March 2012 to April 2013) study of particle fluxes in this canyon and the adjacent continental slope. Three mooring lines equipped with automated sequential sediment traps, high-accuracy conductivity-temperature recorders and current meters allowed measuring total mass fluxes and their major components (lithogenics, calcium carbonate, opal and organic matter) in the settling material jointly with a set of environmental parameters. The integrated analysis of the data obtained from the moorings together with remote sensing images and meteorological and hydrographical data has shed light on the sources of particles and the across- and along margin mechanisms involved in their transfer to the deep.

Our results allow interpreting the dynamics of the sedimentary particles in the study area. Two factors play a critical role: (i) direct delivery of river-sourced material to the narrow continental shelf, and (ii) major resuspension events caused by large waves and near bottom currents developing at the occasion of the rather frequent severe storms that are typical of the Cantabrian Sea. Wind direction and subsequent wind-driven currents largely determine the way sedimentary particles reach the canyon. While westerly winds favour the injection of sediments into the Avilés Canyon mainly by building an offshore transport in the bottom Ekman layer, easterly winds ease the offshore advection of particulate matter towards the Avilés Canyon and its adjacent western slope principally through the surface Ekman layer. Furthermore, repeated cycles of semidiurnal tides add an extra amount of energy to the prevailing bottom currents and actively contribute to keep a permanent background of suspended particles in near-bottom waters.

High contents of lithogenics in settling particles at the three mooring stations confirm that riverine inputs are the principal source of particles to the Avilés Canyon, including the lowermost canyon, and the adjacent open slope. Primary production also has a strong influence on the amount and the composition of particulate matter, with more than 30% of the total mass flux being of biogenic origin (organic matter, opal and calcium carbonate).

1. Introduction

Submarine canyons are large seafloor geomorphological features connecting the shallower with the deeper sections of continental margins (Shepard, 1981; Nittrouer and Wright, 1994; Xu et al., 2002; Canals et al., 2006; Mulder et al., 2012). Multiple studies have demonstrated that submarine canyons act as pathways for water movements, lithogenic and biogenic materials (Gardner, 1989; Puig and Palanques, 1998; Hung et al., 2003; Palanques et al., 2006a), hot spots of biodiversity and biological productivity (Vetter, 1994; Vetter and Dayton, 1998; Gili et al., 1999; Vetter et al., 2010).

One of the main aims of the Spanish DOS MARES project (Deep-water submarine canyons and slopes in the Mediterranean and Cantabrian seas: from synchrony of external forcings to living resources) was to understand how the signal of different forcings is transferred and how it affects the deep ecosystem in submarine canyons and continental slopes around the Iberian Peninsula, with an emphasis on the Avilés Canyon in the Cantabrian margin of the Bay of Biscay. Processes controlling particulate matter transport (e.g. atmosphere and gravitational-driven) have been studied in submarine canyons all over the world (Drake and Gorsline, 1973; Hickey et al., 1986; Durrieu de Madron, 1994; van Weering et al.,

* Corresponding author.
E-mail address: miquelcanals@ub.edu (M. Canals).

http://dx.doi.org/10.1016/j.pocean.2016.03.004
0079-6611/

2002; Puig et al., 2004a; Paull et al., 2005; Xu et al., 2010; Pierau et al., 2011). In the Iberian Peninsula there is a strong contrast between Atlantic margin settings and Mediterranean ones, including physiography and water depth, water mass structure and ocean dynamics.

In the Western Mediterranean Sea, east of the Iberian Peninsula, the best-studied canyons are those located in the Gulf of Lion and the Catalan margin. Some of those canyons, especially Cap de Creus Canyon, experience high energy events in the form of seasonal dense shelf water cascading, a type of flow that erodes the shelf and slope floor and funnels large volumes of water and sediments into the deep margin and basin (Canals et al., 2006; Heussner et al., 2006). Cascading is triggered by strong, persistent, cold and dry northern winds, causing heat loss and an increase in the density of shelf waters that eventually overflow the shelf and cascade down the slope. Coastal downwelling caused by eastern storms also enhances downcanyon sediment transport (Martín et al., 2006; Palanques et al., 2006a; Bonnin et al., 2008; Sànchez-Vidal et al., 2012). In addition to heavy precipitation and river floods carrying significant amounts of sediments and forming surface plumes along the coast, Eastern winds push surface waters against the coastline, where high waves and associated currents lead to major resuspension events of inner shelf sediments. Part of the sediment load resulting both from river floods and shelf resuspension is ultimately captured by canyons having their heads at short distance from the coastline and then is exported down-canyon (Canals et al., 2013). River floods have also been identified as the main drivers for down-canyon sediment transport in submarine canyons off southern Spain, in the Alborán Sea (Palanques et al., 2005). Bottom trawling practiced on the shelf around canyon heads and along canyon flanks also results in sediment gravity flows that move into the canyon axis, as recently shown in La Fonera Canyon, in the north Catalan margin (Puig et al., 2012).

The Atlantic continental margin west of Iberia hosts some particularly large submarine canyons according to global standards, such as Nazaré, Lisbon-Setúbal and Cascais canyons (Arzola et al., 2008; Tyler et al., 2009; Martín et al., 2011; de Stigter et al., 2011). In contrast with micro-tidal environments such as the Western Mediterranean Sea, Atlantic tidal currents are strong enough to trigger resuspension and remobilise particulate matter (Oliveira et al., 2007), especially in upper canyon sections (de Stigter et al., 2007, 2011). The role of shelf storms, eventually combined with river floods, over particulate matter transport from the upper to the middle course of Nazaré Canyon is discussed in Martín et al. (2011). Also in the Atlantic is the northern Iberian, or Cantabrian margin forming the southern bound of the Bay of Biscay. The Cantabrian margin is cut by several, deeply incised submarine canyons and is bounded to the east by the large, more than 2000 km long Cap Breton Canyon, where tidally-induced hydrodynamic events are able to remobilise and sustain a permanent up- and down-canyon transport of particulate matter (Mulder et al., 2012). Shelf storms also play a key role in modulating sediment transport down Cap Breton Canyon. However, in the Cap Ferret submarine canyon, in the eastern margin of the Bay of Biscay, Schmidt et al. (2014) found only a limited downslope particle transfer from the shelf to the basin along the canyon attributed to the disconnection of this canyon from major sediment sources. Further north, in the north-eastern margin of the Bay of Biscay, in the Audierne and Blackmud canyons, particulate matter is resuspended and remobilised by strong tidal hydrodynamics (Mulder et al., 2012).

These studies support the relevance of external forcings on sediment dynamics and particle fluxes within submarine canyons and in the adjacent continental slopes. The external forcings referred to in the previous paragraphs are either atmospherically driven (wind storms, river floods, winter cooling and mixing), gravity driven (tides) or anthropogenic driven (trawling induced resuspension) and all of them are capable of triggering significant sediment transport events in the submarine canyons off the Iberian Peninsula. In addition, the overall margin configuration, including the distance of canyon heads to the nearest shoreline, largely determines the capability of submarine canyons to trap coastal sediment and funnel it down course (Canals et al., 2013).

The above-mentioned background information underlines the existence of a knowledge gap on the behaviour of submarine canyons incised in the Cantabrian margin that our study contributes to fill in, as it is the first of its nature in the central Cantabrian margin. The present study focuses on sediment transfer and particle fluxes from shallow to deep, thus aiming to improve the understanding of the functioning of submarine canyons at large and of Avilés Canyon in particular. Avilés Canyon can be considered as a representative of submarine canyons in the Northeast Atlantic, so that the high productivity and biodiversity associated with these features (Vetter, 1994; De Leo et al., 2010; Vetter et al., 2010) can be better understood, assessed and managed.

2. Regional setting

The Avilés Canyon is the main, 80 km long trunk of a canyon system that consists of three main branches with contrasting morphologies: the El Corbiro and La Gaviera canyons to the east and the Avilés Canyon itself to the west (Fig. 1). El Corbiro and La Gaviera merge before opening into the lowermost course of the Avilés Canyon, which opens to the Biscay abyssal plain at 4765 m depth (Lastras et al., 2012; Gómez-Ballesteros et al., 2013).

Several rivers discharge along the Cantabrian coastline. Their flows are modulated by a typical oceanic climate, with a rainy season starting in November and ending in May and a drier season taking place from June to October (Prego et al., 2008). The main contributor of freshwater and terrigenous sediment to the coastline close to Avilés Canyon head is the 138 km long Nalón River opening into the 15 km long Pravia estuary. The Nalón River is fed by a 4893 km^2 catchment area and has an annual average flow of 109 $m^3\ s^{-1}$ according to Prego et al. (2008), with annual peaks up to 1250 $m^3\ s^{-1}$. These values make the Nalón River watershed and flow the largest in the Cantabrian river system (Prego et al., 2008). Its main tributary is the 111 km long Narcea River with a catchment area of 1135 km^2 and a mean annual discharge of 16 $m^3\ s^{-1}$ ("Confederación Hidrográfica del Cantábrico" online resources in http://chcantabrico.es/index.php/es/atencionciudadano/documentos/documentos-de-la-web/search/lang,es-es/). The Nalón River discharge presents a strong seasonal character following the above-referred rainy and dry seasons. Eight main dams in the Nalón watershed, of which the tallest are Tanes in Nalón River upper course and La Barca in Narcea River, with 95 and 74 m of dam height, respectively (www.seprem.es), and a number of smaller ones, do not have an influence strong enough to wipe off the natural seasonal regime. However, the amounts of sediment trapped behind those dams has not been quantified yet. Of the twenty-eight Cantabrian rivers investigated by Prego et al. (2008), the Nalón River is the one with the highest load (836 $m^3\ s^{-1}$) of total suspended solids (TSS) and is identified as the most important Cantabrian river in terms of TSS contribution to the Bay of Biscay with 379.900 $t\ y^{-1}$ representing 33% of the total.

Consistently with its geographical location, the water column structure in the Bay of Biscay, and the Cantabrian Sea in particular, corresponds to the Northeast Atlantic one (Lavín et al., 2006). Namely: (1) surface waters extending down to the winter maximum depth (~250 m) of the mixed layer (González-Pola et al., 2007), which are characterized by a pronounced inter-annual

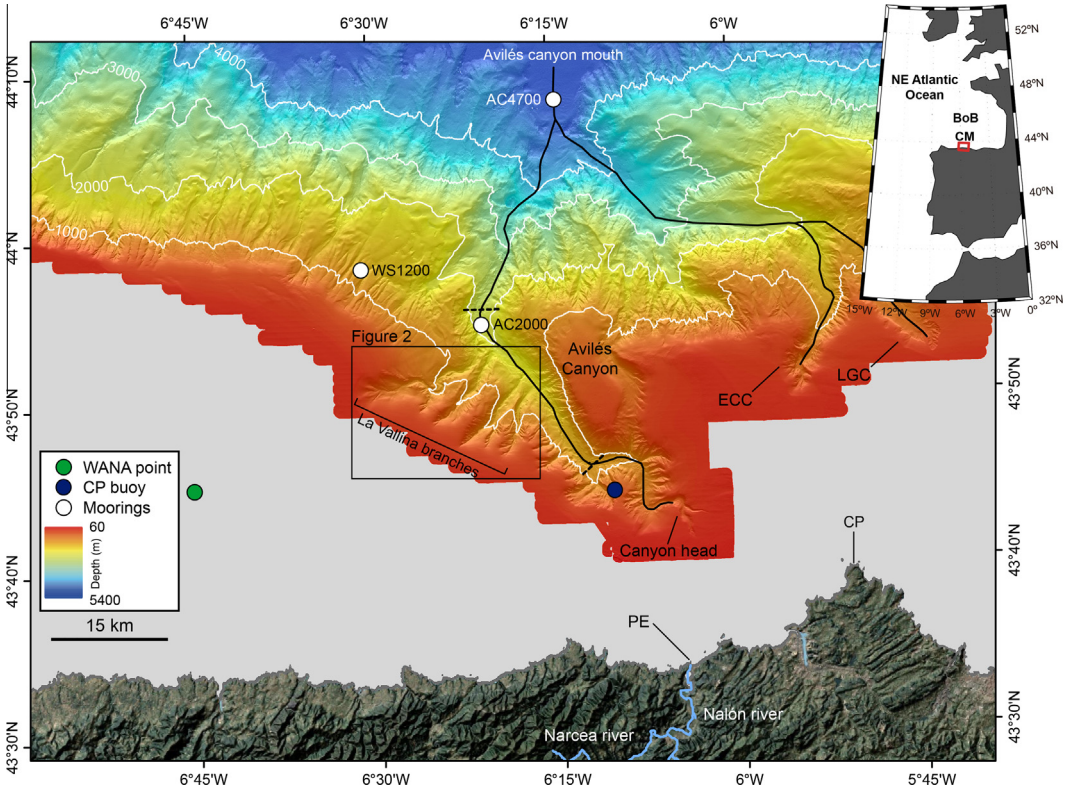

Fig. 1. Shaded relief bathymetric map of the Avilés submarine canyon and surrounding shelf, slope and deep basin. The location of the El Corbiro Canyon (ECC) and the La Gaviera Canyon (LGC) are indicated. Location of moorings (white dots), Cabo Peñas coastal buoy (blue dot) and WANA point 1053075 (green dot) are also presented. Dashed black lines mark the boundaries of the upper and middle canyon course. The black box includes La Vallina branches illustrated in Fig. 2. Land topography from the NASA's Lance rapid response MODIS satellite true colour images. Depth is in meters. The top right map represents the NE Atlantic Ocean with the Cantabrian margin (CM) forming the southern bound of the Bay of Biscay (BoB). (For interpretation of the references to colour in this figure legend, the reader is referred to the web version of this article.)

variability linked to seasonal cycles; (2) the East North Atlantic Central Water (ENACW) from the base of the mixed layer down to 400–600 m; (3) the Mediterranean Outflow Water (MOW) that is located below the ENACW and extends down to depths of 500–1500 m (Iorga and Lozier, 1999a); and (4) the Bottom Water (BW) extending down to the seafloor as a deep water mass formed after the mixing of several water masses including the North Atlantic Deep Water (NADW), the Lowered Deep Water (LDW) and Antarctic Bottom Water (ABW) (Botas et al., 1989; Pingree and Le Cann, 1992; van Aken, 2000a).

The ENACW results from winter mixing over the area surrounded by the North Atlantic Current (NAC) and the Azores Current (AC) (Pollard and Pu, 1985; Pollard et al., 1996). Two varieties of ENACW are defined according to their origin, temperature and salinity (Ríos et al., 1992). The denser variety, or subpolar mode of the ENACW, forms in the southern border of the NAC. In the Bay of Biscay it flows weakly and experiences an anticyclonic recirculation (Pingree, 1993). The lighter variety, or subtropical mode of the ENACW, forms at the northern boundary of the AC and is conveyed along the northwestern and north Iberian upper continental slope by the Iberian Poleward Current (IPC) (Haynes and Barton, 1990). The IPC circulates poleward along the western and northern Iberian continental shelf and slope, eventually reaching the French Armorican shelf (Pingree and Le Cann, 1990). The MOW results from the outflow of Mediterranean dense deep water into the Atlantic Ocean through the Gibraltar Strait. The northern branch of the MOW flows along the Western Iberian margin as a slope current (Iorga and Lozier, 1999a, 1999b; van Aken, 2000b) and reaches the Bay of Biscay with speeds between 2 and 3 cm s^{-1} (Pingree and Le Cann, 1990; Díaz del Río et al., 1998). The BW draws a cyclonic recirculation cell over the Biscay abyssal plain with a poleward current velocity of 1.2 cm s^{-1} nearby the foot of the continental margin (Dickson et al., 1985; Paillet and Mercier, 1997).

Seasonal wind patterns have a significant impact on the sea surface circulation over the shelf and slope of the study area (Charria et al., 2013). NNE to easterly winds, typically more common from April to September, induce a westward shelf and slope surface circulation and promote coastal upwelling. The presence of the Avilés Canyon system seems to enhance upwelling during such situations, which results in an up-canyon flow (Ruiz-Villarreal et al., 2004). In contrast, NW winds, which can be very strong and usually are dominant from October to March, lead to an eastward shelf and slope surface circulation and coastal downwelling. Under these conditions, the submarine canyon does not seem to have any effect on the incident slope current (Ruiz-Villarreal et al., 2004). The influence of the IPC surface flow over the western Iberian and Cantabrian slopes in winter extends to the first 200–300 m depth so impacting the upper slope (Frouin et al., 1990; Haynes and Barton, 1990; Pingree and Le Cann, 1990, 1992; Serpette et al., 2006; Friocourt et al., 2007; Le Cann and Serpette, 2009).

Semi-diurnal tidal oscillations on the Avilés shelf are highly energetic and can dominate current dynamics (Fanjul et al., 1997). Barotropic tides above steep topographies such as submarine canyons give rise to internal tides, especially where the slope gradient becomes critical (i.e. wherever the topographic slope matches the propagation angle of the internal tide beams) (Baines, 1982; Cacchione et al., 2002). According to data from "Puertos del Estado", the mean meso-tidal range at the coast close to Avilés Canyon for the period 1996–2013 ranged between 1.95 m and 4.68 m at neap and spring tides, respectively, and exceeded 5 m during equinoctial tides. In the Bay of Biscay, the dominance

of the semi-diurnal barotropic forcing over the shelf-break and slope makes the internal tide to be markedly semi-diurnal (Pingree and New, 1989). The capability of such tides to influence sedimentary processes by triggering bottom currents fast enough to resuspend sediment has been described in the nearby Aquitanian margin of the Bay of Biscay (Durrieu de Madron et al., 1999).

3. Materials and methods

3.1. Forcing conditions

Wind speed and direction at 3 m above the sea surface and wave height and direction were obtained from Cabo Peñas Seawatch buoy measuring waves as well as atmospheric and oceanographic parameters at an hourly frequency (Álvarez Fanjul et al., 2003). The buoy, which belongs to the Deep Water Network from "Puertos del Estado", is moored at 615 m of water depth on a sort of plateau in the western flank of the Avilés Canyon upper course (Fig. 1). Near surface currents are not corrected for platform motion and all the data gathered by the network buoys is subject to a quality control procedure to find inconsistencies and other anomalies in the datasets.

The buoy data have been crosschecked by linear correlation (not shown) with the coded WANA point 1053075 (see location in Fig. 1) in order to further validate the wind and wave data used in our work. The WANA network delivers hourly averaged time series of wind (at 10 m above the sea surface) and wave parameters obtained from a reanalysis product performed by "Puertos del Estado" in collaboration with "Agencia Estatal de Meteorología".

The wind-drag-induced Ekman transport perpendicular to the coastline (Q_y) is normally taken as an Upwelling Index (UI). This index is an estimate of across-slope transport depending on local wind. In our study, the dominant orientation of the coastline is in the east–west direction and the UI magnitude expresses volume of water transported in the north–south direction by lineal km of shore (in $m^3\ s^{-1}\ km^{-1}$). UI has been calculated from Cabo Peñas buoy wind data according to Bakun (1973) using equation

$$\mathrm{UI} = Q_y = -\frac{\tau_x}{f \cdot \rho_w}, \quad (1)$$

where τ_x is the wind stress for the x component, f is the Coriolis parameter calculated as $f = 2\Omega \sin \Phi$ at 43° of latitude, and ρ_w is seawater density (1025 kg m^{-3}). Upwelling is characterized by positive values of Q_y whereas negative values are indicative of water masses piling up towards the coast (i.e. downwelling). The wind stress for the x component is calculated with equation

$$\tau_x = \rho_a \cdot C_d \cdot \sqrt{U^2 + V^2} \cdot U, \quad (2)$$

where ρ_a is the density of air, U and V are the eastward and northward wind components, respectively, and C_d is the neutral drag air coefficient computed following Smith (1988).

Discharges by Nalón River and its main tributary, the Narcea River, measured from gauging stations located at 23 and 22 km from the river mouth, respectively, have been obtained from EDP group of companies.

Estimates of Chl-a concentrations are from the Giovanni online data system, developed and maintained by the NASA Goddard Earth Sciences (GES) Data and Information Services Center (DISC), using the Moderate Resolution Imaging Spectroradiometer (MODIS) as our data source. Data have been gridded from 43.4°N to 45°N, and from 7.5°W to 4°W in order to include the mooring locations and the areas adjacent to Avilés Canyon. Net primary production data were downloaded from the Ocean Productivity website (http://www.science.oregonstate.edu/ocean.productivity/) and calculated using the Vertically Generalized Production Model (VGPM) (Behrenfeld and Falkowski, 1997). For VGPM, net primary production is a function of chlorophyll, available light, and the photosynthetic efficiency.

Forcing conditions have also been considered indirectly by means of a two-way statistical ANOVA analysis intended to examine the factors responsible for the variability of Total Mass Fluxes (TMFs) in the Avilés Canyon and in its western slope. For this analysis, two fixed factors were considered: month of collection and trap depth (Table 2; see Section 4.3).

A cross-correlation analysis has been performed in ordert to check the extent of the correlation between the external forcings and the TFMs temporal variability (Table 3; see Section 4.3). Given that raw time series with different time steps ranging from hourly to daily periods present occasional gaps, data were resampled at regular and continuous time series prior to the statistical analysis. All data were re-sampled to a time step equivalent to the sampling period of the sediment traps and such time lapse has been used as a "lag" to evaluate time-lagged correlations between time series. Gaps in TMFs in AC2000T trap were linearly interpolated considering the low variability of TMFs in the other sediment traps during the data gap (Fig. 4).

3.2. Multibeam data acquisition

Prior to the deployment of the mooring lines, and in order to accurately identify the more convenient locations to install them, a seabed high-resolution bathymetric survey including the acoustic characterization of the seabed of the Avilés Canyon and the adjacent continental slope was performed. Multibeam data covering 5682 km^2 of the Cantabrian margin around the Avilés Canyon was acquired in October–November 2011 during the COCAN cruise onboard R/V "Miguel Oliver". Data were obtained with a Simrad EM302D multibeam echo-sounder operated in equidistant mode with swath widths between 600 m on the shelf and 6000 m on the abyssal plain. The complete dataset was processed onboard using Caris HIPS and SIPS software, resulting in a general 20 m-grid-size digital terrain model.

3.3. Experimental design

The high-resolution multibeam bathymetry maps evidenced the complex morphology of the Avilés Canyon system and the adjacent continental slope. Jointly with backscatter imagery (not shown), multibeam bathymetry served as background information to decide where to deploy the mooring lines to investigate the across margin transport of particulate matter and characterise the associated ambience conditions, both within and outside the Avilés Canyon. Two moorings (AC2000 and AC4700) where placed in the middle course and lowermost course of the canyon at 2000 m and 4700 m depth, respectively (Fig. 1 and Table 1). AC2000 was deployed in order to capture sediment fluxes eventually arriving from both the shelf-incising set of tributaries known as La Vallina branches and from the Avilés Canyon head and upper course (see Section 4.1). AC4700 was deployed in a very flat area where the Avilés Canyon widens significantly and opens into the Biscay abyssal plain down course of La Gaviera Canyon mouth which main tributary is El Corbiro Canyon (Fig. 1). Therefore, AC4700 was well suited to capture sediment fluxes arriving from the entire Avilés Canyon system. A third mooring (WS1200) was deployed as a control station at 1200 m depth in the open slope west of Avilés Canyon (Fig. 1).

All mooring lines were equipped with automated sequential sediment traps, high-accuracy conductivity-temperature recorders and current meters. They were deployed during one complete

Table 1
Average annual fluxes (g m^{-2} d^{-1}) and relative contribution of each of the major constituents to particle fluxes in the Avilés Canyon and adjacent open slope to the west.

Station	Water depth (m)	Meters above the bottom (m)	Meters below surface (m)	TWF (g m^{-2} d^{-1})	Lithogenic		$CaCO_3$		OM		Opal	
					%	Flux (g m^{-2} d^{-1})	%	Flux (g m^{-2} d^{-1})	%	Flux (g m^{-2} d^{-1})	%	Flux (g m^{-2} d^{-1})
WS1200	1200	46	1154	0.99	61.42	0.54	26.78	0.30	8.62	0.078	3.09	0.09
AC2000T (mid-water)	2000	822	1178	0.43	61.32	0.30	24.93	0.14	10.25	0.05	3.00	0.021
AC2000B (near-bottom)	2000	46	1954	1.98	66.98	1.37	24.42	0.47	6.52	0.14	2.20	0.07
AC4700	4700	46	4654	0.33	53.05	0.17	35.19	0.12	7.42	0.025	4.36	0.017

annual cycle in two consecutive periods, from March 2012 to September 2012 and from September 2012 to March 2013.

The AC2000 mooring line was equipped with two Aquadopp current meters at 44 and 820 m above the bottom (mab), and two PPS3 sediment traps coupled with SBE37 recorders at 46 m and 822 mab. Hereafter, AC2000T and AC2000B will be used to refer to the mid-water (at 820 mab or 1200 m of water depth) and near-bottom levels in this mooring, respectively. The AC4700 mooring line was equipped with a single RCM8 current meter at 44 mab and a PPS3 sediment trap at 46 mab. The WS1200 mooring line was equipped with a pair of current meters, which were an Aquadopp acoustic Doppler current meter at 160 mab and an Aanderaa RCM8 rotor current meter at 44 mab, and a Technicap PPS3 sediment trap coupled with a SBE37 high-accuracy conductivity-temperature recorder at 46 mab.

The PPS3 Technicap sequential sediment traps have a 0.125 m^2 collecting surface and a 2.5 height/diameter ratio in its cylindrical part. They are equipped with 12 receiving cups (Heussner et al., 1990), which were filled with a buffered 5% (v/v) formaldehyde solution in 0.45 μm filtered seawater. This solution is used to prevent the degradation of the collected particles in the retrieving cups and also to avoid fragmentation and degradation of swimmers occasionally entering the sampling cups. All traps collected settling particles synchronously and uninterruptedly with a sampling interval of 15–16 days during the first and second deployment periods except the last three collecting bottles of February 2013, which remained opened 7 days in order to adjust the total sampling interval to the scheduled recovery dates. Traps worked properly from 16th March 2012 to 23rd September 2012, and from 1st October 2012 to 8th March 2013, except AC2000T, which stopped collecting samples before the end of the first deployment period, on the first of August 2012.

Aandera and Aquadopp current meters were set to collect data at 15 minutes intervals at upper levels and 30 minutes near the bottom. A technical failure of the current meter deployed at AC4700 resulted in the complete data loss at this water depth.

3.4. Trap collection efficiency

Trap collection efficiency has been checked by examining the pitch and roll sensors of the current meters. Efficiency can be compromised by trap tilting (Gardner, 1985) and also due to the potential of perturbation of trap mouths on lateral flows causing biases in the collection of sinking particles (e.g. Baker et al., 1988; Gardner et al., 1997; Buesseler et al., 2007 and references therein).

Data from the current meter pressure sensors show that sediment trap tilting never exceeded 11°, even during current speeds as high as 40 cm s^{-1}. According to Gardner (1985) TMFs would not have been affected (see explanation on how TMFs have been calculated in Section 3.5). Our results compare well with those obtained by Bonnin et al. (2008) in their collecting efficiency experiment using the same PPS3 Technicap sediment traps. These authors concluded that their mooring lines were maintained taut, close to vertical, never tilting more than 15°, during strong current episodes (up to 82 cm s^{-1}).

Since we do not have enough information to detect any effect of perturbation by trap mouths on lateral flows, and in order to be consistent with the extensive published data using the same sediment traps in other locations around the Iberian Peninsula and beyond (e.g. Heussner et al., 1999; Fabrés et al., 2002; Miquel et al., 2011; Stabholz et al., 2013), we assume that hydrodynamics over the trap mouth did not bias mass fluxes.

3.5. Sediment trap sample processing and analytical methods

After recovery, samples were stored in the dark at 4 °C until they were processed following a modified version of the methodology of Heussner et al. (1990). Swimming organisms were removed in two steps according to its size: large swimmers were removed by wet sieving through a 1 mm nylon mesh and organisms of less than 1 mm were handpicked using fine tweezers under a microscope. A high-precision peristaltic pump robot was used to split samples into aliquots through repeated division of the sample. Samples were then rinsed repeatedly with Milli-Q water, centrifuged to remove formaldehyde and salt, and freeze-dried before chemical analyses. The dried fraction was weighted to obtain the total mass. TMFs were calculated as follows:

$$\text{TMF}\ (\text{g m}^{-2}\ \text{d}^{-1}) = \frac{\text{Sample dry weight}\ (\text{g})}{\text{Collecting area}\ (\text{m}^2) \cdot \text{Sampling interval}\ (\text{days})} \quad (3)$$

Total carbon, organic carbon (OC) and nitrogen (N) contents were analysed at "Centres Científics i Tecnològics" of "Universitat de Barcelona" using an elemental analyser Thermo EA Flash 1112. In order to determine the OC content, samples were first decarbonated with 25% HCl through repeated addition of 100 μL aliquots until no effervescence was observed. Between each acidification, samples were dried during 8 h at 60 °C. Organic matter (OM) content was calculated as twice the organic carbon content. Inorganic carbon content was calculated as total carbon minus organic carbon. Carbonate content was calculated assuming that all inorganic carbon is contained within calcium carbonate ($CaCO_3$), using the molecular mass ratio of 100/12.

Biogenic silica was analysed by extracting the amorphous silica by means of a two-step 2.5 h extraction with 0.5 M Na_2CO_3 separated by centrifugation of the leachates according to Fabrés et al. (2002). Si and Al contents of leachates were analysed with Inductive Coupled Plasma Atomic Emission Spectrometer (ICP-AES). The Si content of the first leachate was corrected by the Si/Al ratio of the second one, and corrected biogenic Si concentrations were transformed to opal by multiplying by a factor of 2.4 (Mortlock and Froelich, 1989).

Abundance of the lithogenic fraction was obtained by subtracting from the total mass the part corresponding to major biogenic components, assuming that the amount of lithogenics (%) was = 100 − (%OM + %$CaCO_3$ + %opal).

3.6. Calculation of lateral fluxes of suspended sediment

Advection of suspended matter in Avilés Canyon and in the slope west to the canyon has been calculated from data acquired by the current and turbidity meters deployed near the bottom. Recorded Nephelometric Turbidity Units (NTU) have been converted to suspended sediment concentration (SSC) using Eq. (4) by Guillén et al. (2000):

$$\mathrm{SSC}\ (\mathrm{g\ m^{-3}}) = 1.74 \cdot \mathrm{Turbidity}\ (\mathrm{NTU}) - 1.32 \quad (4)$$

SSC has been multiplied by current speed to obtain the magnitude (in g m^{-2} s^{-1}) of lateral fluxes (LF).

4. Results

4.1. Morphology of the Avilés Canyon

The Avilés Canyon is incised about 25 km in the central Cantabrian continental shelf, which is 45 km wide west of the canyon but only 13 km wide ahead of the canyon tip located 18 km WNW of the large coastal promontory of Cabo Peñas (Fig. 1). The tip of the canyon is at 130 m water depth and opens to a canyon head and upper course that display three sharp bends probably related to the underlying tectonic lineations (Lastras et al., 2012). Several tributaries join the Avilés Canyon upper and middle course, mostly through its western flank at axial depths ranging between 1300 and 2100 m (Fig. 1). The group named La Vallina branches includes four main tributaries, which are SW–NE oriented and also markedly incised on the shelf (Fig. 2a–c). With the only exception of the western most branch, La Vallina branches are straight or nearly straight. The two eastern branches show smoothened right flanks along the length incised in the continental shelf, which oppose to gullied left flanks (Fig. 2b and c). In the two western branches, the two flanks look moderately smoothened with some gullies occurring locally. The lower Avilés Canyon is SSW–NNE oriented and its increasingly wide floor is interrupted by a series of overdeepenings (Lastras et al., 2012). The Avilés Canyon mouth opens to the Biscay abyssal plain in an area occupied by a faint sedimentary wave field (Gómez-Ballesteros et al., 2013).

4.2. External forcings

Nalón River discharge time series show increased values in early February 2012 (up to 1071 m^3 s^{-1}), mid April 2012 (602 m^3 s^{-1}), late January 2013 (853 m^3 s^{-1}), and late March 2013 (669 m^3 s^{-1}). Other less marked increased discharge episodes occurred in November and December 2012 (up to 300 m^3 s^{-1}) and February–March 2013 (up to 484 m^3 s^{-1}) (Fig. 3a).

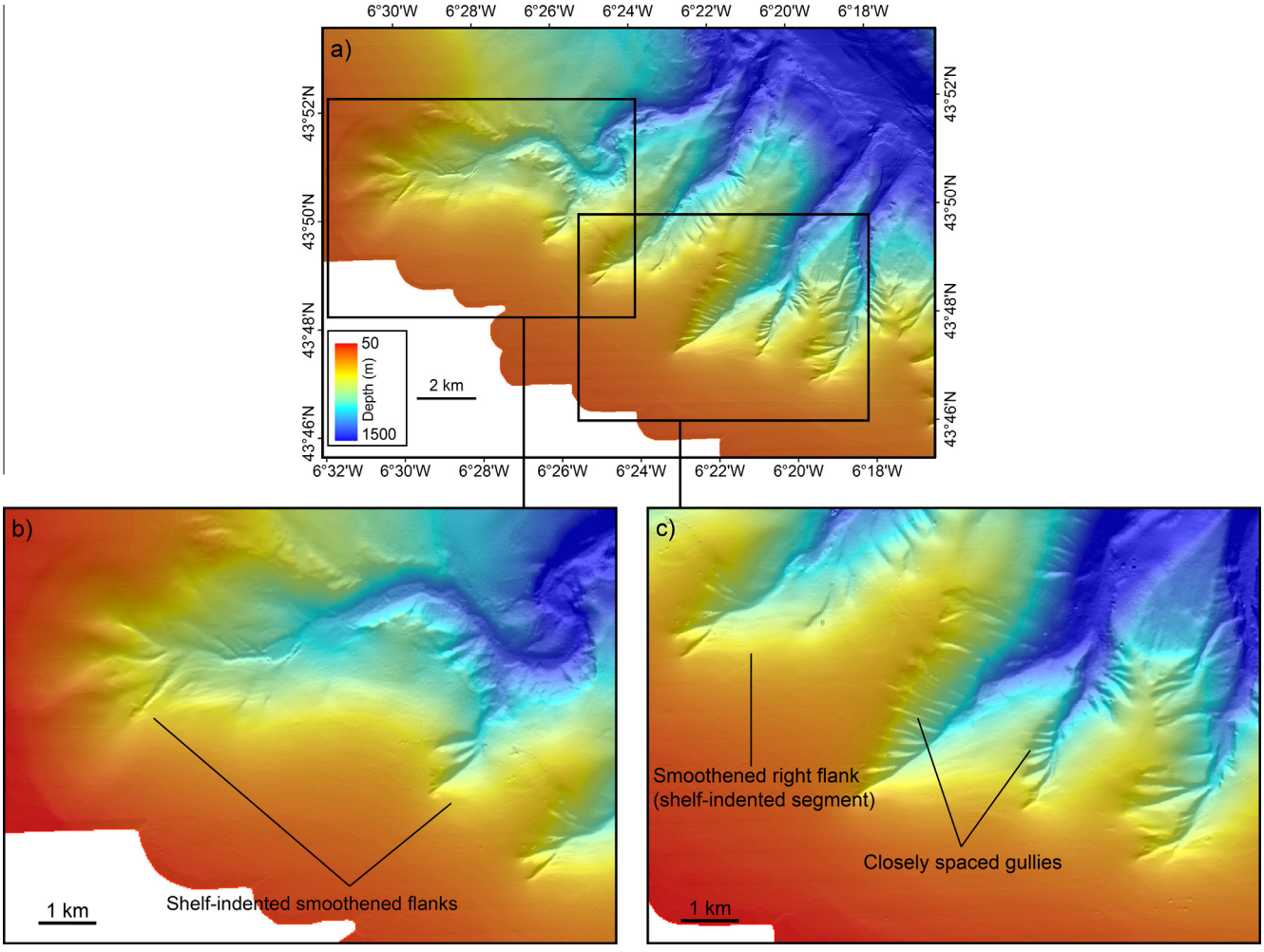

Fig. 2. Shaded relief images of tributaries entering the Avilés Canyon from its western flank. (a) General view of tributaries incised in the western flank of the Avilés Canyon middle course and lower upper course. (b) Zoom in of La Vallina westernmost branch showing a dominantly smoothened relief. (c) Zoom in of a set of La Vallina branches showing a smoothened relieve mainly of the right flanks of shelf-incised segments. Note the presence of some flank gullies locally forming closely spaced sets. See Fig. 1 for location. (For interpretation to colour in this figure, the reader is referred to the web version of this article.)

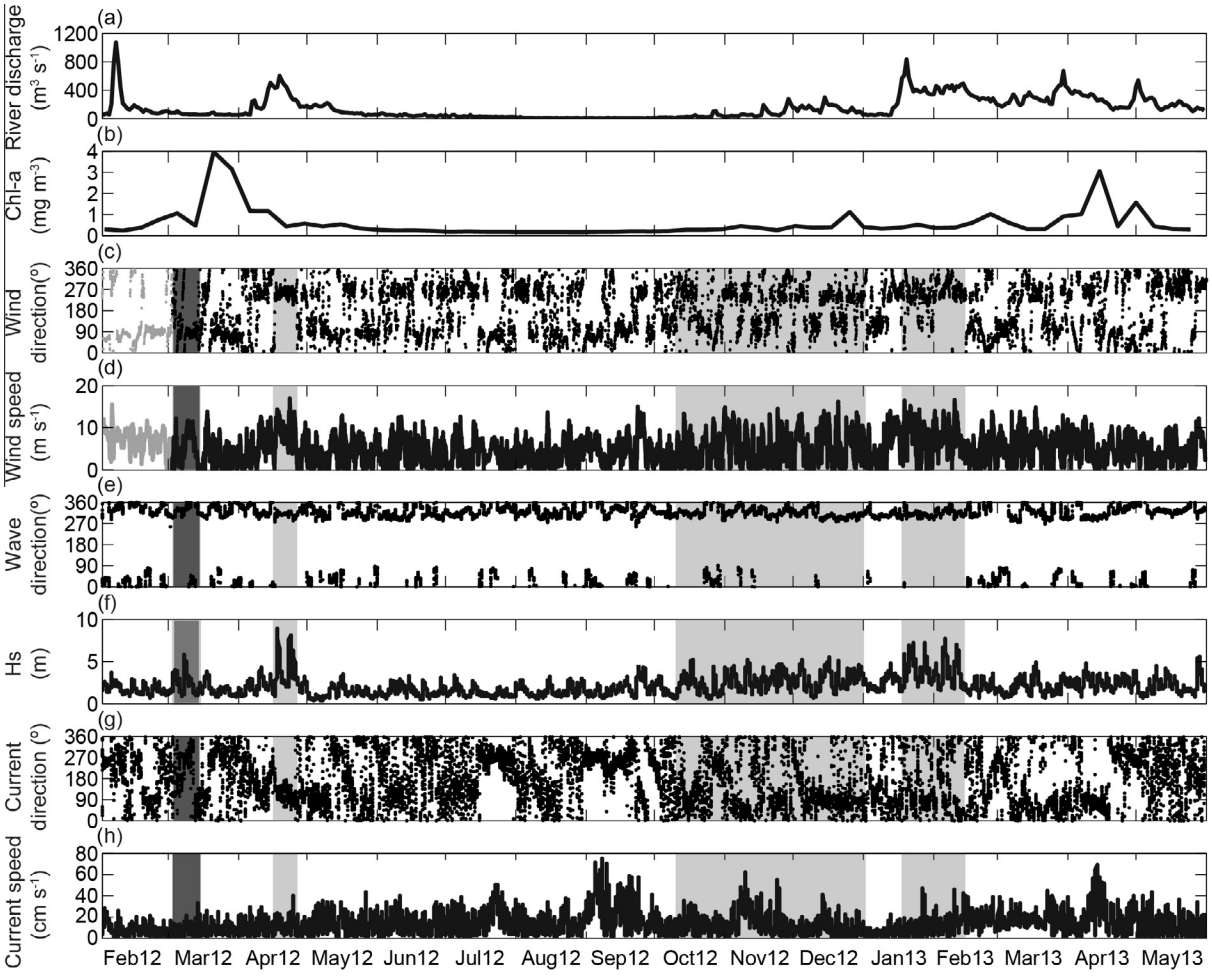

Fig. 3. (a) Water discharge of Nalón River encompassing the studied annual cycle (March 2012–April 2013). (b) Temporal evolution of monthly mean Chlorophyll-a concentration centred over the Avilés Canyon. (c) Wind direction at Cabo Peñas coastal buoy with dots representing the direction from which the wind is blowing. (d) Wind speed. (e) Wave direction at Cabo Peñas coastal buoy with dots representing the direction from which the waves are arriving. (f) Significant wave height (Hs) at Cabo Peñas Seawatch coastal buoy. (g) Current direction measured by the currentmeter installed in the Cabo Peñas buoy at 3 m depth. (h) Current speed at 3 m depth measured by the currentmeter of the Cabo Peñas buoy. Note that wind direction and speed records start about one month later (in grey data from the WANA point 1053075, see location in Fig. 1) than wave and current data due to a technical failure of the buoy's meteorological sensors. Shaded areas highlight specific events discussed in the text.

High Chl-a concentrations during March 2012 and April 2013 (Fig. 3b) correspond to the well-known seasonal phytoplankton spring bloom in the region (e.g. Fernández and Bode, 1991).

The wind regime during the entire monitoring period from March 2012 to March 2013 is characterized by a recurrent alternation between easterly and westerly winds as a response to the coastal polarization of winds (Fig. 3c). Higher wind speeds were recorded during westerly wind bursts (Fig. 3c and d). However, there were also several periods of strong winds with an important meridional component (such as December 2012, Fig. 3c and d). Wave direction (i.e. the direction from which waves arrive to the study area in degrees counted clockwise from the geographical North) shows a marked northwest component during the studied period (Fig. 3e). Maximum significant wave heights (Hs) were recorded in mid April 2012 and during late January–early February 2013 (Fig. 3f) under predominant westerly winds.

4.3. Spatial distribution and variability of mass fluxes

The time series of vertical TMFs recorded in the sediment traps deployed in the Avilés Canyon and on the nearby open slope are shown in Fig. 4. TMFs fluctuate at least one order of magnitude within all stations.

At the WS1200 (near-bottom) open slope station west of Avilés Canyon, TMFs reached a maximum of 11.94 g m^{-2} d^{-1} in March 2012, whereas during the rest of the experiment, values remained below 1 g m^{-2} d^{-1}, with a minor increase in autumn 2012 (Fig. 4a).

In the Avilés Canyon middle course AC2000 station, TMFs increase with increasing trap depth. At the near-bottom level (AC2000B), higher fluxes occurred during the mid-end of winter and in spring (15.65 g m^{-2} d^{-1} in April 2012, which represents the top value of TMFs recorded in all stations, and up to 5.24 g m^{-2} d^{-1} in February 2013). Relatively low fluxes were recorded during the rest of the year (between 0.19 and 2.12 g m^{-2} - d^{-1}) (Fig. 4b), although a continuously increasing trend in TMF took place from October 2012 until almost the end of the experiment. In contrast, in the upper level (AC2000T), TMFs varied from a maximum of 2.57 g m^{-2} d^{-1} in April 2012 to a relative minimum of 0.047 g m^{-2} d^{-1} in July 2012. In October 2012 TMFs increased again until reaching a second relative maximum of 0.74 g m^{-2} d^{-1} in November and December 2012. From December 2012 to the end of the experiment, TMFs decreased progressively to 0.046 g m^{-2} - d^{-1} recorded in February 2013 (Fig. 4b). In comparison with the deeper AC2000B trap, variability in TMFs at the shallower AC2000T is much smaller.

When compared with previous stations the TMFs at the near-bottom AC4700 canyon lowermost course station are much lower,

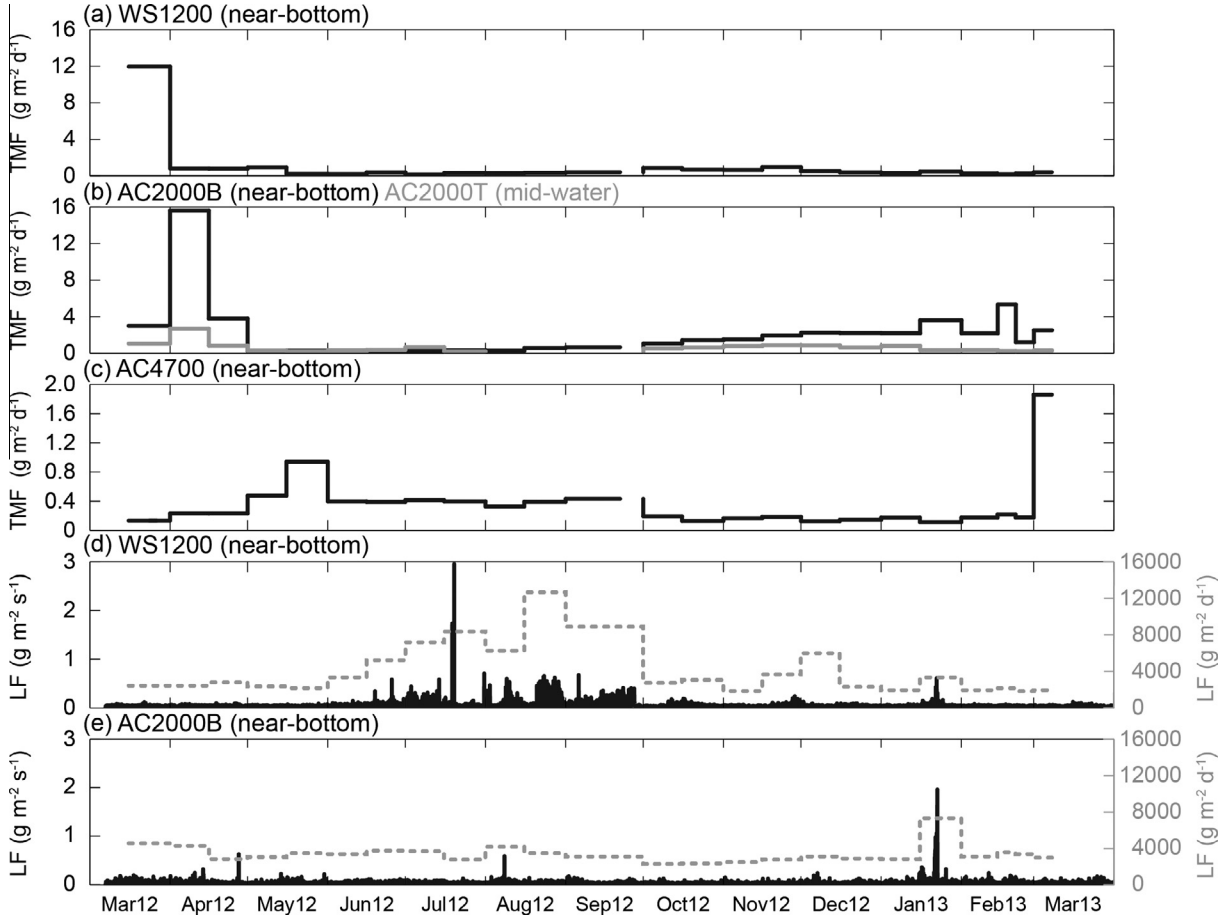

Fig. 4. Total mass fluxes (TMF) and lateral fluxes (LF) in the mooring stations deployed within the Avilés Canyon and on the open upper slope to the west. (a) TMFs at the open upper slope station WS1200 (near-bottom) west of the canyon. (b) TMFs in the middle course station for levels AC2000B (black stepped line, near-bottom) and AC2000T (grey stepped line, mid-water). (c) TMFs in the lowermost canyon course station AC4700 (near-bottom). (d and e) LFs at WS1200 (near-bottom) and AC2000B (near-bottom) in black. The grey dashed line represents re-sampled lateral fluxes adjusted to time steps equal to the sampling interval of the sediment traps.

usually around or below 0.35 g m^{-2} d^{-1}, except for two peaks of up to 0.94 and 1.86 g m^{-2} d^{-1} recorded in May 2012 and March 2013, respectively (Fig. 4c).

The ANOVA analysis shows that the interaction between the month of collection and the trap depth are the main source of variance in the studied area (31%). The month of collection by itself is also significant, representing 21% of the overall variability, which by extension suggests that the variability in TMFs mostly relates to the seasonality of the external forcings. Therefore, these two variables account for 52% of TMFs variability. However, 40% of the variability remains unexplained (residual) (Table 2).

As shown in Table 3, the highest correlation coefficient (>0.7) between time series of external forcings and TMFs corresponds to wave height and wind speed at time lag 1 (15 days) for the mid-water (~1200 m of water depth) trap AC2000T. Good correlation coefficients (~0.6) are also found for these two variables again at time lag 1 for the near-bottom (1954 m of water depth) trap AC2000B. There is a good correlation (~0.7) for the same middle canyon station AC2000 at both levels, mid-water and near-bottom, with total river discharge at time lag 3 (45 days). At the near-bottom, western open slope trap WS1200 the correlation of TMFs and the three variables considered in Table 3 is weaker (~0.4–0.5) and occurs at time lag 2 (30 days) for wave height and wind speed and at time lag 4 (60 days) for total river discharge. Except for wind speed, high cross-correlation coefficients between AC4700 and the external forcings in Table 3 have been found at negative time lags, which are non-representative and therefore will not be considered in the discussion.

LFs are markedly different in the near-bottom stations WS1200 and AC2000B (Fig. 4d and e). In the open slope station WS1200, LFs show a background level close or slightly above 0.05 g m^{-2} s^{-1} and below 0.1 g m^{-2} s^{-1} during most of the time, with some spikes from

Table 2
Results of the three-way ANOVA performed on total mass fluxes (TMFs). The sum of the squares (SS), the degree of freedom (DF), the relative contribution to the overall variability of TMFs of each of the factors considered, and the *F* value and its probability "*p*" are presented.

Factors	SS	DF	% Total variability	*F*	*p*
Trap depth	5.22E+08	2	8	134.23	<0.001
Month of collection	1.35E+09	11	21	134.23	<0.001
Trap depth * month of collection	1.99E+09	22	31	46.60	<0.001
Residual (unexplained)	2.53E+09	1303	40		
Total	7.67E+09	1338	100		

Table 3
Overall cross-correlation coefficients between time series of external forcings and total mass fluxes during the studied period. Each time lag unit corresponds to 15 days.

Station		Wind speed	Wave height	Total river discharge
WS1200	Correlation coefficient	0.458 (lag 2)	0.459 (lag 2)	0.507 (lag 4)
AC2000T (mid-water)	Correlation coefficient	0.716 (lag 1)	0.722 (lag 1)	0.681 (lag 3)
AC2000B (near-bottom)	Correlation coefficient	0.626 (lag 1)	0.639 (lag 1)	0.667 (lag 3)
AC4700 (near-bottom)	Correlation coefficient	0.73 (lag 0)	0.68 (lag −3)	0.69 (lag −3)

June to September 2012 and in January 2013. The most prominent of them occurred in July 2012 reaching 3 g m^{-2} s^{-1} (Fig. 4d). It was also in January 2013 when peak LFs (up to 2 g m^{-2} s^{-1}) were recorded in station AC2000B, where a few minor spikes are also visible (e.g. at the end of April 2012 and in the first half of August 2012, both with 0.6 g m^{-2} s^{-1}) above a similar background level than in WS1200 (Fig. 4e).

4.4. Mean composition of particle fluxes and changes through time

Lithogenics clearly dominate settling particles at all stations, with averaged annual values between 53.05% and 66.98%, and fluxes around 0.17 and 1.37 g m^{-2} d^{-1} (Table 1). The temporal variability of the lithogenic content is quite similar between all stations but AC2000B (Fig. 5a), with higher values during autumn and winter (i.e. from September 2012 to February 2013) and lower values during spring and summer (i.e. from March 2012 to August 2012). AC2000B shows the highest averaged annual value and also the lowest range of interannual variation (i.e. from 62.42% to 74.11%) (Fig. 5a and Table 1). The lithogenic contribution to TMFs is never less than 37% (Fig. 5a). On average it is almost six percentage points lower in AC2000T (mid-water) than in AC2000B (near-bottom), and fourteen percentage points lower in AC4700 (near-bottom) than in AC2000B. This results evidence a decrease in the percentage of lithogenics with, first, increasing distance to the seafloor and, second, increasing canyon depth.

Annualy averaged $CaCO_3$ fluxes are lower than lithogenics, ranging between 0.12 and 0.47 g m^{-2} d^{-1} (Table 1). $CaCO_3$ relative contents display a trend opposite to the lithogenics one, with lower percentage values during autumn and winter (i.e. from September 2012 to February 2013) and slightly higher values during spring and summer (i.e. from March to August 2012) (Fig. 5b). Higher variations were recorded during spring especially at the lowermost canyon and open western slope, where the $CaCO_3$ annualy averaged percentage is the highest among all traps. Similarly to the lithogenics, AC2000B shows the lowest range of interannual variation (i.e. from 17.16% to 30.7%), in parallel with the lowest annually averaged value, close to the one of AC2000T, with 24.42% and 24.93%, respectively (Fig. 5b and Table 1). For the two near-bottom traps deployed inside the canyon, the $CaCO_3$ annual mean content increases with water depth, being about ten percentage points higher at the lowermost canyon (AC4700) than in the middle canyon (AC2000B) (Table 1). It is noteworthy that during the second half of the studied period, $CaCO_3$ records in all traps present a rather similar evolution.

OM fluxes are relatively low, with averaged annual values ranging from 0.025 to 0.14 g m^{-2} d^{-1} and averaged percentages around 8–10% (Table 1). The atomic N to OC ratio (N:OC), which is widely used to examine OM sources and source changes in settling particles, is on average ~0.11 for all traps (Fig. 5c). Our time series show enhanced N:OC ratios (0.12–0.16) and OM relative abundance (16–18%) at station WS1200 in May 2012 and March 2013, thus indicating a marked spring seasonal signal on settling particles at this station. Similar variations were recorded at the upper trap AC2000T of station AC2000 (Fig. 5c), which also displays the highest annual OM contents (Table 1). Both traps, WS1200 and AC2000T, are in the 1150–1200 m depth range below the sea surface (Table 1). In contrast, settling particles at the near-bottom traps AC2000B and AC4700 within the canyon show rather stable N:OC ratios and OM relative abundances (around 0.8–0.13% and 6.5–8.6%, respectively), with only minor fluctuations except for a peak recorded at AC4700 in June 2012 (reaching 12%). By the end of the time series OM contents at all traps and stations reached minimum values to start increasing again till the end of the sampling period in March 2013. This increase was particularly important at WS1200 and AC2000T (Fig. 5c). The parallelism of the OM records for these two traps is noticeable and, except for the above-mentioned final part of the time series, they do not seem to be correlated with the near-bottom traps AC2000B and AC4700 (Fig. 5c).

Averaged annual opal fluxes range between 0.017 and 0.09 g m^{-2} d^{-1} (Table 1) and opal relative abundance shows different patterns depending on mooring location and water depth (Fig. 5d). At the two traps in the same depth range below the sea surface, the western open slope WS1200 (near-bottom) and the AC2000T (mid-water) over the middle canyon, opal content shows an obvious temporal variability peaking up at 12% in March 2012 and March 2013. In the other two, in-canyon, near-bottom traps AC2000B and AC4700, opal contents do not show a clear seasonal signal and the fluctuation rate is much lower, especially for AC2000B (Fig. 5c). Similarly to OM, enhanced opal relative abundances were recorded by the end of the observational period at all stations, weakly at AC2000B and strongly at WS1200 and AC2000T. Contribution of opal relative abundance to the total mass does not represent more than 15% at any trap, and opal mean annual content remains in the range from 2.20% to 4.36%, with the lowest and highest values corresponding to the near-bottom canyon traps AC2000B and AC4700, respectively. WS1200 and AC2000T display very similar values (3% and 3.09%).

5. Discussion

5.1. Particle sources and dispersal patterns

Our results show the dominance of river-sourced lithogenics in sinking particles in the study area. Quartz, feldspars, heavy minerals and aluminosilicates mainly constitute these particles. The dispersion of riverine water and lithogenic particles in the vicinity of the Avilés submarine canyon appears to be affected by seasonal reversals of sea surface circulation. During autumn and winter, the prevailing westerly winds induce an eastward shelf-slope circulation associated with downwelling conditions, which pushes sediment-loaded river plumes away from Avilés Canyon to the east, towards Cabo Peñas and beyond, as shown in the MODIS image of 21 January 2013 (Fig. 6a). Eastward surface currents associated with an onshore surface Ekman transport may also lead to the coastal confinement of river plumes, as also shown in Fig. 6a. Below the surface layer where Ekman transport occurs, there must be a compensatory circulation, directed in opposite sense. Downwelling conditions due to westerly wind forcing will then lead to an eastward shelf current that (if interacting with the bottom, which is generally the case under winter high energy conditions) corresponds to offshore transport in the bottom Ekman layer. This

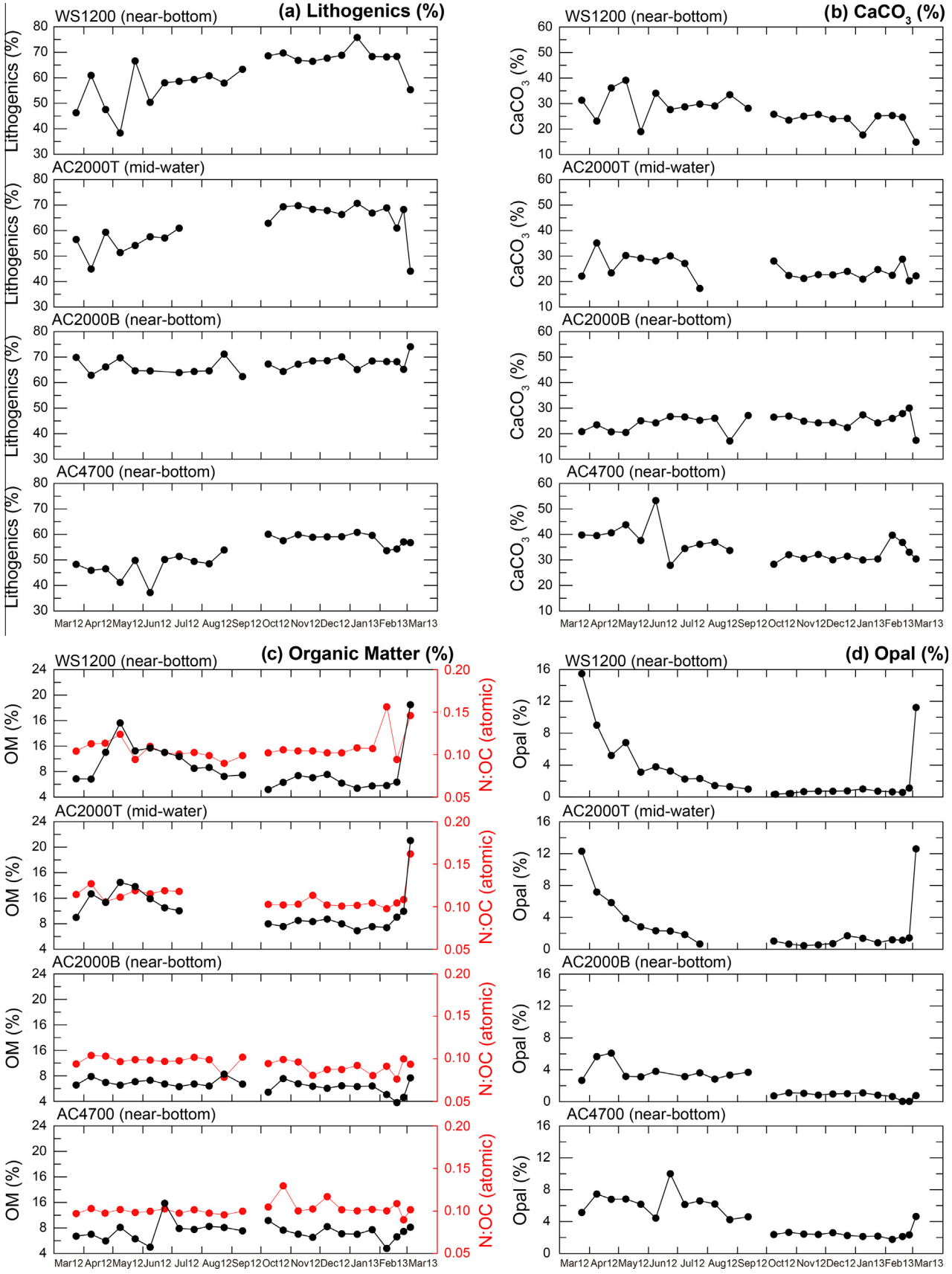

Fig. 5. Temporal variability of the main components of the settling particle fluxes collected by the sediment traps in the mooring stations deployed within and on the open slope west of Avilés Canyon during the studied annual cycle (March 2012–April 2013). (a) Lithogenics. (b) $CaCO_3$. (c) Organic matter (black dots), molar nitrogen:organic carbon ratios (N:C, red dots). (d) Opal. Codes of mooring stations and levels correspond to those in Figs. 1 and 5, and in Table 1. (For interpretation of the references to colour in this figure legend, the reader is referred to the web version of this article.)

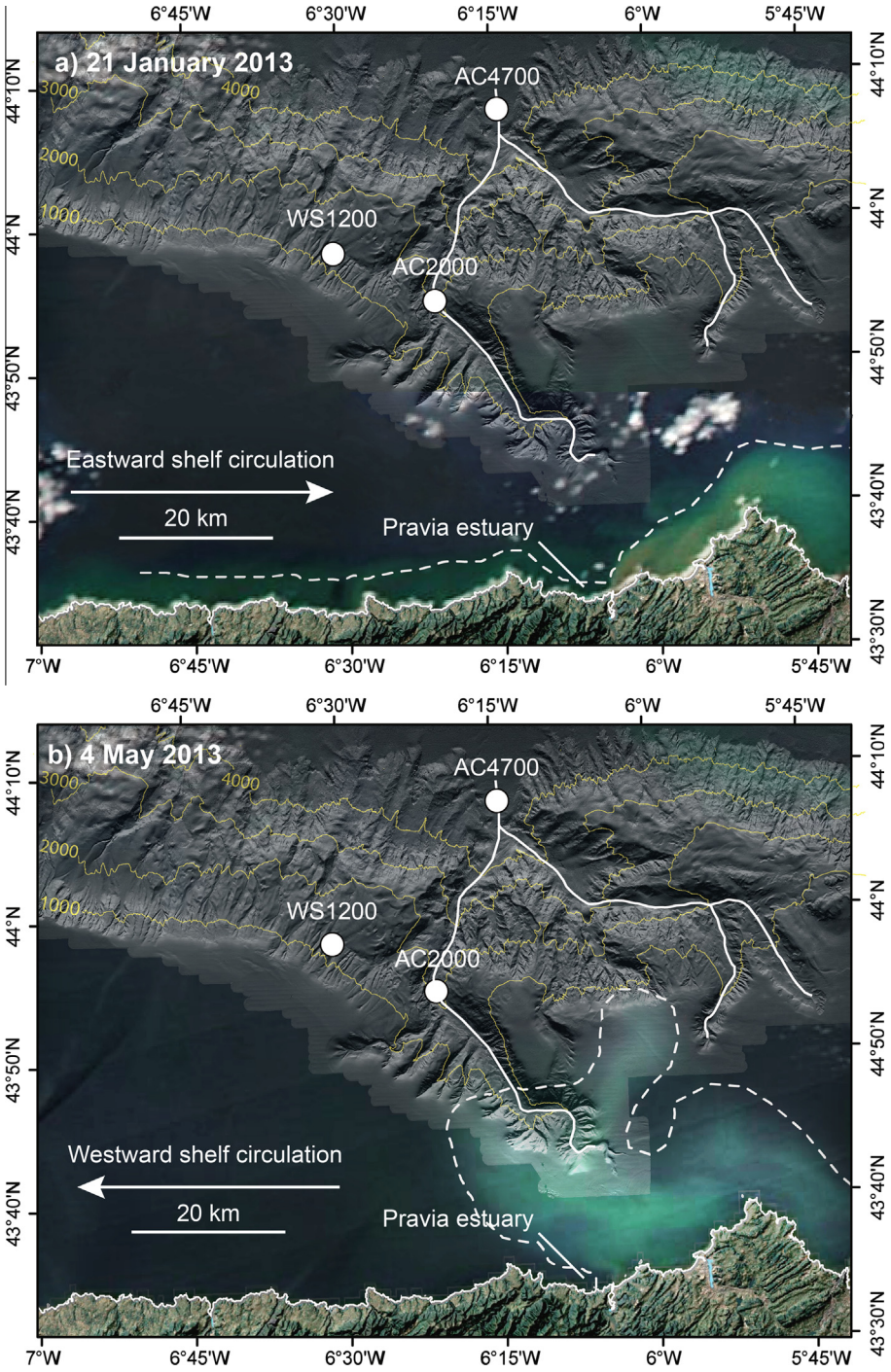

Fig. 6. Lance rapid response MODIS satellite true colour images from the NASA Earth Observing System Data and Information System (EOSDIS) with the shaded relief bathymetry of the Avilés Canyon and adjacent open slope as background layer. White dots indicate the mooring sites. Dashed white lines follow the outer limit of coast-derived sediment plumes at sea surface. (a) Image from 21 January 2013 illustrating plume dispersal under a westward surface circulation. (b) Image from 4 May 2013 illustrating plume dispersal under an eastward surface circulation. (For interpretation of the references to colour in this figure legend, the reader is referred to the web version of this article.)

is because in a bottom Ekman layer the Ekman transport is directed to the right of the bottom stress, in the same way that in a surface Ekman layer the Ekman transport is directed 90° to the right of the wind stress in the Northern Hemisphere. However, given that the stress at the seafloor is in the opposite direction of the prevailing current, the bottom Ekman transport is 90° to the left of the surface current, with the Ekman spiral turning counterclockwise with increasing depth in the Northern Hemisphere (Taylor and Sarkar, 2008).

Westerly wind pulses also reinforce the entrance of the eastward-flowing poleward slope currents over the Cantabrian margin (e.g. González-Pola et al., 2005), which extend from the surface to about 250–400 m depth (Pingree and Le Cann, 1990; Gil and Gomis, 2008). On the contrarily, during spring and summer, with prevailing easterly winds, the shelf circulation is mainly westward (Charria et al., 2013). This surface currents are associated with an upwelling component capable of entraining river plumes and resuspended shelf sediments towards the shelf edge, as shown

in the MODIS image of 4 May 2013 (Fig. 6b), taken after an enhancement in the discharge of Nalón River (Fig. 3a). The same wind forcing then builds a westward coastal jet, which originates onshore transport at the bottom of the Ekman layer and thus favours the retention of resuspended sediments over the shelf. Similarly, in the nearby continental shelf of the Basque country to the east, Jouanneau et al. (2008) reported that prevailing winds and surface currents also redistribute preferentially suspended sediment river plumes, with particle settling occurring during periods of calm.

The relation between increases in river discharge (Fig. 3a) and TMFs in the Avilés Canyon and the western open slope (Fig. 4a and b) is an interesting point of discussion. Our dataset seems to suggest a connection between sustained high river discharge conditions from January to February 2013 and the increases of TMFs in near-bottom traps AC2000B and, AC4700 although the later being less clear and somewhat delayed (Fig. 4a–c). However, this connection is not apparent neither for AC2000T and WS1200 nor for other shorter events of enhanced river discharge, such as the one in April 2012, which apparently had no effect on TMFs in the shallower stations, as shown by high TMFs occurring before the discharge peak (Figs. 3a and 4a, b). The relation of the sharp discharge peak of February 2012 (Fig. 4a) with TMF peaks in early 2012 is also unclear, as the TMF largest peak appears in March in WS1200, which is far from Pravia estuary, and in April in the closer AC2000 at both levels, although with markedly different intensities (Fig. 4a and b). The March 2012 prominent peak in WS1200 is synchronous with a major chlorophyll-a peak under the dominance of easterly winds and resulting westward circulation. However, river discharge, wind speed, wave height and current speed were low during that time (Fig. 4). The composition of mass fluxes at WS1200 in March 2012 (Fig. 5) indicates a phytoplankton signal overprinted on the generally dominant lithogenic component (see Section 4.4).

Without totally precluding some direct connection between the river and the submarine canyon under specific conditions, it is worth considering other dispersion mechanisms that may act either by themselves or in combination with a more direct connection and among themselves. The normal winter mixed layer in the region hardly exceeds the depth of the shelf-break, as it is only about 250 m thick (González-Pola et al., 2007). Therefore, a direct influence of winter convective mixing events on sedimentary particle dynamics at depths where the moorings were deployed should not be expected and, at the most, can only be indirect and likely minor. Only exceptionally the mixed layer reaches larger depths (e.g. in 2005; Somavilla et al., 2009), thus increasing the chances to directly imprint sedimentary processes in the canyon. During winters 2012 and 2013 atmospheric forcings were not exceptionally strong and the mixed layer did not reach unusual depths (R. Somavilla, personal communication). Below the maximum winter mixed layer, the density gradient characteristic of the local permanent pycnocline (van Aken, 2001) may hinder the vertical transport of particulate matter, especially of the lighter fractions. In this context, processes favouring lateral advection of sediments from the shelf become good candidates for triggering major arrivals of river-sourced particles into the canyon. Our hypothesis is that river-sourced particles temporarily accumulate on the shelf until high-energy forcing conditions (see Section 5.2) capable to resuspend and lead to bottom Ekman layer transport carry them into the canyon. This involves a critical assessment of the bottom transport against the surface transport to avoid misleading interpretations (see Section 5.2.1). A similar mechanism of delayed transfer to the continental slope and submarine canyons has been described in other margin settings, such as the Gulf of Lion and the North Catalan margin, where dense shelf water cascading and eastern storms provide such high-energy conditions (Canals et al., 2006; Ulses et al., 2008a; Sànchez-Vidal et al., 2012).

Marine primary production is the second main source of sinking particles in the study area. In the shelf and offshore waters of the Cantabrian margin there is a seasonal succession of phytoplankton species that relates directly to the hydrographical variability (Fernández and Bode, 1994). In winter and spring, intense vertical mixing leads to a homogenized, nutrient-rich water column and noticeable diatom-dominated phytoplanktonic blooms (Fernández and Bode, 1994), as shown in March–April 2012 and April–May 2013 (Figs. 3b and 7). In contrast, in summer and autumn, reduced vertical mixing accompanied by enhanced solar heating leads to a nutrient-depleted stratified upper layer and low primary production. Under these conditions, dinoflagellates, which are able to migrate towards nutrient-rich layers, dominate the phytoplanktonic community (Fernández and Bode, 1994). Occasionally, upwelling alters the above-described hydrographic pattern by reinforcing vertical mixing, injecting extra inputs of inorganic nutrients to the surface layers and increasing primary production (González-Quirós et al., 2003). Upwelling events can be traced as intermittent cold-water tongues close to the coast, often nearby Cabo Peñas promontory, where topographic effects enhance this process (Botas et al., 1989). During the studied period, the spring primary production bloom in 2012 occurred mostly offshore in the central part of the Bay of Biscay, while in 2013 the bloom maximum was observed closer to the Cantabrian coast (Fig. 7). More persistent upwelling favourable conditions in 2013 than in 2012, especially from mid March to late April (Fig. 8), likely led to a higher supply of new nutrients close to the shoreline along the entire Cantabrian margin, thus resulting in a pronounced coast-parallel phytoplankton bloom (Fig. 7). A stronger and more constant river discharge during 2013 (Fig. 3a), also contributing new nutrients to the coastal area, could have also enhanced the coast-parallel primary production. It should be noted, however, that the algorithms used to estimate primary production are susceptible to interference caused by the complex optical properties of the constituents commonly found in coastal waters, where the influence of river outflows, riverine suspended sediments and dissolved OM may confuse the interpretation of satellite-based ocean colour data (Moreno-Madriñán and Fischer, 2013). Further elaboration on this aspect is hampered by the closure of the last collecting cup before the 2013 phytoplanktonic bloom.

The composition of settling particles allows defining two settling regimes. First, the record of the shallower sediment traps both on the open slope (WS1200, near-bottom) and the canyon middle course (AC2000T, mid-water) was markedly seasonal and showed relatively high contents of OM and opal, which most likely resulted from pelagic settling of biogenic particles. Second, the record of the near-bottom traps at the canyon middle and lowermost course AC2000B and AC4700 did not show any evidence of seasonality because of the dilution of biogenic components amidst more abundant, laterally advected lithogenic material. In the shallower environment including the mid-water AC2000T and the near-bottom WS1200 sediment traps, relatively high opal abundance (>12%) found in March 2012 (Fig. 5d) can be directly related to the pelagic settling of material derived from blooms dominated by oceanic tychoplanktonic diatoms and chrysophyceans with siliceous skeletons and/or cysts. It is noteworthy that in April 2012, 16–30 days after the opal peak at AC2000T, an increase is also observed at AC2000B (Fig. 5d). This suggests that particles settling at 1200 m of water depth most probably reached the seafloor. The 800 m of depth difference between AC2000T and AC2000B, and the 30 days of delay result in a siliceous skeletons and/or cysts sinking speed of about 26 m d^{-1}, which is within the range published by Asper (1987) for sinking diatom aggregates.

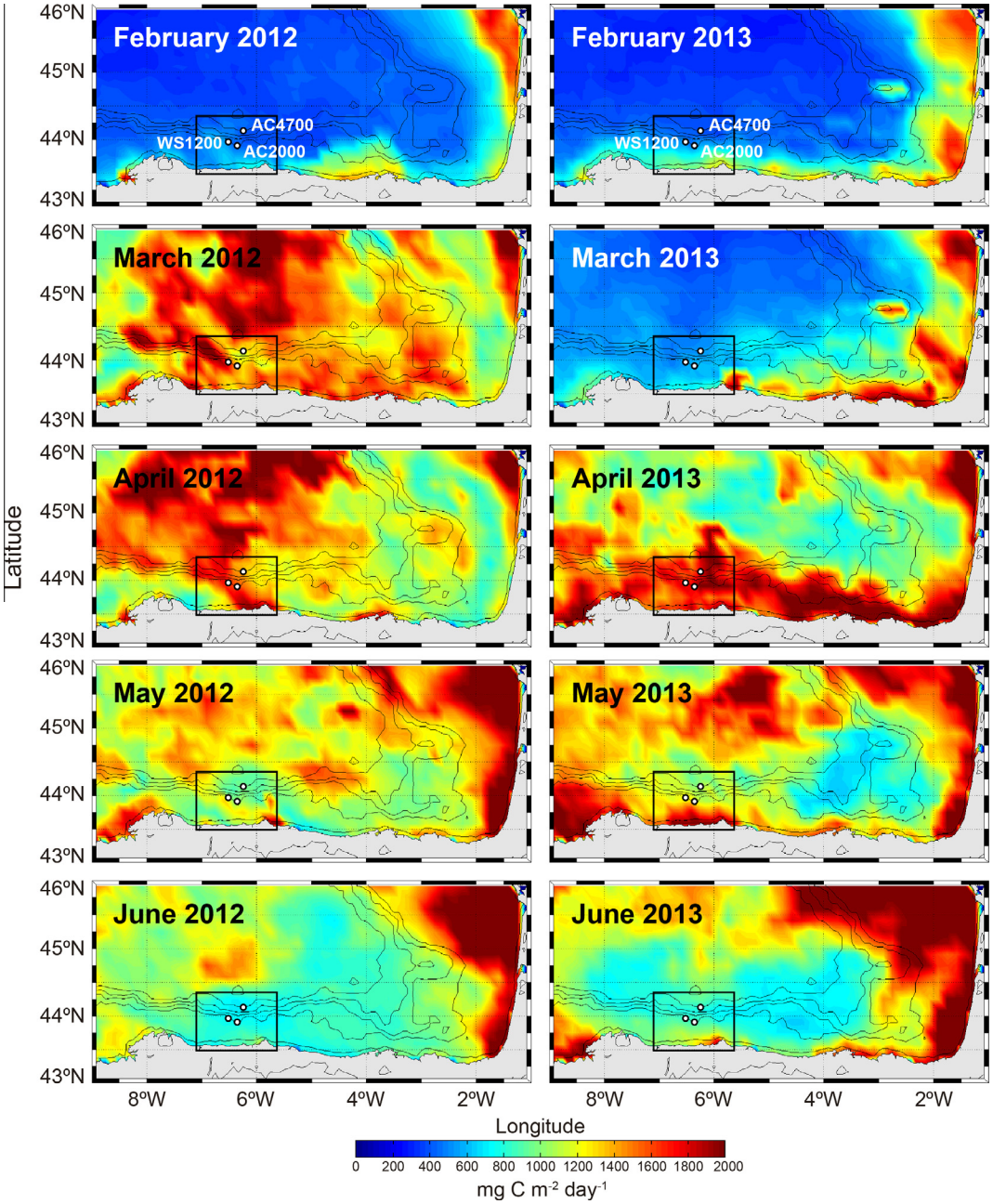

Fig. 7. MODIS-based net primary production maps (mg C m^{-2} d^{-1}) showing the development of phytoplanktonic blooms that occurred in spring 2012 and 2013. Black squares correspond to the area shown in Fig. 1 and white dots indicate mooring locations. (For interpretation of the references to colour in this figure legend, the reader is referred to the web version of this article.)

Following the opal peak in March 2012, an increase in OM relative abundance was also detected in May 2012 in the shallower WS1200 (near-bottom) and AC2000T (mid-water) traps. The OM peak following that in opal relative abundance can be explained by a growth response of consumers (zooplankton) after an increase in phytoplankton, which is in agreement with Stenseth et al. (2006). During this period, in the same two traps N:OC ratios were slightly higher than during most of the following fall and winter months, which according to the high N content of marine OM (N:OC > 0.12), might be a direct signal of the arrival of OM from marine algae. Slightly higher OM relative abundances were recorded from October to December 2012 at both WS1200 and AC2000T, which might be connected to an autumn phytoplankton bloom that may occur in the region during the transitional stage from stratification to mixing (Fernández and Bode, 1991). In September 2012, prevailing easterly winds and accompanying westward surface currents (Fig. 3c and g) led to a prolonged upwelling-favourable situation. This situation, jointly with some short-lived easterly wind episodes in October and November, might have favoured the nutrient replenishment of the surface layer and thus, phytoplankton growth. Bottom-up processes, driven ultimately by meteorological and hydrodynamic forcings, have been widely recognized as key factors in modulating phytoplankton growth and population dynamics (Margalef, 1978).

About the similarities in the evolution of OM relative contents of WS1200 (near-bottom) and AC2000T (mid-water), located at about the same depth (1150–1200 m) below the surface (see Section 4.4), it must be pointed out that both traps lie within the background flow of the slope currents (e.g. Pingree and Le Cann, 1990), which may help homogenizing OM relative contents because of

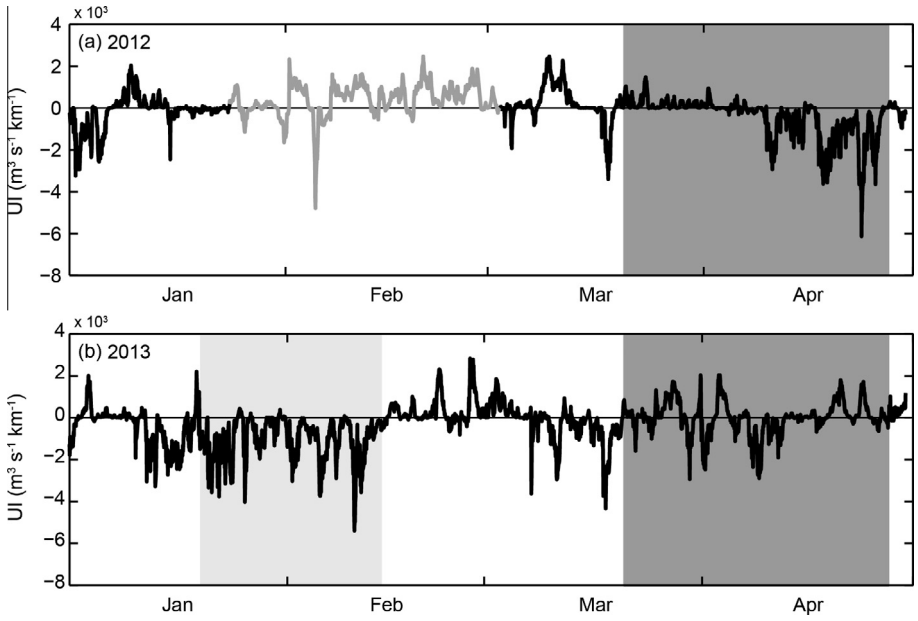

Fig. 8. Time series of upwelling index (UI) during (a) January to April 2012, and (b) January to April 2013. The grey line represents data from the WANA point 1053075. Shaded areas highlight specific events discussed in the text. Note that albeit we do not have particle flux data during January and February 2012, data on UI during such months have been included to note the more persistent upwelling favourable conditions during winter 2013 than during the previous winter.

along slope transport. The persistently high relative abundance of lithogenics in the near-bottom AC2000B trap (Fig. 5a) suggests a dilution effect of OM and opal biogenic particles. Higher opal relative abundance in AC4700 than in AC2000B and, for most of the time, the shallower traps (Fig. 5d), suggests a distinct behaviour of the lower canyon course, that seems to be more influenced by pelagic settling and less by advective transport from the inner continental margin. OM relative abundance is also slightly higher at AC4700 than at AC2000B during most of the time (Fig. 5c).

The lowermost canyon trap AC4700 is the one showing the highest relative content of $CaCO_3$ (Fig. 5b and Table 1), with the most prominent peak occurring in June 2012. The fact that this $CaCO_3$ peak is synchronous with OM and opal peaks (Fig. 5b–d) following three months of rather high primary production (Fig. 7) points to pelagic sedimentation of material derived from the spring phytoplanktonic bloom. This view is further supported by relatively high presence of foraminifera and pteropod shells in trap samples, which evidences a significant contribution of biogenic carbonate particles. Berner and Honjo (1981) reported a ~12% contribution of pteropod shells to the total carbonate flux in open ocean sites of the Atlantic Ocean. Given that labile organic material can be degraded while being transported to lower canyon environments (de Stigter et al., 2007; Pasqual et al., 2011), the higher $CaCO_3$ relative abundance at AC4700 probably results from a good preservation of pelagic carbonate shells. Furthermore, N:OC ratios also point to a marine, pelagic origin. It is to be noted that the calcium carbonate compensation depth (CCD) in the region is several hundred meters deeper (~5200 m) than the deployment depth of our deeper trap AC4700 (Biscaye et al., 1976), which prevents significant dissolution of $CaCO_3$ particles. Also some contribution of terrestrial, river-sourced $CaCO_3$ cannot be totally discarded, as Nalón River drains from limestone formations and advection processes might bring light carbonate particles to the outer continental margin.

Compared to other locations in the Bay of Biscay, peaks in TMFs in the upper open slope west of the Avilés Canyon (WS1200) are higher than, for instance, those recorded by Schmidt et al. (2009) in the western slope adjacent to the nearby Cap Ferret submarine canyon. Similarly, TMFs peaks in AC2000T and AC2000B are also higher than those recorded both in the water column (1350 m water depth, 950 m above the bottom) and near-bottom (at 2250 m water depth, 50 m above the bottom) by Heussner et al. (1999) in the mid Cap Ferret Canyon at 2300 m of water depth, where neither variability in river discharge nor in wind dynamics (see Section 5.2.1) seem to be related to the observed rapid changes (e.g. from 57 mg m^{-2} d^{-1} to 2630 mg m^{-2} d^{-1}) in particulate fluxes. Instead, variability in particle fluxes in the mid Cap Ferret Canyon seems to be mainly controlled by oceanographic forcing, namely short-term fluctuations of the along-slope current (Heussner et al., 1999). The links of atmospheric, oceanographic and other forcings with particle fluxes in the Avilés Canyon area are discussed in the next chapter.

5.2. Physical controls on particle fluxes

5.2.1. Storms

Increased wave height due to storms and their effects on the water column and on the resuspension of seabed sediments seem to be the main driver of TMFs temporal variability in the Avilés submarine canyon. This is supported by the good correlation coefficients (~0.6–0.7) of TMFs with wave height and wind speed at time lag 1 (15 days) for AC2000T and AC2000B (see Section 4.3), which also indicates that in terms of sediment dynamics the middle reaches of the Avilés Canyon respond relatively quick (15 days) to external forcings such as waves and wind. Given its shallower depth, it is to be supposed that the upper canyon reaches respond even faster. Such relationship is in agreement with observations made by several authors who have shown that submarine canyons ease the transport of particulate matter from coastal and shelf environments to the deep sea, often during storms associated to large wave heights and subsequent current intensification (Guillén et al., 2006; Palanques et al., 2008, 2009; Ulses et al., 2008b; Sànchez-Vidal et al., 2012). Other authors have also pointed out that in some continental margins, particles from the shelf reach the deep margin and basin after experiencing several cycles of deposition and resuspension (e.g. Palanques et al., 2012; Rumín-Caparrós et al., 2013).

The good correlation (~0.7) of both levels of AC2000 with total river discharge means that riverine inputs have a clear impact on TMFs in the Avilés Canyon mid course, although with some delay as this coefficient corresponds to time lag 3 (45 days). Several storm events occurred during the monitoring period. The first event took place in early March 2012 after a February increase in riverine discharge up to almost 1100 $m^3 s^{-1}$ (Fig. 3a), which likely resulted in the arrival of large amounts of particulate matter to the shelf. During this event, easterly winds up to 12 $m s^{-1}$ (Fig. 3c and d) coexisted with up to 6 m Hs swell waves from the NW–N quadrant reaching the study area (dark grey shaded area in Fig. 3e and f). The combination of easterly winds and high swell waves led to a surface westward shelf current peaking at 37 $cm s^{-1}$ (dark grey shaded areas in Fig. 3g and h), involving a westwards and offshore transport of particles in the surface Ekman layer. This situation favoured the surface advection and subsequent settling of particulate matter originating from the shelf into the Avilés Canyon down to depths of at least 2000 m eventually reaching also the open slope to the west towards La Vallina branches (Figs. 1, 2 and 4a). However, the transport in the bottom Ekman layer, should favour a shoreward flow thus hampering the bottom nepheloid layer to reach the shelf edge and beyond. The opposite situation occurred during the April 2012 and the late January–early February 2013 storm (see further down). This supports the relative importance of surface nepheloid layer transport vs. bottom nepheloid layer transport under different situations. The scenario described above explains why no significant LFs were recorded in AC2000B and WS12000 in March 2012 (Fig. 4d and e). It is worth referring here to the discrepancies between sediment trap-based vertical mass TMFs and turbidity sensor-based LFs (Fig. 4). This topic has been discussed often in the literature where discrepancies are attributed to the inefficiency of sediment traps to collect laterally advected particulate matter under high current speeds, and also to the presence of coarse particles that settle rapidly and give low turbidity readings (e.g. Gardner, 1989; Gardner and Walsh, 1990; Walsh and Gardner, 1992; Bonnin et al., 2008). The lack of data on the sizes of suspended sedimentary particles in our study area prevents us to further discuss this aspect.

The weaker correlation (~0.4–0.5) of TMFs during the studied period and the three variables considered in Table 3 for the near-bottom, western open slope trap WS1200, together with its fit with time lag 2 (30 days) for wave height and wind speed and time lag 4 (60 days) for total river discharge points to a different behaviour of the canyon and the upper open slope west of it. This also implies that, if affected by advection from the shelf, the open upper slope west of the Avilés Canyon will be impacted with a noticeable delay (eventually involving shifts in the meteoceanic conditions) and to a lesser extent than the Avilés Canyon mid (and probably upper) course.

A second, more severe storm was recorded in late April 2012, which was practically concomitant with a >600 $m^3 s^{-1}$ peak in riverine discharge (Fig. 3a) bringing river-sourced particles to the shelf. During this storm, western wind bursts of 17.1 $m s^{-1}$ (Fig. 3c and d) were accompanied by an 8-day period of waves from the northwest (light grey shaded areas in Fig. 3e) exceeding 8 m of Hs (Fig. 3f) that may have caused again shelf sediment resuspension adding to river-sourced inputs. Prevailing wind-driven surficial eastward shelf currents (light grey shaded areas in Fig. 3g and h) opposed to the arrival of shelf resuspended settling particles within the surface Ekman layer into the Avilés Canyon and its western open slope. It is noteworthy that during this storm an increase in raw near-bottom current speed up to 34 $cm s^{-1}$ occurred at AC2000B (Fig. 9). Filtered current speed also increased in WS1200, reaching a peak value of 10.8 $cm s^{-1}$. However, filtered current speed in AC2000B remained greatly unchanged despite the large increment of the raw velocity data. A possible supporting evidence of some near-bottom advection of particles during the April 2012 event is the small LFs spike in AC2000B. This suggests that part of the material supplied by the river and eventually resuspended from the shelf floor could have been transported offshore in the bottom Ekman layer having an impact initially restricted to the canyon upper and mid courses, which may explain the increase in LFs recorded in AC2000B (Fig. 4e). The lack of a concurrent increase in LFs in WS1200 is in agreement with the view of a different behaviour of the upper open slope compared to the canyon.

The concurrent though smaller peak of TMF in April 2012 at AC2000T (mid-water) is tentatively attributed to intermediate nepheloid layers detaching from the canyon head and upper course, or from the upper continental slope. Nepheloid layers spreading along isopycnal surfaces have been found at intermediate depths over the continental slope of the nearby Celtic Sea, where near-bottom nepheloid layers have been identified too (e.g. McCave et al., 2001). Several studies demonstrate that such nepheloid layers mainly result from particle resuspension triggered by storms associated to high waves and increased bottom currents, with internal waves eventually playing a role in such particle loading (e.g. Biscaye and Andersson, 1994; Durrieu de Madron et al., 1999; Bonnin et al., 2002; Puig et al., 2004b).

In an attempt to asses if sedimentary particles could be carried from the mid to the lowermost canyon reaches we built the progressive vector diagram in Fig. 10 using near-bottom raw (non-filtered) currents recorded at the location of AC2000B (near-bottom). We selected the period of April–May 2012 as it corresponds to the highest TMFs in the canyon mid course and also includes a significant storm and river discharge event, so that it could be considered representative of enhanced transport along the canyon. We also assume that the overall circulation pattern in the upper–middle canyon course (as represented by station AC2000) could be extrapolated to the canyon lowermost course. The composition depicted in Fig. 10 therefore represents the horizontal displacement that a particle should follow if the horizontal current field was homogenous in the study area. The plot shows that particles which on the 1st of April 2012 were at ~2000 m depth on the position of mooring AC2000 (AC2000B at 44 mab) could move horizontally roughly following the direction of the canyon from AC2000 to AC4700, and reach the position of AC4700 (still at ~2000 m depth) around the 10th of May 2012. This scenario is in agreement with the pattern of increments in TMFs in both stations, first in AC2000 in April 2012, and 30 days later in AC4700 (Fig. 4b and c). However, these results and their interpretation have to be taken with care, as the characteristics of the near bottom transit of particles would depend on the deeper circulation of Avilés Canyon, not necessarily connected to the circulation at upper layers. The lack of significance of cross-correlation coefficients between AC4700 and the external forcings in Table 3 points towards a different behaviour of the lowermost canyon compared to the shallower canyon reaches and open upper slope.

The significance of residual currents that can be derived from the hodograph in Fig. 10 is discussed further down within Section 5.2.2 on tidal currents.

A set of moderate storms with Hs never exceeding 5.4 m occurred from October to December 2012 (Fig. 3f). During this period, prevailing westerly winds (Fig. 3c) triggering eastward coastal currents (Fig. 3g) led to bottom Ekman transport directed offshore, likely contributing to the particle loading of bottom nepheloid layers in the mid and outer shelf and advecting particles in suspension towards the Avilés Canyon head, which were carried subsequently into the canyon upper and middle sections, as recorded by the progressive increase in TMF at AC2000B (near-bottom) (Fig. 4b). The fact that a slight increase in TMF is also observed at AC2000T suggests that in addition to the bottom nepheloid layer, also

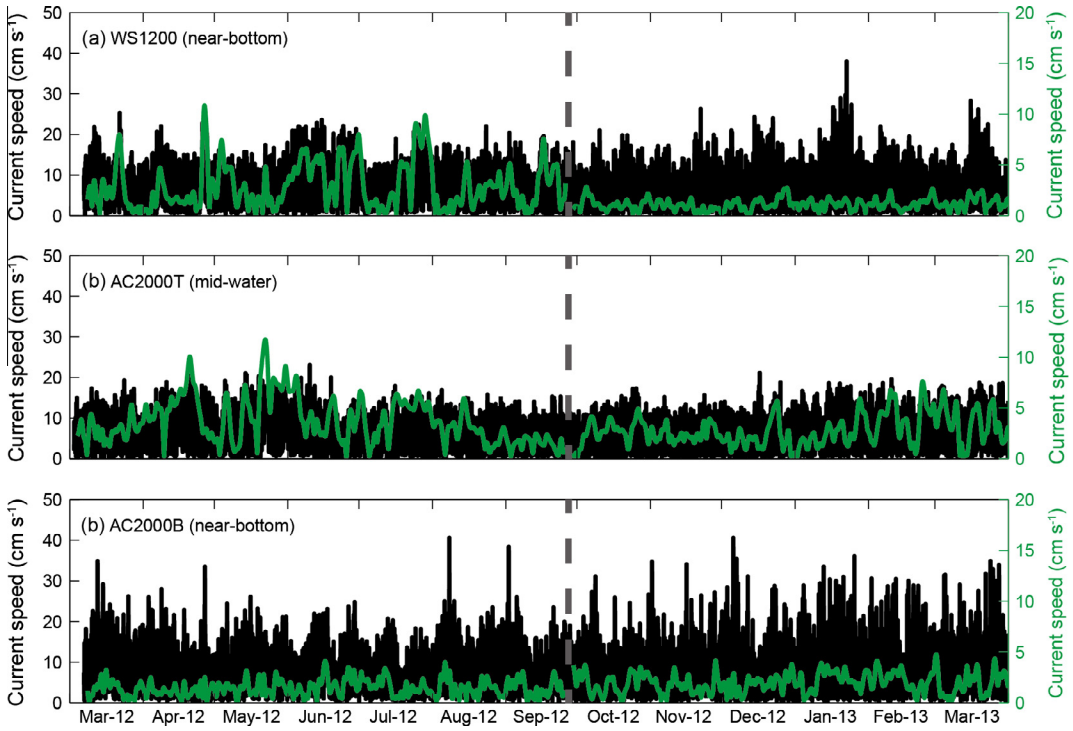

Fig. 9. Current speed (black line) and de-tided current speed (green line) over (a) the continental slope west of Avilés Canyon at 1200 m depth near-bottom (WS1200); (b) the Avilés Canyon middle course (AC2000T) at mid-water depth (1200 m); and (c) the Avilés Canyon (AC2000B) middle course near-bottom. The vertical grey dashed line marks the boundary between the two observational periods (see Section 3.3). (For interpretation of the references to colour in this figure legend, the reader is referred to the web version of this article.)

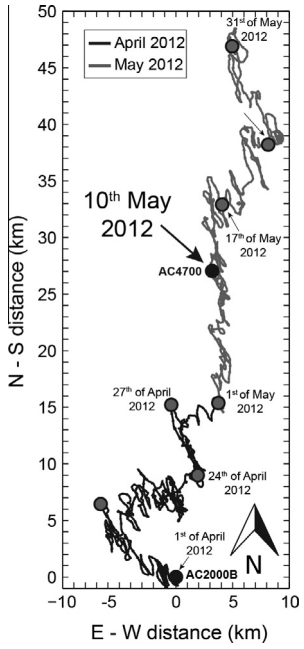

Fig. 10. Progressive vector diagram built after near-bottom raw (non-filtered) currents recorded at the location of AC2000B (near-bottom) in Avilés Canyon from 1 April 2012 to 31 May 2012. The position of the mooring stations in the middle canyon (AC2000) and the lowermost canyon (AC4700) is indicated with black dots.

intermediate nepheloids eventually detaching from the upper canyon and/or slope reached the location of AC2000 mooring station in the middle canyon (Fig. 4b). Durrieu de Madron et al. (1990) found that nepheloid structures extending seaward along isopycnals in the Gulf of Lion may increase the frequency of injection of sediment to the water column over the continental slope and sediment fluxes along submarine canyons.

The last stormy period with an impact on particle fluxes in the Avilés Canyon and the adjacent slope to the west lasted 27 days in January and February 2013. That event started synchronously with an increase in discharge of the Nalón River exceeding 800 $m^3 s^{-1}$, which likely resulted in the arrival of large amounts of material to the continental shelf (Fig. 3a). During this stormy period, westerly winds of about 18 $m s^{-1}$ blowing along the Cantabrian coast raised waves up to 7.5 m of Hs arriving from the northwest (light grey shaded areas in Fig. 3c–f), induced downwelling pulses (Fig. 8) and promoted an eastward Ekman surface transport (Fig. 6a). However, the eastward coastal currents that these wind conditions generate along the shelf, might also lead to bottom Ekman transport directed offshore, potentially advecting sediments into the canyon head and slope as indicated by LF increases up to 1.97 and 0.61 $g m^{-2} s^{-1}$ in AC2000B and WS1200, respectively (Fig. 4d and e).

Unlike the storm of late April 2012, this one was not accompanied by an increase in near-bottom filtered current speed in WS1200 (Fig. 9a), where the current meter provided negligible low-passed Godin $(A^2A_{25})/(24^225)$ currents (Godin, 1972), likely because it fell in a gully during the second deployment period from September 2012 to March 2013, thus lying in the shadow of along-slope currents. A 70 m deeper deployment depth during the second period compared to the first deployment period supports this view. Noticeably, raw near-bottom current speed (amplitude of tidal currents) reached the highest value (39 cm s^{-1}) in late January 2013 in WS1200. However, the location of the mooring obscures establishing the link between this increase and the passage of the stormy period here described.

Vertical TMFs also augmented in AC2000B during the occurrence of the January–February 2013 storm and shortly after up to a maximum of 5.24 $g m^{-2} d^{-1}$ by mid-February, following the

above-mentioned increase in LFs in January (Fig. 4b and e). Within this stormy period, filtered currents were also rather low in AC2000B, similarly to WS1200, while raw near-bottom currents were fluctuating markedly around a mean value close to 22 cm s^{-1}, peaking at 37 cm s^{-1} (Fig. 9a and c). The increase in LFs and TMFs at AC2000B is interpreted as indicative of the arrival to the mid Avilés Canyon of bottom nepheloid layers triggered by the storm and increased river discharge, which further supports the offshore transport hypothesis in the bottom Ekman layer. Our observations also indicate that the nepheloid layers entering the canyon had practically no impact on TMFs in the open slope to the west (Fig. 4a). It is also plausible that the bottom nepheloid layer has been supplied by particles settling down from intermediate nepheloid layers. The peak values in TMFs recorded in early March 2013 at AC4700 could also be related to the transfer of the storm signal from AC2000B downcanyon (Fig. 4c). The higher contents of lithogenics at AC4700 during the second deployment period (September 2012 to March 2013) compared to the first one (March to September 2012) (Fig. 5a) support this view, as such higher values could be interpreted as a result of the set of moderate storms from October to December 2012 and the January–February 2013 storm, with concomitant increases of TMFs at AC2000B (Fig. 4b). The downcanyon propagation of bottom nepheloid layers, eventually leading to intermediate nepheloid layers too, has been noticed in other submarine canyons around Iberia, such as the Nazaré Canyon (van Weering et al., 2002; Martín et al., 2011).

The coastal downwelling conditions in early 2013, together with the concurrent increase in river discharge (Fig. 3a) and the phytoplankton bloom near Cabo Peñas and more generally along the coastal area, already visible in March 2013 (Fig. 7), help explaining the enrichment in OM and opal visible in all stations by March 2013 (Fig. 5c and d). In addition to the general meteorological and hydrological conditions in the Bay of Biscay, it is likely that the new nutrients brought by the sustained high river discharge from mid-January 2013 onwards by Nalón River (Fig. 3a) and also other Cantabrian rivers (data not shown) contributed to the coastal phytoplankton bloom starting in March 2013 and continuing for the following months (Fig. 7). The overall situation would have resulted in the formation of turbid layers enriched in biogenic constituents that were spreading over the margin at various levels, eventually eased by Ekman intermediate and bottom transport, including nepheloid layers detaching from the seabed at certain depths. The impact of the OM and opal-rich turbid layers extending over the continental margin was, however, much larger at mid depths, both in the water column and near-bottom (i.e. ~1200 m of water depth) and not restricted to the canyon, as shown by the records of traps AC2000T and WS1200. This impact was much lower, though it was still visible, in the deeper near-bottom traps AC2000B and AC4700 in the mid and lower canyon (Fig. 5c and d). The marine algal contribution to the particle load was especially remarkable at mid depths, as indicated by the prominent increases in the N:OC ratios at AC2000T and WS1200 traps, likely resulting from downwelling and pelagic settling. Such a signal, however, barely reached the deeper levels either because of consumption, dilution or retention at shallower levels (e.g. at density boundaries).

Overall, our set of observations indicates that the direction of wind, especially when it blows over a threshold of 12 m s^{-1} (Fig. 3d), and the wind-triggered currents determine whether river-contributed and resuspended shelf particulate matter reaches Avilés Canyon or not, and if this occurs mostly at surface, intermediate or near-bottom levels (Fig. 11). Clearly, there are two contrasting situations: (i) during westerly wind conditions an eastward shelf circulation is established and sea surface plumes tend to pile up along the coast while the Ekman bottom transport can carry sedimentary particles offshore; and (ii) during easterly wind conditions a westward shelf circulation is established and sea surface plumes can move over the canyon head and upper course while the bottom nepheloid layer would be pushed shoreward.

According to Ruiz-Villarreal et al. (2004), during the upwelling season eased by the prevailing easterly winds in spring–summer, mean westward flows would enhance upwelling over the head and upper reaches of the Avilés Canyon. This situation may enhance the westwards and seawards transport of particles in the surface Ekman Layer and thus, the advection and subsequent settling of particulate matter from the shelf into the Avilés Canyon and the open continental slope west of it (Fig. 11). Following the same authors, during the downwelling season induced by the prevailing westerly winds in autumn–winter, near-bottom flows in the upper reaches of the Avilés Canyon are variable but directed offshore, which would enhance the propagation of bottom nepheloid layers from the canyon head into the canyon upper and middle sections and possibly beyond.

5.2.2. Tidal currents

The influence of tidal currents on sediment transport along submarine canyons has attracted since long the attention of researchers (e.g. Shepard et al., 1979 and references therein). Observations in the Baltimore Canyon showed how internal tides focussing in the upper and middle canyon course resulted in sediment resuspension and ultimately in a net down-canyon sediment transport (Gardner, 1989). In the Nazaré Canyon, off Portugal, de Stigter et al. (2007) demonstrated how 15–25 cm s^{-1} semidiurnal tidal currents in the upper and middle canyon course were able to trigger sudden increases in suspended particulate matter and to promote net down-canyon sediment transport.

The spectral analysis carried out in the near-bottom AC2000B and WS1200 current meters within the Avilés Canyon and on the adjacent open slope, respectively, reveals that the main tidal component is semidiurnal (M2) with frequencies of 0.0805 cycles per hour (cph) (12.42 h) (not shown). Other less energetic peaks are also present in the inertial frequency (f) of 0.0605 cph (16.52 h), as a mix of diurnal species (mostly K1) with 0.0410 cph (24.38 h), and as higher harmonic species M4 and M6 with 0.1621 cph (6.17 h) and 0.2441 cph (4.10 h), respectively. This underlines the relevance of tidal currents in the dynamics of the upper and middle Avilés Canyon and its adjacent slope. The Godin $(A^2A_{25})/(24^225)$ filter applied to obtain tidal period variations and extract subinertial series, shows that during the study period, tidal currents represented, at least, 60% in average of all currents recorded both at Avilés Canyon and on the open continental slope west of it.

One further aspect that can be derived from the currentmeter time series, and is well depicted in the hodograph of Fig. 10, is the existence of two directions of polarization of the residual current at AC2000B. In a first time the current measured at that depth consisted in a residual movement towards NW (hodograph ending at about 5 km North/5 km West), so suggesting the presence of a residual current coming downcanyon along the Avilés Canyon axis. Then the residual movement due to horizontal currents at AC2000B becomes directed towards NE (hodograph end at about 10 km North/3 km East). This would imply the presence at AC2000B, during this period, of a current coming from the slope southwest of the mooring position and directed towards NE roughly. This would be a residual current coming from La Vallina tributary branches located in the westward flank of Avilés Canyon (Figs. 1 and 2). In evolution that follows, periods when this residual current was flowing down-canyon coming from the Avilés Canyon axis can be distinguished from periods (that seem to predominate) when the residual current came from La Vallina branches.

During the entire period there were also short-lived current fluctuations overprinted on these residual currents, which are

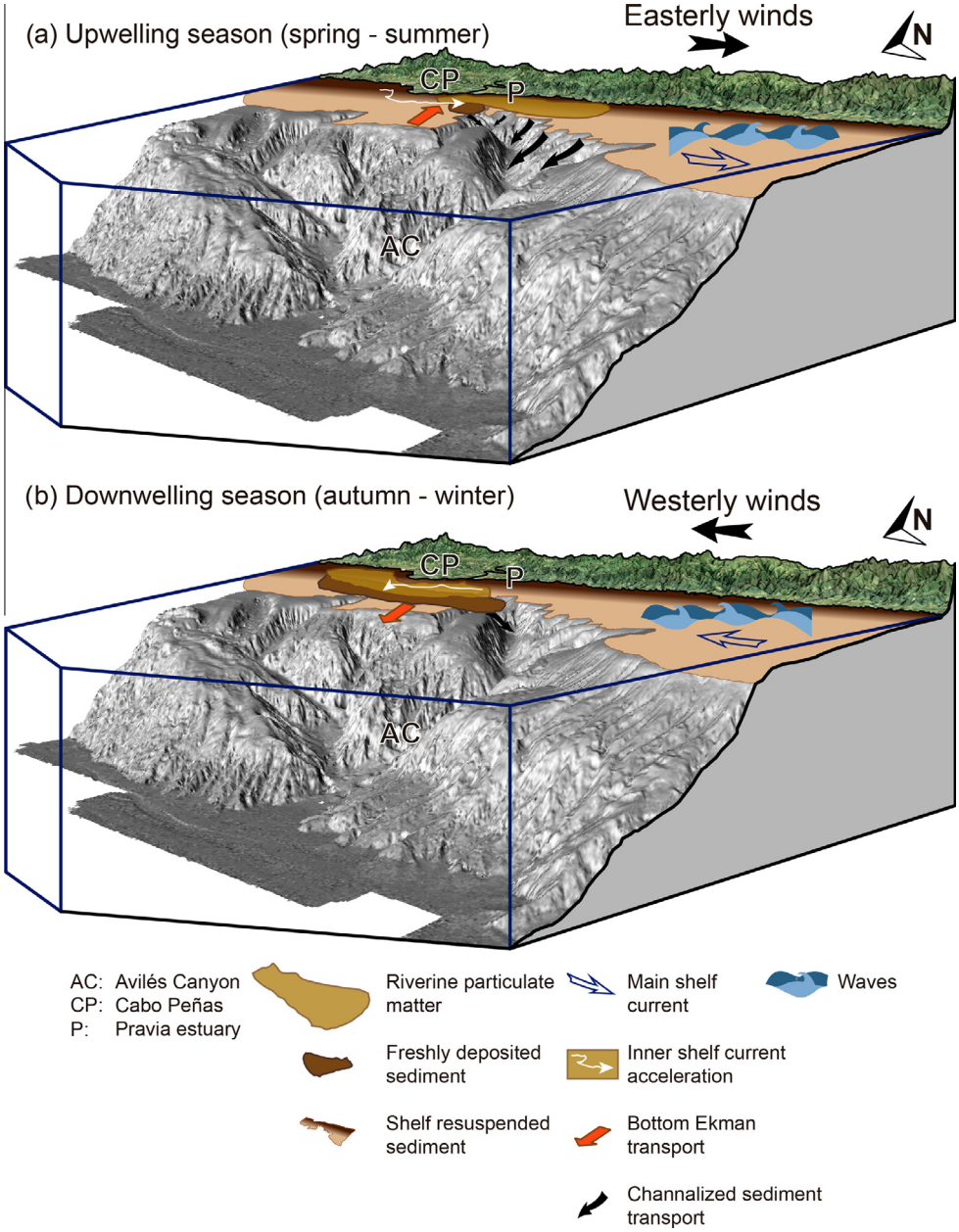

Fig. 11. Scheme illustrating wind regimes and associated processes including sediment transport (a) during spring and summer, when easterly winds induce a westward circulation and favour the advection of coast-derived sea surface sediment plumes towards Avilés Canyon and its adjacent open slope, and (b) during autumn and winter, when westerly winds induce and eastward circulation pushing sea surface sediment plumes against the shoreline, i.e. away from the canyon head and upper course. Note, however, that the bottom Ekman transport is directed offshore (see Section 5.1). (For interpretation to colour in this figure, the reader is referred to the web version of this article.)

apparently polarized along the Avilés Canyon axis. These short period fluctuations have periods from half a day (that would be the semidiurnal tidal currents) to one or two days and the particle excursions associated with these movements seem to align very well with the orientation of the Avilés Canyon axis no matter the orientation of the residual flow.

Tidal currents add, therefore, an extra amount of energy to the prevailing bottom currents, which may actively favour sediment transport along the Avilés submarine canyon system. Repeated cycles of semidiurnal tides shorten the intervals during which particles might settle, thus contributing to keep a permanent background of suspended particles in near-bottom waters (Fig. 4d and e), which is about 0.04 g m^{-2} d^{-1}. De Stigter et al. (2007) noticed a similar situation in the Nazaré Canyon off the western Iberian margin. Also, during quiet summer conditions when the water column is stratified the turbulence associated to internal waves likely has the capability to resuspend and remobilize sedimentary deposits on the continental slope and possibly the outer and mid-shelf (e.g. Quaresma et al., 2007).

The above observations further suggest the important role being played by the La Vallina tributary branches, in the westward flank of Avilés Canyon. The significance of these tributaries is further discussed in the next section.

5.2.3. Coastal and seafloor physiography

The interaction of the regional circulation with shoreline and seafloor morphological irregularities has been proven to influence the long-term sediment dispersal and accumulation in continental

margins. In the study area, the interaction of the Cabo Peñas headland and the Avilés Canyon system topography with the wind-forced circulation adds complexity to the understanding of sediment transport.

As pointed out by DeGeest et al. (2008), headlands behave as sediment bypass areas where alongshore currents accelerate and deviate offshore. This is well illustrated, amongst other examples, by Cape Creus coastal promontory, in the Gulf of Lion, northwestern Mediterranean Sea, which accelerates and deviates shelf water flows offshore into the Cap de Creus Canyon (Canals et al., 2006; Lastras et al., 2007; Ulses et al., 2008a). Cabo Peñas headland (Fig. 1) might play a similar a role, i.e. deflecting and accelerating the regional along shelf circulation, thus conveying sediment off the nearshore belt into the Avilés Canyon. This would be associated with the specific interactions of Cabo Peñas promontory, and also the canyon head, with the prevailing westward and eastward shelf and slope surface circulation favouring coastal upwelling and downwelling, respectively (see Sections 2 and 5.2.1).

Based on morphological criteria, La Vallina tributary branches seem to play a relevant role in feeding the Avilés Canyon. After the canyon head, the heads of this set of tributaries are the most indented into the continental shelf west of Cabo Peñas (Fig. 1). Therefore, they might be able to capture sediment fluxes reaching the outer shelf. Interestingly, the main La Vallina branches but the westernmost one are markedly asymmetric with dominantly smoothened right flanks and gullied left flanks (Fig. 2a–c). The westernmost branch, which is the largest and most open one, displays a similar smoothening in both flanks (Fig. 2b). These features suggest preferential sediment deposition on the right flanks of the shelf-indented La Vallina branches, with a more widespread sedimentation over the larger westernmost branch. Furthermore, the dominant gullied character of the left flanks of La Vallina branches (Fig. 2c) points to erosion. Such features might be related not only to the location of La Vallina branches but also to recirculation induced by Cabo Peñas Promontory and topographic effects caused by the presence of the head of the Avilés Canyon under the two dominant wind regimes and the associated Ekman transport at various depths. The sedimented, smoothened character of the shelf-indented segments of the right (eastern) flank of several of the La Vallina branches points to a significant role of the bottom Ekman transport during periods of persistent eastward shelf circulation. Part of the sediment captured by La Vallina branches likely ends up into the Avilés Canyon main trunk up-course of the location of our AC2000 mid-canyon mooring. Therefore, this set of tributaries may constitute a relevant side sediment source opening directly into the Avilés Canyon mid-course.

In situ inspection with towed cameras have shown the rough, rocky and sediment-starved nature of the Avilés Canyon head (Sánchez-Delgado et al., 2014), which on one side indicates that sedimentary particles do not settle possibly due to the prevailing intense hydrodynamics occurring there and, on another side, reinforces the role of the La Vallina branches as significant sediment feeders of the canyon mid-course. This is supported by observations made by Sánchez et al. (2014) in the neighbouring La Gaviera Canyon (Fig. 1), where the intensification of hydrodynamic activity at the very canyon head is a consequence of the regional circulation, especially during high-energy events such as storms, and the semidiurnal tidal cycle causing bore-like structures and strong resuspension.

The two main directions of polarization depicted in Fig. 10 illustrate the swinging behaviour of residual currents at AC2000B, with periods of northwestward residual movement followed by periods of northeastward movement and so on (see Section 5.2.2). These directions correspond to residual currents flowing down the main trunk of the Avilés Canyon alternating with currents coming from La Vallina branches, and therefore further support the significant role of La Vallina tributaries in the dynamics and sediment fluxes of the Avilés Canyon system.

The smaller tributaries situated between la Vallina group and the main canyon head do not look particularly asymmetric in terms of flank smoothening and gullies appear only locally, without forming closely spaced sets as in some of the flanks of la Vallina branches (Fig. 1). Their overall appearance also suggests some sediment smoothening, although not as pronounced as in the shelf-indented segments of the (mostly right) flanks of La Vallina branches, which could be related to the shorter incision distance into the continental shelf of these smaller tributaries, subsequently resulting in a lessened ability to capture sediment escaping from the shelf, but also to an extended effect of the intense hydrodynamics in the main canyon head preventing particles to settle, as described above.

5.2.4. Bottom trawling

The role of bottom trawling in resuspending sediments and inducing sediment gravity flows within submarine canyons has been documented by several authors, in particular in La Fonera Canyon, in the northwestern Mediterranean Sea (Palanques et al., 2006b; Martín et al., 2008; Puig et al., 2012; Martín et al., 2014a, b). These authors have shown how the action of trawlers on the seabed triggers sharp near-bottom turbidity peaks associated with increases in downslope near-bottom currents. Amongst other authors, Pusceddu et al. (2014) and Martín et al. (2015) have investigated other far-reaching consequences of recurrent bottom trawling.

In the western slope adjacent to Avilés Canyon there is an active commercial bottom trawling fishery down to 600 m of water depth that mainly targets blue whiting (Sánchez-Delgado et al., 2014, their Fig. 8.2.5A). As shown by satellite-based vessel tracking data (Sánchez-Delgado et al., 2014), this fishery mainly operates during periods of fair weather by means of pair trawling, a highly aggressive fishing technique able to resuspend large amounts of unconsolidated bottom sediment. An impact of bottom trawling on the Avilés Canyon area, and especially on the canyon head and upper course but also on the adjacent upper open slope is, therefore, likely. This view is supported by the increase in LFs at WS1200 (near-bottom) (Fig. 4d, grey dashed lines) during the calm seas period extending from June to September 2012, when some prominent peaks were also noticed (Fig. 4d, black solid lines). Unfortunately, there are no TMF or LF data available that could help assessing the impact of bottom trawling in the canyon head and upper course. The bottom trawl triggered resuspension does not seem to reach the middle canyon where AC2000 was deployed (Fig. 4b).

6. Conclusions

The dominance of lithogenics (averaged annual values between 53.05% and 66.98% of TMFs) in settling particulate matter shows that riverine inputs represent the main source of particles arriving into the Avilés Canyon and its adjacent open slope. However, we did not detect a univocal direct control of river discharge on the temporal variability of TMFs neither in the middle and lower course of the Avilés Canyon, nor in the open upper slope west of the canyon, which suggests that other factors should control particle fluxes beyond the continental shelf edge. Indeed, certain hydrodynamic processes such as storms involve enough energy to enhance the transport of particles from coastal and shelf environments beyond that boundary.

Marine primary production is the second main source of sedimentary particles settling down in the study area. Biological components represented in average more than 30% in weight of the

particles collected at all sediment traps during the monitoring period. In the lowermost canyon course (station AC4700) the $CaCO_3$ content of the biogenic fraction reaching the seabed is higher due to an enhanced flux of carbonate particles compared to siliceous ones. Furthermore, a CCD deeper (~5200 m) than our deepest sediment traps prevents significant dissolution of $CaCO_3$ particles.

Two different particle settling regimes have been identified. The first involves the shallower sediment traps in the open slope to the west (WS1200, near-bottom) and in the middle canyon course (AC2000T, mid-water). This regime encompasses a clear seasonal signal with relatively high contents of biogenic particles. The second regime refers to the deeper, near-bottom traps in the canyon middle (AC2000B) and lowermost (AC4700) course, where no seasonal signal has been identified. Instead, resuspended, lithogenic-rich particulate matter diluting biogenic particles characterises this regime. The 16–30 days of delay in biogenic fraction increases recorded between the mid water AC2000T trap and the near-bottom AC2000B trap in the middle canyon course indicate some degree of connection through pelagic settling between different depth levels within the Avilés Canyon. Furthermore, the trajectory of particles between AC2000B in the middle canyon course and AC4700 in the lowermost canyon course points to an effective horizontal along canyon transport, at least at the depth level of AC2000B. However, this does not prove that the near-bottom circulation on Avilés Canyon is connected to the circulation at upper layers.

Storms are the main physical driver of particle fluxes in the Avilés Canyon area. Wind direction and wind-driven currents determine whether resuspended shelf particulate matter may reach the canyon, and if this will occur by surface or bottom transport. Winds blowing from the west induce an onshore surface Ekman transport that pushes river-sourced and shelf-resuspended sedimentary particles away from the Avilés canyon head and upper course. However, under the same situation, the bottom Ekman transport is directed offshore and, therefore, favours the injection of particles into the Avilés Canyon. In contrast, winds blowing from the east induce coastal upwelling and favour the advection in the surface layer of particulate matter towards the Avilés Canyon and the adjacent western open slope. The same wind forcing triggers a bottom Ekman transport easing the retention of resuspended sediments on the shelf.

The Avilés Canyon head displays a very rough topography and a sediment-starved character. We suggest this to be caused, at least partly, by current deflection and turbulence induced by Cabo Peñas promontory. Such current deflection causes the bypass of suspended material over the Avilés Canyon head while steering the collection and funnelling of sediment fluxes into the main trunk of the canyon through La Vallina branches further west, as suggested by the smoothened nature of the shelf-incised segments in the right flanks of these set of tributaries, which could also respond to bottom trawling resuspension and subsequent setting there. The enhancement of hydrodynamic activity at the canyon head associated to high-energy events and tides likely plays a role too in making it sediment-starved.

Tidal currents actively contribute to sediment transport both in the upper–middle canyon course and over the western open slope. Repeated cycles of semidiurnal tides prevent particles to settle, thus resulting in a permanent background of suspended particles in near-bottom waters.

Increases in LFs occurring in summer months under calm sea conditions with no apparent relationship with meteoceanic external forcings are hypothesized to be also a consequence of commercial bottom trawling in the area. This anthropogenic disturbance may intensify the input of suspended matter all over the slope adjacent to the Avilés Canyon, and sporadically trigger shelf-slope sediment flows.

Finally, the specific physiography and orientation of the central Cantabrian margin, with a narrow continental shelf ahead of the Avilés Canyon and the presence of the nearby major coastal promontory of Cabo Peñas might help explaining its sensitivity to atmospheric and associated oceanographic forcings. The impact of these forcings on shallow waters would trigger a direct response propagating across the margin, which may explain the higher TMFs peaks in the Avilés Canyon compared to other canyons in the Bay of Biscay, such as Cap Ferret Canyon.

Acknowledgements

This research has been supported mainly by the DOS MARES Spanish project (CTM2010-21810-C03-01). Generalitat de Catalunya supported GRC Geociències Marines through grant 2009 SGR 1305 (now 2014 SGR 1068). We thank the crew of R/V Sarmiento de Gamboa, Universitat de Barcelona and Instituto Español de Oceanografía staff involved in sampling at sea and in the maintenance of the mooring lines. We also thank the crew of R/V Miguel Oliver and the COCAN cruise shipboard party for multibeam bathymetry data acquisition and processing. R. Pedrosa-Pàmies and M. Guart were extremely helpful during sea going and laboratory work. M. Romero and R. Roca assisted us during ICP-AES and EA analyses. D.L. Jones provided the Fathom Toolbox for Matlab and made it freely available for download. The mission scientists and principal investigators from Giovanni system provided chlorophyll-a data. X. Rayo assisted us with the ArcGis software, X. Tubau contributed with valuable comments and L. D. Pena improved the English. ASV is supported by a Ramon y Cajal contract by the Spanish Ministry for Science and Innovation.

References

Álvarez Fanjul, E., Alfonso, M., Ruiz, M.I., López, J.D., Rodríguez, I., 2003. Building the European capacity in operational oceanography. Proceedings of the third international conference on EuroGOOS. Elsevier Oceanography Series 69, 398–402.

Arzola, R.G., Wynn, R.B., Lastras, G., Masson, D.G., Weaver, P.P.E., 2008. Sedimentary features and processes in the Nazaré and Setúbal submarine canyons, west Iberian margin. Marine Geology 250, 64–88.

Asper, V.L., 1987. Measuring the flux and sinking speed of marine snow aggregates. Deep Sea Research Part A: Oceanographic Research Papers 34, 1–17.

Baines, P.G., 1982. On internal tide generation models. Deep Sea Research Part A: Oceanographic Research Papers 29, 307–338.

Baker, E.T., Milburn, H.B., Tennant, D.A., 1988. Field assessment of sediment trap efficiency under varying flow conditions. Journal of Marine Research 46, 573–592.

Bakun, A., 1973. Coastal Upwelling Indices, West Coast of North America, 1946-71. US. Dep. Comm. NOAA. Tech. Rep. NMFS-SSRF 671.

Behrenfeld, M.J., Falkowski, P.G., 1997. Photosynthetic rates derived from satellite-based chlorophyll concentration. Limnology and Oceanography 42, 1–20.

Berner, R.A., Honjo, S., 1981. Pelagic sedimentation of aragonite: its geochemical significance. Science 211, 940–942.

Biscaye, P.E., Kolla, V., Turekian, K.K., 1976. Distribution of calcium carbonate in surface sediments of the Atlantic Ocean. Journal of Geophysical Research 81, 2595–2603.

Biscaye, P.E., Andersson, R.F., 1994. Fluxes of particulate matter on the slope of the southern Middle Atlantic Bight: SEEP-II. Deep Sea Research Part II: Topical Studies in Oceanography 41, 459–509.

Bonnin, J., Van Raaphorst, W., Brummer, G.J., Van Haren, H., Malschaert, H., 2002. Intense mid-slope resuspension of particulate matter in the Faeroe-Shetland Channel: short-term deployment of near-bottom sediment traps. Deep Sea Research Part I: Oceanographic Research Papers 49, 1485–1505.

Bonnin, J., Heussner, S., Calafat, A., Fabrés, J., Palanques, A., Durrieu de Madron, X., Canals, M., Puig, P., Avril, J., Delsaut, N., 2008. Comparison of horizontal and downward particle fluxes across canyons of the Gulf of Lions (NW Mediterranean): meteorological and hydrodynamical forcing. Continental Shelf Research 28, 1957–1970.

Botas, J.A., Fernández, E., Bode, A., Anadón, R., 1989. Water masses off the central Cantabrian coast. Scientia Marina 53, 755–761.

Buesseler, K.O., Antia, A.N., Chen, M., Fowler, S.W., Gardner, W.D., Gustafsson, O., Harada, K., Michaels, A.F., Rutgers van der Loeff, M., Sarin, M., Steinberg, D.K., Trull, T., 2007. An assessment of the use of sediment traps for estimating upper ocean particle fluxes. Journal of Marine Research 65, 345–416.

Cacchione, D.A., Pratson, L.F., Ogston, A.S., 2002. The shaping of continental slopes by internal tides. Science 296, 724–727.

Canals, M., Puig, P., de Madron, X.D., Heussner, S., Palanques, A., Fabrés, J., 2006. Flushing submarine canyons. Nature 444, 354–357.
Canals, M., Company, J.B., Martín, D., Sànchez-Vidal, A., Ramírez-Llodra, E., 2013. Integrated study of Mediterranean deep canyons: novel results and future challenges. Progress in Oceanography 118, 1–27.
Charria, G., Lazure, P., Le Cann, B., Serpette, A., Reverdin, G., Louazel, S., Batifoulier, F., Dumas, F., Pichon, A., Morel, Y., 2013. Surface layer circulation derived from Lagrangian drifters in the Bay of Biscay. Journal of Marine Systems 109, S60–S76.
DeGeest, A.L., Mullenbach, B.L., Puig, P., Nittrouer, C.A., Drexler, T.M., Durrieu de Madron, X., Orange, D.L., 2008. Sediment accumulation in the western Gulf of Lions, France: the role of Cap de Creus canyon in linking shelf and slope sediment dispersal systems. Continental Shelf Research 28, 2031–2047.
De Leo, F.C., Smith, C.R., Rowden, A.A., Bowden, D.A., Clark, M.R., 2010. Submarine canyons: hotspots of benthic biomass and productivity in the deep sea. Proceedings of the Royal Society of London B: Biological Sciences 277, 2783–2792.
de Stigter, H.C., Boer, W., de Jesus Mendes, P.a., Jesus, C.C., Thomsen, L., van den Bergh, G.D., van Weering, T.C.E., 2007. Recent sediment transport and deposition in the Nazaré Canyon, Portuguese continental margin. Marine Geology 246, 144–164.
de Stigter, H.C., Jesus, C.C., Boer, W., Richter, T.O., Costa, A., van Weering, T.C.E., 2011. Recent sediment transport and deposition in the Lisbon-Setúbal and Cascais submarine canyons, Portuguese continental margin. Deep Sea Research Part II: Topical Studies in Oceanography 58, 2321–2344.
Díaz del Río, G., González, N., Marcote, D., 1998. The intermediate Mediterranean water inflow along the northern slope of the Iberian Peninsula. Oceanologica Acta 21, 157–163.
Dickson, R.R., Gould, W.J., Müller, T.J., Maillard, C., 1985. Estimates of the mean circulation in the deep (>2,000 m) layer of the Eastern North Atlantic. Progress in Oceanography 14, 103–127.
Drake, D.E., Gorsline, D.S., 1973. Distribution and transport of suspended particulate matter in Hueneme, Redondo, Newport and La Jolla submarine canyons. Geological Society of America Bulletin 84, 3949–3968.
Durrieu de Madron, X., Nyffeler, F., Godet, C.H.C., 1990. Hydrographic structure and nepheloid spatial distribution in the Gulf of Lions continental margin. Continental Shelf Research 10, 915–929.
Durrieu de Madron, X., 1994. Hydrography and nepheloid structures in the Grand-Rhône canyon. Continental Shelf Research 14, 457–477.
Durrieu De Madron, X., Castaing, P., Nyffeler, F., Courp, T., 1999. Slope transport of suspended particulate matter on the Aquitanian margin of the Bay of Biscay. Deep-Sea Research Part II 46, 2003–2027.
Fabrés, J., Calafat, A., Sànchez-Vidal, A., Canals, M., Heussner, S., 2002. Composition and spatio-temporal variability of particle fluxes in the Western Alboran Gyre, Mediterranean Sea. Journal of Marine Systems 34, 431–456.
Fanjul, E.A., Gómez, B.P., Sánchez-Arévalo, I.R., 1997. A description of the tides in the Eastern North Atlantic. Progress in Oceanography 40, 217–244.
Fernández, E., Bode, A., 1991. Seasonal patterns of primary production in the Central Cantabrian Sea (Bay of Biscay). Scientia Marina 55, 629–636.
Fernández, E., Bode, A., 1994. Succession of phytoplankton assemblages in relation to the hydrography in the southern Bay of Biscay: a multivariate approach. Scientia Marina 58, 191–205.
Friocourt, Y., Levier, B., Speich, S., Blanke, B., Drijfhout, S.S., 2007. A regional numerical ocean model of the circulation in the Bay of Biscay. Journal of Geophysical Research: Oceans 112, 1–19.
Frouin, R., Fiúza, A.F.G., Ambar, I., Boyd, T.J., 1990. Observations of a poleward surface current off the coasts of Portugal and Spain during winter. Journal of Geophysical Research: Oceans 95, 679–691.
Gardner, W.D., 1985. The effect of tilt on sediment trap efficiency. Deep Sea Research Part A: Oceanographic Research Papers 32, 349–361.
Gardner, W.D., 1989. Baltimore Canyon as a modern conduit of sediment to the deep sea. Deep Sea Research Part A: Oceanographic Research Papers 36, 323–358.
Gardner, W.D., Walsh, I.D., 1990. Distribution of macroaggregates and fine-grained particles across a continental margin and their potential role in fluxes. Deep Sea Research Part A: Oceanographic Research Papers 37, 401–411.
Gardner, W.D., Biscaye, P.E., Richardson, M.J., 1997. A sediment trap experiment in the Vema Channel to evaluate the effect of horizontal particle fluxes on measured vertical fluxes. Journal of Marine Research 55, 995–1028.
Gil, J., Gomis, D., 2008. The secondary ageostrophic circulation in the Iberian Poleward Current along the Cantabrian Sea (Bay of Biscay). Journal of Marine Systems 74, 60–73.
Gili, J., Bouillon, J., Palanques, A., Puig, P., 1999. Submarine canyons as habitats of prolific plankton populations: three new deep-sea Hydroidomedusae in the western Mediterranean. Zoological Journal of the Linnean Society 125, 313–329.
Godin, G., 1972. The Analysis of Tides. Univ. Toronto, Toronto, Canada, 264pp.
Gómez-Ballesteros, M., Druet, M., Muñoz, A., Arrese, B., Rivera, J., Sánchez, F., Cristobo, J., Parra, S., García-Alegre, A., González-Pola, C., Gallástegui, J., Acosta, J., 2013. Geomorphology of the Avilés Canyon System, Cantabrian Sea (Bay of Biscay). Deep Sea Research Part II: Topical Studies in Oceanography, 1–19.
González-Pola, C., Ruiz-Villarreal, M., Lavín, A., Cabanas, J.M., Álvarez-Fanjul, E., 2005. A subtropical water intrusion spring-event in the shelf-slope of the south-western Bay of Biscay after strong wind-forcing pulses. Journal of Atmospheric and Ocean Science 10, 343–359.
González-Pola, C., Fernández-Díaz, J.M., Lavín, A., 2007. Vertical structure of the upper ocean from profiles fitted to physically consistent functional forms. Deep Sea Research Part I: Oceanographic Research Papers 54, 1985–2004.
González-Quirós, R., Cabal, J., Álvarez-Marqués, F., Isla, A., 2003. Ichthyoplankton distribution and plankton production related to the shelf break front at the Avilés Canyon. ICES Journal of Marine Science 60, 198–210.
Guillén, J., Palanques, A., Puig, P., Durrieu de Madron, X., Nyffeler, F., 2000. Field calibration of optical sensors for measuring suspended sediment concentration in the western Mediterranean. Scientia Marina 64, 427–435.
Guillén, J., Bourrin, F., Palanques, A., Durrieu de Madron, X., Puig, P., Buscail, R., 2006. Sediment dynamics during wet and dry storm events on the Têt inner shelf (SW Gulf of Lions). Marine Geology 234, 129–142.
Haynes, R., Barton, E.D., 1990. A poleward flow along the Atlantic coast of the Iberian Peninsula. Journal of Geophysical Research: Oceans 95, 11425–11441.
Heussner, S., Ratti, C., Carbonne, J., 1990. The PPS 3 time-series sediment trap and the trap sample processing techniques used during the ECOMARGE experiment. Continental Shelf Research 10, 943–958.
Heussner, S., Durrieu de Madron, X., Radakovitch, O., Beaufort, L., Biscaye, P.E., Carbonne, J., Delsaut, N., Etcheber, H., Monaco, A., 1999. Spatial and temporal patterns of downward particle fluxes on the continental slope of the Bay of Biscay (northeastern Atlantic). Deep-Sea Research II 46, 2101–2146.
Heussner, S., Durrieu de Madron, X., Calafat, A., Canals, M., Carbonne, J., Delsaut, N., Saragoni, G., 2006. Spatial and temporal variability of downward particle fluxes on a continental slope: lessons from an 8-yr experiment in the Gulf of Lions (NW Mediterranean). Marine Geology 234, 63–92.
Hickey, B., Baker, E., Kachel, N., 1986. Suspended particle movement in and around Quinault submarine canyon. Marine Geology 71, 35–83.
Hung, J.-J., Lin, C.-S., Chung, Y.-C., Hung, G.-W., Liu, W.-S., 2003. Lateral fluxes of biogenic particles through the Mien-Hua canyon in the southern East China Sea slope. Continental Shelf Research 23, 935–955.
Iorga, M.C., Lozier, M.S., 1999a. Signatures of the Mediterranean outflow from a North Atlantic climatology: 1. Salinity and density fields. Journal of Geophysical Research 104, 25985–26009.
Iorga, M.C., Lozier, M.S., 1999b. Signatures of the Mediterranean outflow from a North Atlantic climatology: 2. Diagnostic velocity fields. Journal of Geophysical Research: Oceans 104, 26011–26029.
Jouanneau, J.-M., Weber, O., Champilou, N., Cirac, P., Muxika, I., Borja, A., Pascual, A., Rodríguez-Lázaro, J., Donard, O., 2008. Recent sedimentary study of the shelf of the Basque country. Journal of Marine Systems 72, 397–406.
Lastras, G., Canals, M., Urgelès, R., Amblàs, D., Ivanov, M., Droz, L., Dennielou, B., Fabrés, J., Schoolmeester, T., Akhmetzhanov, A., Orange, D., García-García, A., 2007. A walk down the Cap de Creus canyon, northwestern Mediterranean Sea: recent processes inferred from morphology and sediment bedforms. Marine Geology 246, 176–192.
Lastras, G., Canals, M., Amblàs, D., Calafat, A.M., Durán, R., Muñoz, A., Pedrosa-Pàmies, R., Sànchez-Vidal, A., Rayo, X., Rumin, A., Tubau, X., Veres, O., 2012. The Avilés submarine canyon drainage system, northern Iberian margin. The Deep-Sea and Sub-Seafloor Frontiers Conf. 11–14 March, Spain, Abstr., vol. P085.
Lavín, A., Valdés, L., Sénchez, F., Abaunza, P., Forest, A., Boucher, J., Lazure, P., Jegou, A.-M., 2006. The Bay of Biscay: the encountering of the ocean and the shelf. Seas Harvard Press 14, 933–1001.
Le Cann, B., Serpette, A., 2009. Intense warm and saline upper ocean inflow in the southern Bay of Biscay in autumn-winter 2006–2007. Continental Shelf Research 29, 1014–1025.
Margalef, R., 1978. Life-forms of phytoplankton as survival alternatives in an unstable environment. Oceanologica Acta 1, 493–509.
Martín, J., Palanques, A., Puig, P., 2006. Composition and variability of downward particulate matter fluxes in the Palamós submarine canyon (NW Mediterranean). Journal of Marine Systems 60, 75–97.
Martín, J., Puig, P., Palanques, A., Masqué, P., García-Orellana, J., 2008. Effect of commercial trawling on the deep sedimentation in a Mediterranean submarine canyon. Marine Geology 252, 150–155.
Martín, J., Palanques, A., Vitorino, J., Oliveira, A., de Stigter, H.C., 2011. Near-bottom particulate matter dynamics in the Nazaré submarine canyon under calm and stormy conditions. Deep Sea Research Part II: Topical Studies in Oceanography 58, 2388–2400.
Martín, J., Puig, P., Palanques, A., Ribó, M., 2014a. Trawling-induced daily sediment resuspension in the flank of a Mediterranean submarine canyon. Deep Sea Research Part II: Topical Studies in Oceanography 104, 174–183.
Martín, J., Puig, P., Masqué, P., Palanques, A., Sánchez-Gómez, A., 2014b. Impact of bottom trawling on deep-sea sediment properties along the flanks of a submarine canyon. PLoS ONE 9, e104536.
Martín, J., Puig, P., Palanques, A., Giamportone, A., 2015. Commercial bottom trawling as a driver of sediment dynamics and deep seascape evolution in the Anthropocene. Anthropocene 7, 1–15.
McCave, I.N., Hall, I.R., Antia, a.N., Chou, L., Dehairs, F., Lampitt, R.S., Thomsen, L., Van Weering, T.C.E., Wollast, R., 2001. Distribution, composition and flux of particulate material over the European margin at 47°–50°N. Deep Sea Research Part II: Topical Studies in Oceanography 48, 3107–3139.
Miquel, J.C., Martín, J., Gasser, B., Rodríguez-y-Baena, A., Toubal, T., Fowler, S.W., 2011. Dynamics of particle flux and carbon export in the northwestern Mediterranean Sea: a two decade time-series study at the DYFAMED site. Progress in Oceanography 91, 461–481.
Moreno-Madriñán, M.J., Fischer, A.M., 2013. Performance of the MODIS FLH algorithm in estuarine waters: a multi-year (2003–2010) analysis from

Tampa Bay, Florida (USA). International Journal of Remote Sensing 34, 6467–6483.
Mortlock, R.A., Froelich, P.N., 1989. A simple method for the rapid determination of biogenic opal in pelagic marine sediments. Deep Sea Research Part A: Oceanographic Research Papers 36, 1415–1426.
Mulder, T., Zaragosi, S., Garlan, T., Mavel, J., Cremer, M., Sottolichio, a., Sénéchal, N., Schmidt, S., 2012. Present deep-submarine canyons activity in the Bay of Biscay (NE Atlantic). Marine Geology 295–298, 113–127.
Nittrouer, C.A., Wright, L.D., 1994. Transport of particles across continental shelves. Reviews of Geophysics 32, 85–113.
Oliveira, A., Santos, A.I., Rodrigues, A., Vitorino, J., 2007. Sedimentary particle distribution and dynamics on the Nazaré canyon system and adjacent shelf (Portugal). Marine Geology 246, 105–122.
Paillet, J., Mercier, H., 1997. An inverse model of the eastern North Atlantic general circulation and thermocline ventilation. Deep Sea Research Part I: Oceanographic Research Papers 44, 1293–1328.
Palanques, A., El Khatab, M., Puig, P., Masqué, P., Sánchez-Cabeza, J.A., Isla, E., 2005. Downward particle fluxes in the Guadiaro submarine canyon depositional system (north-western Alboran Sea), a river flood dominated system. Marine Geology 220, 23–40.
Palanques, A., Durrieu de Madron, X., Puig, P., Fabrés, J., Guillén, J., Calafat, A., Canals, M., Heussner, S., Bonnin, J., 2006a. Suspended sediment fluxes and transport processes in the Gulf of Lions submarine canyons. The role of storms and dense water cascading. Marine Geology 234, 43–61.
Palanques, A., Martín, J., Puig, P., Guillén, J., Company, J.B., Sardà, F., 2006b. Evidence of sediment gravity flows induced by trawling in the Palamós (Fonera) submarine canyon (northwestern Mediterranean). Deep Sea Research Part I: Oceanographic Research Papers 53, 201–214.
Palanques, A., Guillén, J., Puig, P., Durrieu de Madron, X., 2008. Storm-driven shelf-to-canyon suspended sediment transport at the southwestern Gulf of Lions. Continental Shelf Research 28, 1947–1956.
Palanques, A., Puig, P., Latasa, M., Scharek, R., 2009. Deep sediment transport induced by storms and dense shelf-water cascading in the northwestern Mediterranean basin. Deep Sea Research Part I: Oceanographic Research Papers 56, 425–434.
Palanques, A., Puig, P., Durrieu de Madron, X., Sànchez-Vidal, A., Pasqual, C., Martín, J., Calafat, A., Heussner, S., Canals, M., 2012. Sediment transport to the deep canyons and open-slope of the western Gulf of Lions during the 2006 intense cascading and open-sea convection period. Progress in Oceanography 106, 1–15.
Pasqual, C., Lee, C., Goñi, M., Tesi, T., Sànchez-Vidal, A., Calafat, A., Canals, M., Heussner, S., 2011. Use of organic biomarkers to trace the transport of marine and terrigenous organic matter through the southwestern canyons of the Gulf of Lion. Marine Chemistry 126, 1–12.
Paull, C.K., Mitts, P., Ussler, W., Keaten, R., Greene, H.G., 2005. Trail of sand in upper Monterey Canyon: offshore California. Geological Society of America Bulletin 117, 1134–1145.
Pierau, R., Henrich, R., Preiß-Daimler, I., Krastel, S., Geersen, J., 2011. Sediment transport and turbidite architecture in the submarine Dakar Canyon off Senegal, NW-Africa. Journal of African Earth Sciences 60, 196–208.
Pingree, R.D., 1993. Flow of surface waters to the west of the British Isles and in the Bay of Biscay. Deep Sea Research Part II: Topical Studies in Oceanography 40, 369–388.
Pingree, R.D., Le Cann, B., 1990. Structure, strength and seasonality of the slope currents in the Bay of Biscay region. Journal of the Marine Biological Association of the United Kingdom 70, 857–885.
Pingree, R.D., Le Cann, B., 1992. Anticyclonic eddy X91 in the southern Bay of Biscay, May 1991 to February 1992. Journal of Geophysical Research: Oceans 97, 14353–14367.
Pingree, R.D., New, A.L., 1989. Downward propagation of internal tidal energy into the Bay of Biscay. Deep Sea Research Part A: Oceanographic Research Papers 36, 735–758.
Pollard, R.T., Pu, S., 1985. Structure and circulation of the Upper Atlantic Ocean northeast of the Azores. Progress in Oceanography 14, 443–462.
Pollard, R.T., Griffiths, M.J., Cunningham, S.A., Read, J.F., Pérez, F.F., Ríos, A.F., 1996. Vivaldi 1991 – a study of the formation, circulation and ventilation of Eastern North Atlantic Central Water. Progress in Oceanography 37, 167–192.
Prego, R., Boi, P., Cobelo-García, A., 2008. The contribution of total suspended solids to the Bay of Biscay by Cantabrian Rivers (northern coast of the Iberian Peninsula). Journal of Marine Systems 72, 342–349.
Puig, P., Palanques, A., 1998. Temporal variability and composition of settling particle fluxes on the Barcelona continental margin (Northwestern Mediterranean). Journal of Marine Research 56, 639–654.
Puig, P., Ogston, A.S., Mullenbach, B.L., Nittrouer, C.A., Parsons, J.D., Sternberg, R.W., 2004a. Storm-induced sediment gravity flows at the head of the Eel submarine canyon, northern California margin. Journal of Geophysical Research 109, C03019.
Puig, P., Palanques, a., Guillén, J., El Khatab, M., 2004b. Role of internal waves in the generation of nepheloid layers on the northwestern Alboran slope: implications for continental margin shaping. Journal of Geophysical Research: Oceans C109, 1–11.
Puig, P., Canals, M., Company, J.B., Martín, J., Amblàs, D., Lastras, G., Palanques, A., Calafat, A.M., 2012. Ploughing the deep sea floor. Nature 489, 286–289.
Pusceddu, A., Bianchelli, S., Martín, J., Puig, P., Palanques, A., Masqué, P., Danovaro, R., 2014. Chronic and intensive bottom trawling impairs deep-sea biodiversity and ecosystem functioning. Proceedings of the National Academy of Sciences 111 (24), 8861–8866.
Quaresma, L.S., Vitorino, J., Oliveira, A., da Silva, J., 2007. Evidence of sediment resuspension by nonlinear internal waves on the western Portuguese mid-shelf. Marine Geology 246, 123–143.
Ríos, A.F., Pérez, F.F., Fraga, F., 1992. Water masses in the upper and middle North Atlantic Ocean east of the Azores. Deep Sea Research Part A: Oceanographic Research Papers 39, 645–658.
Ruiz-Villarreal, M., Coelho, H., Díaz del Río, G., Nogueira, J., 2004. Slope Current in the Cantabrian: Observations and Modeling of Seasonal Variability and Interaction with Aviles Canyon. ICES CM 2004/N:12, 23pp.
Rumín-Caparrós, A., Sànchez-Vidal, A., Calafat, A., Canals, M., Martín, J., Puig, P., Pedrosa-Pàmies, R., 2013. External forcings, oceanographic processes and particle flux dynamics in Cap de Creus submarine canyon, NW Mediterranean Sea. Biogeosciences 10, 3493–3505.
Sánchez, F., González-Pola, C., Druet, M., García-Alegre, A., Acosta, J., Cristobo, J., Parra, S., Ríos, P., Altuna, Á., Gómez-Ballesteros, M., Muñoz-Recio, A., Rivera, J., del Río, G.D., 2014. Habitat characterization of deep-water coral reefs in La Gaviera Canyon (Avilés Canyon System, Cantabrian Sea). Deep Sea Research Part II: Topical Studies in Oceanography 106, 118–140.
Sánchez-Delgado, F., Gómez-Ballesteros, M., Parra-Descalzo, S., Cristobo, J., Serrano-López, A., Druet-Vélez, M., García-Alegre-Garralda, A., Rodríguez-Cabello-Ródenas, M.C., Preciado-Ramírez, M.I., Tello-Antón, M.O., Punzón-Merino, A. M., Blanco-Giner, M.Á., Ríos, P., Frutos-Parralejo, M.I., González-Pola, C., Acosta-Yepes, J., Rivera, J., 2014. Caracterización ecológica del área marina del sistema de cañones submarinos de Avilés. Informe final área LIFE+ INDEMARES (LIFE07/NAT/E/000732). Instituto Español de Oceanografía. Coordinación: Fundación Biodiversidad, Madrid, 243pp.
Sànchez-Vidal, A., Canals, M., Calafat, A.M., Lastras, G., Pedrosa-Pàmies, R., Menéndez, M., Medina, R., Company, J.B., Hereu, B., Romero, J., Alcoverro, T., 2012. Impacts on the deep-sea ecosystem by a severe coastal storm. PLoS ONE 7, e30395.
Schmidt, S., Howa, H., Mouret, A., Lombard, F., Anschutz, P., Labeyrie, L., 2009. Particle fluxes and recent sediment accumulation on the Aquitanian margin of Bay of Biscay. Continental Shelf Research 29, 1044–1052.
Schmidt, S., Howa, H., Diallo, A., Martín, J., Cremer, M., Duros, P., Fontanier, C., Deflandre, B., Metzger, E., Mulder, T., 2014. Recent sediment transport and deposition in the Cap-Ferret Canyon, South-East margin of Bay of Biscay. Deep Sea Research Part II: Topical Studies in Oceanography 104, 134–144.
Serpette, A., Le Cann, B., Colas, F., 2006. Lagrangian circulation of the North Atlantic Central Water over the abyssal plain and continental slopes of the Bay of Biscay: description of selected mesoscale features. Scientia Marina 70, 27–42.
Shepard, F.P., 1981. Submarine canyons: multiple causes and long-time persistence. American Association of Petroleum Geologists Bulletin 65, 1062–1077.
Shepard, F.P., Marshall, N.F., McLoughlin, P.A., Sullivan, G.G., 1979. Currents in submarine canyons and other seavalleys. AAPG Studies in Geology 8, 173.
Smith, S.D., 1988. Coefficients for sea surface wind stress, heat flux, and wind profiles as a function of wind speed and temperature. Journal of Geophysical Research 93, 15467–15472.
Somavilla, R., González-Pola, C., Rodríguez, C., Josey, S.A., Sánchez, R.F., Lavín, A., 2009. Large changes in the hydrographic structure of the Bay of Biscay after the extreme mixing of winter 2005. Journal of Geophysical Research 114, 1–14.
Stabholz, M., Durrieu de Madron, X., Canals, M., Khripounoff, A., Taupier-Letage, I., Testor, P., Heussner, S., Kerhervé, P., Delsaut, N., Houpert, L., Lastras, G., Dennielou, B., 2013. Impact of open-ocean convection on particle fluxes and sediment dynamics in the deep margin of the Gulf of Lions. Biogeosciences 10, 1097–1116.
Stenseth, N.C., Llope, M., Anadón, R., Ciannelli, L., Chan, K.-S., Hjermann, D.Ø., Bagøien, E., Ottersen, G., 2006. Seasonal plankton dynamics along a cross-shelf gradient. Proceedings of the Royal Society of London B: Biological Sciences 273, 2831–2838.
Taylor, J.R., Sarkar, S., 2008. Stratification effects in a bottom Ekman layer. Journal of Physical Oceanography 38, 2535–2555.
Tyler, P., Amaro, T., Arzola, R., Cunha, M.R., de Stigter, H., Gooday, A., Huvenne, V., Ingels, J., Kiriakoulakis, K., Lastras, G., Masson, D., Oliveira, A., Pattenden, A., Vanreusel, A., Van Weering, T., Vitorino, J., Witte, U., Wolff, G., 2009. Europe's grand canyon: Nazaré submarine canyon. Oceanography 22, 46–57.
Ulses, C., Estournel, C., Bonnin, J., Durrieu de Madron, X., Marsaleix, P., 2008a. Impact of storms and dense water cascading on shelf-slope exchanges in the Gulf of Lion (NW Mediterranean). Journal of Geophysical Research 113, 1–18.
Ulses, C., Estournel, C., Durrieu de Madron, X., Palanques, A., 2008b. Suspended sediment transport in the Gulf of Lions (NW Mediterranean): impact of extreme storms and floods. Continental Shelf Research 28, 2048–2070.
van Aken, H.M., 2000a. The hydrography of the mid-latitude Northeast Atlantic Ocean. I: the deep water masses. Deep Sea Research Part I: Oceanographic Research Papers 47, 757–788.
van Aken, H.M., 2000b. The hydrography of the mid-latitude Northeast Atlantic Ocean. II: the intermediate water masses. Deep Sea Research Part I: Oceanographic Research Papers 47, 789–824.
van Aken, H.M., 2001. The hydrography of the mid-latitude Northeast Atlantic Ocean – part III: the subducted thermocline water mass. Deep Sea Research Part I: Oceanographic Research Papers 48, 237–267.
van Weering, T.C.E., de Stigter, H.C., Boer, W., de Haas, H., 2002. Recent sediment transport and accumulation on the NW Iberian margin. Progress in Oceanography 52, 349–371.
Vetter, E.W., 1994. Hotspots of benthic production. Nature 372, 47.

Vetter, E.W., Dayton, P.K., 1998. Macrofaunal communities within and adjacent to a detritus-rich submarine canyon system. Deep Sea Research Part II: Topical Studies in Oceanography 45, 25–54.
Vetter, E.W., Smith, C.R., De Leo, F.C., 2010. Hawaiian hotspots: enhanced megafaunal abundance and diversity in submarine canyons on the oceanic islands of Hawaii. Marine Ecology 31, 183–199.
Walsh, I.D., Gardner, W.D., 1992. A comparison of aggregate profiles with sediment trap fluxes. Deep Sea Research Part A: Oceanographic Research Papers 39, 1817–1834.
Xu, J., Noble, M., Eittreim, S.L., Rosenfeld, L.K., Schwing, F.B., Pilskaln, C.H., 2002. Distribution and transport of suspended particulate matter in Monterey Canyon, California. Marine Geology 181, 215–234.
Xu, J.P., Swarzenski, P.W., Noble, M., Li, A.-C., 2010. Event-driven sediment flux in Hueneme and Mugu submarine canyons, southern California. Marine Geology 269, 74–88.